frontiers | Research Topics

The molecular landscape and promising therapeutic targets in aggressive B-cell non-Hodgkin lymphomas

Edited by
Niklas Gebauer, Hanno Maximilian Witte, Axel Künstner, Francesco Piazza and Gaël Roué

Coordinated by
Emil Chteinberg

Published in
Frontiers in Oncology
Frontiers in Medicine

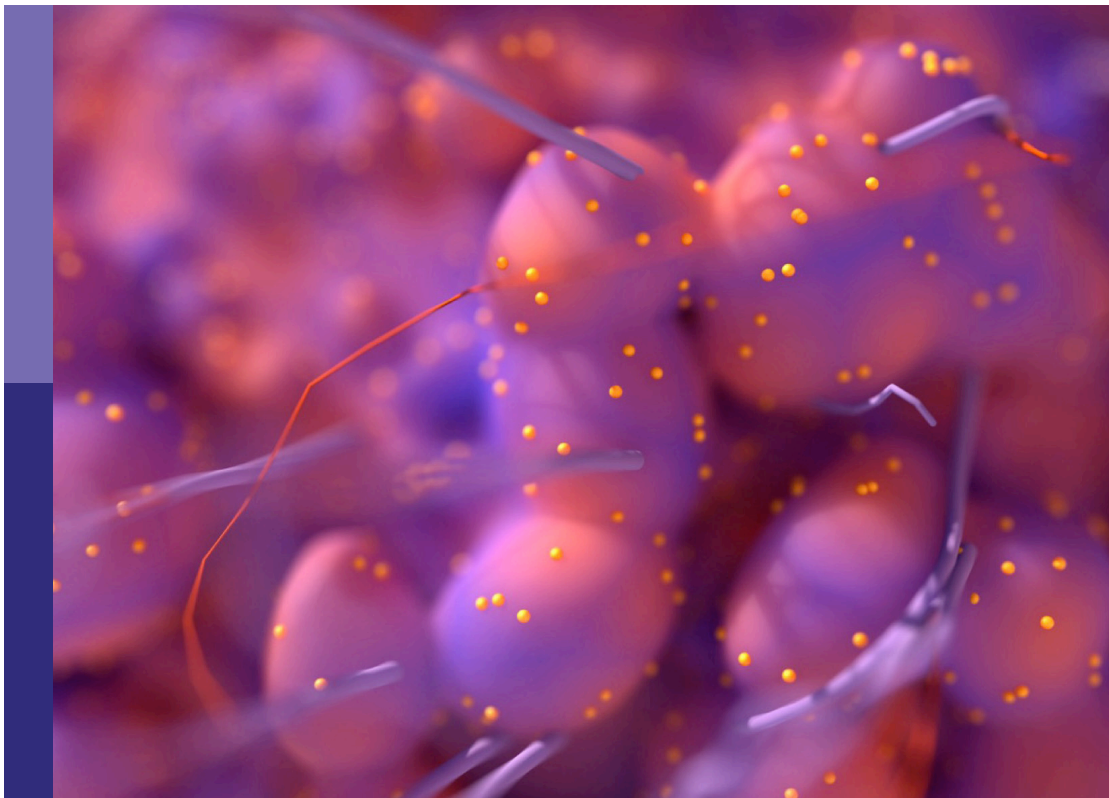

ISSN 1664-8714
ISBN 978-2-8325-3474-8
DOI 10.3389/978-2-8325-3474-8

About Frontiers

Frontiers is more than just an open access publisher of scholarly articles: it is a pioneering approach to the world of academia, radically improving the way scholarly research is managed. The grand vision of Frontiers is a world where all people have an equal opportunity to seek, share and generate knowledge. Frontiers provides immediate and permanent online open access to all its publications, but this alone is not enough to realize our grand goals.

Frontiers journal series

The Frontiers journal series is a multi-tier and interdisciplinary set of open-access, online journals, promising a paradigm shift from the current review, selection and dissemination processes in academic publishing. All Frontiers journals are driven by researchers for researchers; therefore, they constitute a service to the scholarly community. At the same time, the *Frontiers journal series* operates on a revolutionary invention, the tiered publishing system, initially addressing specific communities of scholars, and gradually climbing up to broader public understanding, thus serving the interests of the lay society, too.

Dedication to quality

Each Frontiers article is a landmark of the highest quality, thanks to genuinely collaborative interactions between authors and review editors, who include some of the world's best academicians. Research must be certified by peers before entering a stream of knowledge that may eventually reach the public - and shape society; therefore, Frontiers only applies the most rigorous and unbiased reviews. Frontiers revolutionizes research publishing by freely delivering the most outstanding research, evaluated with no bias from both the academic and social point of view. By applying the most advanced information technologies, Frontiers is catapulting scholarly publishing into a new generation.

What are Frontiers Research Topics?

Frontiers Research Topics are very popular trademarks of the *Frontiers journals series*: they are collections of at least ten articles, all centered on a particular subject. With their unique mix of varied contributions from Original Research to Review Articles, Frontiers Research Topics unify the most influential researchers, the latest key findings and historical advances in a hot research area.

Find out more on how to host your own Frontiers Research Topic or contribute to one as an author by contacting the Frontiers editorial office: frontiersin.org/about/contact

The molecular landscape and promising therapeutic targets in aggressive B-cell non-Hodgkin lymphomas

Topic editors

Niklas Gebauer — University Medical Center Schleswig-Holstein, Germany
Hanno Maximilian Witte — Bundeswehrkrankenhaus, Germany
Axel Künstner — University of Lübeck, Germany
Francesco Piazza — University of Padua, Italy
Gaël Roué — Josep Carreras Leukaemia Research Institute (IJC), Spain

Topic Coordinator

Emil Chteinberg — Ulm University Medical Center, Germany

Citation

Gebauer, N., Witte, H. M., Künstner, A., Piazza, F., Roué, G., Chteinberg, E., eds. (2023). *The molecular landscape and promising therapeutic targets in aggressive B-cell non-Hodgkin lymphomas*. Lausanne: Frontiers Media SA. doi: 10.3389/978-2-8325-3474-8

Table of contents

frontiers | Frontiers in Oncology

TYPE Editorial
PUBLISHED 30 August 2023
DOI 10.3389/fonc.2023.1278169

OPEN ACCESS

EDITED AND REVIEWED BY
Adrián Mosquera Orgueira,
University Hospital of Santiago de Compostela, Spain

*CORRESPONDENCE
Hanno Maximilian Witte
hanno.witte@uni-ulm.de

RECEIVED 15 August 2023
ACCEPTED 21 August 2023
PUBLISHED 30 August 2023

CITATION
Witte HM, Künstner A, Chteinberg E, Piazza F, Roué G and Gebauer N (2023) Editorial: The molecular landscape and promising therapeutic targets in aggressive B-cell non-Hodgkin lymphomas. *Front. Oncol.* 13:1278169. doi: 10.3389/fonc.2023.1278169

Editorial: The molecular landscape and promising therapeutic targets in aggressive B-cell non-Hodgkin lymphomas

Hanno Maximilian Witte[1,2,3]*, Axel Künstner[3,4], Emil Chteinberg[5], Francesco Piazza[6], Gaël Roué[7] and Niklas Gebauer[2,3]

[1]Department of Hematology and Oncology, Bundeswehrkrankenhaus Ulm, Ulm, Germany, [2]Department of Hematology and Oncology, University Hospital of Schleswig-Holstein, Lübeck, Germany, [3]University Cancer Center Schleswig-Holstein, University Hospital of Schleswig-Holstein, Lübeck, Germany, [4]Medical Systems Biology Group, University of Lübeck, Lübeck, Germany, [5]Institute of Human Genetics Ulm University and Ulm University Medical Center, Ulm, Germany, [6]Department of Medicine, Hematology and Clinical Immunology Unit, University of Padova and Myeloma and Lymphoma Pathobiology Laboratory, Veneto Istituto of Molecular Medicine, Padova, Italy, [7]Lymphoma Translational Group, Josep Carreras Leukaemia Research Institute, Badalona, Spain

KEYWORDS

aggressive B-cell lymphoma, non-Hodgkin lymphoma, genomics, transcriptomics, multi-omics, precision oncology

Editorial on the Research Topic
The molecular landscape and promising therapeutic targets in aggressive B-cell non-Hodgkin lymphomas

Precision oncology attempts to translate the results of next-generation sequencing and array-based methods into molecularly stratified therapeutic concepts for cancer. To date, aggressive B-cell non-Hodgkin lymphomas (B-cell-NHL) have received only marginal access to molecularly stratified therapeutic approaches. In addition to the most common entity, diffuse-large B-cell lymphoma (DLBCL), the spectrum of aggressive B-cell-NHL includes 25 other distinct entities. Molecular analyses have been performed in varying degrees for most of these entities, revealing their therapeutic vulnerabilities. However, particularly with the advancements in novel molecular technologies (e.g., single-cell RNA-sequencing, spatial-transcriptomics), some of these entities remain insufficiently characterized. Novel technologies allow a subjacent understanding of molecular tumor-biology, making individual risk-stratification more precise and molecularly stratified therapy recommendations increasingly specific. In addition, new dimensions of tumor-biology, such as phylogenetic evolution, cell-cell interactions or epigenetic regulation of lymphomas can be considered for treatment decision-making in precision oncology.

This editorial presents the results of ten published articles in the *Frontiers in Oncology* Research-Topic "*The Molecular Landscape and Promising Therapeutic Targets in Aggressive B-cell Non-Hodgkin Lymphomas*".

The original research article by Zhang et al. highlights the prognostic implications of cuproptosis in DLBCL, a copper-induced form of programmed cell-death that is tightly interconnected with mitochondrial metabolism. Here, the authors characterized

cuproptosis-related genes (CRG) in DLBCL and identified two biologically and prognostically distinct subtypes. Moreover, the two CRG-clusters differed in terms of immune-cell infiltration and treatment response. The authors constructed a prognostic model incorporating CRG gene-expression and demonstrated the prognostic superiority of this model over the International-Prognostic-Index (IPI).

The success of rituximab in DLBCL treatment is undisputed. To date, the synergistic molecular mechanisms between the CD20-antibody and also those of the next generation (ofatumumab) with components of chemotherapy (CHOP-protocol) are poorly understood. In a preclinical cell-culture approach, Lee et al. addressed this question using transcriptome-sequencing. Based on transcriptional profiles, the authors discovered that CD20-antibodies modulate genes in the JNK and p38 MAPK-family, and thus apoptosis and proliferation of lymphoma-cells through different mechanisms. These findings contribute significantly to our understanding the molecular mechanism of action of CD20-antibodies in DLBCL.

CAR-T-cell therapy is an essential component of novel targeted options for the treatment of lymphoma. The article of the international workgroup of Albendea et al. highlights the existing problems of access and challenges of CAR-T-cell therapy within European healthcare-systems. Comparatively, country-specific measures and solutions are discussed in this manuscript to improve the CAR-T-cell provisioning structure and manufacturing.

In the original research article by Xu et al., panel-sequencing (121 genes) was performed on 259 DLBCL-patients. The molecular alterations were then placed in the context of genomic-clusters according to Wright et al. (1). Subsequently, the presence of dyslipidemia, a risk-factor for cardiovascular disease, was correlated with genomic clusters in DLBCL. Strikingly, DLBCL belonging to the EZB-cluster, in particular, was significantly more frequently associated with dyslipidemia. Pathophysiologically, DLBCL of the EZB-cluster is closely associated with the pathogenesis of follicular lymphoma. Consequently, the rate of dyslipidemia was significantly higher in DLBCL with *BCL2*-fusions (t(14;18)) which represents the genomic hallmark in FL. Ultimately, dyslipidemia had no prognostic impact on overall-survival (OS) in DLBCL.

NTRK is an increasingly common therapeutic target in molecular oncology. A separate ESMO-guideline has already been published on this topic. Despite single references indicating that *NTRK* is also detectable in aggressive B-cell-NHL, Ghandili et al. demonstrated on tissue-microarrays that *NTRK* does not represent a promising target for DLBCL-treatment.

At the recent ASH Annual-Meeting, the 5-year update of the REMoDL-B trial was presented, in which DLBCL-patients treated with R-CHOP were randomized to the addition of bortezomib and their benefits were analyzed based on gene expression profiles (whole-genome cDNA-mediated assay) (2, 3). In our Research Topic, Orguirea et al. presents the application of an artificial intelligence approach (LymForest-25 profile) to the data from the REMoDL-B trial, considering not only clinical but also transcriptomic characteristics. The result is a significant improvement in individual risk-stratification, leading to a 30% risk-reduction in half of the (molecularly) high-risk DLBCL-patients in the study.

A subgroup among DLBCL-patients, for whom the greatest challenge in treatment remains to strike an optimal balance between therapy intensity, life-expectancy, and adverse-event management, is represented by geriatric patients. In recent years, the evaluation of nutritional status has become increasingly important with regard to risk stratification of cancer patients. In a comprehensive review article (2,353 cases), Cao and Zhang summarize the available evidence on the Geriatric-Nutritional-Risk-Index (GNRI) and demonstrate that a low GNRI is associated with unfavorable prognosis and disease-progression in elderly and/or frail DLBCL-patients.

Our Research-Topic also included articles on other aggressive B-cell NHL entities. A meta-analysis by Zeremski et al. addressed the still existing question of the value of treatment-intensification in high-grade B-cell lymphomas with MYC and BCL2- and/or BCL6-rearrangements (HGBL-DH/TH). Despite the consideration of some limitations (e.g., retrospective study design, renewed WHO-classification), this meta-analysis provides evidence that chemotherapy-intensification benefits 2-year-PFS and -OS in HGBL-DH/TH.

Plasmablastic lymphoma (PBL) is one of the most aggressive entities in the spectrum of B-cell NHL. Almost no targeted options have been investigated for the treatment of this CD20-negative and rare neoplasm. After progression on first-line chemotherapy, few treatment options are available for these patients representing an urgent unmet clinical need. In a virtual molecular tumor board discussing whole exome and whole transcriptome data from 14 primary-refractory PBL cases, Witte et al. demonstrate that numerous targeted therapeutic vulnerabilities can be evaluated for this difficult-to-treat entity.

The Research-Topic is completed by the presentation of a novel primary renal lymphoma cell line and the corresponding gene expression signature. Li et al. give an outlook on the clinical relevance of this cell line and its application in animal experimental approaches.

The Research-Topic article-collection contains interesting contributions to improve individual risk-stratification, molecular diagnostics and therapeutic implications in aggressive B-cell NHL. On the one hand, the articles demonstrate profound insights into molecular lymphoma biology and on the other hand, they illustrate potential future directions in lymphoma research. The felicitous spectrum of experimental, translational and clinical topics also underlines the multimodality of precision oncology in the field of aggressive B-cell NHL.

Author contributions

HW: Conceptualization, Data curation, Formal Analysis, Funding acquisition, Investigation, Methodology, Project administration, Resources, Visualization, Writing – original draft, Writing – review & editing. AK: Methodology, Software, Validation, Visualization, Writing – review & editing. EC: Investigation,

Resources, Writing – review & editing. FP: Conceptualization, Project administration, Supervision, Writing – review & editing. GR: Conceptualization, Project administration, Supervision, Writing – review & editing. NG: Conceptualization, Data curation, Formal Analysis, Funding acquisition, Investigation, Methodology, Project administration, Resources, Supervision, Writing – review & editing.

Funding

HW received support from Soldatentumorhilfe and Stefan-Morsch-Stiftung. NG was supported by Stefan-Morsch-Stiftung, the Damp-Stiftung, the Wilhelm-Sander-Stiftung, the Jose Carreras Leukämie-Stiftung. GR was supported by the Spanish Ministry of Science and Innovation (PID2021-123039OB-C21) and the Catalan Agency for Management of University and Research Grants (2021SGR01535).

Conflict of interest

The authors declare that the research was conducted in the absence of any commercial or financial relationships that could be construed as a potential conflict of interest.

The authors declared that they were an editorial board member of Frontiers, at the time of submission. This had no impact on the peer review process and the final decision.

Publisher's note

References

1. Wright GW, Huang DW, Phelan JD, Coulibaly ZA, Roulland S, Young RM, et al. A probabilistic classification tool for genetic subtypes of diffuse large B cell lymphoma with therapeutic implications. *Cancer Cell* (2020) 37(4):551–568 e514. doi: 10.1016/j.ccell.2020.03.015

2. Davies A, Cummin TE, Barrans S, Maishman T, Mamot C, Novak U, et al. Gene-expression profiling of bortezomib added to standard chemoimmunotherapy for diffuse large B-cell lymphoma (REMoDL-B): an open-label, randomised, phase 3 trial. *Lancet Oncol* (2019) 20(5):649–62. doi: 10.1016/S1470-2045(18)30935-5

3. Davies AJ, Stanton L, Caddy J, Barrans S, Wilding S, Saunders GN, et al. Five-year survival results from the remodl-B trial (ISRCTN 51837425) show improved outcomes in diffuse large B-cell lymphoma molecular subgroups from the addition of bortezomib to R-CHOP chemoimmunotherapy. *Blood* (2022) 140(Supplement 1):1770–2. doi: 10.1182/blood-2022-159976

frontiers | Frontiers in Oncology

TYPE Original Research
PUBLISHED 12 January 2023
DOI 10.3389/fonc.2022.1020566

OPEN ACCESS

EDITED BY
Francesco Piazza,
University of Padua, Italy

REVIEWED BY
Qian Xu,
Nanyang Normal University, China
Xiuli Wu,
Jinan University, China

*CORRESPONDENCE
Yongyong Ma
mayy@wmu.edu.cn

SPECIALTY SECTION
This article was submitted to Hematologic Malignancies, a section of the journal Frontiers in Oncology

RECEIVED 26 August 2022
ACCEPTED 22 December 2022
PUBLISHED 12 January 2023

CITATION
Zhang B, Zhang T, Zheng Z, Lin Z, Wang Q, Zheng D, Chen Z and Ma Y (2023) Development and validation of a cuproptosis-associated prognostic model for diffuse large B-cell lymphoma.
Front. Oncol. 12:1020566.
doi: 10.3389/fonc.2022.1020566

Development and validation of a cuproptosis-associated prognostic model for diffuse large B-cell lymphoma

Bingxin Zhang[1], Tianyu Zhang[1], Ziwei Zheng[1], Zhili Lin[1], Quanqiang Wang[1], Dong Zheng[1], Zixing Chen[2] and Yongyong Ma[1]*

[1]Department of Hematology, The First Affiliated Hospital of Wenzhou Medical University, Wenzhou, Zhejiang, China, [2]Department of Hepatobiliary Surgery, The Second Affiliated Hospital and Yuying Children's Hospital of Wenzhou Medical University, Wenzhou, Zhejiang, China

Diffuse large B-cell lymphoma (DLBCL) is a highly heterogeneous disease. Therefore, more reliable biomarkers are required to better predict the prognosis of DLBCL. Cuproptosis is a novel identified form of programmed cell death (PCD) that is different from oxidative stress-related cell death (e.g., apoptosis, ferroptosis, and necroptosis) by Tsvetkov and colleagues in a recent study released in Science. Cuproptosis is copper-dependent PCD that is closely tied to mitochondrial metabolism. However, the prognostic value of cuproptosis-related genes (CRGs) in DLBCL remains to be further elucidated. In the present study, we systematically evaluated the molecular changes of CRGs in DLBCL and found them to be associated with prognosis. Subsequently, based on the expression profiles of CRGs, we characterized the heterogeneity of DLBCL by identifying two distinct subtypes using consensus clustering. Two isoforms exhibited different survival, biological functions, chemotherapeutic drug sensitivity, and immune microenvironment. After identifying differentially expressed genes (DEGs) between CRG clusters, we built a prognostic model with the Least absolute shrinkage and selection operator (LASSO) Cox regression analysis and validated its prognostic value by Cox regression analysis, Kaplan-Meier curves, and receiver operating characteristic (ROC) curves. In addition, the risk score can predict clinical characteristics, levels of immune cell infiltration, and prognosis. Furthermore, a nomogram incorporating clinical features and risk score was generated to optimize risk stratification and quantify risk assessment. Compared to the International Prognostic Index (IPI), the nomogram has demonstrated more accuracy in survival prediction. Furthermore, we validated the prognostic gene expression levels through external experiments. In conclusion, cuproptosis-related gene signature can serve as a potential prognostic predictor in DLBCL patients and may provide new insights into cancer therapeutic targets.

KEYWORDS

diffuse large B-cell lymphoma, cuproptosis, subtypes, prognostic gene signature, overall survival, tumor microenvironment

1 Introduction

Diffuse large B-cell lymphoma (DLBCL) is the most common non-Hodgkin's lymphoma (NHL) in adults and represents a highly heterogeneous group of tumors in terms of morphology, phenotype, molecular features, clinical course, and response to therapy (1, 2). Based on gene expression profile, DLBCL can be classified from the cell of origin (COO) into at least two subtypes, germinal center B-cell-like (GCB) and activated B-cell-like (ABC), while 10-20% of cases remain unclassified (3). R-CHOP (rituximab, cyclophosphamide, doxorubicin, vincristine, and prednisone) is currently the first-line treatment for patients with DLBCL and contributes to a significant improvement in prognosis (4, 5). However, many patients of DLBCL do not respond to treatment and usually have a poor prognosis, especially in patients with the ABC subtype (6, 7). Tumor heterogeneity and the inevitable acquisition of drug resistance make DLBCL still incurable. Therefore, there is an urgent need to identify novel and reliable biomarkers that can aid in clinical risk stratification and the guidance of precision therapy.

Copper is an enzyme cofactor involved in a variety of biological functions in humans and other mammals, including cellular respiration, regulation of energy production and other redox reactions, neurotransmitter biosynthesis, and connective tissue formation (8). Moreover, copper is a key regulator of cellular signal transduction pathways, regulating or triggering multiple biological pathways in response to external stimuli (9). Therefore, the maintenance of copper homeostasis plays a crucial role in the biological activities of the organism. Many associations have been observed between cancer and copper. Several studies have reported elevated copper levels in serum and tumor tissue of patients with various malignancies, including lymphomas, compared to normal tissue (10–16). Copper accumulation has been associated with the promotion of proliferation and growth, angiogenesis, metastasis, and drug resistance (17–22). In lymphoma, serum copper level is an independent prognostic factor, closely related to tumor activity (23–25). Copper compounds are considered to be effective inducers of apoptosis in lymphoma cells (26–28). In addition, targeting mitochondria with the copper chelator drug ATN-224 may serve as an important therapeutic strategy for apoptosis-resistant DLBCL (29). A completely new form of cell death has recently been proposed that differs from all other known programmed cell death mechanisms, including apoptosis, ferroptosis, pyroptosis, and necroptosis (30). Characterized by protein lipoylation in the tricarboxylic acid (TCA) cycle, it causes acute proteotoxic stress through lipid-acylated protein aggregation and subsequent loss of iron-sulfur cluster protein, ultimately leading to cell death. Additionally, they identified seven genes (*FDX1*, *LIAS*, *LIPT1*, *DLD*, *DLAT*, *PDHA1*, and *PDHB*) that sensitized the cells to cuproptosis by genome-wide CRISPR-Cas9 loss-of-function screen, while three genes (*MTF1*, *GLS*, and *CDKN2A*) with resistance to cuproptosis. Copper importer *(SLC31A1)* and copper exporter (*ATP7B*) have also been found to promote and inhibit cuproptosis, respectively, by regulating intracellular copper concentrations (30). As we know, cuproptosis mainly targets mitochondrial respiration and the TCA cycle. In another study, the consistent cluster classification scheme identified three isoforms of DLBCL by molecular analysis, the BCR/proliferative cluster (BCR-DLBCL), OxPhos cluster (OxPhos-DLBCL), and host response cluster. Among them, the OxPhos-DLBCL was significantly enriched in genes regulating oxidative phosphorylation (OxPhos), mitochondrial membrane potential, and electron transport chain (31). A subsequent study unearthed that the OxPhos-DLBCL was insensitive to conventional drugs targeting the BCR signaling axis. With enhanced mitochondrial energy transduction, the OxPhos cluster exhibited an increased admixture of nutrient carbon in the TCA cycle (32). Furthermore, another study used immunohistochemical markers of glycolysis and mitochondrial OxPhos metabolism to explore the metabolic phenotype of human DLBCL tumors. Compared to non-tumor lymphoid tissue, the OxPhos phenotype was highly expressed in tumor lymphocytes in DLBCL samples, while stromal cells strongly expressed the glycolytic phenotype. They hypothesized that tumor cells meet their own TCA cycle substrate requirements by mediating stromal cell metabolic reorganization (33). Not surprisingly, the oxidative phosphorylation inhibitor Gboxin analog was found to have a strong proliferation inhibitory and cell cycle blocking effect on DLBCL with specific selectivity for it (34). Several recent studies have revealed the potential role of CRGs in the prognosis of cancers, such as kidney cancer (35–42), hepatocellular carcinoma (43–47), lung cancer (48–53), head and neck squamous cell carcinoma (53–60), glioma (61–66), breast cancer (67–70), endometrial carcinoma (71, 72), melanoma (73–75), pancreatic cancer (76, 77), colorectal cancer (78–81) and so on. However, no reports describe any effects of the cuproptosis regulatory mechanism on DLBCL.

Abbreviations: DLBCL, diffuse large B-cell lymphoma; PCD, programmed cell death; CRGs, cuproptosis-related genes; OS, overall survival; DEGs, differentially expressed genes; LASSO, least absolute shrinkage and selection operator; ROC, receiver operating characteristic; IPI, International Prognostic Index; NHL, non-Hodgkin's lymphoma; GCB, germinal center B-cell-like; ABC, activated B-cell-like; TCA, tricarboxylic acid; GEO, Gene Expression Omnibus; TCGA, The Cancer Genome Atlas; FFPE, formalin-fixed paraffin-embedded; GDC, Genomic Data Commons; SNV, single nucleotide variant; CNV, copy number variation; GSCA, Gene Set Cancer Analysis; PCA, principal component analysis; ssGSEA, single-sample gene set enrichment analysis; GSVA, gene set variation analysis; KEGG, Kyoto Encyclopedia of Genes and Genomes; GSEA, Gene Set Enrichment Analysis; CCLE, Cancer Cell Line Encyclopedia; time-ROC curve, time-dependent receiver operating characteristic curve; AUC, area under the curve; GO, Gene Ontology; FP, forward primer; RP, reverse primer; qRT-PCR, quantitative real-time PCR; TME, tumor microenvironment; DSS, disease-specific survival; STRING, Search Tool for the Retrieval of Interacting Genes; Tregs, regulatory T cells; ECOG, Eastern Cooperative Oncology Group; LDH, lactate dehydrogenase; ES, extranodal sites; COO, cell of origin; BCR, B-cell receptor; OxPhos, oxidative phosphorylation.

This study divided 400 DLBCL samples into two subtypes based on the 12 cuproptosis-related genes (CRGs) mentioned above. The differences in survival, drug sensitivity, and immune cell infiltration between subtypes were also integrated. Subsequently, we constructed a prognostic model to stratify patients at risk. Furthermore, we developed a nomogram integrating clinical features and risk scores to quantify risk assessment and predict the overall survival (OS) of DLBCL patients. The results showed that the nomogram was an effective prognostic indicator. Finally, we performed an experimental verification on our clinical samples.

2 Materials and methods

2.1 Data acquisition

Gene expression and the relevant prognostic and clinicopathological data of DLBCL were downloaded from the public database Gene Expression Omnibus (GEO) (https://www.ncbi.nlm.nih.gov/geo/) and The Cancer Genome Atlas (TCGA) (https://portal.gdc.cancer.gov/). Microarray expression profiles of DLBCL patients were obtained from GSE10846, GSE31312, and GSE87371 datasets using Affymetrix Human Genome U133 Plus 2.0 platform. Transcriptional data for 48 DLBCL samples from TCGA were retrieved from UCSC Xena (https://xenabrowser.net/datapages/). All the microarray data included were normalized and log2 transformed. Probe IDs were mapped to gene symbols according to the corresponding annotation files, expression measurements for all probes associated with the same gene were averaged and the maximum value was finally taken. The pathology image data (formalin-fixed paraffin-embedded (FFPE) slide) were downloaded from the Genomic Data Commons (GDC; https://portal.gdc.cancer.gov/). After excluding samples with missing survival information or survival time of less than one month, the GSE10846, GSE31312, and GSE87371 included 400, 466, and 216 tumor specimens of DLBCL respectively. GSE10846 was used as the training dataset for constructing the subtype and prognostic model, while GSE31312 and TCGA-DLBCL were the validation sets for subtype identification and GSE87371 was the validation for the prognostic model. 12 CRGs (*FDX1*, *LIAS*, *LIPT1*, *DLD*, *DLAT*, *PDHA1*, *PDHB*, *MTF1*, *GLS*, *CDKN2A*, *SLC31A1*, and *ATP7B*) were obtained from the article by Tsvetkov et al. (30).

2.2 Clinical samples

The FFPE lymphoma tissue samples were collected from 7 patients with incipient untreated DLBCL in the First Affiliated Hospital of Wenzhou Medical University, and normal lymphoid tissues in the control group were taken from a healthy volunteer. The histological diagnosis was established according to the World Health Organization (WHO) classification (82). The study was approved by the Review Board of the First Affiliated Hospital of Wenzhou Medical University with informed consent obtained from all subjects in accordance with the Declaration of Helsinki. The clinical data of the patients are listed in Supplementary Table 1.

2.3 Gene interaction network and the effects of genetic alterations

The correlation network of 12 CRGs was derived from the "corrr" R package. To determine the somatic mutations of 12 CRGs, the single nucleotide variant (SNV) data of these 12 CRGs in all cancers, as well as the copy number variation (CNV) data in DLBCL, were mined in Gene Set Cancer Analysis (GSCA) (http://bioinfo.life.hust.edu.cn/GSCA/) (83). We also used GSCA to analyze the relationships between survival and gene expression, CNV, gene methylation, and the relationship between expression and pathway activity in DLBCL.

2.4 Consensus clustering analysis of CRGs

Consistent unsupervised clustering analysis was performed using the R package "ConsensusClusterPlus" (84) to classify patients based on CRG expression. Consensus clustering is based on resampling to verify the rationality of clustering, whose main purpose is to assess the stability of the clustering. The maximum number of classifications (maxK) was set to 6. The K-Means clustering algorithm was chosen and euclidean calculated the distances. 80% of the samples were resampled 1000 times by this procedure to ensure the stability and reproducibility of the classification. The optimal number of clusters k was determined by combining the graphs of each clustering result and the proportion of ambiguous clustering (PAC) method (85). GSE31312 and TCGA-DLBCL were also used for unsupervised clustering analysis to verify the accuracy of clustering. Principal component analysis (PCA) was generated by "scatterplot3d" packages to further determine the validity of the clustering. Furthermore, the differences in survival among different subtypes were assessed using Kaplan-Meier curves derived from the "survival" and "survminer" R packages. Heatmap created by the "pheatmap" software package displayed the clinical characteristics and survival differences of the different clusters.

2.5 Evaluation of tumor microenvironment and biological function in the cuproptosis subtypes

The infiltration fractions of 22 human immune cell subsets of every DLBCL sample were calculated by the CIBERSORT

algorithm (86). Furthermore, we also used the single-sample gene set enrichment analysis (ssGSEA) algorithm (87) to validate the difference in immune cell infiltration between the subtypes in TCGA-DLBCL. Additionally, through TCGA Pathology Slides, we were able to confirm the above analysis. To investigate the differences of CRGs subtypes in biological processes, gene set variation analysis (GSVA) was performed with the Kyoto Encyclopedia of Genes and Genomes (KEGG) gene set (c2. cp. kegg. v7.2) obtained from Gene Set Enrichment Analysis (GSEA) database (http://www.gsea-msigdb.org/gsea/msigdb). Furthermore, we used the R software package "pRRophetic" (88) to evaluate the chemotherapeutic sensitivity between different subgroups.

2.6 Construction and validation of the prognostic signature based on the DEGs between the CRG clusters

Identification of DEGs between different subtypes using the R package "limma" (|logFC|>2, adjusted P <0.01) (89). Then prognosis-related DEGs were obtained by Cox regression analysis (P<0.001). Based on prognostic DEGs associated with cuproptosis, the Least absolute shrinkage and selection operator (LASSO) Cox regression analysis was used to minimize the risk of overfitting with the "glmnet" R package (90, 91). After 1000-fold cross-validation of the maximum likelihood estimate of penalty, a cuproptosis-related prognostic model was finally constructed. According to the median risk score, patients in the training and validation datasets were divided into low-risk and high-risk groups respectively, then subjected to Kaplan-Meier survival analysis. The prognostic value of the model was confirmed by univariate and multivariate Cox regression. Further validation of the model was performed with the gene expression data in lymphoma from the Cancer Cell Line Encyclopedia database (CCLE, https://portals.broadinstitute.org/ccle). Time-dependent receiver operating characteristic curve (time-ROC curve) analysis was conducted using the "timeROC" R package (92) to obtain the area under the curve (AUC) value and evaluate the predictive power of the signature. The "ggrisk" package integrated the ranking dot map, scatter map, and heatmap to show the difference in survival and gene expression between high- and low-risk groups.

2.7 Comprehensive analysis of CRGs-related prognostic model

The co-expression matrix of CRGs and genes in the prognostic model was established using the "ggcorrplot" package in R. For the DEGs between risk groups identified by the "limma" package, we conducted Gene Ontology (GO) enrichment analysis using the "clusterProfiler" package (93, 94). Spearman correlation analysis was used to test the correlation between tumor microenvironment (TME) and risk score.

2.8 Construction and evaluation of a combined nomogram

A predictive nomogram integrating the clinical characteristics and risk score was developed using the "rms" package according to the outcome of the independent prognosis analysis. Calibration plots of the nomogram were used to measure the consistency of predicted survival events and actual observed results at 1-, 2- and 3 years. Time-ROC curves for 1-, 2- and 3-year survival were performed for the assessment of accuracy in DLBCL prognosis.

2.9 RNA extraction and reverse transcription

RNA was extracted from the FFPE samples using the Paraffin-Embedded Tissue RNA Extraction Kit (AIDISHENG, Yancheng, China) according to the manufacturer's instructions. Reverse transcription was performed with the cDNA synthesis kit (Vazyme, Nanjing, China) to generate cDNAs.

2.10 Quantitative real-time PCR

Taq Pro Universal SYBR qPCR Master Mix (Vazyme, Nanjing, China) was then used for quantitative PCR. β-ACTIN was used as an internal control, and each sample was repeated in triplicate. The relative fold-change in expression with respect to a control group was calculated by the 2-ΔΔCt method. The PCR cycle conditions were 95 °C for 30 s, followed by 40 cycles of 95 °C (10 s) and 60 °C (30 s). Three biological replicates were performed. The PCR primers used were as follows:

TUBB4A forward primer (FP): 5′-GAGTTCCCAGACC GCATCA-3′;

TUBB4A reverse primer (RP): 5′-CGGAAACAGATGTC GTAGAGTG-3′;

SLC38A5 FP: 5′-AACAGCAATGGAGAGTGAAGC-3′;

SLC38A5 RP: 5′-ACCTCAGGGTGGCAGACAA-3′;

TEX9 FP: 5′-TTTATGAGACAGCAGCGAACA-3′;

TEX9 RP: 5′-GAACCTCTGTGGCACTTTGAC-3′;

S100B FP: 5′-GGAAGGGAGGGAGACAAGCA-3′;

S100B RP: 5′-CTGGAAGTCACATTCGCCGT-3′;

ACTIN FP: 5′-TCAAGATCATTGCTCCTCCTGAG-3′;

ACTIN RP: 5′-ACATCTGCTGGAAGGTGGACA-3′;

2.11 Statistical analyses

All statistical analyses were performed with R version 4.1.1, GraphPad Prism 9.0.0, and SPSS software version 26.0. Student's t-test or one-way analysis of variance was used to analyze differences between groups in variables with a normal distribution. Wilcoxon test was used to analyze the differences between groups of skewed distribution variables. And we used the Kaplan-Meier method for survival analysis and the log-rank test to analyze the differences in overall survival. $P < 0.05$ was considered statistically significant.

3 Results

3.1 Genetic alterations and interactions of CRGs in DLBCL

The detailed clinical characteristics of patients from the three GEO datasets are summarized in Table 1. The interaction of these 12 genes was shown in Figure 1A. Among the 12 CRGs, 10 of them were mutated in 98.23% (941/958) of tumor samples in pan-cancer analysis with the TCGA database (Figure 1B). The missense mutation was the most common mutation variant. *CDKN2A* was the most frequent mutated CRG (42%), followed by *ATP7B*, *MTF1*, *GLS*, and *DLD* (22%, 13%, 9% and 9% respectively). Next, we investigated somatic copy number changes in these CRGs of DLBCL and found widespread copy number alterations in all 12 CRGs (Figure 1C). Among them, the copy number variations (CNVs) of *FDX1*, *DLAT*, *DLD*, *SLC31A1*, *PDHB*, *GLS*, and *ATP7B* were mainly amplifications, while the CNVs of *CDKN2A*, *MTF1*, *PDHA1*, *LIAS*, and *LIPT1* were mainly deletions (Figure 1C). Furthermore, we explored the relationships between CNV, gene expression, gene methylation, and survival in the TCGA DLBCL dataset. The difference in survival between CNV and wide type was shown in Supplementary Figure 1A. The CNVs of *MTF1*, *GLS*, *LIPT1*, and *LIAS* were closely related to the survival of DLBCL patients ($P<0.05$). Meanwhile, the results showed that the expression of *ATP7B*, *GLS*, *MTF1*, and *LIPT1* were negatively correlated with the overall survival (OS) of DLBCL ($P<0.05$), and the first three genes were previously identified as negative regulators of cuproptosis (30). In addition to these 4 genes, the other 8 CRGs were positively correlated with OS ($P<0.05$) (Supplementary Figure 1B). We then explored the correlation between the expression of 12 genes and pathway activity. *SLC31A1* may have a potential activating effect on apoptosis (FDR=0.0114) and a possible inhibiting effect on DNA damage (FDR=0.0105) response (Figure 1D). *CDKN2A* may potentially inhibit the TSC/mTOR pathway (FDR=0.0260) (Figure 1D). As for methylation, hypermethylation of *SLC31A1*, *DLAT*, *DLD*, *ATP7B*, *GLS*, and *FDX1* was associated with shorter disease-specific survival (DSS) ($P<0.05$) (Supplementary Figure 1C). In addition, we explored the relationship between the proteins encoded by CRGs based on the Search Tool for the Retrieval of Interacting Genes (STRING) network (95) (Figure 1E).

3.2 Identification and assessment of the CRG subtypes

To further understand the expression characteristics of CRGs in DLBCL, we used a consistent clustering algorithm to classify patients with DLBCL according to the expression profiles of 12 CRGs (Figure 2A). Our results indicated that k=2 appeared to be the best choice for dividing the entire cohort into A subtype (n=194) and B subtype (n=206) (Figure 2A). PCA revealed significant differences in the cuproptosis transcription profiles between the two subtypes (Figure 2B). Additionally, we used GSE31312 and TCGA-DLBCL to verify the repeatability of the clustering. Unsupervised clustering of this cohort also clearly identified 2 distinct subtypes (Supplementary Figure 2). The Kaplan-Meier curve showed that patients with subtype A had worse survival compared to those with subtype B ($P<0.001$; HR=1.881 [1.328, 2.664], $P<0.001$) (Figure 2C). Heatmap revealed differences in CRGs expression between subtypes as well as clinical features (Figure 2D). *GLS*, *MTF1*, and *ATP7B* were highly expressed in subtype A and were previously found to inhibit cuproptosis (30). In contrast, *PDHB*, *FDX1*, *DLD*, *DLAT*, *LIPT1*, *LIAS*, and *SLC31A1* were highly expressed in subtype B.

3.3 Characteristics of TME cell infiltration and biological function in the cuproptosis subtypes

To investigate TME differences in CRGs-related subtypes, the enrichment fraction of 22 kinds of immune cells in both two clusters was evaluated using the CIBERSORT algorithm (86). Significant differences in the infiltration of most immune cells between the two subtypes were observed (Figure 3A). The infiltration levels of naive B cells, memory B cells, resting $CD4^+$ memory T cells, regulatory T cells (Tregs), follicular helper T cells, and activated natural killer (NK) cells were higher in subtype A, while $CD8^+$ T cells, activated $CD4^+$ memory T cells, gamma delta T cells, M1 macrophages, plasma cells had significantly lower infiltration in subtype A compared to those in subtype B. In addition, we also carried out the ssGSEA algorithm in TCGA-DLBCL to further validate the differences in TME cell infiltration between the cuproptosis subtypes (Figure 4A). In conclusion, a higher level of immune infiltration was observed in subtype B. TCGA Pathology Slides further confirmed the difference (Figure 4B) (P-value < 0.05 was considered statistically significant).

10.3389/fonc.2022.1020566

TABLE 1 The clinical characteristics of the training and validation cohorts.

Characteristics	Training cohort	Validation cohort	Validation cohort
	GSE10846	GSE31312	GSE87371
	n=400	*n*=466	*n*=216
Gender			
Female	167(41.75%)	196(42.06%)	101(46.76%)
Male	216(54.00%)	270(57.94%)	115(53.24%)
Unknown	17(4.25%)	–	–
Age			
≤60 years	185(46.25%)	200(42.92%)	113(52.31%)
>60 years	215(53.75%)	266(57.08%)	103(47.69%)
Stage			
I- II	186(46.50%)	–	71(32.87%)
III-IV	208(52.00%)	–	145(67.13%)
Unknown	6(1.50%)	–	–
COO			
GCB	181(45.25%)	–	82(37.96%)
Non-GCB	219(54.75%)	–	134(62.04%)
ECOG PS			
0-1	291(72.75%)	372(79.83%)	–
2-4	86(21.50%)	94(20.17%)	–
Unknown	23(5.75%)	–	–
LDH			
Normal	167(41.75%)	148(31.76%)	–
>ULN	175(43.75%)	275(59.01%)	–
Unknown	58(14.50%)	43(9.23%)	–
ES			
<2	342(85.50%)	364(78.11%)	–
≥2	29(7.25%)	102(21.89%)	–
Unknown	29(7.25%)	–	–
Survival status			
OS years (median)	2.45	2.95	3.06
Censored(%)	151(37.75)	167(35.84)	45(20.83)

COO, cell of origin; GCB, germinal center B-cell-like subtype; ECOG PS, The Eastern Cooperative Oncology Group performance score; LDH, lactate dehydrogenase; ULN, the upper limit of normal; ES, extranodal sites; OS, overall survival.

To better understand the survival differences between the two subtypes, GSVA enrichment analysis of the KEGG pathway was conducted on these two clusters to assess the functional and biological differences. The results showed that the subtype A was mainly enriched in cell signal transduction pathways and immune-related pathways, such as the Notch signaling pathway, MAPK signaling pathway, VEGF signaling pathway, ERBB signaling pathway, primary immunodeficiency, and Fc

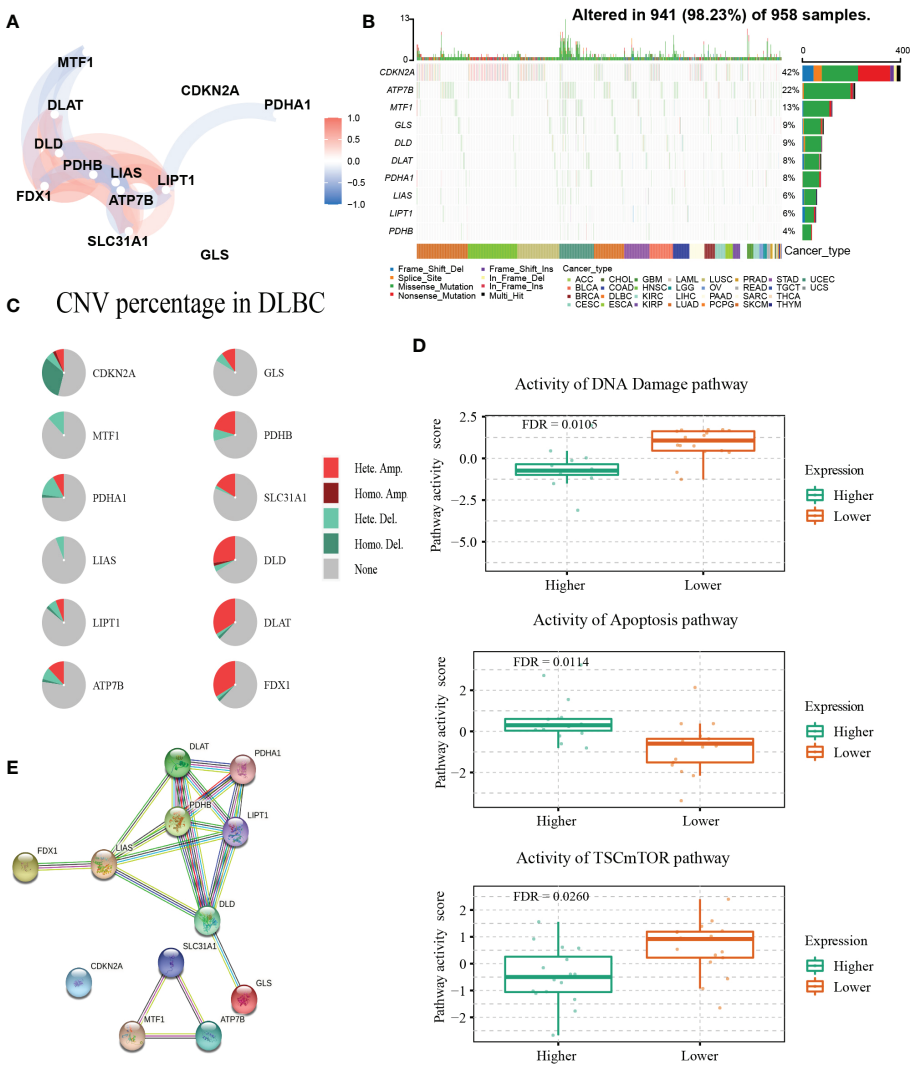

FIGURE 1
Genetic alterations and interactions of CRGs in DLBCL. **(A)** The correlation network of 12 CRGs. The correlation coefficients are represented by different colors. **(B)** The tumor mutation burden frequency of CRGs in pan-cancer analysis. **(C)** The CNV percentage of 12 CRGs in DLBCL. **(D)** The associations between expression of *SLC31A1* and activity of DNA damage and apoptosis pathway and the relationship between *CDKN2A* expression and mTOR pathway activity in DLBCL. **(E)** The PPI network encoded by CRGs in DLBCL. CNV, copy number variation; PPI, protein-protein interaction.

epsilon RI signaling pathway. B subtype was mainly enriched in the p53 signaling pathway and metabolism-related pathways, including the metabolism of sugar, protein, fat, and nucleotide (Figure 3B).

We then evaluated the therapeutic responsiveness of chemotherapeutic agents between the two subgroups, subtype A exhibited a resistance tendency to bleomycin, cisplatin, doxorubicin, etoposide, vincristine, vinorelbine and elesclomol, a kind of copper ionophore, while B was more resistant to paclitaxel and methotrexate (Figure 3C; Supplementary Figure 3) (*P*-value < 0.05 was considered statistically significant).

3.4 Construction and validation of the prognostic signature based on the DEGs between the CRG clusters

To explore the potential biological functions of the cuproptosis subgroups in DLBCL, we identified the DEGs between the two clusters with the "limma" R package, and 180 genes were obtained (|logFC|>2, adjusted P <0.01). Univariable Cox regression analysis was then performed to acquire 66 DEGs associated with prognosis (p< 0.001). Finally, the candidate genes were incorporated into the construction of the

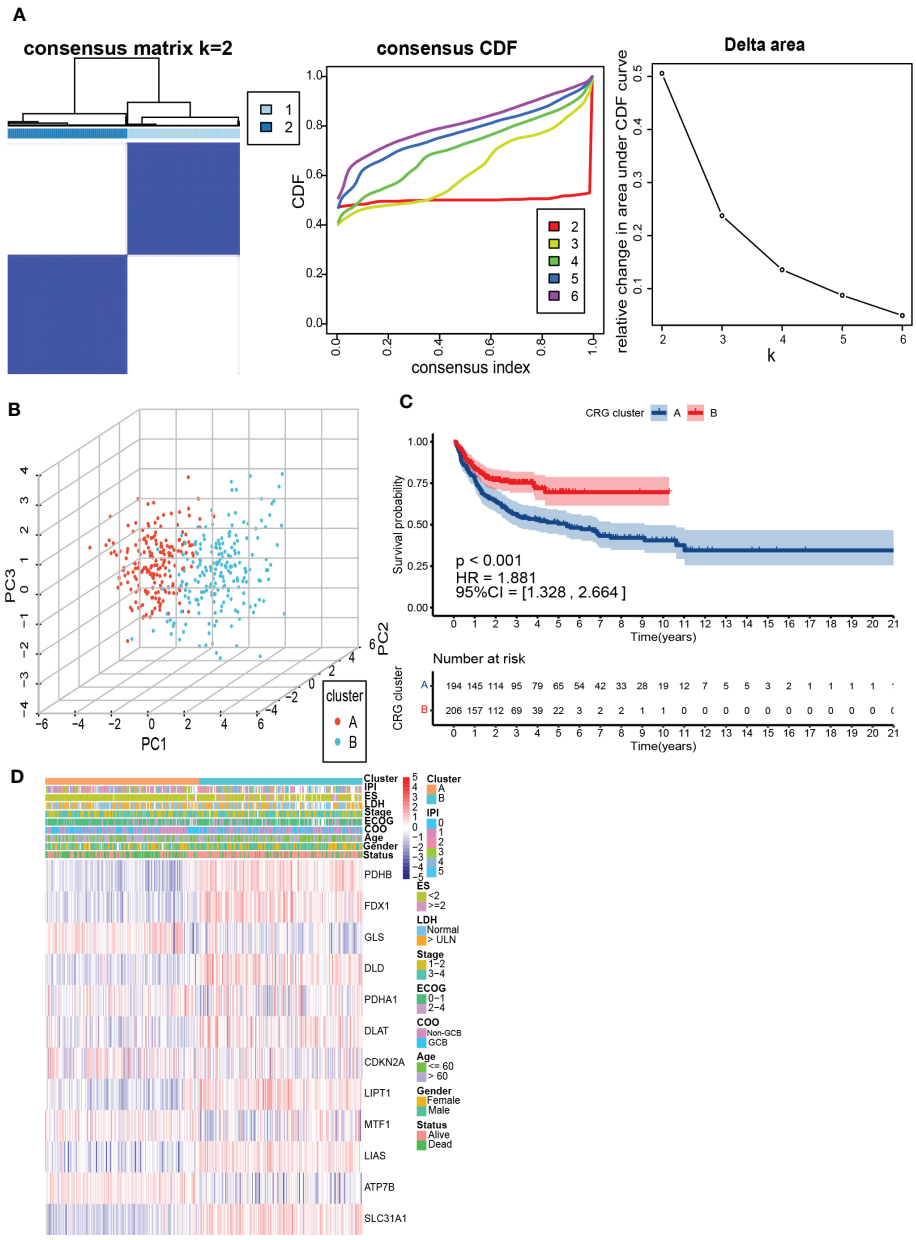

FIGURE 2
Identification and assessment of the CRG subtypes. **(A)** The consensus matrix, consensus cumulative distribution function (CDF), and delta area by cluster analysis based on CRGs. Two clusters (k=2) would be best. **(B)** Principal component analysis of two CRG clusters. **(C)** Kaplan-Meier survival curves of two CRG clusters ($p < 0.001$). **(D)** Heatmap of clinical features and CRGs expressions between subtypes. LDH, lactate dehydrogenases; ES, extranodal sites; ECOG, The Eastern Cooperative Oncology Group performance score; COO, cell of origin; IPI, International Prognostic Index.

prognostic model using LASSO Cox regression analysis, and a signature of 5 genes (*S100B*, *TUBB4A*, *SLC38A5*, *LOC100507477*, and *TEX9*) was discovered. The optimal weighting coefficient for each gene was determined by the regularization parameter lambda using the min standard (Figure 5A).

The risk model was constructed as follows: risk score = (0.1239 × expression of *SLC38A5*) + (0.0194 × expression of *TUBB4A*) + (0.0458 × expression of *LOC100507477)* – (0.0192 × expression of *S100B)* – (0.0541× expression of *TEX9*). According to the median risk score of the corresponding datasets, the patients with DLBCL were divided into high-scoring and low-scoring groups respectively in training and validation datasets.

Multivariate Cox regression analysis showed that the risk score was an independent prognostic factor for DLBCL (Figure 5B). Next, we performed the external validation on the expression of these four genes in lymphoma using the online

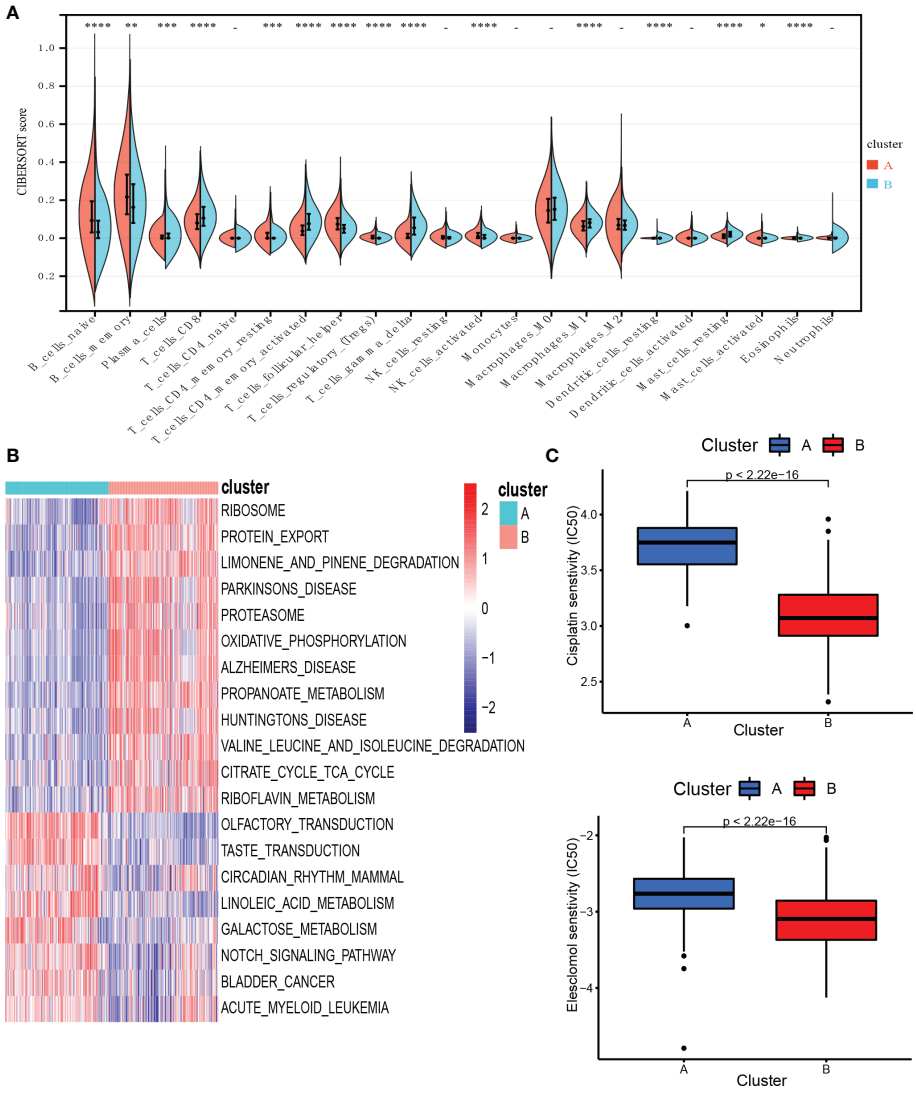

FIGURE 3
Characteristics of TME and biological function in the cuproptosis subtypes. **(A)** The abundance of different infiltrating immune cells in the two clusters. **(B)** GSVA of biological pathways between two distinct subtypes. **(C)** Prediction of drug responsiveness in the subtypes. * $P < 0.05$, ** $P < 0.01$, *** $P < 0.001$, **** $P < 0.0001$, - P > 0.05. TME, tumor microenvironment; IC50, half maximal inhibitory concentration.

database CCLE (no data was available for *LOC100507477*), and the expression levels of *S100B* and *TEX9* were relatively low, consistent with the above formula (Figure 5C). The Kaplan-Meier survival curve showed a significant difference between the groups. The high-risk group had a poor prognosis in the GSE10846 (P<0.0001; HR=2.280 [1.593, 3.263], P<0.001) (Figure 5D). In the GSE87371, the ability of the model to predict patient prognosis was further verified (P=0.040; HR=1.829 [1.019, 3.282], P=0.043) (Supplementary Figure 4A). Additionally, the 1-year, 2-year, and 3-year survival predicted by the risk score exhibited AUC values of 0.625, 0.637, and 0.636, respectively (Figure 5E). AUCs for the validation dataset were shown in Supplementary Figure 4B. The ranked dot demonstrated that the prognostic model can well distinguish high-risk groups from others. The scatter plot further revealed the worse survival outcome in the high-scoring group compared to the low-scoring group (Figure 5F). The same was true in the validation queue (Supplementary Figure 4C).

3.5 Comprehensive analysis of cuproptosis-related prognostic model

To further analyze the differences between high- and low-risk groups, we investigated the relationship between different clinical characteristics and risk scores. The risk scores were higher in those LDH above normal levels and non-GCB subgroups (P<0.05) (Supplementary Figure 5A). And these factors were also

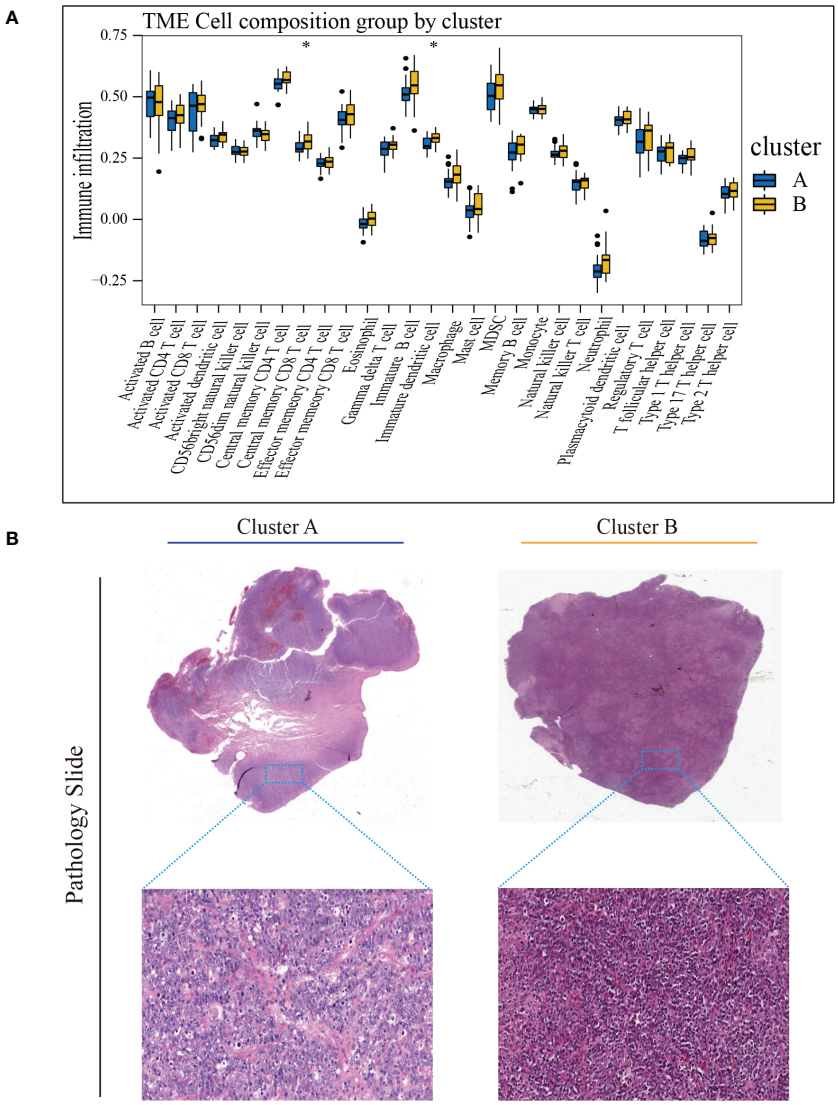

FIGURE 4
Characteristics of TME in the cuproptosis subtypes of TCGA-DLBCL. **(A)** The abundance of different infiltrating immune cells in the two clusters. **(B)** Representative images of pathological H&E staining of two cuproptosis subtypes. * $P < 0.05$; ns, not significant. TME, tumor microenvironment.

identified as risk factors for poor prognosis of DLBCL in previous studies (96). A high score was also closely associated with subtype A ($P<0.05$), consistent with the previous results of poor prognosis for subtype A (Supplementary Figure 5A).

Then we constructed the co-expression matrix of CRGs and genes in the prognostic model to further explore the association between cuproptosis and the model. The results revealed widespread correlations in these genes (Figure 6A). For instance, *LIPT1* and *PDHB* ($r=0.64$, $P<0.05$) were positively correlated, while *LIPT1* was negatively correlated with *TUBB4A* ($r=-0.58$, $P<0.05$). Alluvial diagram is plotted for a better display of clinical characteristics and survival differences between CRG clusters and risk groups (Figure 6B).

To better understand the difference in survival in the prognostic signature, the analysis of the molecular alterations in five genes of the prognostic model was performed. The summary report showed that four of them were mutated at a high frequency in tumor specimens (Figure 6C). Mutations were present in all 228 samples (100%) (Figure 6C). Among them, *TUBB4A* had the highest mutation frequency (45%), followed by *SLC38A5* (29%). The proportion of the CNV for each gene was summarized in Supplementary Figure 5B.

To further explore the biological differences between different risk groups, we investigated the DEGs between the two groups, which generated 2624 genes (|logFC|>1, adjusted P <0.01) (Figure 6D). GO enrichment analysis indicated that the

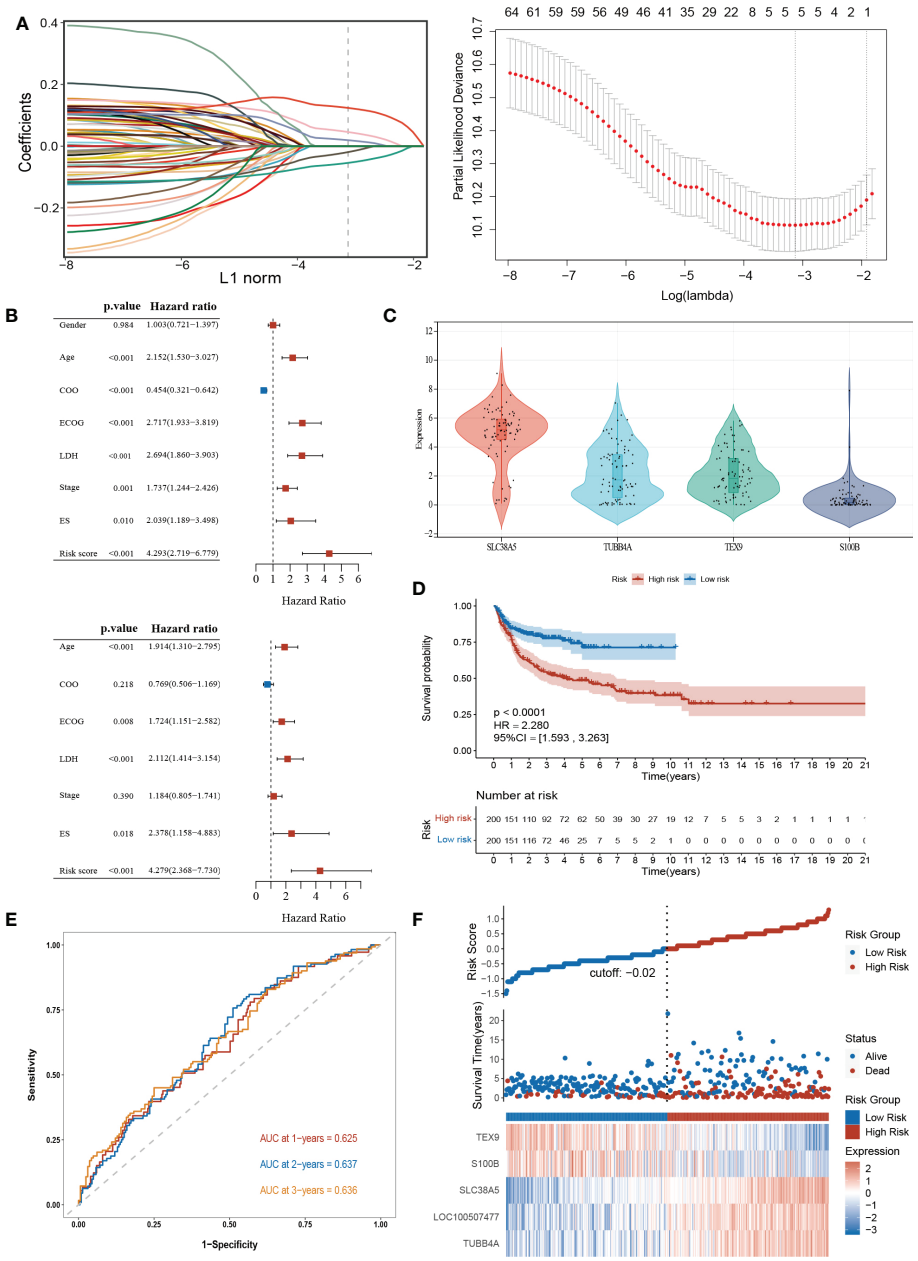

FIGURE 5
Construction and validation of the prognostic signature according to cuproptosis-related DEGs. **(A)** Construction of the prognostic model using LASSO Cox regression analysis. **(B)** Univariate and multivariate Cox regression analysis of clinical features and risk score in the training dataset. **(C)** Expression of the 4 genes in the CCLE database. **(D)** Kaplan-Meier curve in the high- and low-risk group. **(E)** Sensitivity and specificity of the risk score model assessed by time-dependent ROC analysis. **(F)** Ranked dot and scatter plots showing the risk score distribution and patients' survival status. LASSO, the Least absolute shrinkage and selection operator; ROC, receiver operating characteristic. LDH, lactate dehydrogenases; ES, extranodal sites; ECOG, The Eastern Cooperative Oncology Group performance score.

functions of the DEGs were predominantly related to ion transport, such as regulation of metal ion transport and regulation of transmembrane transporter activity (Figure 6E).

The association between CRGs and the abundance of immune cells had been previously demonstrated, and here we also investigated the correlation between DEGs-related risk core and immune cell infiltration. As shown in the correlation scatter plot, Tregs, follicular helper T cells, activated and resting NK cells, naive B cells, memory B cells, and activated dendritic cells were positively correlated with the risk score. However, a negative correlation was found between the risk score and gamma delta T cells, activated memory $CD4^+$ T cells, $CD8^+$ T

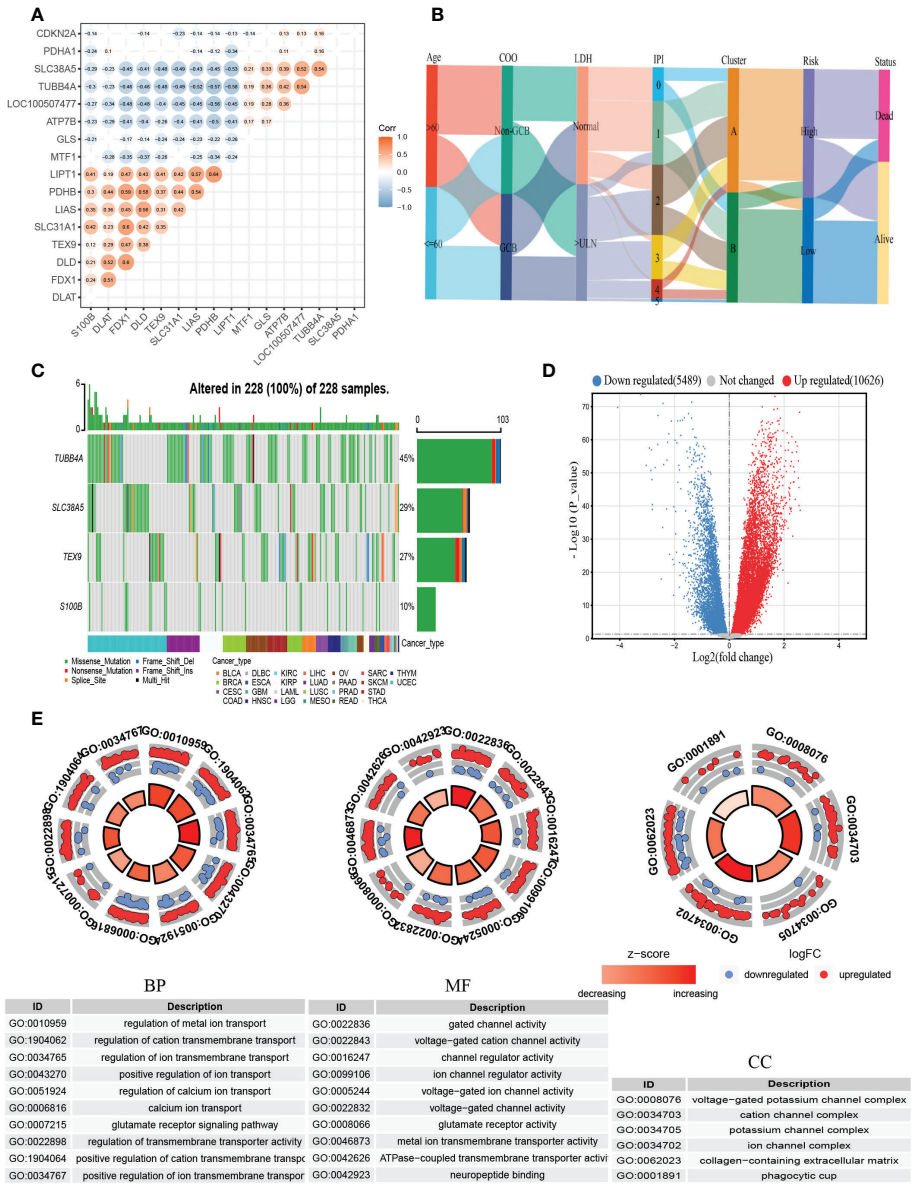

BP

ID	Description
GO:0010959	regulation of metal ion transport
GO:1904062	regulation of cation transmembrane transport
GO:0034765	regulation of ion transmembrane transport
GO:0043270	positive regulation of ion transport
GO:0051924	regulation of calcium ion transport
GO:0006816	calcium ion transport
GO:0007215	glutamate receptor signaling pathway
GO:0022898	regulation of transmembrane transporter activity
GO:1904064	positive regulation of cation transmembrane transpc
GO:0034767	positive regulation of ion transmembrane transpor

MF

ID	Description
GO:0022836	gated channel activity
GO:0022843	voltage−gated cation channel activity
GO:0016247	channel regulator activity
GO:0099106	ion channel regulator activity
GO:0005244	voltage−gated ion channel activity
GO:0022832	voltage−gated channel activity
GO:0008066	glutamate receptor activity
GO:0046873	metal ion transmembrane transporter activity
GO:0042626	ATPase−coupled transmembrane transporter activi
GO:0042923	neuropeptide binding

CC

ID	Description
GO:0008076	voltage−gated potassium channel complex
GO:0034703	cation channel complex
GO:0034705	potassium channel complex
GO:0034702	ion channel complex
GO:0062023	collagen−containing extracellular matrix
GO:0001891	phagocytic cup

FIGURE 6
Comprehensive analysis of the cuproptosis-related prognostic model. **(A)** Correlations between CRGs and the prognostic model. The results of *P*>0.05 were not shown. **(B)** Alluvial diagram showing clinical characteristics distribution and survival differences of CRG clusters and risk groups. **(C)** The tumor mutation burden frequency of genes in the prognostic model in the pan-cancer analysis. **(D)** The DEGs between high- and low-risk groups. **(E)** GO enrichment analyses of DEGs. COO, cell of origin; LDH, lactate dehydrogenases; IPI, International Prognostic Index; DEGs, differentially expressed genes; GO, Gene Ontology; BP, biological process; CC, cellular component; MF, molecular function.

cells, M1 macrophages, resting mast cells, and resting dendritic cells (Supplementary Figure 5C).

3.6 Construction and evaluation of combined nomogram

To improve the predictive accuracy as well as the clinical utility of the prognostic model, we constructed a nomogram based on multivariate Cox regression analysis, and the nomogram incorporated age, the Eastern Cooperative Oncology Group (ECOG), lactate dehydrogenase (LDH), extranodal sites (ES), and risk sore (Figure 7A). A C-index of 0.735 indicated that the nomogram had a good predictive value. The calibration plot for survival probability exhibited a satisfactory consensus between the prediction and observation (Figure 7B). The 1-, 2- and 3-year AUC of the nomogram were 77.61%, 75.09%, and 76.36%, respectively, higher than the AUC

10.3389/fonc.2022.1020566

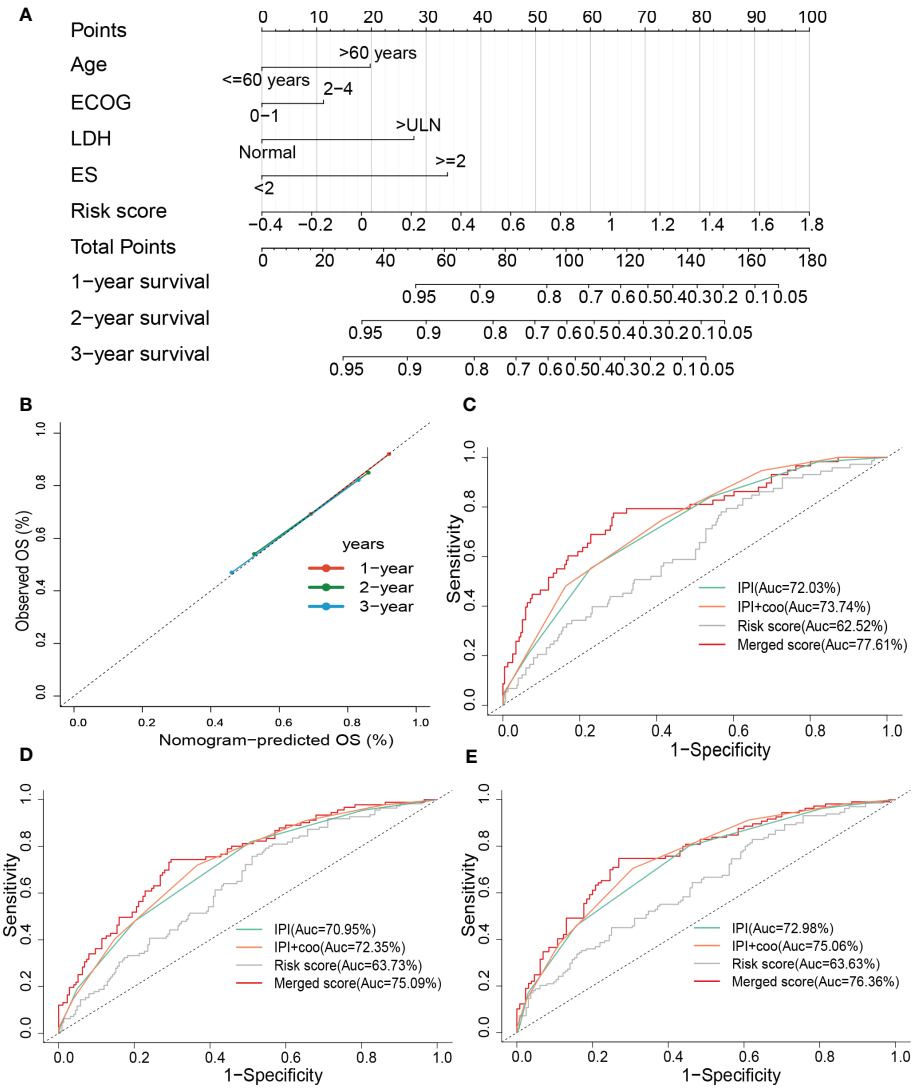

FIGURE 7
Constructing and evaluating the combined nomogram. **(A)** The nomograms with age, LDH, ES, ECOG, and risk score. **(B)** Calibration curves of the nomogram for predicting 1-, 2-, and 3-year survival. ROC curves of the nomogram, risk score, COO+IPI, and IPI score for **(C)** 1-year and **(D)** 2-year, and **(E)** 3-year survival prediction. LDH, lactate dehydrogenases; ES, extranodal sites; ECOG, The Eastern Cooperative Oncology Group performance score; ROC, receiver operating characteristic; COO, cell of origin; IPI, International Prognostic Index.

of the cell of origin (COO) plus/or International Prognostic Index (IPI) alone (Figures 7C–E). IPI is the current prognostic benchmark for DLBCL.

3.7 External experimental validation of prognostic genes

To validate the expression changes of these prognostic signature genes in patients with DLBCL, we collected 7 clinical samples of DLBCL and detected the mRNA expression of these four genes (*TUBB4A*, *SLC38A5*, *S100B*, and *TEX9*) using qRT-PCR. The trend of gene expression in the qRT-PCR analysis was basically consistent with our prognostic model. Compared with the normal lymphoid tissue in the control sample, the expression of risk genes (*TUBB4A* and *SLC38A5*) was up-regulated, while the expression of protective genes (*S100B* and *TEX9*) was down-regulated in most DLBCL samples ($P < 0.05$) (Figures 8A–D).

4 Discussion

Copper is a trace metal essential to life. The amount of copper in the organism is strictly controlled. Due to the close relationship between copper and the occurrence and development of cancer, copper ionophores (disulfiram/DSF,

10.3389/fonc.2022.1020566

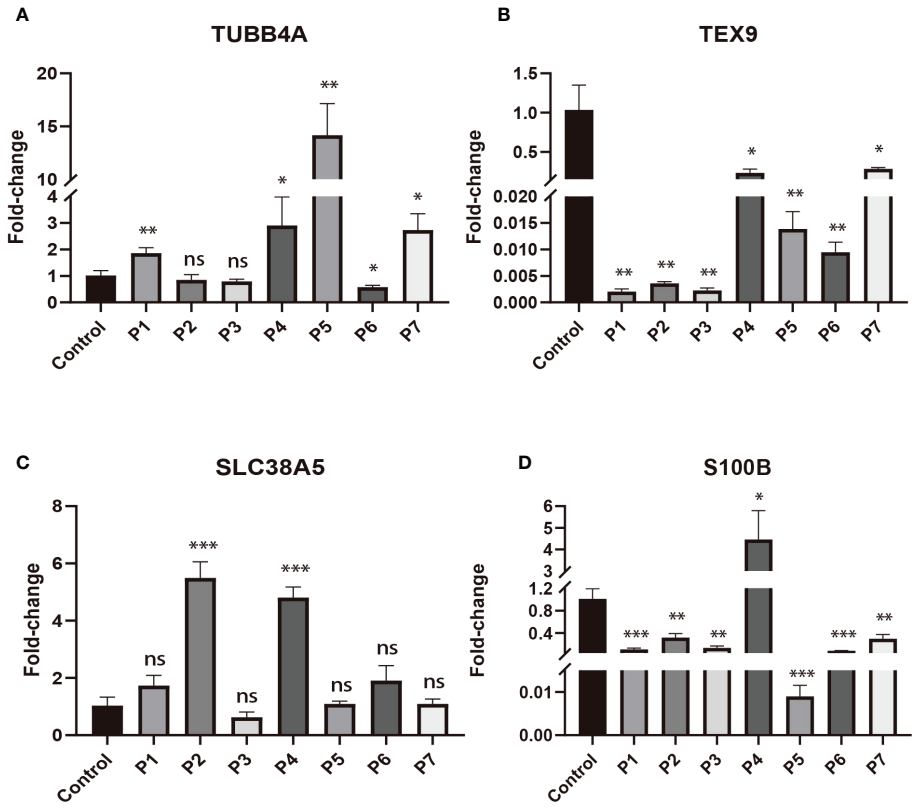

FIGURE 8
The expressions of four signature genes were validated by quantitative real-time PCR (qRT-PCR). *P< 0.05; **P< 0.01; ***P< 0.001; ns, no significance. **(A)** The expression of TUBB4A in DLBCL patients. **(B)** The expression of TEX9 in DLBCL patients. **(C)** The expression of SLC38A5 in DLBCL patients. **(D)** The expression of S100B in DLBCL patients.

dithiocarbamates, elesclomol, etc.) and copper chelators (trientine, tetrathiomolybdate, etc.) have been applied in anticancer treatment (97, 98). Cu-DSF has strong cytotoxicity to leukemic stem cell-like cells in a dose-dependent manner, whereas it does not affect normal hematopoietic progenitor cells (99). This may be related to the ability of cancer cells to accumulate copper, but also to their oxidative sensitivity. Elesclomol has been included in the clinical trial for acute myeloid leukemia (100). Copper chelating agents, known to have anti-angiogenic and anti-tumor activity, have been demonstrated the rate-limiting effects on tumor growth (101–104). Choline tetrathiomolybdate (ATN-224) was found to induce mitochondrial dysfunction and caspase-independent cell death in DLBCL (29). Recently, a novel mode of cell death that relies on the TCA cycle and mitochondrial oxidative respiration has been proposed, called cuproptosis (30). TCA cycle and OxPhos are also known to play important roles in DLBCL. B-cell lymphoma uses glucose and glutamine to fuel the TCA cycle for producing energy and metabolic precursors to support cell growth and proliferation (32, 105). Glucose-independent glutamine metabolism promotes the proliferation and survival of human lymphoma cells through the TCA cycle (105). Impaired TCA cycling has been reported to induce autophagy (106), which acts as a tumor suppressor in DLBCL (107). Currently, efforts to capture the molecular heterogeneity of DLBCL depend on gene expression profiles. In another transcriptomic approach, consensus cluster classification identified three subgroups, the BCR/proliferative cluster (BCR-DLBCL), showing upregulation of genes encoding B-cell receptor (BCR) signaling components, OxPhos cluster (OxPhos-DLBCL), which was significantly enriched in mitochondrial OxPhos-related genes, host response tumors were characterized by active host inflammatory infiltration (31). The OxPhos subset was characterized by non-functional BCR signaling and increased mitochondrial metabolism. Compared with BCR-DLBCL, OxPhos-DLBCL showed enhanced mitochondrial energy transduction, greater incorporation of nutrient-derived carbon into the TCA cycle, and consequent activation of antioxidant defense mechanisms (108). The OxPhos molecular marker provided these subpopulations with alternative survival benefits independent of the BCR network (32). In a study of the metabolic phenotype of DLBCL, neoplastic lymphocytes in DLBCL samples expressed a significant OxPhos phenotype, whereas stromal cells strongly exhibited a glycolytic phenotype, compared with non-tumor lymphoid tissues from control samples. This suggests that

tumor lymphocytes in DLBCL undergo a significant degree of mitochondrial oxidative metabolism rather than aerobic glycolysis. They then hypothesized that DLBCL's multi-compartment metabolism is a result of adapting to its high metabolic demands. Neoplastic cells metabolically reorganize the surrounding stroma to undergo aerobic glycolysis, providing them with substrates for the TCA cycle (33). As an OxPhos inhibitor, the Gboxin analog 5d has specific selectivity for DLBCL. Given its strong proliferation inhibition and cell cycle-blocking effects on DLBCL, 5d is considered a candidate agent for DLBCL alternative drug development (34). In conclusion, the TCA cycle and mitochondrial oxidative respiration are closely associated with DLBCL. However, the role of cuproptosis in DLBCL has not been explored.

Identifying tumor subgroups with different pathogenesis and possible therapeutic targets to characterize the genetic heterogeneity of DLBCL will facilitate a deeper understanding and precise treatment of the disease. In this study, we identified two isoforms by consensus clustering based on the expression profiles of 12 CRGs. Meanwhile, we explored the CNV, gene expression, and methylation of 12 CRGs in the TCGA DLBCL dataset. Due to the small number of samples in the dataset (n=48), we performed a pan-cancer analysis of the SNVs in 12 CRGs. The results showed that 10 of 12 genes were mutated in 98.23% (941/958) of tumor samples, of which *CDKN2A* was the most (42%). In addition, CNVs were present in all 12 CRGs. Among them, the most frequent were *CDKN2A* (predominantly deletion) and *FDX1* (predominantly amplification). *FDX1* is known to regulate protein lipoylation and is a key regulator in the process of cuproptosis (30). Furthermore, the CNVs of *MTF1*, *GLS*, *LIPT1*, and *LIAS* were closely related to the survival time of DLBCL patients. We then found that the high expressions of 3 genes identified as cuproptosis-negative regulators (*MTF1*, *GLS*, and *ATP7B*) (30) were associated with shorter OS. In addition, in the study of the correlation between gene expression and pathway activity, *SLC31A1* was found to have a potential activating effect on the apoptosis pathway and a potentially inhibiting effect on DNA damage. And *CDKN2A* exhibited potential inhibition of the TSC/mTOR pathway. All of these pathways are known to play a critical role in tumor growth and progression. *SLC31A1* and *ATP7B* are copper importer (109, 110) and copper efflux transporter, respectively (30). *SLC31A1* has been reported to be an important pathway for platinum drug import into cells (111). In addition, a lower expression level of *SLC31A1* is usually associated with increased cisplatin resistance in tumors (112). Conversely, *ATP7B* is involved in the efflux and sequestration of cisplatin, thereby increasing the resistance of tumor cells to platinum treatment (113, 114). *CDKN2A*, an important tumor suppressor gene, which is frequently mutated or absent in a variety of tumors, is capable of inducing cell cycle arrest in G1 and G2 phases (115). *CDKN2A* deletion is the most common gene copy number abnormality in DLBCL, which is associated with poor prognosis (116–118). Metal-responsive transcription factor-1 (*MTF1*) is a candidate susceptibility gene for lymphoma. Since the products of targets such as metallothionein can suppress cellular stress generated by ionizing radiation (119). Glutaminase (*GLS*) is a mitochondrial enzyme that catalyzes the conversion of glutamine to glutamate (120). Highly expressed in cancers including lymphoma, blocking its enzymatic activity or gene knockout has been shown to have antitumor activity (121, 122). Under the stress of PD-1-expressing γδ T cells, *GLS* confers immunosuppressive properties to ABC-DLBCL cells by enhancing mitochondrial bioenergetics and consequent STAT3 activation and PD-L1 expression in ABC-DLBCL cells (123). These analyses above have demonstrated the potential role of cuproptosis in the prognosis of DLBCL.

In the subsequent comparative analysis of the two subtypes, we found that subtype A had poorer survival than B, and the four cuproptosis-negative regulatory genes (*CDKN2A*, *MTF1*, *GLS*, and *ATP7B*) were more highly expressed in subtype A. The difference in the expression of CRGs between the two subtypes may be a potential reason for their distinct prognosis. Next, potential biological differences between subtypes were explored by GSVA. The results showed that subtype A was mainly enriched in pathways closely related to tumor growth and development, such as the Notch signaling pathway, MAPK signaling pathway, VEGF signaling pathway, and ERBB signaling pathway. For instance, Notch2 is a key membrane receptor for B-cell function and plays a critical role in the pathogenesis of lymphoma (124). The main enriched pathways of subtype B include the p53 signaling pathway and metabolism-related pathways, such as oxidative phosphorylation and the TCA cycle. Subtype B may be closely related to OxPhos-DLBCL identified by Monti et al. (31).

Given the increasing importance of TME in cancer treatment and prognosis, immune cell infiltration between the two subtypes was assessed by the CIBERSORT algorithm. Tregs and resting $CD4^+$ memory T cells were more infiltrated in subtype A, whereas $CD8^+$ T cells, gamma delta T cells, and $CD4^+$ memory-activated T cells were more infiltrated in subtype B. Similarly, the immune infiltration ssGSEA scores in TCGA-DLBCL and the pathological slide data showed a higher immune infiltration in cluster B. In the subsequent drug sensitivity prediction analysis, subgroup A exhibited resistance to doxorubicin, bleomycin, etoposide, elesclomol, and cisplatin. Resistance to cisplatin may be related to higher expression of *ATP7B* and lower expression of *SLC31A1* in subgroup A. Differences in immune status and treatment responsiveness between subtypes may contribute to the differences in survival outcomes.

Based on DEGs between cuproptosis-related subpopulations, we constructed and validated a prognostic model integrating five genes (*S100B*, *TEX9*, *TUBB4A*, *SLC38A5*, *LOC100507477*) using LASSO regression analysis. The model was identified as an independent prognostic factor in Cox regression analysis.

Different clinical characteristics and prognoses were demonstrated between high- and low-risk groups. The prognosis of the high-risk group was worse compared to the low-risk group. Subtype A, LDH>ULN, and non-GCB subpopulations tended to have a higher risk score.

Furthermore, four of the five genes in the prognostic model had SNVs in all 228 samples (100%) of the pan-cancer analysis, with the most variant being *TUBB4A* (45%). All four genes had copy number abnormalities in patients with DLBCL. The human microtubulin β-IVa class (*TUBB4A*), which pertains to the β-microtubulin family, has little or no expression in most normal tissues but is highly expressed in a variety of human cancer cell lines (125). *TUBB4A* deletion has been reported to reduce prostate tumor growth and metastasis by inhibiting the activation of NF-κB, cell cycle protein D1, and c-MYC signaling (126). It is also involved in the resistance of multiple cancer cells to chemotherapy and radiotherapy (127–129). Likewise, *TEX9* is a testis-expressed protein that belongs to cancer/testis antigen (CTA) and is normally expressed only in the testis, except in early-developing embryos and the placenta. *TEX9* expression can be induced in tumor cells when cancer occurs. *TEX9* has been shown the promotion of proliferation and migration and has an inhibitory effect on the apoptosis of esophageal squamous carcinoma cells (130). *S100* calcium-binding protein B (*S100B*) is a Ca^{+2}/Zn^{+2}-*p53* binding protein that blocks phosphorylation and acetylation sites on *p53* important for transcriptional activation (131). In addition, it appears as a key signaling molecule in many physiological and pathological processes, including inflammation, apoptosis, and cell growth (132). High expression of *S100B* in antigen-presenting cells correlates with a good prognosis (133). *SLC38A5* is a sodium-coupled transporter upregulated in multiple cancers, mediating the influx of glutamine, serine, glycine, and methionine into cancer cells. It responds to the metabolic reprogramming of cancer cells to meet the expansive demands of tumor growth and proliferation (134). Furthermore, the gene co-expression matrix revealed the close association of 12 CRGs with genes in the prognostic model. However, the relationship between these genes in model and DLBCL still needs to be further investigated.

According to GO enrichment analysis, DEGs between high- and low-risk groups were closely associated with the metal ion transport-related pathways. This suggests that there may be differences in copper transport capacity between the high and low-risk groups, which may be one of the potential reasons for the different prognoses in the two groups. Since serum copper levels have previously been shown to be positively correlated with disease status in non-Hodgkin lymphoma, with significantly higher levels in active or relapsed patients than in patients in remission (16, 23–25).

Correlation analysis of risk score and immune cell infiltration indicated that the risk score was positively correlated with the infiltration of Tregs, but negatively correlated with the abundance of gamma delta T cells, $CD8^+$ T cells, and activated $CD4^+$ memory T cells. This may have led to the difference in survival between the high- and low-risk groups. Ultimately, a nomogram integrating clinical features and risk scores was constructed. IPI is the main clinical tool used to predict the prognosis of patients with aggressive NHL and is the current prognostic benchmark for DLBCL (2, 96). Compared with IPI, the nomogram demonstrated higher accuracy and discrimination in predicting survival.

To further verify the expression level of signature genes in DLBCL, we performed qRT-PCR on our clinical samples to quantify the mRNA expression of these four genes (*TUBB4A*, *SLC38A5*, *S100B*, and *TEX9*). qRT-PCR analysis showed that the expression of risk genes (*TUBB4A* and *SLC38A5)* was up-regulated, while the expression of protective genes (*S100B* and *TEX9*) was down-regulated in DLBCL. This was generally consistent with our prognostic model.

Our study has several limitations. Firstly, our clustering typing strategy and prognostic signature need to be further validated for their robustness and clinical utility in a larger sample. Secondly, since the establishment and validation of the prognostic model were primarily based on public databases, further validations are required through cell experiments and larger clinical samples. In addition, the specific mechanism of CRG in DLBCL and the underlying mechanism between CRGs and tumor immunity in DLBCL are currently unclear and require further study.

In conclusion, we performed systematic analyses on the molecular alterations of CRGs in DLBCL, and our study suggests that these genes may play a key role in the prognosis of DLBCL. The two subtypes identified based on the CRGs expression signature were significantly different in biological function, immune cell infiltration, treatment responsiveness, and clinical prognosis. In addition, the prognostic model constructed from CRG performed well in predicting the survival of DLBCL patients and was significantly correlated with the level of immune infiltration. Furthermore, we built a nomogram combining clinical features and risk scores that improved the predictive power of DLBCL. Finally, we carried out an external experiment to verify the level of prognostic gene expression. Our work provides new directions for prognostic prediction and potential therapeutic targets in DLBCL and may provide the basis for more in-depth studies in the future.

Data availability statement

The original contributions presented in the study are included in the article/Supplementary Material. Further inquiries can be directed to the corresponding author.

Author contributions

BZ conceived the study design, completed data analysis and interpretation, and manuscript writing. QW assisted in the completion of experiments. TZ, ZZ, ZL, DZ, and ZC provided suggestions for the data analysis. YM provided critical revisions to the paper. All authors contributed to the article and approved the submitted version.

Funding

The study was supported by the Natural Science Foundation of Zhejiang Province (Item No.: LY20H080003).

Conflict of interest

The authors declare that the research was conducted in the absence of any commercial or financial relationships that could be construed as a potential conflict of interest.

Publisher's note

Supplementary material

The Supplementary Material for this article can be found online at: https://www.frontiersin.org/articles/10.3389/fonc.2022.1020566/full#supplementary-material

SUPPLEMENTARY FIGURE 1
(A) Correlation analysis of CNV and survival in DLBCL. **(B)** The relationships between expression of CRGs and survival in DLBCL. **(C)** Correlation analysis of gene methylation of CRGs and survival in DLBCL. The bubble color from blue to red represents the hazard ratio from low to high, and bubble size is positively correlated with the Cox P value significance. The black outline border indicates Cox P value ≤ 0.05.

SUPPLEMENTARY FIGURE 2
Validation of CRG clusters. **(A, C)** The consensus matrix of the consensus clustering. **(B, D)** The sample clustering consistency diagram. A and B were for GSE31312. C and D were for TCGA-DLBCL. Two clusters (k=2) would be best.

SUPPLEMENTARY FIGURE 3
Prediction of drug responsiveness in the distinct subtypes. IC50, half maximal inhibitory concentration.

SUPPLEMENTARY FIGURE 4
Validation of the prognostic signature in GSE87371. **(A)** Kaplan-Meier curve in the high- and low-risk group. **(B)** Sensitivity and specificity of the risk score model assessed by time-depend ROC analysis. **(C)** Ranked dot and scatter plots showing the risk score distribution and patients' survival status.

SUPPLEMENTARY FIGURE 5
(A) Differences in risk scores among groups with distinct clinical characteristics. **(B)** The CNV percentage of genes in the model of DLBCL. **(C)** Correlation between risk score and immune infiltration in DLBCL. COO, cell of origin; LDH, lactate dehydrogenases; CNV, copy number variation.

References

1. Chan WC, Armitage JO, Gascoyne R, Connors J, Close P, Jacobs P, et al. A clinical evaluation of the international lymphoma study group classification of non-hodgkin's lymphoma. the non-hodgkin's lymphoma classification project. *Blood* (1997) 89(11):3909–18. doi: 10.1182/blood.V89.11.3909

2. Sehn LH, Salles G. Diffuse large b-cell lymphoma. *N Engl J Med* (2021) 384 (9):842–58. doi: 10.1056/NEJMra2027612

3. Alizadeh AA, Eisen MB, Davis RE, Ma C, Lossos IS, Rosenwald A, et al. Distinct types of diffuse large b-cell lymphoma identified by gene expression profiling. *Nature* (2000) 403(6769):503–11. doi: 10.1038/35000501

4. Coiffier B, Lepage E, Briere J, Herbrecht R, Tilly H, Bouabdallah R, et al. Chop chemotherapy plus rituximab compared with chop alone in elderly patients with diffuse large-b-cell lymphoma. *N Engl J Med* (2002) 346(4):235–42. doi: 10.1056/NEJMoa011795

5. Feugier P, Van Hoof A, Sebban C, Solal-Celigny P, Bouabdallah R, Ferme C, et al. Long-term results of the r-chop study in the treatment of elderly patients with diffuse large b-cell lymphoma: a study by the groupe d'etude des lymphomes de l'adulte. *J Clin Oncol* (2005) 23(18):4117–26. doi: 10.1200/JCO.2005.09.131

6. Karube K, Enjuanes A, Dlouhy I, Jares P, Martin-Garcia D, Nadeu F, et al. Integrating genomic alterations in diffuse large b-cell lymphoma identifies new relevant pathways and potential therapeutic targets. *Leukemia* (2018) 32(3):675–84. doi: 10.1038/leu.2017.251

7. Lenz G, Wright G, Dave SS, Xiao W, Powell J, Zhao H, et al. Stromal gene signatures in large-b-cell lymphomas. *N Engl J Med* (2008) 359(22):2313–23. doi: 10.1056/NEJMoa0802885

8. Wachnik A. The physiological role of copper and the problems of copper nutritional deficiency. *Nahrung* (1988) 32(8):755–65. doi: 10.1002/food.19880320811

9. Grubman A, White AR. Copper as a key regulator of cell signalling pathways. *Expert Rev Mol Med* (2014) 16:e11. doi: 10.1017/erm.2014.11

10. Yaman M, Kaya G, Yekeler H. Distribution of trace metal concentrations in paired cancerous and non-cancerous human stomach tissues. *World J Gastroenterol* (2007) 13(4):612–8. doi: 10.3748/wjg.v13.i4.612

11. Yaman M, Kaya G, Simsek M. Comparison of trace element concentrations in cancerous and noncancerous human endometrial and ovary tissues. *Int J Gynecol Cancer* (2007) 17(1):220–8. doi: 10.1111/j.1525-1438.2006.00742.x

12. Mao S, Huang S. Zinc and copper levels in bladder cancer: A systematic review and meta-analysis. *Biol Trace Elem Res* (2013) 153(1-3):5–10. doi: 10.1007/s12011-013-9682-z

13. Ressnerova A, Raudenska M, Holubova M, Svobodova M, Polanska H, Babula P, et al. Zinc and copper homeostasis in head and neck cancer: Review and meta-analysis. *Curr Med Chem* (2016) 23(13):1304–30. doi: 10.2174/0929867323666160405111543

14. Lener MR, Scott RJ, Wiechowska-Kozlowska A, Serrano-Fernandez P, Baszuk P, Jaworska-Bieniek K, et al. Serum concentrations of selenium and copper in patients diagnosed with pancreatic cancer. *Cancer Res Treat* (2016) 48 (3):1056–64. doi: 10.4143/crt.2015.282

15. Shen F, Cai WS, Li JL, Feng Z, Cao J, Xu B. The association between serum levels of selenium, copper, and magnesium with thyroid cancer: A meta-analysis. *Biol Trace Elem Res* (2015) 167(2):225–35. doi: 10.1007/s12011-015-0304-9

16. Gozdasoglu S, Cavdar AO, Arcasoy A, Akar N. Serum copper and zinc levels and copper/zinc ratio in pediatric non-hodgkin's lymphoma. *Acta Haematol* (1982) 67(1):67–70. doi: 10.1159/000207027

17. Ishida S, Andreux P, Poitry-Yamate C, Auwerx J, Hanahan D. Bioavailable copper modulates oxidative phosphorylation and growth of tumors. *Proc Natl Acad Sci U.S.A.* (2013) 110(48):19507–12. doi: 10.1073/pnas.1318431110

18. Vella V, Malaguarnera R, Lappano R, Maggiolini M, Belfiore A. Recent views of heavy metals as possible risk factors and potential preventive and therapeutic agents in prostate cancer. *Mol Cell Endocrinol* (2017) 457:57–72. doi: 10.1016/j.mce.2016.10.020

19. Tisato F, Marzano C, Porchia M, Pellei M, Santini C. Copper in diseases and treatments, and copper-based anticancer strategies. *Med Res Rev* (2010) 30(4):708–49. doi: 10.1002/med.20174

20. De Luca A, Barile A, Arciello M, Rossi L. Copper homeostasis as target of both consolidated and innovative strategies of anti-tumor therapy. *J Trace Elem Med Biol* (2019) 55:204–13. doi: 10.1016/j.jtemb.2019.06.008

21. Shanbhag V, Jasmer-McDonald K, Zhu S, Martin AL, Gudekar N, Khan A, et al. Atp7a delivers copper to the lysyl oxidase family of enzymes and promotes tumorigenesis and metastasis. *Proc Natl Acad Sci U.S.A.* (2019) 116(14):6836–41. doi: 10.1073/pnas.1817473116

22. Arnesano F, Natile G. Interference between copper transport systems and platinum drugs. *Semin Cancer Biol* (2021) 76:173–88. doi: 10.1016/j.semcancer.2021.05.023

23. Cohen Y, Epelbaum R, Haim N, McShan D, Zinder O. The value of serum copper levels in non-hodgkin's lymphoma. *Cancer* (1984) 53(2):296–300. doi: 10.1002/1097-0142(19840115)53:2<296::aid-cncr2820530219>3.0.co;2-u

24. Hisamitsu S, Shibuya H, Hoshina M, Horiuchi J. Prognostic factors in head and neck non-hodgkin's lymphoma with special reference to serum lactic dehydrogenase and serum copper. *Acta Oncol* (1990) 29(7):879–83. doi: 10.3109/02841869009096383

25. Shah-Reddy I, Khilanani P, Bishop CR. Serum copper levels in non-hodgkin's lymphoma. *Cancer* (1980) 45(8):2156–9. doi: 10.1002/1097-0142(19800415)45:8<2156::aid-cncr2820450824>3.0.co;2-c

26. Spengler G, Kincses A, Racz B, Varga B, Watanabe G, Saijo R, et al. Benzoxazole-based Zn(Ii) and Cu(Ii) complexes overcome multidrug-resistance in cancer. *Anticancer Res* (2018) 38(11):6181–7. doi: 10.21873/anticanres.12971

27. Ng CH, Kong SM, Tiong YL, Maah MJ, Sukram N, Ahmad M, et al. Selective anticancer copper(ii)-mixed ligand complexes: targeting of ros and proteasomes. *Metallomics* (2014) 6(4):892–906. doi: 10.1039/c3mt00276d

28. Easmon J, Purstinger G, Heinisch G, Roth T, Fiebig HH, Holzer W, et al. Synthesis, cytotoxicity, and antitumor activity of copper(ii) and iron(ii) complexes of (4)n-azabicyclo[3.2.2]nonane thiosemicarbazones derived from acyl diazines. *J Med Chem* (2001) 44(13):2164–71. doi: 10.1021/jm000979z

29. Lee K, Hart MR, Briehl MM, Mazar AP, Tome ME. The copper chelator atn-224 induces caspase-independent cell death in diffuse large b cell lymphoma. *Int J Oncol* (2014) 45(1):439–47. doi: 10.3892/ijo.2014.2396

30. Tsvetkov P, Coy S, Petrova B, Dreishpoon M, Verma A, Abdusamad M, et al. Copper induces cell death by targeting lipoylated tca cycle proteins. *Science* (2022) 375(6586):1254–61. doi: 10.1126/science.abf0529

31. Monti S, Savage KJ, Kutok JL, Feuerhake F, Kurtin P, Mihm M, et al. Molecular profiling of diffuse large b-cell lymphoma identifies robust subtypes including one characterized by host inflammatory response. *Blood* (2005) 105(5):1851–61. doi: 10.1182/blood-2004-07-2947

32. Caro P, Kishan AU, Norberg E, Stanley IA, Chapuy B, Ficarro SB, et al. Metabolic signatures uncover distinct targets in molecular subsets of diffuse large b cell lymphoma. *Cancer Cell* (2012) 22(4):547–60. doi: 10.1016/j.ccr.2012.08.014

33. Gooptu M, Whitaker-Menezes D, Sprandio J, Domingo-Vidal M, Lin Z, Uppal G, et al. Mitochondrial and glycolytic metabolic compartmentalization in diffuse large b-cell lymphoma. *Semin Oncol* (2017) 44(3):204–17. doi: 10.1053/j.seminoncol.2017.10.002

34. Yao S, Yin J, Liu W, Li Y, Huang J, Qi C, et al. A novel gboxin analog induces oxphos inhibition and mitochondrial dysfunction-mediated apoptosis in diffuse large b-cell lymphoma. *Bioorg Chem* (2022) 127:106019. doi: 10.1016/j.bioorg.2022.106019

35. Bian Z, Fan R, Xie L. A novel cuproptosis-related prognostic gene signature and validation of differential expression in clear cell renal cell carcinoma. *Genes (Basel)* (2022) 13(5):851. doi: 10.3390/genes13050851

36. Ji ZH, Ren WZ, Wang HQ, Gao W, Yuan B. Molecular subtyping based on cuproptosis-related genes and characterization of tumor microenvironment infiltration in kidney renal clear cell carcinoma. *Front Oncol* (2022) 12:919083. doi: 10.3389/fonc.2022.919083

37. Mei W, Liu X, Jia X, Jin L, Xin S, Sun X, et al. A cuproptosis-related gene model for predicting the prognosis of clear cell renal cell carcinoma. *Front Genet* (2022) 13:905518. doi: 10.3389/fgene.2022.905518

38. Li K, Tan L, Li Y, Lyu Y, Zheng X, Jiang H, et al. Cuproptosis identifies respiratory subtype of renal cancer that confers favorable prognosis. *Apoptosis* (2022) 27(11-12):1004–14. doi: 10.1007/s10495-022-01769-2

39. Zhang G, Chen X, Fang J, Tai P, Chen A, Cao K. Cuproptosis status affects treatment options about immunotherapy and targeted therapy for patients with kidney renal clear cell carcinoma. *Front Immunol* (2022) 13:954440. doi: 10.3389/fimmu.2022.954440

40. Yuan H, Qin X, Wang J, Yang Q, Fan Y, Xu D. The cuproptosis-associated 13 gene signature as a robust predictor for outcome and response to immune- and targeted-therapies in clear cell renal cell carcinoma. *Front Immunol* (2022) 13:971142. doi: 10.3389/fimmu.2022.971142

41. Xu S, Liu D, Chang T, Wen X, Ma S, Sun G, et al. Cuproptosis-associated lncrna establishes new prognostic profile and predicts immunotherapy response in clear cell renal cell carcinoma. *Front Genet* (2022) 13:938259. doi: 10.3389/fgene.2022.938259

42. Huili Y, Nie S, Zhang L, Yao A, Liu J, Wang Y, et al. Cuproptosis-related lncrna: prediction of prognosis and subtype determination in clear cell renal cell carcinoma. *Front Genet* (2022) 13:958547. doi: 10.3389/fgene.2022.958547

43. Wang Y, Zhang Y, Wang L, Zhang N, Xu W, Zhou J, et al. Development and experimental verification of a prognosis model for cuproptosis-related subtypes in hcc. *Hepatol Int* (2022) 16(6):1435–47. doi: 10.1007/s12072-022-10381-0

44. Liu Y, Liu Y, Ye S, Feng H, Ma L. Development and validation of cuproptosis-related gene signature in the prognostic prediction of liver cancer. *Front Oncol* (2022) 12:985484. doi: 10.3389/fonc.2022.985484

45. Zhang G, Sun J, Zhang X. A novel cuproptosis-related lncrna signature to predict prognosis in hepatocellular carcinoma. *Sci Rep* (2022) 12(1):11325. doi: 10.1038/s41598-022-15251-1

46. Zhang Z, Zeng X, Wu Y, Liu Y, Zhang X, Song Z. Cuproptosis-related risk score predicts prognosis and characterizes the tumor microenvironment in hepatocellular carcinoma. *Front Immunol* (2022) 13:925618. doi: 10.3389/fimmu.2022.925618

47. Fu J, Wang S, Li Z, Qin W, Tong Q, Liu C, et al. Comprehensive multiomics analysis of cuproptosis-related gene characteristics in hepatocellular carcinoma. *Front Genet* (2022) 13:942387. doi: 10.3389/fgene.2022.942387

48. Yun Y, Wang Y, Yang E, Jing X. Cuproptosis-related gene - slc31a1, fdx1 and atp7b polymorphisms are associated with risk of lung cancer. *Pharmgenomics Pers Med* (2022) 15:733–42. doi: 10.2147/PGPM.S372824

49. Wang F, Lin H, Su Q, Li C. Cuproptosis-related lncrna predict prognosis and immune response of lung adenocarcinoma. *World J Surg Oncol* (2022) 20(1):275. doi: 10.1186/s12957-022-02727-7

50. Hu Q, Wang R, Ma H, Zhang Z, Xue Q. Cuproptosis predicts the risk and clinical outcomes of lung adenocarcinoma. *Front Oncol* (2022) 12:922332. doi: 10.3389/fonc.2022.922332

51. Zhang H, Shi Y, Yi Q, Wang C, Xia Q, Zhang Y, et al. A novel defined cuproptosis-related gene signature for predicting the prognosis of lung adenocarcinoma. *Front Genet* (2022) 13:975185. doi: 10.3389/fgene.2022.975185

52. Gao C, Kong N, Zhang F, Zhou L, Xu M, Wu L. Development and validation of the potential biomarkers based on m6a-related lncrnas for the predictions of overall survival in the lung adenocarcinoma and differential analysis with cuproptosis. *BMC Bioinf* (2022) 23(1):327. doi: 10.1186/s12859-022-04869-7

53. Wang S, Xing N, Meng X, Xiang L, Zhang Y. Comprehensive bioinformatics analysis to identify a novel cuproptosis-related prognostic signature and its cerna regulatory axis and candidate traditional chinese medicine active ingredients in lung adenocarcinoma. *Front Pharmacol* (2022) 13:971867. doi: 10.3389/fphar.2022.971867

54. Xu M, Mu J, Wang J, Zhou Q, Wang J. Construction and validation of a cuproptosis-related lncrna signature as a novel and robust prognostic model for colon adenocarcinoma. *Front Oncol* (2022) 12:961213. doi: 10.3389/fonc.2022.961213

55. Zhang S, Zhang L, Lu H, Yao Y, Liu X, Hou J. A cuproptosis and copper metabolism-related gene prognostic index for head and neck squamous cell carcinoma. *Front Oncol* (2022) 12:955336. doi: 10.3389/fonc.2022.955336

56. Tang S, Zhao L, Wu XB, Wang Z, Cai LY, Pan D, et al. Identification of a novel cuproptosis-related gene signature for prognostic implication in head and neck squamous carcinomas. *Cancers (Basel)* (2022) 14(16):3986. doi: 10.3390/cancers14163986

57. Li G, Luo Q, Wang X, Zeng F, Feng G, Che G. Deep learning reveals cuproptosis features assist in predict prognosis and guide immunotherapy in lung adenocarcinoma. *Front Endocrinol (Lausanne)* (2022) 13:970269. doi: 10.3389/fendo.2022.970269

58. Ding Q, Chen X, Hong W, Wang L, Liu W, Cai S, et al. The prognostic role of cuproptosis in head and neck squamous cell carcinoma patients: a comprehensive analysis. *Dis Markers* (2022) 2022:9996946. doi: 10.1155/2022/9996946

59. Yang L, Yu J, Tao L, Huang H, Gao Y, Yao J, et al. Cuproptosis-related lncrnas are biomarkers of prognosis and immune microenvironment in head and neck squamous cell carcinoma. *Front Genet* (2022) 13:947551. doi: 10.3389/fgene.2022.947551

60. Chen Y. Identification and validation of cuproptosis-related prognostic signature and associated regulatory axis in uterine corpus endometrial carcinoma. *Front Genet* (2022) 13:912037. doi: 10.3389/fgene.2022.912037

61. Chen B, Zhou X, Yang L, Zhou H, Meng M, Zhang L, et al. A cuproptosis activation scoring model predicts neoplasm-immunity interactions and personalized treatments in glioma. *Comput Biol Med* (2022) 148:105924. doi: 10.1016/j.compbiomed.2022.105924

62. Bao JH, Lu WC, Duan H, Ye YQ, Li JB, Liao WT, et al. Identification of a novel cuproptosis-related gene signature and integrative analyses in patients with lower-grade gliomas. *Front Immunol* (2022) 13:933973. doi: 10.3389/fimmu.2022.933973

63. Wang W, Lu Z, Wang M, Liu Z, Wu B, Yang C, et al. The cuproptosis-related signature associated with the tumor environment and prognosis of patients with glioma. *Front Immunol* (2022) 13:998236. doi: 10.3389/fimmu.2022.998236

64. Yan X, Wang N, Dong J, Wang F, Zhang J, Hu X, et al. A cuproptosis-related lncrnas signature for prognosis, chemotherapy, and immune checkpoint blockade therapy of low-grade glioma. *Front Mol Biosci* (2022) 9:966843. doi: 10.3389/fmolb.2022.966843

65. Ye Z, Zhang S, Cai J, Ye L, Gao L, Wang Y, et al. Development and validation of cuproptosis-associated prognostic signatures in who 2/3 glioma. *Front Oncol* (2022) 12:967159. doi: 10.3389/fonc.2022.967159

66. Ouyang Z, Zhang H, Lin W, Su J, Wang X. Bioinformatic profiling identifies the glutaminase to be a potential novel cuproptosis-related biomarker for glioma. *Front Cell Dev Biol* (2022) 10:982439. doi: 10.3389/fcell.2022.982439

67. Sha S, Si L, Wu X, Chen Y, Xiong H, Xu Y, et al. Prognostic analysis of cuproptosis-related gene in triple-negative breast cancer. *Front Immunol* (2022) 13:922780. doi: 10.3389/fimmu.2022.922780

68. Li X, Ma Z, Mei L. Cuproptosis-related gene slc31a1 is a potential predictor for diagnosis, prognosis and therapeutic response of breast cancer. *Am J Cancer Res* (2022) 12(8):3561–80.

69. Li L, Li L, Sun Q. High expression of cuproptosis-related slc31a1 gene in relation to unfavorable outcome and deregulated immune cell infiltration in breast cancer: an analysis based on public databases. *BMC Bioinf* (2022) 23(1):350. doi: 10.1186/s12859-022-04894-6

70. Cheng T, Wu Y, Liu Z, Yu Y, Sun S, Guo M, et al. Cdkn2a-mediated molecular subtypes characterize the hallmarks of tumor microenvironment and guide precision medicine in triple-negative breast cancer. *Front Immunol* (2022) 13:970950. doi: 10.3389/fimmu.2022.970950

71. Shan J, Geng R, Zhang Y, Wei J, Liu J, Bai J. Identification of cuproptosis-related subtypes, establishment of a prognostic model and tumor immune landscape in endometrial carcinoma. *Comput Biol Med* (2022) 149:105988. doi: 10.1016/j.compbiomed.2022.105988

72. Lei L, Tan L, Sui L. A novel cuproptosis-related gene signature for predicting prognosis in cervical cancer. *Front Genet* (2022) 13:957744. doi: 10.3389/fgene.2022.957744

73. Lv H, Liu X, Zeng X, Liu Y, Zhang C, Zhang Q, et al. Comprehensive analysis of cuproptosis-related genes in immune infiltration and prognosis in melanoma. *Front Pharmacol* (2022) 13:930041. doi: 10.3389/fphar.2022.930041

74. Zhou Y, Shu Q, Fu Z, Wang C, Gu J, Li J, et al. A novel risk model based on cuproptosis-related lncrnas predicted prognosis and indicated immune microenvironment landscape of patients with cutaneous melanoma. *Front Genet* (2022) 13:959456. doi: 10.3389/fgene.2022.959456

75. Yang X, Wang X, Sun X, Xiao M, Fan L, Su Y, et al. Construction of five cuproptosis-related lncrna signature for predicting prognosis and immune activity in skin cutaneous melanoma. *Front Genet* (2022) 13:972899. doi: 10.3389/fgene.2022.972899

76. Huang X, Zhou S, Toth J, Hajdu A. Cuproptosis-related gene index: a predictor for pancreatic cancer prognosis, immunotherapy efficacy, and chemosensitivity. *Front Immunol* (2022) 13:978865. doi: 10.3389/fimmu.2022.978865

77. Liu T, Liu Q, Wang Y, Yang R, Tian F. Cuproptosis scoring model predicts overall survival and assists in immunotherapeutic decision making in pancreatic carcinoma. *Front Genet* (2022) 13:938488. doi: 10.3389/fgene.2022.938488

78. Li Y, Wang RY, Deng YJ, Wu SH, Sun X, Mu H. Molecular characteristics, clinical significance, and cancer immune interactions of cuproptosis and ferroptosis-associated genes in colorectal cancer. *Front Oncol* (2022) 12:975859. doi: 10.3389/fonc.2022.975859

79. Hou D, Tan JN, Zhou SN, Yang X, Zhang ZH, Zhong GY, et al. A novel prognostic signature based on cuproptosis-related lncrna mining in colorectal cancer. *Front Genet* (2022) 13:969845. doi: 10.3389/fgene.2022.969845

80. Du Y, Lin Y, Wang B, Li Y, Xu D, Gan L, et al. Cuproptosis patterns and tumor immune infiltration characterization in colorectal cancer. *Front Genet* (2022) 13:976007. doi: 10.3389/fgene.2022.976007

81. Wang L, Cao Y, Guo W, Xu J. High expression of cuproptosis-related gene fdx1 in relation to good prognosis and immune cells infiltration in colon adenocarcinoma (COAD). *J Cancer Res Clin Oncol [Preprint]* (2022). doi: 10.1007/s00432-022-04382-7

82. Swerdlow SH, Campo E, Pileri SA, Harris NL, Stein H, Siebert R, et al. The 2016 revision of the world health organization classification of lymphoid neoplasms. *Blood* (2016) 127(20):2375–90. doi: 10.1182/blood-2016-01-643569

83. Liu CJ, Hu FF, Xia MX, Han L, Zhang Q, Guo AY. Gscalite: A web server for gene set cancer analysis. *Bioinformatics* (2018) 34(21):3771–2. doi: 10.1093/bioinformatics/bty411

84. Wilkerson MD, Hayes DN. Consensusclusterplus: A class discovery tool with confidence assessments and item tracking. *Bioinformatics* (2010) 26 (12):1572–3. doi: 10.1093/bioinformatics/btq170

85. Senbabaoglu Y, Michailidis G, Li JZ. Critical limitations of consensus clustering in class discovery. *Sci Rep* (2014) 4:6207. doi: 10.1038/srep06207

86. Sturm G, Finotello F, Petitprez F, Zhang JD, Baumbach J, Fridman WH, et al. Comprehensive evaluation of transcriptome-based cell-type quantification methods for immuno-oncology. *Bioinformatics* (2019) 35(14):i436–i45. doi: 10.1093/bioinformatics/btz363

87. Rooney MS, Shukla SA, Wu CJ, Getz G, Hacohen N. Molecular and genetic properties of tumors associated with local immune cytolytic activity. *Cell* (2015) 160(1-2):48–61. doi: 10.1016/j.cell.2014.12.033

88. Geeleher P, Cox N, Huang RS. Prrophetic: An r package for prediction of clinical chemotherapeutic response from tumor gene expression levels. *PloS One* (2014) 9(9):e107468. doi: 10.1371/journal.pone.0107468

89. Ritchie ME, Phipson B, Wu D, Hu Y, Law CW, Shi W, et al. Limma powers differential expression analyses for rna-sequencing and microarray studies. *Nucleic Acids Res* (2015) 43(7):e47. doi: 10.1093/nar/gkv007

90. Friedman J, Hastie T, Tibshirani R. Regularization paths for generalized linear models *via* coordinate descent. *J Stat Softw* (2010) 33(1):1–22.

91. Simon N, Friedman J, Hastie T, Tibshirani R. Regularization paths for cox's proportional hazards model *via* coordinate descent. *J Stat Softw* (2011) 39(5):1–13. doi: 10.18637/jss.v039.i05

92. Blanche P, Dartigues JF, Jacqmin-Gadda H. Estimating and comparing time-dependent areas under receiver operating characteristic curves for censored event times with competing risks. *Stat Med* (2013) 32(30):5381–97. doi: 10.1002/sim.5958

93. Yu G, Wang LG, Han Y, He QY. Clusterprofiler: An r package for comparing biological themes among gene clusters. *OMICS* (2012) 16(5):284–7. doi: 10.1089/omi.2011.0118

94. Wu T, Hu E, Xu S, Chen M, Guo P, Dai Z, et al. Clusterprofiler 4.0: A universal enrichment tool for interpreting omics data. *Innovation (Camb)* (2021) 2 (3):100141. doi: 10.1016/j.xinn.2021.100141

95. Szklarczyk D, Franceschini A, Kuhn M, Simonovic M, Roth A, Minguez P, et al. The string database in 2011: functional interaction networks of proteins, globally integrated and scored. *Nucleic Acids Res* (2011) 39(Database issue):D561–8. doi: 10.1093/nar/gkq973

96. International Non-Hodgkin's Lymphoma Prognostic Factors P. A predictive model for aggressive non-hodgkin's lymphoma. *N Engl J Med* (1993) 329(14):987–94. doi: 10.1056/NEJM199309303291402

97. Babak MV, Ahn D. Modulation of intracellular copper levels as the mechanism of action of anticancer copper complexes: clinical relevance. *Biomedicines* (2021) 9(8):852. doi: 10.3390/biomedicines9080852

98. Oliveri V. Selective targeting of cancer cells by copper ionophores: An overview. *Front Mol Biosci* (2022) 9:841814. doi: 10.3389/fmolb.2022.841814

99. Xu B, Wang S, Li R, Chen K, He L, Deng M, et al. Disulfiram/copper selectively eradicates aml leukemia stem cells in vitro and in vivo by simultaneous induction of ros-jnk and inhibition of nf-kappab and Nrf2. *Cell Death Dis* (2017) 8 (5):e2797. doi: 10.1038/cddis.2017.176

100. Hedley D, Shamas-Din A, Chow S, Sanfelice D, Schuh AC, Brandwein JM, et al. A phase i study of elesclomol sodium in patients with acute myeloid leukemia. *Leuk Lymphoma* (2016) 57(10):2437–40. doi: 10.3109/10428194.2016.1138293

101. Brem SS, Zagzag D, Tsanaclis AM, Gately S, Elkouby MP, Brien SE. Inhibition of angiogenesis and tumor growth in the brain. suppression of endothelial cell turnover by penicillamine and the depletion of copper, an angiogenic cofactor. *Am J Pathol* (1990) 137(5):1121–42.

102. Yoshii J, Yoshiji H, Kuriyama S, Ikenaka Y, Noguchi R, Okuda H, et al. The copper-chelating agent, trientine, suppresses tumor development and angiogenesis in the murine hepatocellular carcinoma cells. *Int J Cancer* (2001) 94(6):768–73. doi: 10.1002/ijc.1537

103. Pan Q, Kleer CG, van Golen KL, Irani J, Bottema KM, Bias C, et al. Copper deficiency induced by tetrathiomolybdate suppresses tumor growth and angiogenesis. *Cancer Res* (2002) 62(17):4854–9.

104. Cox C, Teknos TN, Barrios M, Brewer GJ, Dick RD, Merajver SD. The role of copper suppression as an antiangiogenic strategy in head and neck squamous cell carcinoma. *Laryngoscope* (2001). doi: 10.1097/00005537-200104000-00024

105. Le A, Lane AN, Hamaker M, Bose S, Gouw A, Barbi J, et al. Glucose-independent glutamine metabolism *via* tca cycling for proliferation and survival in b cells. *Cell Metab* (2012) 15(1):110–21. doi: 10.1016/j.cmet.2011.12.009

106. Martinez-Reyes I, Diebold LP, Kong H, Schieber M, Huang H, Hensley CT, et al. Tca cycle and mitochondrial membrane potential are necessary for diverse biological functions. *Mol Cell* (2016) 61(2):199–209. doi: 10.1016/j.molcel.2015.12.002

107. Li M, Chiang YL, Lyssiotis CA, Teater MR, Hong JY, Shen H, et al. Non-oncogene addiction to sirt3 plays a critical role in lymphomagenesis. *Cancer Cell* (2019) 35(6):916–31 e9. doi: 10.1016/j.ccell.2019.05.002

108. Chen L, Monti S, Juszczynski P, Daley J, Chen W, Witzig TE, et al. Syk-dependent tonic b-cell receptor signaling is a rational treatment target in diffuse large b-cell lymphoma. *Blood* (2008) 111(4):2230–7. doi: 10.1182/blood-2007-07-100115

109. Ishida S, Lee J, Thiele DJ, Herskowitz I. Uptake of the anticancer drug cisplatin mediated by the copper transporter ctr1 in yeast and mammals. *Proc Natl Acad Sci U.S.A.* (2002) 99(22):14298–302. doi: 10.1073/pnas.162491399

110. Lin X, Okuda T, Holzer A, Howell SB. The copper transporter ctr1 regulates cisplatin uptake in saccharomyces cerevisiae. *Mol Pharmacol* (2002) 62 (5):1154–9. doi: 10.1124/mol.62.5.1154

111. Holzer AK, Manorek GH, Howell SB. Contribution of the major copper influx transporter ctr1 to the cellular accumulation of cisplatin, carboplatin, and oxaliplatin. *Mol Pharmacol* (2006) 70(4):1390–4. doi: 10.1124/mol.106.022624

112. Song IS, Savaraj N, Siddik ZH, Liu P, Wei Y, Wu CJ, et al. Role of human copper transporter ctr1 in the transport of platinum-based antitumor agents in cisplatin-sensitive and cisplatin-resistant cells. *Mol Cancer Ther* (2004) 3(12):1543–9.

113. Komatsu M, Sumizawa T, Mutoh M, Chen ZS, Terada K, Furukawa T, et al. Copper-transporting p-type adenosine triphosphatase (atp7b) is associated with cisplatin resistance. *Cancer Res* (2000) 60(5):1312–6.

114. Samimi G, Safaei R, Katano K, Holzer AK, Rochdi M, Tomioka M, et al. Increased expression of the copper efflux transporter atp7a mediates resistance to cisplatin, carboplatin, and oxaliplatin in ovarian cancer cells. *Clin Cancer Res* (2004) 10(14):4661–9. doi: 10.1158/1078-0432.CCR-04-0137

115. Liggett WHJr., Sidransky D. Role of the P16 tumor suppressor gene in cancer. *J Clin Oncol* (1998) 16(3):1197–206. doi: 10.1200/JCO.1998.16.3.1197

116. Jardin F, Ruminy P, Kerckaert JP, Parmentier F, Picquenot JM, Quief S, et al. Detection of somatic quantitative genetic alterations by multiplex polymerase chain reaction for the prediction of outcome in diffuse large b-cell lymphomas. *Haematologica* (2008) 93(4):543–50. doi: 10.3324/haematol.12251

117. Jardin F, Jais JP, Molina TJ, Parmentier F, Picquenot JM, Ruminy P, et al. Diffuse large b-cell lymphomas with cdkn2a deletion have a distinct gene expression signature and a poor prognosis under r-chop treatment: a gela study. *Blood* (2010) 116(7):1092–104. doi: 10.1182/blood-2009-10-247122

118. Lenz G, Wright GW, Emre NC, Kohlhammer H, Dave SS, Davis RE, et al. Molecular subtypes of diffuse large b-cell lymphoma arise by distinct genetic pathways. *Proc Natl Acad Sci U.S.A.* (2008) 105(36):13520–5. doi: 10.1073/pnas.0804295105

119. Tamura Y, Maruyama M, Mishima Y, Fujisawa H, Obata M, Kodama Y, et al. Predisposition to mouse thymic lymphomas in response to ionizing radiation depends on variant alleles encoding metal-responsive transcription factor-1 (Mtf-1). *Oncogene* (2005) 24(3):399–406. doi: 10.1038/sj.onc.1208197

120. Wise DR, DeBerardinis RJ, Mancuso A, Sayed N, Zhang XY, Pfeiffer HK, et al. Myc regulates a transcriptional program that stimulates mitochondrial glutaminolysis and leads to glutamine addiction. *Proc Natl Acad Sci U.S.A.* (2008) 105(48):18782–7. doi: 10.1073/pnas.0810199105

121. Wang JB, Erickson JW, Fuji R, Ramachandran S, Gao P, Dinavahi R, et al. Targeting mitochondrial glutaminase activity inhibits oncogenic transformation. *Cancer Cell* (2010) 18(3):207–19. doi: 10.1016/j.ccr.2010.08.009

122. Gross MI, Demo SD, Dennison JB, Chen L, Chernov-Rogan T, Goyal B, et al. Antitumor activity of the glutaminase inhibitor cb-839 in triple-negative breast cancer. *Mol Cancer Ther* (2014) 13(4):890–901. doi: 10.1158/1535-7163.MCT-13-0870

123. Xia X, Zhou W, Guo C, Fu Z, Zhu L, Li P, et al. Glutaminolysis mediated by malt1 protease activity facilitates pd-l1 expression on abc-dlbcl cells and contributes to their immune evasion. *Front Oncol* (2018) 8:632. doi: 10.3389/fonc.2018.00632

124. Zhang X, Shi Y, Weng Y, Lai Q, Luo T, Zhao J, et al. The truncate mutation of notch2 enhances cell proliferation through activating the nf-kappab signal pathway in the diffuse large b-cell lymphomas. *PloS One* (2014) 9(10):e108747. doi: 10.1371/journal.pone.0108747

125. Luduena RF. Are tubulin isotypes functionally significant. *Mol Biol Cell* (1993) 4(5):445–57. doi: 10.1091/mbc.4.5.445

126. Gao S, Wang S, Zhao Z, Zhang C, Liu Z, Ye P, et al. Tubb4a interacts with myh9 to protect the nucleus during cell migration and promotes prostate cancer *via* Gsk3beta/Beta-catenin signalling. *Nat Commun* (2022) 13(1):2792. doi: 10.1038/s41467-022-30409-1

127. Atjanasuppat K, Lirdprapamongkol K, Jantaree P, Svasti J. Non-adherent culture induces paclitaxel resistance in h460 lung cancer cells *via* erk-mediated up-regulation of betaiva-tubulin. *Biochem Biophys Res Commun* (2015) 466(3):493–8. doi: 10.1016/j.bbrc.2015.09.057

128. Tamura D, Arao T, Nagai T, Kaneda H, Aomatsu K, Fujita Y, et al. Slug increases sensitivity to tubulin-binding agents *via* the downregulation of betaiii and betaiva-tubulin in lung cancer cells. *Cancer Med* (2013) 2(2):144–54. doi: 10.1002/cam4.68

129. Kavallaris M, Kuo DY, Burkhart CA, Regl DL, Norris MD, Haber M, et al. Taxol-resistant epithelial ovarian tumors are associated with altered expression of specific beta-tubulin isotypes. *J Clin Invest* (1997) 100(5):1282–93. doi: 10.1172/JCI119642

130. Xu F, Zhang S, Liu Z, Gu J, Li Y, Wang L, et al. Tex9 and Eif3b functionally synergize to promote the progression of esophageal squamous cell carcinoma. *BMC Cancer* (2019) 19(1):875. doi: 10.1186/s12885-019-6071-9

131. van Dieck J, Teufel DP, Jaulent AM, Fernandez-Fernandez MR, Rutherford TJ, Wyslouch-Cieszynska A, et al. Posttranslational modifications affect the interaction of s100 proteins with tumor suppressor P53. *J Mol Biol* (2009) 394 (5):922–30. doi: 10.1016/j.jmb.2009.10.002

132. Donato R, Sorci G, Riuzzi F, Arcuri C, Bianchi R, Brozzi F, et al. S100b's double life: intracellular regulator and extracellular signal. *Biochim Biophys Acta* (2009) 1793(6):1008–22. doi: 10.1016/j.bbamcr.2008.11.009

133. Chan WJ. Pathogenesis of diffuse large b cell lymphoma. *Int J Hematol* (2010) 92(2):219–30. doi: 10.1007/s12185-010-0602-0

134. Sniegowski T, Korac K, Bhutia YD, Ganapathy V. Slc6a14 and slc38a5 drive the glutaminolysis and serine-glycine-one-carbon pathways in cancer. *Pharm (Basel)* (2021) 14(3):216. doi: 10.3390/ph14030216

frontiers | Frontiers in Oncology

TYPE Original Research
PUBLISHED 27 February 2023
DOI 10.3389/fonc.2023.1129405

OPEN ACCESS

EDITED BY
Satoshi Yoshihara,
Hyogo Medical University, Japan

REVIEWED BY
Stefano Aldo Pileri,
University of Bologna, Italy
Jorge Castillo,
Dana–Farber Cancer Institute,
United States

*CORRESPONDENCE
Hanno M. Witte
hanno.witte@uksh.de

†These authors have contributed equally to this work

‡These authors share senior authorship

SPECIALTY SECTION
This article was submitted to Hematologic Malignancies, a section of the journal Frontiers in Oncology

RECEIVED 21 December 2022
ACCEPTED 13 February 2023
PUBLISHED 27 February 2023

CITATION
Witte HM, Fähnrich A, Künstner A, Riedl J, Fliedner SMJ, Reimer N, Hertel N, von Bubnoff N, Bernard V, Merz H, Busch H, Feller A and Gebauer N (2023) Primary refractory plasmablastic lymphoma: A precision oncology approach. *Front. Oncol.* 13:1129405. doi: 10.3389/fonc.2023.1129405

Primary refractory plasmablastic lymphoma: A precision oncology approach

Hanno M. Witte[1,2*†], Anke Fähnrich[3,4,5†], Axel Künstner[3,4,5], Jörg Riedl[1,6], Stephanie M. J. Fliedner[1,5], Niklas Reimer[3,4,5], Nadine Hertel[1], Nikolas von Bubnoff[1,5], Veronica Bernard[6], Hartmut Merz[5], Hauke Busch[3,4,5‡], Alfred Feller[6‡] and Niklas Gebauer[1,5‡]

[1]Department of Hematology and Oncology, University Hospital of Schleswig-Holstein, Lübeck, Germany, [2]Department of Hematology and Oncology, Federal Armed Forces Hospital, Ulm, Germany, [3]Medical Systems Biology Group, Lübeck Institute of Experimental Dermatology, University of Lübeck, Lübeck, Germany, [4]Institute for Cardiogenetics, University of Lübeck, Lübeck, Germany, [5]University Cancer Center Schleswig-Holstein, University Hospital of Schleswig- Holstein, Lübeck, Germany, [6]Hämatopathologie Lübeck, Reference Centre for Lymph Node Pathology and Hematopathology, Lübeck, Germany

Introduction: Hematologic malignancies are currently underrepresented in multidisciplinary molecular-tumor-boards (MTB). This study assesses the potential of precision-oncology in primary-refractory plasmablastic-lymphoma (prPBL), a highly lethal blood cancer.

Methods: We evaluated clinicopathological and molecular-genetic data of 14 clinically annotated prPBL-patients from initial diagnosis. For this proof-of-concept study, we employed our certified institutional MTB-pipeline (University-Cancer-Center-Schleswig-Holstein, UCCSH) to annotate a comprehensive dataset within the scope of a virtual MTB-setting, ultimately recommending molecularly stratified therapies. Evidence-levels for MTB-recommendations were defined in accordance with the NCT/DKTK and ESCAT criteria.

Results: Median age in the cohort was 76.5 years (range 56-91), 78.6% of patients were male, 50% were HIV-positive and clinical outcome was dismal. Comprehensive genomic/transcriptomic analysis revealed potential recommendations of a molecularly stratified treatment option with evidence-levels according to NCT/DKTK of at least m2B/ESCAT of at least IIIA were detected for all 14 prPBL-cases. In addition, immunohistochemical-assessment (CD19/CD30/CD38/CD79B) revealed targeted treatment-recommendations in all 14 cases. Genetic alterations were classified by treatment-baskets proposed by Horak et al. Hereby, we identified tyrosine-kinases (TK; n=4), PI3K-MTOR-AKT-pathway (PAM; n=3), cell-cycle-alterations (CC; n=2), RAF-MEK-ERK-cascade (RME; n=2), immune-evasion (IE; n=2), B-cell-targets (BCT; n=25) and others (OTH; n=4) for targeted treatment-recommendations. The minimum requirement for consideration of a drug within the scope of the study was FDA-fast-track development.

Discussion: The presented proof-of-concept study demonstrates the clinical potential of precision-oncology, even in prPBL-patients. Due to the aggressive course of the disease, there is an urgent medical-need for personalized treatment approaches, and this population should be considered for MTB inclusion at the earliest time.

KEYWORDS

molecular tumor board, plasmablastic lymphoma, whole exome sequencing, whole transcriptome sequencing, recurrent aberrations, targeted therapy

Introduction

The success of targeted cancer therapies depends on the therapeutic detection of the targetable biomarker rather than the histologic subtype (1). Consequently, the number of basket trials investigating the efficacy of molecularly stratified therapeutic options is continuously increasing in recent years (2). Abandoning omnidirectional and unspecific treatment strategies, implementing multidisciplinary molecular tumor boards (MTB), and synchronous advancements in genomic profiling rapidly expand the spectrum of existing treatment strategies in cancer patients (3–5). To date, the implementation rate of effective MTB recommendations resulting in a beneficial outcome for cancer patients is in great need of improvement as most patients in the MTB setting are heavily pre-treated and at a very late stage within the course of the disease. Furthermore, the turn-around time for molecular and genetic diagnostic workups is between three and four weeks. Consecutively, recommended treatments are implemented in a minority of cases (4). Additionally, the performance of genomic profiling and allocation to rational therapies within the context of MTB evaluations is extremely heterogeneous (6, 7). Some Cancer Centers derive MTB recommendations merely from targeted panel sequencing, whereas others perform whole exome/genome sequencing (WES/WGS) potentially complemented with entire transcriptome sequencing (WTS) and epigenetic analyses resulting in a more refined understanding of variants and processes driving each cancer (6, 8, 9). However, the representation of hematologic malignancies in MTBs remains disproportionally low (4, 10) and MTB activities focus on solid tumors in most cases (4). Through implementing MTB platforms and growing experience with molecular diagnostics in a clinical setting, vast datasets for molecularly stratified treatments were generated (11). Consecutively, clinical outcome in personalized cancer therapies is steadily improving (12). At the same time, high-throughput sequencing and single-cell profiling allowed the refinement of the taxonomy, e.g. of aggressive B-cell non-Hodgkin lymphomas (B-NHL), uncovering novel potential therapeutically targetable vulnerabilities for personalized treatment strategies (13–17). Notably, the fusion of both fields, incorporating the advantages of state-of-the-art MTB diagnostics and decision-making as well as a growingly refined molecular understanding of hematological malignancies appear exceptionally promising, especially in rare entities associated with a dismal outcome such as plasmablastic lymphoma (PBL) (18). Poor prognosis and frequent concomitant HIV infections in younger PBL patients or immunodeficiency of other causes (e.g,. age-related immunosenescence or secondary to organ transplant recipients) underline the urgent need for novel therapeutic strategies (19, 20).

Moreover, this heterogeneous clientele of patients entails a relevant subgroup frequently not eligible for intensive treatment (21). The present study aimed to evaluate a subcohort of primary refractory (pr) PBL patients from a previous study by our group from the precision hematologist's perspective applying the certified institutional MTB pipeline (University Cancer Center Schleswig-Holstein, UCCSH) to a highly lethal blood cancer (20). Based on the histopathological and immunophenotypic assessment, whole exome and transcriptome sequencing data, immunological and genetic targets were individually annotated within the scope of a virtual MTB setting. This resulted in recommending immunologically and/or molecularly stratified treatment strategies for prPBL patients.

Methods

Study design and patient characteristics

For this proof-of-concept study, a virtual MTB approach was conducted in a retrospectively assembled cohort of prPBL aiming to address an urgent unmet medical need in an extremely rare and aggressive subtype of B-cell non-Hodgkin lymphoma of post-germinal origin. As previously reported, screening of our institutional database revealed 76 PBL cases whose biopsy specimens were transferred to the reference center for Haematopathology, University Hospital Schleswig Holstein Campus Lübeck and Haematopathology Lübeck for centralized histopathologic expert review between January 1998 and December 2020. Due to the rarity of this entity, the sample size was not statistically predetermined. The number of cases included in the study corresponds to all PBL cases that have been referred to the reference center of Hematopathology within two decades. Investigations were not randomized, and investigators were not blinded. After excluding PBL cases with insufficient or

unrepresentative tissue samples, the molecular landscape of PBL was characterized based on WES and WTS from 33 and 20 PBL cases, respectively (20). From this cohort, 14 PBL cases presented with the primary refractory disease were selected, deducing potential advantages from applying a certified MTB-pipeline approach in the era of precision oncology. No data were excluded from analyses.

Genomic and transcriptomic analysis

Sample preparation, whole exome, and RNA-sequencing from formalin-fixed, paraffin-embedded (FFPE) tissue sections, as well as the process of raw data preparation, filtering, and the detection of single nucleotide variants (SNVs), short insertions and deletions (indels), somatic copy number aberrations (SCNAs) and fusion genes, were performed as previously described by Witte et al. (20) and Künstner et al. (22). MSI sensor was applied for the detection of microsatellite instability (MSI). For gene expression analysis from RNA-seq data, STAR ALIGNER (version 2.7.2b) and MIXNORM were used. The hg19 genome served as the reference genome. Several steps of bioinformatic analysis are integrated into the institutional MTB pipeline at University Cancer Center Schleswig-Holstein (UCCSH), which is certified for routine clinical diagnostics (Figure 1).

MTB data preparation

Standardized sheets (genomic reports) that were constructed for MTB database research upon Medical Informatics for Research and Care in University Medicine (MIRACUM) pipeline analysis list the tumor mutational burden (TMB) and the percentual content of tumor cells (23). Apart from microsatellite (MSI) status, we calculated the *BRCA*ness score (cut-off ≥ 20%), and variant allele frequency (VAF) for each mutation and provided information regarding tumor heterogeneity as we reported on tumor subclones. Genomic reports were provided by the Medical Systems Biology Group (University of Lübeck). An individual genomic report was prepared for each case.

ANNOVAR was used for the annotation of filtered variants. Coverage for reference and alternative alleles for each variant was extracted using VCF- QUERY (VCFTOOLS version 0.1.13). Somatic variants were filtered as follows: at least 8 reads per base, minimum VAF of 5%, and only variants with a frequency below 0.001 in 1000 genomes, gnomAD, or ExAC, were considered for subsequent downstream analysis. Serving as a component for treatment prioritization, the effect of strong deleterious effects (CADD phred score > 20) was assessed per sample, and a gene set variation analysis was performed for WES and RNA-seq data against HALLMARK gene sets. More details on bioinformatics are provided in the Supplementary Material.

MTB annotation and data analysis

In the first step, the recurrence of a genomic alteration was checked to employ the databases COSMIC, OncoKB (prognostic & diagnostic levels), ClinVar (clinically relevant variation), and cBioPortal. Afterward the functional relevance of an alteration was verified with ProteinPaint. Once an alteration was found to be recurrent as well as functionally relevant, its therapeutic vulnerability was annotated with CIVIC, OncoKB (therapeutic & FDA levels), Cancer-Genome-Interpreter (CGI), and the Drug-Gene-Interaction database (DGIdb) in a third step of database research (Figure 1). Apart from genomic alterations, we included immunohistochemical findings identified upon histopathologic diagnostics (CD19, CD30, CD38, and CD79B) to potentially serve as a relevant therapeutic target (Supplemental Table 1). A rationale for an immunotherapeutic strategy was recommended if a high TMB status was detected (≥10 mut/Mb) or in samples with MSI high status.

Finally, the annotation ended up concluding research of ongoing studies on https://clinicaltrials.gov and preclinical data on https://pubmed.ncbi.nlm.nih.gov. Only resources open for academic research purposes were considered for MTB recommendations. Evidence levels for MTB recommendations were defined in accordance with the NCT/DKTK MASTER program (Figure 1) and with the European Society for Medical Oncology Scale for Actionability of Molecular Targets (ESCAT) (4, 24). Additionally, genetic alterations were classified by biomarker/treatment baskets proposed by Horak et al. (Figure 1) (4).

Prioritization of therapeutic vulnerabilities

The relevance of genomic alterations was considered based on VAF and CADD score. Variants of unknown significance were excluded. Each recommended drug was either approved by the Food and Drug Administration (FDA) and/or European Medicines Agency (EMA) or at least designated for FDA fast-track development as a minimum requirement for consideration within the scope of this study (cutoff date 31st October 2022).

Treatment was recommended if at least one agent targeted at least one genomic alteration, one protein with relevant expression levels or if the TMB status was high. As data on the efficacy of agents targeting a non-mutated pathway component up- or downstream in an altered pathway detected upon gene set enrichment analysis remains insufficient, such agents were not considered for MTB recommendations. We excluded immunotherapeutic rationales based on the mutational signature SBS26, which was found in 6 cases as this rationale represents a biological rationale, so far lacking clinical validation (25).

Considering the matching score (MS) calculation by Sicklick et al., we adapted the calculation to our retrospective virtual MTB setting and provided a modified matching score (mMS) for each PBL case (26). The calculation was performed by dividing the number of alterations serving as a potential target for recommended drugs by the total number of characteristic alterations after excluding variants of unknown significance and a VAF lower than 5%. Apart from genomic alterations, immunohistochemical targets and immunotherapeutic rationales (TMB > 10mut/Mb, MSI status), as well as positive *BRCA*ness scoring pleading for PARP-inhibition, were considered equally for

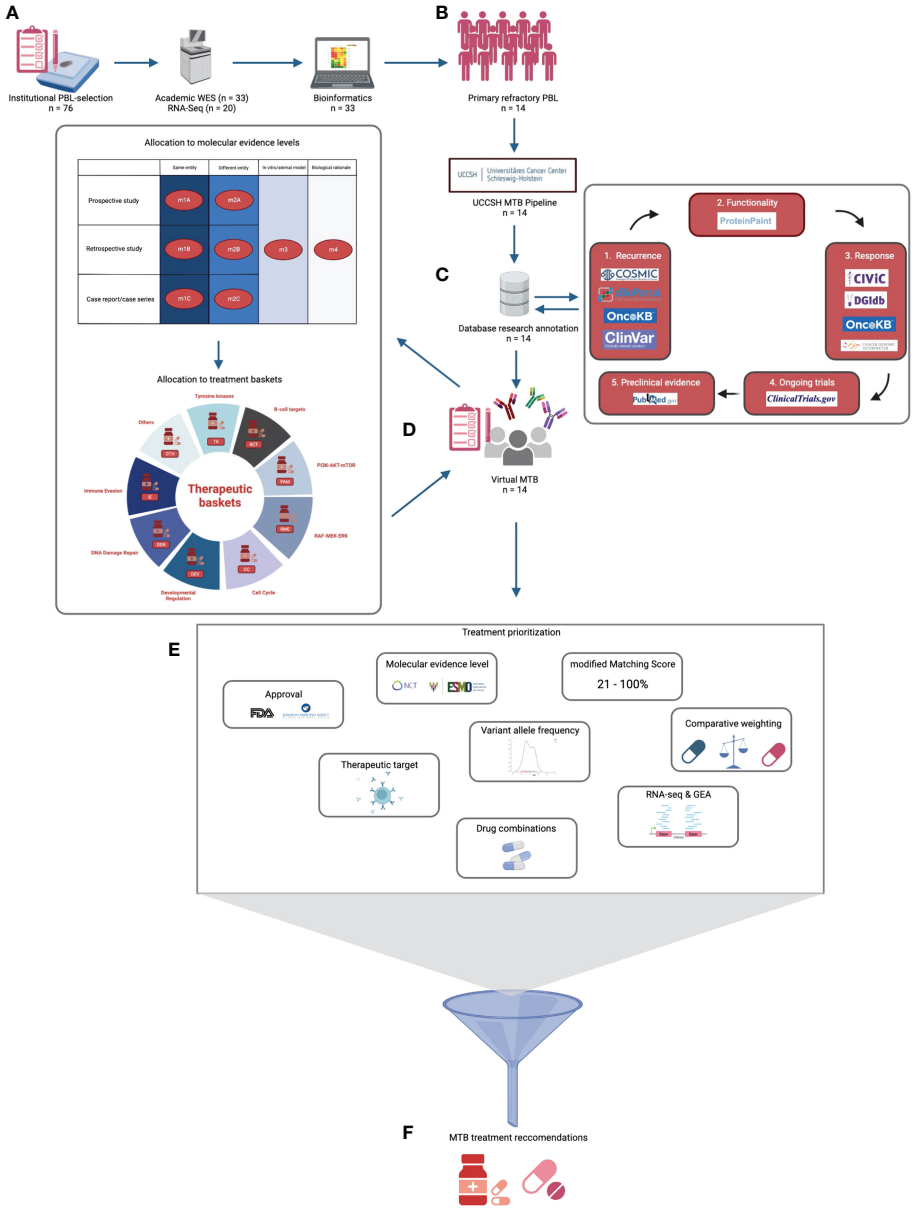

FIGURE 1
Virtual UCCSH molecular tumor board workflow for primary refractory plasmablastic lymphomas (prPBL). **(A)** After institutional PBL selection, academic WES and RNA-seq were performed in 33 and 20 cases, respectively. **(B)** Consecutively, 14 prPBL cases were identified and underwent UCCSH MTB pipeline evaluation. **(C)** Afterwards, manual database research annotation was conducted for each relevant variant. **(D)** In a virtual MTB setting, each prPBL case was discussed. Potential therapeutic vulnerabilities were allocated to molecular evidence levels and to treatment baskets. **(E)** Multifactorial treatment prioritization process revealed **(F)** MTB treatment recommendations.

mMS calculation. In the present calculation, a synergistic and well-established drug combination targeting the same aberration (such as dabrafenib plus trametinib for *BRAF* mutations) the impact was counted as one. Results ranged from 0% to 100%. Higher scores represented better matches.

$$mMs(\%) = \frac{x}{y} \times 100$$

x = number of targetable vulnerabilities

(genomic alterations + IHC + MSI - high status + TMB - high status + BRCAness score)

y = number of characteristic and significant alterations

(targetable + un - targetable with a VAF ≥ 5%)

Combinations of drugs were considered and recommended according to the I-PREDICT study (9). Congruent to the approach of Sicklick et al. (9), the participating pharmacist screened each potential combination for feasibility in the light of drug interactions.

Each mutation was proved for its biological relevance and conclusiveness based on VAF, gene set enrichment analysis, and RNA-sequencing data, if available.

In summary, the prioritization of MTB recommendations was a multifactorial process simultaneously considering several considerations (Figure 1, Supplementary Table 2).

Virtual MTB setting

The detailed MTB workflow is visualized in Figure 1. In total, we performed three rounds of virtual multicentre MTB conferences in accordance with the institutional standards of UCCSH, retrospectively discussing the 14 prPBL cases (1st round: 4 cases; 2nd round: 5 cases; 3rd round: 5 cases). A board-certified hematologist presented the case. The conference included at least a molecular oncologist, a bioinformatician, a pathologist, a pharmacist, a radiologist, and a medical geneticist. Centralized documentation of MTB recommendations was conducted in each case (Supplementary Material).

Data availability

Data was taken from accession number EGAD00001006795 (European genome-phenome archive (EGA)).

Ethical regulation

This retrospective study was approved by the ethics committee of the University of Lübeck (reference no. 18-311), conducted in accordance with the Declaration of Helsinki, and patients have provided written informed consent regarding routine diagnostic and academic assessment, including genomic studies of their biopsy specimen in addition to the transfer of their clinical data.

Results

Patient characteristics and clinical outcome

Here, we report on the potential of molecularly stratified treatment options in 14 cases presenting with prPBL (median age 76.5 years, range 56 - 91). Additional PBL cases responding to initial cytoreductive treatment served as a comparison cohort (n = 19) (20). The majority of patients were male (11/14; 79%) and presented with advanced-stage disease (10/14; 71%) as well as an adverse prognostic constellation (11/14; 79% had an NCCN-IPI scoring ≥4). All patients had elevated lactate dehydrogenase (LDH) serum levels and the frequency of reduced performance status, according to the Eastern Cooperative Oncology Group (ECOG), demonstrated the frailty of patients included in the present cohort. Half of the current cohort was HIV positive (7/14 cases) and had underlying EBV (7/14 cases) infections at initial diagnosis. In 6 cases, we detected both HIV and EBV infections (43%). Cytoreductive treatment was applied in 13/14 cases (92.8%). More than half of the patients (8/14; 57%) received a CHOP-based (cyclophosphamide, hydroxydaunorubicin, vincristine, and prednisolone) treatment in 1st line setting. In relapsed or refractory settings, 10/14 (71.4%) patients were eligible for 2nd line cytoreductive treatment. Across any line of treatment, only five PBL patients responded to therapy (partial remission; PR), and another five PBL patients had stable disease (SD) as the best response. Three PBLs were completely refractory (progressive disease; PD) towards any treatment approach, and one PBL died shortly after initial clinical presentation. This underlines the urgent unmet clinical need for individualized treatment options among rare entities in hematology, such as PBL. Tumor cell content, immunohistochemical findings, and the contribution of *MYC* alterations were comparable between primary refractory cases and the comparison cohort. All baseline clinicopathological characteristics are summarized in Table 1.

The course of the disease, information on clinical characteristics, and treatment sequences for each prPBL case is visualized in Figure 2A. Survival analysis revealed significantly inferior PFS ($p< 0.0001$) and OS ($p = 0.002$) in prPBL compared to those cases responding to first-line treatment (Figure 2B).

Genomic profiling in primary refractory plasmablastic lymphomas

Since the genomic and transcriptomic landscape of PBL recently has been described comprehensively (20, 27, 28), we

TABLE 1 Baseline clinicopathological characteristics in primary refractory PBL.

Characteristic	Primary refractory PBL (n = 14)	Comparison cohort PBL (n = 19)
Age, median (range), y	76.5 (56 – 91)	60 (32 - 83)
Sex		
Female	3 (21%)	7 (37%)
Male	11 (79%)	12 (63%)
HIV positivity	7 (50%)	7 (37%)
EBV positivity	7 (50%)	13 (68%)
HIV and EBV positivity	6 (43%)	10 (53%)

(Continued)

10.3389/fonc.2023.1129405

TABLE 1 Continued

Characteristic	Primary refractory PBL (n = 14)	Comparison cohort PBL (n = 19)
NCCN-IPI		
Low risk	-	3 (16%)
Low intermediate risk	3 (21%)	7 (37%)
High intermediate risk	4 (29%)	3 (16%)
High risk	7 (50%)	6 (32%)
Stage (Ann Arbor)		
I - II	4 (29%)	10 (53%)
III - IV	10 (71%)	9 (47%)
B-symptoms	8 (57%)	7 (37%)
Extranodal sites		
0	3 (21%)	1 (5%)
1 - 2	10 (71%)	17 (89%)
>2	1 (7%)	1 (5%)
ECOG-PS		
0 - 1	4 (29%)	12 (63%)
≥ 2	10 (71%)	7 (37%)
Elevated LDH	14 (100%)	9 (47%)
Tumor cell content, median (range)	70% (60 - 90%)	70% (55 - 85%)
Immunohistochemistry		
CD38	14 (100%)	19 (100%)
CD19	5 (36%)	8 (42%)
CD30	2 (14%)	5 (26%)
CD79B	4 (29%)	6 (32%)
Ki-67, median (range)	78% (60 - 90%)	80% (60 - 90%)
Chromosomal aberration		
MYC overall	10 (71%)	16 (84%)
MYC amplification	5 (36%)	7 (37%)
MYC split	5 (36%)	9 (47%)
Median TMB in mut/Mb (range)	4.06 (2.18 - 9.87)	3.09 (1.38 - 8.42)
Frontline therapy regimen		
CHOP-like	8 (57%)	13 (68%)
Bendamustine-like	3 (21%)	-
Others	2 (14%)	4 (21%)
Refusal or no treatment	1 (7%)	2 (11%)
Frontline therapy SAE (grade 3-5)		
Polyneuropathy	2 (14%)	3 (16%)
Acute kidney injury	3 (21%)	2 (11%)
Febrile neutropenia	4 (29%)	4 (21%)
Sepsis	5 (36%)	2 (11%)

CHOP, cyclophosphamide/hydroxydaunorubicin/vincristine/prednisolone; EBV, Epstein Barr virus; ECOG-PS, Eastern Cooperative Oncology Group performance status; HIV, human immunodeficiency virus; LDH, lactate dehydrogenase; Mb, megabase; mut, mutations; NCCN-IPI, National Comprehensive Cancer Network International Prognostic Index; PBL, plasmablastic lymphoma; SAE, severe adverse event; TMB, tumor mutational burden; y, years.

carved out genomic features of primary refractory cases to detect potential therapeutic vulnerabilities in this difficult-to-treat hematologic malignancy and verified their biological significance based on transcriptomic data.

Our WES analysis revealed 3,955 SNVs and indels involving 2,700 genes after variant filtering. Investigations regarding the functionality of such mutations revealed that 17.1% were functionally relevant, whereas 26.5% were functionally neutral, and 56.4% were found to be functionally inconclusive. Across the detected mutations, the most frequent alterations were missense mutations (74.2%), followed by frameshift mutations (16.1%; indels) and nonsense mutations (9.7%). Further investigations revealed loss of function (LOF) in 48.4% and gain of function (GOF) in 51.6% among the spectrum of mutations (Figure 2C). The median TMB was slightly higher in primary refractory cases (4.06 mut/Mb in primary refractory PBL vs. 3.09 mut/Mb in the comparison cohort; Figure 2D; Supplemental Table 3). Given the limited sample size, this result was statistically insignificant ($p = 0.337$). TMB values in PBL displayed an overall low to intermediate TMB (29, 30). As previously reported, no evidence for MSI-based hypermutations in PBL, and matched germline DNA was not available for comparative analysis (20). After the identification of

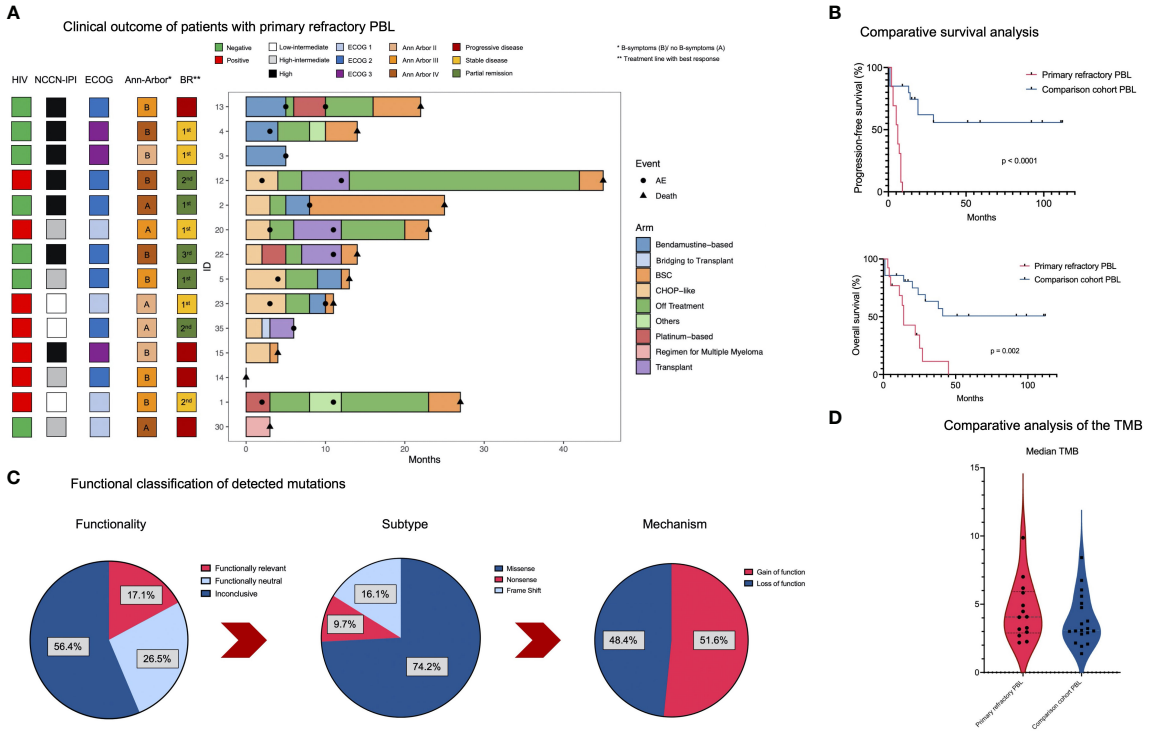

FIGURE 2
Clinical and genomic features in prPBL. **(A)** The swimmer plot illustrates the clinical course of the disease for each prPBL case. **(B)** Kaplan Meier survival analysis (PFS and OS) comparing prPBL cases and the comparison cohort which were not associated with primary refractory disease. **(C)** Pie charts outlining functionality, the mutational subtype and the mechanism of detected mutations. **(D)** Comparative median TMB calculation between prPBL and the comparison group.

mutational subtypes and their functionality, the MIRACUM pipeline analysis identified 26 relevant genes carrying driver mutations (Figure 3A).

Annotation of therapeutic vulnerabilities

In total, MIRACUM pipeline analysis identified 47 variants potentially driving cancer growth across 26 genes in the cohort of 14 prPBL. Among these variants, individualized database research assigned potential treatment recommendations for 15 variants involving 9 genes. For targets amenable to multiple agents, we favored agents with the highest level of evidence according to the NCT/DKTK classification (reference). The heterogeneous spectrum of treatment recommendations comprised well-known agents such as idelalisib (targeting *PI3KCD*) (31) or everolimus (targeting *mTOR*) (32) and novel agents such as eprenetapopt (targeting *TP53*) (33), napabucasin (targeting *STAT3*) (34) or bemarituzumab (targeting *FGFR2*) (35). Moreover, recurrent LOF variants in *TP53* were previously related to treatment recommendations with CDK4/6 inhibitors (e.g., palbociclib/abemaciclib) (4). However, novel data suggest the inefficacy of CDK4/6 inhibitors in *TP53*-mutated malignancies as such mutations promote resistance to this class of drugs prompting us to exclude this recommendation (36). Results from the conducted MIRACUM pipeline analysis are outlined in Figure 3A.

Second, treatment recommendations based on immunohistochemical investigations were found in each case. Among the four immunohistochemical targets, a rationale for anti-CD38 (e.g., daratumumab) (37), anti-CD19 (e.g., tafasitamab) (38), anti-CD30 (brentuximab vedotin) (39) and anti-CD79B (e.g., polatuzumab vedotin) (40) was found in 14/14 (100%), 6/14 (43%), 2/14 (14%) and 2/14 (14%) cases, respectively (Figure 3A).

Third, exhaustive database research and annotation for recurrent genomic alterations beyond the MIRACUM pipeline analysis revealed four additional targetable mutations potentially acting as relevant drivers (*ERBB2, KIT, IDH2*, and *TET2*) (Figure 3B). In the era of precision oncology, alterations in such genes represent trailblazers for molecularly stratified treatment strategies. Further characteristics of annotated mutations are summarized in Supplemental Table 4. Particular attention was paid to the functional alignment concerning the biological significance and conclusiveness of each annotated mutation.

For potential treatment recommendations emerging from the annotation process, FDA approval was available for 14 agents, EMA was approved for 12 agents, and three agents were designated for FDA fast-track development (Figure 3C).

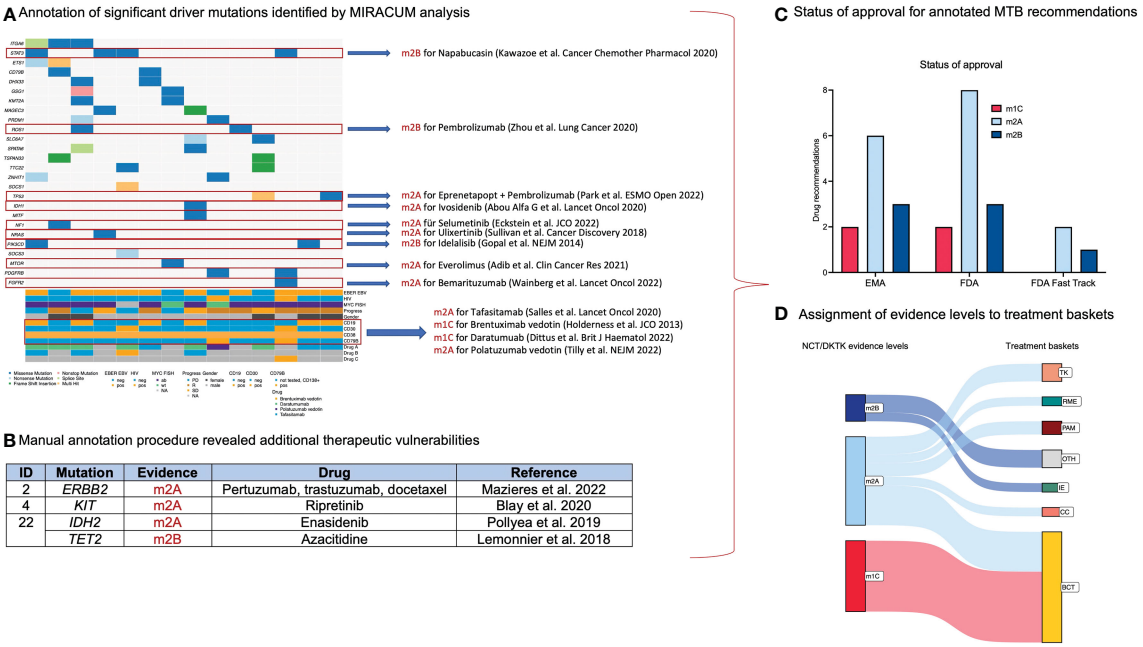

B Manual annotation procedure revealed additional therapeutic vulnerabilities

ID	Mutation	Evidence	Drug	Reference
2	*ERBB2*	m2A	Pertuzumab, trastuzumab, docetaxel	Mazieres et al. 2022
4	*KIT*	m2A	Ripretinib	Blay et al. 2020
22	*IDH2*	m2A	Enasidenib	Pollyea et al. 2019
	TET2	m2B	Azacitidine	Lemonnier et al. 2018

FIGURE 3
Results from manual database research and annotation of relevant genomic alterations. **(A)** Oncoplot summarizes relevant driver mutations and immunohistochemical targets detected upon MIRACUM pipeline analysis and potential therapeutic options. **(B)** Additional therapeutic vulnerabilities resulting from manual annotation procedure. **(C)** Bar plot visualizing the status of approval for annotated therapeutic options. **(D)** Sankey plot assigning molecular evidence levels to treatment baskets.

Immunotherapeutic strategies and homologous recombination deficiency

There exists a rationale for immune checkpoint blockade in tumors with high TMB status and DNA MMR deficiency (41–44). We used a cut-off for TMB-high status of ≥10 mut/Mb (43). Contrary to expectations, all PBL cases presented with a TMB<10 mut/Mb. In six cases, we found a predominant DNA MMR deficiency signature (single base substitution signature SBS26) (25, 45). For this constellation, the rationale for immunotherapy based on a mutational signature associated with DNA MMR deficiency corresponds to a molecular evidence level no higher than m3/m4 (*in vitro* data/biologic rationale). Consequently, there was no TMB- or DNA-MMR-deficiency-related recommendation for immunotherapy in the present prPBL cohort. However, immune checkpoint blockade was recommended in two cases (X%) harboring *ROS1* alterations associated with resistance towards crizotinib and other targeted agents by propagating an immune escape mechanism (46). Moreover, we applied the calculation of the UCCSH MTB-pipeline BRCAness score (based on SBS6 signature) to predict the responsiveness towards PARP inhibitors (47). The *BRCA*ness score incorporates mutations coming along with homologous recombination deficiency (HRD), such as *BRCA1* or *BRCA2* losses or alterations mimicking these losses (*ATM, CHEK2, RAD51*) (48). In the present cohort, *BRCA*ness scoring revealed no evidence for PARP inhibition.

Molecular evidence levels and assignment to therapeutic baskets

This proof-of-concept approach evaluated treatment options associated with NCT-DKTK molecular levels of evidence of at least m2B or higher for each prPBL case beyond anti-CD38 antibodies (daratumumab: 14x m1C rationale, ESCAT tier IIA; 32%). In the light of therapeutically addressable genomic alterations, 19 potential therapeutic vulnerabilities were assigned to m2A (n = 10; 23%) or m2B (n = 9; 20%) rationales. As already stated, immunohistochemical targets displayed a promising therapeutic option in primary refractory PBL. Assignment to molecular evidence levels revealed two m1C (brentuximab vedotin; 5%) and nine m2A (tafasitamab and polatuzumab vedotin; 20%) rationales.

Considering ESMO Scale for Clinical Actionability of molecular Targets (ESCAT) (reference), it has to be mentioned that recommendations based on higher ESCAT levels can hardly be reached in rare entities, especially among the spectrum of hematologic malignancies, due to the lack of prospective (randomized) clinical trials and their underrepresentation in MTB settings. Consequently, the experience in the molecularly stratified treatment of rare hematologic malignancies lags far behind recent developments in the field of solid tumors. However, the assignment of ESCAT evidence levels to therapeutic vulnerabilities found in this difficult-to-treat entity allocated 8 recommendations to ESCAT tier IC (18%), 14 recommendations to ESCAT tier IIA (32%), two recommendations to ESCAT tier IIB (5%) and 20 recommendations

were allocated to ESCAT tier IIIA (45%). More preclinical options (NCT DKTK evidence level m3/m4 or ESCAT tier IV/V) were not considered in the present cohort, characterized by an urgent need for treatment recommendations in primary refractory setting due to the aggressive biologic features in PBL.

The calculation of the mMS ranged from 21% to 100% (median: 50%). In eight cases, a mMS of ≥ 50% was calculated (57%). The prognostic impact of the mMS remains speculative at this point, as no recommended treatment was administered in this virtual setting. However, the higher the mMS, the more alterations and pathways relevant to each case can be addressed upon recommended treatment strategies. Therefore, it can be expected that the mMS will be associated with overall response rates (ORR) and patient outcomes referring to the MS calculation reported in the I-PREDICT study (9).

The assignment to treatment baskets was made under the consideration of the drug's mechanism of action rather than its functionality regarding the targeted alteration. According to baskets, we identified tyrosine kinases (TK; n=5), PI3K-MTOR-AKT pathway (PAM; n=3), cell cycle alterations (CC; n=2), RAF-MEK-ERK cascade (RME; n=2), immune evasion (IE; n=2) and others (OTH; n=4) for targeted treatment recommendations. An additional treatment basket based on B-cell-specific immunohistochemical markers has been added: B-cell targets (BCT; n=25) representing the elementary therapeutic basket in the present study (Figure 3D). Our analysis revealed 3.0 MTB recommendations in the median across the entire cohort of prPBL (range 2 – 5) (Figure 4A). All potential MTB treatment recommendations are summarized in Table 2.

Transcriptomic profiling and verification of biological significance

RNA-sequencing data was available in 10 cases (71.4%). A gene set enrichment analysis and an integrated analysis of WES and RNA-seq data were performed for these cases. RNA expression patterns were used to underline or refute the biological significance of an annotated and potentially addressable mutation (Figure 4B). Based on this integrated analysis, one potential candidate driver mutation (*KIT*) was excluded as we evaluated inconclusive results for mRNA expression. *KIT* represents an oncogene, and consecutively we expected an overexpression of *KIT* mutation-related transcripts. However, the present analysis revealed an inconclusive under-expression. Others (n = 18) were found to be conclusive. We assumed driver mutations to be recurrent based on database research, functionally relevant based on RNA expression patterns, and represent an essential mutation within an altered pathway enriched in a sample (49). Following these criteria, we identified seven conclusive driver mutations (one in a tumor suppressor gene and six in oncogenes) and nine conclusive mutations in oncogenes, as well as one conclusive mutation in a tumor suppressor gene (Figure 4B). However, the significance of specific variants (driver or not) remained unresolved due to the lack of RNA-seq data in four cases. In such cases, a variant was categorized as a provisional mutation but not as a driver mutation.

Apart from this, RNA-seq did not reveal a distinct transcriptomic signature of prPBL compared to the comparison cohort

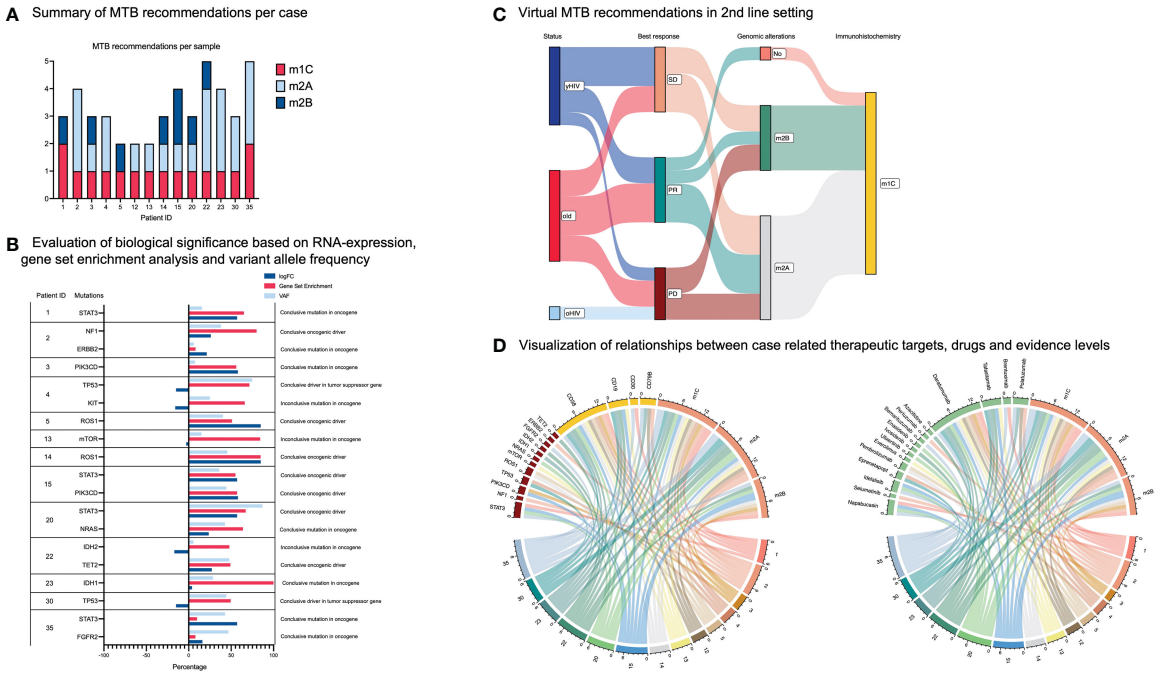

FIGURE 4
Therapeutic targets und treatment recommendations. **(A)** Case-related summary of MTB recommendations and associated molecular evidence levels. **(B)** Evaluation of RNA expression, gene set enrichment analysis and variant allele frequency (VAF) for each mutation serving as a therapeutic vulnerability. **(C)** Sankey plot allocating patients dependent on HIV status and age. The plot shows the best response of prPBL patients after standard chemotherapy. Moreover, the Sankey plot illustrates therapeutic vulnerabilities beyond standard chemotherapy based on genomic alterations and immunohistochemical targets. **(D)** Both chord plots demonstrate the relationships between cases and potential therapeutic targets, drugs and related evidence levels.

10.3389/fonc.2023.1129405

TABLE 2 Summary of MTB treatment recommendations.

ID	Target	Drug	NCT DKTK EL	ESCAT	Approval	mMS
1	CD38	Daratumumab	m1C	IIA	EMA/FDA	50%
	CD30	Brentuximab vedotin	m1C	IIB	EMA/FDA	
	STAT3	Napabucasin	m2B	IC	FDA-FT	
2	CD38	Daratumumab	m1C	IIA	EMA/FDA	44%
	CD79B	Polatuzumab vedotin	m2A	IIIA	EMA/FDA	
	NF1	Selumetinib	m2A	IIIA	EMA/FDA	
	ERBB2	Pertuzumab, trastuzumab, docetaxel	m2A	IIIA	EMA/FDA	
3	CD38	Daratumumab	m1C	IIA	EMA/FDA	50%
	PIK3CD	Idelalisib	m2B	IIIA	EMA/FDA	
4	CD38	Daratumumab	m1C	IIA	EMA/FDA	60%
	TP53	Eprenetapopt + pembrolizumab	m2A	IC	FDA-FT	
	KIT	Ripretinib	m2A	IIIA	EMA/FDA	
5	CD38	Daratumumab	m1C	IIA	EMA/FDA	43%
	ROS1	Pembrolizumab	m2B	IIIA	EMA/FDA	
12	CD38	Daratumumab	m1C	IIA	EMA/FDA	38%
	CD79B	Polatuzumab vedotin	m2A	IIIA	EMA/FDA	
13	CD38	Daratumumab	m1C	IIA	EMA/FDA	40%
	mTOR	Everolimus + pazopanib	m2A	IIIA	EMA/FDA	
14	CD38	Daratumumab	m1C	IIA	EMA/FDA	21%
	CD19	Tafasitamab	m2A	IIIA	EMA/FDA	
	ROS1	Pembrolizumab	m2B	IIIA	EMA/FDA	
15	CD38	Daratumumab	m1C	IIA	EMA/FDA	45%
	CD19	Tafasitamab	m2A	IIIA	EMA/FDA	
	STAT3	Napabucasin	m2B	IC	FDA-FT	
	PIK3CD	Idelalisib	m2B	IIIA	EMA/FDA	
20	CD38	Daratumumab	m1C	IIA	EMA/FDA	57%
	STAT3	Napabucasin	m2B	IC	FDA-FT	
	NRAS	Ulixertinib	m2A	IC	FDA-FT	
22	CD38	Daratumumab	m1C	IIA	EMA/FDA	50%
	CD19	Tafasitamab	m2A	IIIA	EMA/FDA	
	IDH2	Enasidenib + azacitidine	m2A	IIIA	FDA	
	TET2	Azacitidine	m2B	IIIA	EMA/FDA	
23	CD38	Daratumumab	m1C	IIA	EMA/FDA	57%
	CD19	Tafasitamab	m2A	IIIA	EMA/FDA	
	CD79B	Polatuzumab vedotin	m2A	IIIA	EMA/FDA	
	IDH1	Ivosidenib + azacitidine	m2A	IC	FDA	
30	CD38	Daratumumab	m1C	IIA	EMA/FDA	100%
	CD19	Tafasitamab	m2A	IIIA	EMA/FDA	
	TP53	Eprenetapopt + pembrolizumab	m2A	IC	FDA-FT	

(Continued)

TABLE 2 Continued

ID	Target	Drug	NCT DKTK EL	ESCAT	Approval	mMS
35	CD38	Daratumumab	m1C	IIA	EMA/FDA	71%
	CD30	Brentuximab vedotin	m1C	IIB	EMA/FDA	
	CD79B	Polatuzumab vedotin	m2A	IIIA	EMA/FDA	
	STAT3	Napabucasin	m2B	IC	FDA-FT	
	FGFR2	Bemarituzumab	m2A	IIIA	EMA-FT	

(Supplementary Figure 1). However, we found exclusive expression patterns of *TAF9, CCDC125, ALMS1*and *ZNF462* in prPBL but not in the comparison cohort. RNA expression of such genes did not contribute novel insights into the pathogenesis of these difficult-to-treat cases.

Congruent to previous results published by our work group, the current re-evaluation of RNA-seq data did not reveal any novel, recurrent, and therapeutically relevant genomic fusion beyond those affecting *MYC* (Supplemental Table 5).

Drug combinations

MTB recommendations for drug combinations considered insights from previous studies such as the I-PREDICT (NCT02534675) or the TOP-ART trials (NCT03127215) and other studies investigating the efficacy of drug combinations within the context of targeted therapies (9). Previous studies highlighted the advantages of drug combinations in molecularly stratified treatment settings (9). Preferably, drug combinations were chosen based on available datasets demonstrating their feasibility and efficacy in distinct entities or basket trials (11/14 cases; 79%). Novel drug combinations were selected considering the potential of overlapping drug toxicities, the molecular evidence levels for involved single agents, and the availability of such agents. Due to a distinct toxicity profile, immune checkpoint inhibition was a promising component for several drug combinations (4/14 cases; 29%). Moreover, several therapeutic options identified by immunohistochemical assessment harbored the potential for various additional drug combinations in all cases (Supplemental Table 6). There is growing evidence for using immunotherapeutic agents and/or agents targeting immunohistochemical assessable structures in the context of cytoreductive drug combinations in MTB settings as those combinations represent the standard of care among a variety of both solid and hematologic malignancies (40, 50, 51). However, there is still significant room for improvement in determining the combination of targeted therapeutics in the era of precision oncology.

Summary of virtual MTB recommendations

The median turnaround time from DNA/RNA isolation to virtual MTB recommendations was 28 days. In this virtual MTB approach, solely recommendations on treatment but not additional diagnostics were enunciated. After the exclusion of one inconclusive mutation upon integrated WES and RNA-seq analysis, the standardized institutional UCCSH MTB pipeline application revealed 43 treatment recommendations across the 14 cases of prPBL. Because PBL represents an extremely rare and aggressive hematologic malignancy, most recommendations were based on evidence deduced from evidence generated in different entities (m2A-B; 28/43 recommendations; 65%). Subsequently, class m1 evidence (NCT-DKTK) was gained from case reports (m1C; 16/43 recommendations; 37%) as prospective clinical trials are in short supply (37, 39, 52).

As outlined in the methods section, treatment prioritization reflected a multifactorial process that incorporated patient-related clinical features (such as ECOG-PS), drug availability, molecular evidence levels, the calculation of the mMS, the modality of a therapeutic target, the biologic significance of an alteration (based on RNA-seq data, VAF and gene set enrichment analysis) and the feasibility of drug combinations. Most recommendations were based on single agents (38/43; 88%). The spectrum of MTB recommendations expanded when potential drug combinations were considered (28 additional recommendations, Supplementary Table 6), and/or alternative agents to preferred recommendations were considered as well (10 additional recommendations; Supplementary Table 7). The decision towards the preference for a specific agent over another addressing the same target was made based on available molecular evidence levels (e.g., daratumumab = m1C versus isatuximab = m2A).

In summary, whole exome and partially whole transcriptomic sequencing data of 14 primary refractory PBL cases were processed through the UCCSH MTB pipeline. They revealed a total of 43 treatment recommendations in this aggressive and chemo-refractory hematologic B-cell malignancy. Treatment recommendations comprised molecular evidence levels from m2B to m1C rationales. The heterogeneous distribution of treatment basket allocations underlines the diversity of potential treatment strategies in a virtual second-line setting (Figure 4C), and demonstrates the relevance of molecular diagnostics in rare and aggressive B-cell malignancies such as PBL. The interdependence between case-related targets, treatment recommendations, and evidence levels is visualized in Figure 4D.

Discussion

Our virtual approach of a molecular tumor board provides evidence for promising therapeutic options and draws attention to an urgent medical need in this patient population which is yet

underrepresented in MTB efforts. Including 1st line treatment, therapeutic options are limited and often ineffective for PBL (53). Our work provides evidence that applying a validated MTB pipeline might open up therapeutic avenues for prPBL, a highly lethal blood cancer, serving as a role model for rare and aggressive hematologic neoplasms.

Several challenges are coming along with the introduction of an MTB process for patients with highly proliferative hematologic malignancies. One challenge is the transit of a histologic sample from making the correct diagnosis to MTB recommendations within a preferably short timeframe (54). Especially in highly aggressive malignancies, there is a relevant risk of terminal progression of the disease if molecularly targeted therapies are not rapidly identified and applied.

The PETAL trial demonstrated prognostic implications of interim fluorodeoxyglucose positron emission tomography (FDG-PET) imaging in patients with diffuse-large B-cell lymphoma (DLBCL) indicating poor event-free survival rates in patients with remaining PET-positivity after two cycles of R-CHOP-like immunochemotherapy (55). Outcome prediction by PET was independent of the International Prognostic Index (IPI) (55). This sparks the assumption that this observation might be transferred to other aggressive B-cell non-Hodgkin lymphomas such as PBL. Consecutively, PBL-cases with FDG-avidity upon interim PET-imaging may be associated with dismal prognosis and should be considered for early extened molecular testing. Therefore, we suggest including patients with rare, aggressive hematologic malignancies in clinical high-risk settings in precision oncology programs as early as possible, preferentially after the first evaluation of response in terms of interim FDG-PET (55). This would enable the identification of biomarkers for targeted therapeutic options in the relapsed or refractory setting at a point during the course of the disease when a successful bridging therapy may still be feasible. If previously identified biomarkers can be confirmed in the relapsed or refractory settings, this may accelerate the process of MTB treatment recommendations. Otherwise, novel targetable genomic alterations emerge in the relapsed or refractory setting, harboring novel options for targeted treatments (56). Moreover, repeated sampling might provide insights into the clonal evolution in such malignancies (57). This double-tracked strategy seems feasible in the light of cost efficacy, as financial analyses have shown that diagnostics in MTB settings represent 0.3% of total costs (58).

Such strategies require a simple and readily available diagnostic tool for the detection as well as monitoring of targetable genomic alterations over the course of disease. In recent years, liquid biopsy approaches analyzing cell-free DNA fragments (cfDNA)/circulating tumor DNA (ctDNA) from the peripheral blood have steadily evolved into an attractive component in genomic diagnostics (59). Liquid biopsies represent an extract of the current mutational status in a tumor, partially even reflecting subclonal architecture (60). To date, the essential critical aspects regarding the implementation in routine clinical use of liquid biopsy remains the insufficient sensitivity and lack of technological standardization between laboratories as well as pending results from prospective studies showing clinical benefit in a large scale prospective setting (61). Additionally, genomic profiling of tumor sites provides a more decisive overview on its molecular constitution leading to the most reliable identification of therapeutic vulnerabilities (62, 63). However, recent major technical advances have broadened the spectrum of molecular techniques leading to a more and more comprehensive convergence between the molecular studies from primary tumor tissues on the one hand and from the peripheral blood (liquid biopsy) on the other (64). We believe that there will be an essential role for liquid biopsy approaches in the upcoming era of precision oncology. Transferring the potential of liquid biopsy to our virtual MTB approach, we suggest its application from the initiation of a targeted and molecularly stratified treatment recommendation as a tool for drug monitoring, monitoring of response and for the detection of potential escape mechanisms related to the tumor (65, 66).

The lack of suitable basket trials for rare hematologic malignancies poses a significant challenge in applying molecularly stratified treatments. Consecutively, knowledge from MTB settings affecting solid tumors is often extrapolated into the field of hematology and generated molecular evidence, therefore, does hardly ever exceed the m2A level according to NCT/DKTK or ESCAT tier IIIA according to ESCAT recommendations. This also affects the transferability of established biomarkers associated with designated MTB rationales, such as olaparib therapy in malignancies with HRD deficiency or immune checkpoint inhibitor therapy in cancers harboring a DNA MMR mutational signature (24, 67). Moreover, there needs to be standardized practice to draw coherent conclusions from RNA-seq data and gene set enrichment analyses within an MTB setup. Accordingly, we used our RNA-seq data for an integrated analysis to verify the biological significance of mutations previously identified by WES. This integrated analysis supported the functional relevance for most mutations yet led to the exclusion of one modification (*KIT*) as a potential therapeutic target.

Including patients with rare hematologic malignancies in MTBs is associated with several chances. An essential finding of this study is that comprehensive genomic characterization of PBL revealed a broad range of promising therapeutically targetable vulnerabilities. Even today, many novel agents approved in the U.S. (FDA) and/or in Europe (EMA) are available and ready for clinical use, including a drug repurposing approach outside of the approved drug label. However, the steady increase of knowledge regarding the efficacy and toxicity profiles of novel agents in the light of molecularly stratified therapies used as single agents or as components in drug combinations will lead to a variety of therapeutic options in rare hematologic entities in which there is no supporting evidence beyond the application of CHO(E)P or an equivalent chemotherapeutic regimen with or without bortezomib (53, 68). Moreover, there is growing evidence for recommending drug combinations in MTBs (9). The stringent inclusion of rare hematologic malignancies into MTBs and basket trials will help gain experience regarding the application of drug combinations in such entities. Such processes require monitoring by Data Safety

Monitoring Boards (9). Additionally, helpful tools such as matching score calculation should be used to predict the effectiveness and toxicity of single agents or drug combinations. In the present study, the calculation of the mMS is exclusively descriptive in nature. As this proof-of-concept study created a virtual MTB setting in which patients were not treated according to the recommended MTB strategies, the benefit of such strategy on the clinical outcome of PBL and other rare, aggressive hematologic neoplasms has yet to be demonstrated. In addition, further studies are needed to validate the modified way of MS calculation performed here and to define a practical cut-off value in a minimum p-value approach. The era of precision oncology is paralleled with the era of deep learning and machine learning approaches based on artificial intelligence (AI) models. Integrating AI into precision oncology is promising in order to standardize MTBs and to provide information on administered molecularly stratified therapies in a more standardized way (69). The increment of evidence in this rare entity associated with a high prevalence of HIV infections, is challenging as HIV infections pose a central exclusion criterion for the majority of clinical trials (70, 71). Currently, there exist negligible initiative on behalf of pharmaceutic companies regarding funding prospective clinical trials. Consecutively, the MTB setting represents a relevant alternative to gain more evidence in treating PBL and other rare, aggressive hematologic neoplasms.

Limitations of the present study predominantly include its limited sample size and shortcomings inherent to the retrospective nature harboring the potential of incomplete data, a selection bias during the inclusion procedure, and a detection bias during the analysis procedure, as well as limitations coming along with the fact that we present a solely virtual setting. Apart from WES, complete genomic RNA-seq data for each case and matched germline DNA for processing would have been desirable, including comparative analysis (4). In the present cohort, immunotherapeutic recommendations were concluded based on a mutational signature predominantly affecting DNA MMR genes. Immunohistochemical investigations included CD19, CD30, CD38, and CD79B but not programmed cell death ligand-1 (PD-L1) staining. PD-L1 staining probably extends the fraction of cases in which immune checkpoint blockade displays an appropriate therapeutic option, especially as a component of potential drug combinations.

In summary, the presented approach of an MTB for patients with prPBL is theoretical in nature. As none of the molecularly analyzed cases were treated according to the virtually recommended options in a prospective manner, optimal dosing as well as the applicability of considered drugs as monotherapy or as a combination needs further validation within the scope of clinical trials (e.g. umbrella and/or basket trials). A limited number of ongoing clinical trials will amplify the spectrum of therapeutic options in PBL and other rare hematologic malignancies investigating the efficacy of novel agents such as the anti-CD27 antibody varlilumab (NCT03038672) or the BCMA-directed antibody-drug conjugate belantamab mafodotin (NCT04676360).

Conclusion

With the present study, we aim to draw attention to the potential benefits of a more frequent inclusion of rare hematologic malignancies such as PBL in MTB settings, as our work demonstrates the vast potential for molecularly stratified therapeutic approaches with reasonable molecular evidence levels. Such patients should therefore be introduced to precision oncology programs as early as possible due to the aggressive biology of the tumor. Our suggestion intends to initiate a learning process for improved patient care. To the best of our knowledge, this is the first approach of a virtual MTB in hematologic malignancies. Future studies are warranted to demonstrate the effectiveness and tolerability of molecularly stratified treatments in PBL patients and other rare hematologic neoplasms.

Data availability statement

The datasets presented in this study can be found in online repositories. The names of the repository/repositories and accession number(s) can be found in the article.

Ethics statement

The studies involving human participants were reviewed and approved by Ethics committee of the University of Lübeck (reference no. 18-311). The patients/participants provided their written informed consent to participate in this study. Written informed consent was obtained from the individual(s) for the publication of any potentially identifiable images or data included in this article.

Author contributions

Study concept: HW, NG. Data collection: HW, NH, AF, AK, NR, VB, JR, HM, NB, HB, NG.

Data analysis and creation of figures and tables: HW, AF, AK, SF, NR, NB, HM, HB, AF, NG. Initial Draft of manuscript: HW. All authors contributed to the article and approved the submitted version.

Acknowledgments

The authors would like to thank Tanja Oeltermann for her skilled technical assistance. NR, AK and HB acknowledge computational support from the OMICS compute cluster at the University of Lübeck. HB acknowledges funding by the Deutsche Forschungsgemeinschaft (DFG, German Research Foundation) under Germany`s Excellence Strategy – EXC 22167-390884018.

Conflict of interest

The authors declare that the research was conducted in the absence of any commercial or financial relationships that could be construed as a potential conflict of interest.

Publisher's note

All claims expressed in this article are solely those of the authors and do not necessarily represent those of their affiliated organizations, or those of the publisher, the editors and the reviewers. Any product that may be evaluated in this article, or claim that may be made by its manufacturer, is not guaranteed or endorsed by the publisher.

Supplementary material

The Supplementary Material for this article can be found online at: https://www.frontiersin.org/articles/10.3389/fonc.2023.1129405/full#supplementary-material

References

1. Subbiah V, Puzanov I, Blay JY, Chau I, Lockhart AC, Raje NS, et al. Pan-cancer efficacy of vemurafenib in BRAF (V600)-mutant non-melanoma cancers. *Cancer Discovery* (2020) 10(5):657–63. doi: 10.1158/2159-8290.CD-19-1265

2. Larson KL, Huang B, Weiss HL, Hull P, Westgate PM, Miller RW, et al. Clinical outcomes of molecular tumor boards: A systematic review. *JCO Precis Oncol* (2021) 5. doi: 10.1200/PO.20.00495

3. Tempero M. One size fits all? really? *J Natl Compr Canc Netw* (2018) 16(10):1161. doi: 10.6004/jnccn.2018.0080

4. Horak P, Heining C, Kreutzfeldt S, Hutter B, Mock A, Hullein J, et al. Comprehensive genomic and transcriptomic analysis for guiding therapeutic decisions in patients with rare cancers. *Cancer Discovery* (2021) 11(11):2780–95. doi: 10.1158/2159-8290.CD-21-0126

5. Prokosch HU, Acker T, Bernarding J, Binder H, Boeker M, Boerries M, et al. MIRACUM: Medical informatics in research and care in university medicine. *Methods Inf Med* (2018) 57(S 01):e82–91. doi: 10.3414/ME17-02-0025

6. Heinrich K, Miller-Phillips L, Ziemann F, Hasselmann K, Ruhlmann K, Flach M, et al. Lessons learned: the first consecutive 1000 patients of the CCCMunich(LMU) molecular tumor board. *J Cancer Res Clin Oncol* (2022) 7–11. doi: 10.1007/s00432-022-04165-0

7. Tessier-Cloutier B, Grewal JK, Jones MR, Pleasance E, Shen Y, Cai E, et al. The impact of whole genome and transcriptome analysis (WGTA) on predictive biomarker discovery and diagnostic accuracy of advanced malignancies. *J Pathol Clin Res* (2022) 8 (4):395–407. doi: 10.1002/cjp2.265

8. Irmisch A, Bonilla X, Chevrier S, Lehmann KV, Singer F, Toussaint NC, et al. The tumor profiler study: integrated, multi-omic, functional tumor profiling for clinical decision support. *Cancer Cell* (2021) 39(3):288–93. doi: 10.1016/j.ccell.2021.01.004

9. Sicklick JK, Kato S, Okamura R, Schwaederle M, Hahn ME, Williams CB, et al. Molecular profiling of cancer patients enables personalized combination therapy: the I-PREDICT study. *Nat Med* (2019) 25(5):744–50. doi: 10.1038/s41591-019-0407-5

10. Hoefflin R, Geissler AL, Fritsch R, Claus R, Wehrle J, Metzger P, et al. Personalized clinical decision making through implementation of a molecular tumor board: A German single-center experience. *JCO Precis Oncol* (2018) 2. doi: 10.1200/PO.18.00105

11. Rodriguez H, Zenklusen JC, Staudt LM, Doroshow JH, Lowy DR. The next horizon in precision oncology: Proteogenomics to inform cancer diagnosis and treatment. *Cell* (2021) 184(7):1661–70. doi: 10.1016/j.cell.2021.02.055

12. Boehm KM, Khosravi P, Vanguri R, Gao J, Shah SP. Harnessing multimodal data integration to advance precision oncology. *Nat Rev Cancer* (2022) 22(2):114–26. doi: 10.1038/s41568-021-00408-3

13. Wright GW, Huang DW, Phelan JD, Coulibaly ZA, Roulland S, Young RM, et al. A probabilistic classification tool for genetic subtypes of diffuse Large b cell lymphoma with therapeutic implications. *Cancer Cell* (2020) 37(4):551–68.e14. doi: 10.1016/j.ccell.2020.03.015

14. Schmitz R, Wright GW, Huang DW, Johnson CA, Phelan JD, Wang JQ, et al. Genetics and pathogenesis of diffuse Large b-cell lymphoma. *N Engl J Med* (2018) 378 (15):1396–407. doi: 10.1056/NEJMoa1801445

15. Chapuy B, Stewart C, Dunford AJ, Kim J, Kamburov A, Redd RA, et al. Molecular subtypes of diffuse large b cell lymphoma are associated with distinct pathogenic mechanisms and outcomes. *Nat Med* (2018) 24(5):679–90. doi: 10.1038/s41591-018-0016-8

16. Aoki T, Chong LC, Takata K, Milne K, Hav M, Colombo A, et al. Single-cell transcriptome analysis reveals disease-defining T-cell subsets in the tumor microenvironment of classic Hodgkin lymphoma. *Cancer Discovery* (2020) 10 (3):406–21. doi: 10.1158/2159-8290.CD-19-0680

17. Hubschmann D, Kleinheinz K, Wagener R, Bernhart SH, Lopez C, Toprak UH, et al. Mutational mechanisms shaping the coding and noncoding genome of germinal center derived b-cell lymphomas. *Leukemia* (2021) 35(7):2002–16. doi: 10.1038/s41375-021-01251-z

18. Ebert BL. Introduction to a review series on precision hematology. *Blood* (2017) 130(4):408–9. doi: 10.1182/blood-2017-06-735753

19. Hertel N, Merz H, Bernd HW, Bernard V, Kunstner A, Busch H, et al. Performance of international prognostic indices in plasmablastic lymphoma: a comparative evaluation. *J Cancer Res Clin Oncol* (2021) 147(10):3043–50. doi: 10.1007/s00432-021-03580-z

20. Witte HM, Kunstner A, Hertel N, Bernd HW, Bernard V, Stolting S, et al. Integrative genomic and transcriptomic analysis in plasmablastic lymphoma identifies disruption of key regulatory pathways. *Blood Adv* (2022) 6(2):637–51. doi: 10.1182/bloodadvances.2021005486

21. Witte HM, Hertel N, Merz H, Bernd HW, Bernard V, Stolting S, et al. Clinicopathological characteristics and MYC status determine treatment outcome in plasmablastic lymphoma: a multi-center study of 76 consecutive patients. *Blood Cancer J* (2020) 10(5):63. doi: 10.1038/s41408-020-0327-0

22. Kunstner A, Witte HM, Riedl J, Bernard V, Stolting S, Merz H, et al. Mutational landscape of high-grade b-cell lymphoma with MYC-, BCL2 and/or BCL6 rearrangements characterized by whole-exome sequencing. *Haematologica* (2021) 107(8):1850–63. doi: 10.1101/2021.07.13.21260465

23. Metzger P, Scheible R, Maier W, Reimer N, hessmaria, Ritzel C, et al. *AG-Boerries/MIRACUM-Pipe: v4.0.0_beta (v4.0.0_beta)*. Zenodo (2022). Available at: https://zenodo.org/record/7024815/export/xm#.Y-5-MS9XYUE.

24. Mateo J, Chakravarty D, Dienstmann R, Jezdic S, Gonzalez-Perez A, Lopez-Bigas N, et al. A framework to rank genomic alterations as targets for cancer precision medicine: the ESMO scale for clinical actionability of molecular targets (ESCAT). *Ann Oncol* (2018) 29(9):1895–902. doi: 10.1093/annonc/mdy263

25. Degasperi A, Zou X, Amarante TD, Martinez-Martinez A, Koh GCC, Dias JML, et al. Substitution mutational signatures in whole-genome-sequenced cancers in the UK population. *Science* (2022) 376(6591). doi: 10.1126/science.abl9283

26. Sicklick JK, Kato S, Okamura R, Patel H, Nikanjam M, Fanta PT, et al. Molecular profiling of advanced malignancies guides first-line n-of-1 treatments in the I-PREDICT treatment-naive study. *Genome Med* (2021) 13(1):155. doi: 10.1186/s13073-021-00969-w

27. Frontzek F, Staiger AM, Zapukhlyak M, Xu W, Bonzheim I, Borgmann V, et al. Molecular and functional profiling identifies therapeutically targetable vulnerabilities in plasmablastic lymphoma. *Nat Commun* (2021) 12(1):5183. doi: 10.1038/s41467-021-25405-w

28. Liu Z, Filip I, Gomez K, Engelbrecht D, Meer S, Lalloo PN, et al. Genomic characterization of HIV-associated plasmablastic lymphoma identifies pervasive mutations in the JAK-STAT pathway. *Blood Cancer Discovery* (2020) 1(1):112–25. doi: 10.1158/2643-3230.BCD-20-0051

29. Goodman AM, Kato S, Bazhenova L, Patel SP, Frampton GM, Miller V, et al. Tumor mutational burden as an independent predictor of response to immunotherapy in diverse cancers. *Mol Cancer Ther* (2017) 16(11):2598–608. doi: 10.1158/1535-7163.MCT-17-0386

30. Riviere P, Goodman AM, Okamura R, Barkauskas DA, Whitchurch TJ, Lee S, et al. High tumor mutational burden correlates with longer survival in immunotherapy-naive patients with diverse cancers. *Mol Cancer Ther* (2020) 19 (10):2139–45. doi: 10.1158/1535-7163.MCT-20-0161

31. Gopal AK, Kahl BS, de Vos S, Wagner-Johnston ND, Schuster SJ, Jurczak WJ, et al. PI3Kdelta inhibition by idelalisib in patients with relapsed indolent lymphoma. *N Engl J Med* (2014) 370(11):1008–18. doi: 10.1056/NEJMoa1314583

32. Adib E, Klonowska K, Giannikou K, Do KT, Pruitt-Thompson S, Bhushan K, et al. Phase II clinical trial of everolimus in a pan-cancer cohort of patients with mTOR pathway alterations. *Clin Cancer Res* (2021) 27(14):3845–53. doi: 10.1158/1078-0432.CCR-20-4548

33. Park H, Shapiro GI, Gao X, Mahipal A, Starr J, Furqan M, et al. Phase ib study of eprenetapopt (APR-246) in combination with pembrolizumab in patients with advanced or metastatic solid tumors. *ESMO Open* (2022) 7(5):100573. doi: 10.1016/j.esmoop.2022.100573

34. Kawazoe A, Kuboki Y, Bando H, Fukuoka S, Kojima T, Naito Y, et al. Phase 1 study of napabucasin, a cancer stemness inhibitor, in patients with advanced solid tumors. *Cancer Chemother Pharmacol* (2020) 85(5):855–62. doi: 10.1007/s00280-020-04059-3

35. Wainberg ZA, Enzinger PC, Kang YK, Qin S, Yamaguchi K, Kim IH, et al. Bemarituzumab in patients with FGFR2b-selected gastric or gastro-oesophageal junction adenocarcinoma (FIGHT): a randomised, double-blind, placebo-controlled, phase 2 study. *Lancet Oncol* (2022) 23(11):1430–40. doi: 10.1016/S1470-2045(22)00603-9

36. El Shamieh S, Saleh F, Assaad S, Farhat F. Next-generation sequencing reveals mutations in RB1, CDK4 and TP53 that may promote chemo-resistance to palbociclib in ovarian cancer. *Drug Metab Pers Ther* (2019) 34(2). doi: 10.1515/dmpt-2018-0027

37. Dittus C, Miller JA, Wehbie R, Castillo JJ. Daratumumab with ifosfamide, carboplatin and etoposide for the treatment of relapsed plasmablastic lymphoma. *Br J Haematol* (2022) 198(2):e32–e4. doi: 10.1111/bjh.18228

38. Salles G, Duell J, Gonzalez Barca E, Tournilhac O, Jurczak W, Liberati AM, et al. Tafasitamab plus lenalidomide in relapsed or refractory diffuse large b-cell lymphoma (L-MIND): a multicentre, prospective, single-arm, phase 2 study. *Lancet Oncol* (2020) 21(7):978–88. doi: 10.1016/S1470-2045(20)30225-4

39. Holderness BM, Malhotra S, Levy NB, Danilov AV. Brentuximab vedotin demonstrates activity in a patient with plasmablastic lymphoma arising from a background of chronic lymphocytic leukemia. *J Clin Oncol* (2013) 31(12):e197–9. doi: 10.1200/JCO.2012.46.9593

40. Tilly H, Morschhauser F, Sehn LH, Friedberg JW, Trneny M, Sharman JP, et al. Polatuzumab vedotin in previously untreated diffuse Large b-cell lymphoma. *N Engl J Med* (2022) 386(4):351–63. doi: 10.1056/NEJMoa2115304

41. Le DT, Durham JN, Smith KN, Wang H, Bartlett BR, Aulakh LK, et al. Mismatch repair deficiency predicts response of solid tumors to PD-1 blockade. *Science* (2017) 357(6349):409–13. doi: 10.1126/science.aan6733

42. Supek F, Lehner B. Differential DNA mismatch repair underlies mutation rate variation across the human genome. *Nature* (2015) 521(7550):81–4. doi: 10.1038/nature14173

43. Palmeri M, Mehnert J, Silk AW, Jabbour SK, Ganesan S, Popli P, et al. Real-world application of tumor mutational burden-high (TMB-high) and microsatellite instability (MSI) confirms their utility as immunotherapy biomarkers. *ESMO Open* (2022) 7(1):100336. doi: 10.1016/j.esmoop.2021.100336

44. Cristescu R, Aurora-Garg D, Albright A, Xu L, Liu XQ, Loboda A, et al. Tumor mutational burden predicts the efficacy of pembrolizumab monotherapy: a pan-tumor retrospective analysis of participants with advanced solid tumors. *J Immunother Cancer* (2022) 10(1). doi: 10.1136/jitc-2021-003091

45. Mandal R, Samstein RM, Lee KW, Havel JJ, Wang H, Krishna C, et al. Genetic diversity of tumors with mismatch repair deficiency influences anti-PD-1 immunotherapy response. *Science* (2019) 364(6439):485–91. doi: 10.1126/science.aau0447

46. Zhou Y, Jiang W, Zeng L, Mi J, Song L, Lizaso A, et al. A novel ROS1 G2032 K missense mutation mediates lorlatinib resistance in a patient with ROS1-rearranged lung adenocarcinoma but responds to nab-paclitaxel plus pembrolizumab. *Lung Cancer* (2020) 143:55–9. doi: 10.1016/j.lungcan.2020.03.019

47. Alexandrov LB, Kim J, Haradhvala NJ, Huang MN, Tian Ng AW, Wu Y, et al. The repertoire of mutational signatures in human cancer. *Nature* (2020) 578(7793):94–101. doi: 10.1038/s41586-020-1943-3

48. Stok C, Kok YP, van den Tempel N, van Vugt M. Shaping the BRCAness mutational landscape by alternative double-strand break repair, replication stress and mitotic aberrancies. *Nucleic Acids Res* (2021) 49(8):4239–57. doi: 10.1093/nar/gkab151

49. Raphael BJ, Dobson JR, Oesper L, Vandin F. Identifying driver mutations in sequenced cancer genomes: computational approaches to enable precision medicine. *Genome Med* (2014) 6(1):5. doi: 10.1186/gm524

50. Gandhi L, Rodriguez-Abreu D, Gadgeel S, Esteban E, Felip E, De Angelis F, et al. Pembrolizumab plus chemotherapy in metastatic non-Small-Cell lung cancer. *N Engl J Med* (2018) 378(22):2078–92. doi: 10.1056/NEJMoa1801005

51. Nastoupil LJ, Chin CK, Westin JR, Fowler NH, Samaniego F, Cheng X, et al. Safety and activity of pembrolizumab in combination with rituximab in relapsed or refractory follicular lymphoma. *Blood Adv* (2022) 6(4):1143–51. doi: 10.1182/bloodadvances.2021006240

52. Castillo JJ, Lamacchia J, Silver J, Flynn CA, Sarosiek S. Complete response to pembrolizumab and radiation in a patient with HIV-negative, EBV-positive plasmablastic lymphoma. *Am J Hematol* (2021) 96(10):E390–E2. doi: 10.1002/ajh.26291

53. Castillo JJ, Bibas M, Miranda RN. The biology and treatment of plasmablastic lymphoma. *Blood* (2015) 125(15):2323–30. doi: 10.1182/blood-2014-10-567479

54. Luchini C, Lawlor RT, Milella M, Scarpa A. Molecular tumor boards in clinical practice. *Trends Cancer* (2020) 6(9):738–44. doi: 10.1016/j.trecan.2020.05.008

55. Duhrsen U, Muller S, Hertenstein B, Thomssen H, Kotzerke J, Mesters R, et al. Positron emission tomography-guided therapy of aggressive non-Hodgkin lymphomas (PETAL): A multicenter, randomized phase III trial. *J Clin Oncol* (2018) 36(20):2024–34. doi: 10.1200/JCO.2017.76.8093

56. Zhao Y, Murciano-Goroff YR, Xue JY, Ang A, Lucas J, Mai TT, et al. Diverse alterations associated with resistance to KRAS(G12C) inhibition. *Nature* (2021) 599(7886):679–83. doi: 10.1038/s41586-021-04065-2

57. Walens A, Lin J, Damrauer JS, McKinney B, Lupo R, Newcomb R, et al. Adaptation and selection shape clonal evolution of tumors during residual disease and recurrence. *Nat Commun* (2020) 11(1):5017. doi: 10.1038/s41467-020-18730-z

58. Pages A, Foulon S, Zou Z, Lacroix L, Lemare F, de Baere T, et al. The cost of molecular-guided therapy in oncology: a prospective cost study alongside the MOSCATO trial. *Genet Med* (2017) 19(6):683–90. doi: 10.1038/gim.2016.174

59. Poynton E, Okosun J. Liquid biopsy in lymphoma: Is it primed for clinical translation? *EJHaem* (2021) 2(3):616–27. doi: 10.1002/jha2.212

60. Amelio I, Bertolo R, Bove P, Buonomo OC, Candi E, Chiocchi M, et al. Liquid biopsies and cancer omics. *Cell Death Discovery* (2020) 6(1):131. doi: 10.1038/s41420-020-00373-0

61. Pirosa MC, Borchmann S, Jardin F, Gaidano G, Rossi D. Controversies in the interpretation of liquid biopsy data in lymphoma. *Hemasphere* (2022) 6(6):e727. doi: 10.1097/HS9.0000000000000727

62. Lin LH, Allison DHR, Feng Y, Jour G, Park K, Zhou F, et al. Comparison of solid tissue sequencing and liquid biopsy accuracy in identification of clinically relevant gene mutations and rearrangements in lung adenocarcinomas. *Mod Pathol* (2021) 34(12):2168–74. doi: 10.1038/s41379-021-00880-0

63. Esagian SM, Grigoriadou G, Nikas IP, Boikou V, Sadow PM, Won JK, et al. Comparison of liquid-based to tissue-based biopsy analysis by targeted next generation sequencing in advanced non-small cell lung cancer: a comprehensive systematic review. *J Cancer Res Clin Oncol* (2020) 146(8):2051–66. doi: 10.1007/s00432-020-03267-x

64. Lauer EM, Mutter J, Scherer F. Circulating tumor DNA in b-cell lymphoma: technical advances, clinical applications, and perspectives for translational research. *Leukemia* (2022) 36(9):2151–64. doi: 10.1038/s41375-022-01618-w

65. Liu MC, MacKay M, Kase M, Piwowarczyk A, Lo C, Schaeffer J, et al. Longitudinal shifts of solid tumor and liquid biopsy sequencing concordance in metastatic breast cancer. *JCO Precis Oncol* (2022) 6(1):e2100321. doi: 10.1200/PO.21.00321

66. Mauri G, Vitiello PP, Sogari A, Crisafulli G, Sartore-Bianchi A, Marsoni S, et al. Liquid biopsies to monitor and direct cancer treatment in colorectal cancer. *Br J Cancer* (2022) 127(3):394–407. doi: 10.1038/s41416-022-01769-8

67. Janysek DC, Kim J, Duijf PHG, Dray E. Clinical use and mechanisms of resistance for PARP inhibitors in homologous recombination-deficient cancers. *Transl Oncol* (2021) 14(3):101012. doi: 10.1016/j.tranon.2021.101012

68. Castillo JJ, Guerrero-Garcia T, Baldini F, Tchernonog E, Cartron G, Ninkovic S, et al. Bortezomib plus EPOCH is effective as frontline treatment in patients with plasmablastic lymphoma. *Br J Haematol* (2019) 184(4):679–82. doi: 10.1111/bjh.15156

69. Petak I, Kamal M, Dirner A, Bieche I, Doczi R, Mariani O, et al. A computational method for prioritizing targeted therapies in precision oncology: performance analysis in the SHIVA01 trial. *NPJ Precis Oncol* (2021) 5(1):59. doi: 10.1038/s41698-021-00191-2

70. Uldrick TS, Ison G, Rudek MA, Noy A, Schwartz K, Bruinooge S, et al. Modernizing clinical trial eligibility criteria: Recommendations of the American society of clinical oncology-friends of cancer research HIV working group. *J Clin Oncol* (2017) 35(33):3774–80. doi: 10.1200/JCO.2017.73.7338

71. Vora KB, Ricciuti B, Awad MM. Exclusion of patients living with HIV from cancer immune checkpoint inhibitor trials. *Sci Rep* (2021) 11(1):6637. doi: 10.1038/s41598-021-86081-w

frontiers | Frontiers in Oncology

TYPE Original Research
PUBLISHED 14 March 2023
DOI 10.3389/fonc.2023.1146029

OPEN ACCESS

EDITED BY
Niklas Gebauer,
University Medical Center Schleswig-Holstein, Germany

REVIEWED BY
Hanno Maximilian Witte,
Bundeswehrkrankenhaus, Germany
Hajnalka Rajnai,
Semmelweis University, Hungary

*CORRESPONDENCE
Susanne Ghandili
s.ghandili@uke.de

SPECIALTY SECTION
This article was submitted to Hematologic Malignancies, a section of the journal Frontiers in Oncology

RECEIVED 16 January 2023
ACCEPTED 06 March 2023
PUBLISHED 14 March 2023

CITATION
Ghandili S, Dierlamm J, Bokemeyer C, von Bargen CM and Weidemann SA (2023) NTRK fusion protein expression is absent in a large cohort of diffuse large B-cell lymphoma.
Front. Oncol. 13:1146029.
doi: 10.3389/fonc.2023.1146029

NTRK fusion protein expression is absent in a large cohort of diffuse large B-cell lymphoma

Susanne Ghandili[1]*, Judith Dierlamm[1], Carsten Bokemeyer[1], Clara Marie von Bargen[2] and Sören Alexander Weidemann[2]

[1]Department of Oncology, Hematology and Bone Marrow Transplantation with Section Pneumology, University Cancer Center Hamburg, University Medical Center Hamburg-Eppendorf, Hamburg, Germany, [2]Institute of Pathology, University Medical Center Hamburg-Eppendorf, Hamburg, Germany

Background: Even though two NTRK-targeting drugs are available for the treatment of irresectable, metastatic, or progressive NTRK-positive solid tumors, less is known about the role of NTRK fusions in lymphoma. For this reason, we aimed to investigate if NTRK fusion proteins are expressed in diffuse large B-cell lymphoma (DLBCL) by systemic immunohistochemistry (IHC) screening and additional FISH analysis in a large cohort of DLBCL samples according to the ESMO Translational Research and Precision Medicine Working Group recommendations for the detection of NTRK fusions in daily practice and clinical research.

Methods: A tissue microarray of 92 patients with the diagnosis of DLBCL at the University Hospital Hamburg between 2020 and 2022 was built. The clinical data were taken from patient records. Immunohistochemistry for Pan-NTRK fusion protein was performed and positive staining was defined as any viable staining. For FISH analysis only results with quality 2 and 3 were evaluated.

Results: NTRK immunostaining was absent in all analyzable cases. No break apart was detectable by FISH.

Conclusion: Our negative result is consistent with the very sparse data existing on NTRK gene fusions in hematologic neoplasms. To date, only a few cases of hematological malignancies have been described in which NTRK-targeting drugs may provide a potential therapeutic agent. Even though NTRK fusion protein expression was not detectable in our sample cohort, performing systemic screenings for NTRK fusions are necessary to define further the role of NTRK fusions not only in DLBCL but in a multitude of lymphoma entities as long as the lack of reliable data exists.

KEYWORDS

diffuse large B-cell lymphoma, NTRK fusion protein, immunohistochemistry, tissue microarray, molecular landscape

Introduction

With an incidence of 7 cases per 100,000 persons per year, diffuse large B-cell lymphoma (DLBCL) is the most frequently observed histological type of non-Hodgkin lymphoma (NHL), accounting for approximately 25% of all NHL (1–3). DLBCL typically presents as rapidly enlarging lymphoma, commonly with extranodal involvement and/or constitutional symptoms (4). With current treatment approaches mainly consisting of combined therapy with CD20, CD79b-directed monoclonal antibodies, and conventional chemotherapy, DLBCL is curable in approximately 70% of patients (5). However, a lack of chemotherapy sensitivity must be assumed in patients with primary refractory or early relapsing DLBCL. To overcome the dismal prognosis of refractory or relapsed DLBCL, promising newly developed treatment approaches like CD19-directed CAR-T-cell therapies are already approved and available in selected countries or in the case of T-cell-engaging bi-specific antibodies currently investigated during multiple clinical trials (6–11). Nevertheless, despite the high overall response rates, the average time to CAR-T-cell reinfusion is approximately four weeks (12).

For this reason, the need for non-lymphodepleting chemotherapy-free bridging strategies is undisputed. In clinical routine, approved as well as off-label, individual bridging therapies with, for example, tafasitamab/lenalidomide, ibrutinib, or rituximab with polatuzumab vedotin are commonly used. In this setting, precision medicine based on the identification of driver mutations might provide additional treatment possibilities in a subset of DLBCL patients.

The neurotrophic tyrosine receptor kinase (NTRK) genes 1, 2, and 3 encode a tyrosine receptor kinase (TRK) receptor family (TRKA, TRKB, and TRKC), which plays an essential role during embryogenesis in the development of the nervous system and is moreover physiologically expressed in neuronal tissue (13–16). However, a gene rearrangement caused by a fusion of NTRK genes with different fusion partners can result in the development of TRK fusion oncoproteins which themselves lead to constitutive kinase activity or a simple overexpression of the kinase domain with subsequent activation of downstream cellular signaling pathways, which are involved in cell proliferation and survival (17, 18). NTRK fusions can occur with a high frequency (defined as > 25-35%) in a selected spectrum of rare pediatric cancers e.g. congenital infantile fibrosarcoma, congenital mesoblastic nephroma, secretory breast carcinoma or, mammary analog secretory carcinoma of the salivary gland or with an intermediate (>1% but < 25%) or low frequency (< 1%) in common adult solid cancers (19). The role of NTRK fusion genes has been extensively investigated and described in a broad spectrum of solid cancers leading to one of the first tissue-agnostic approvals of a highly effective targeted therapy by the Food and Drug Administration (FDA) when in 2018, larotrectinib was granted accelerated approval by the FDA as the first-in-class selective NTRK-inhibitor for the treatment of adult and pediatric patients with irresectable, metastatic, or progressive NTRK-positive solid tumors (20). However, the occurrence of NTRK-associated molecular findings in large cohorts of patients with hematological malignancies is rarely investigated. In 2020, Joshi et al. analyzed samples of 185 patients with acute myeloid leukemia, acute lymphoblastic leukemia, or myeloproliferative neoplasm. The authors identified a total of nine NTRK mutations, including four novel oncogenic NTRK point mutations potentially targetable by entrectinib (21). Recently, Witte et al. identified two cases of NTRK3 mutation in a cohort of 33 consecutive patients with plasmablastic lymphoma (22).

However, up to now, the occurrence of NTRK fusion protein expression or NTRK gene fusion in DLBCL has yet to be investigated. Since larotrectinib and entrectinib, two approved NTRK-targeted drugs are now available; we aimed to investigate the expression of NTRK fusion proteins in DLBCL by a systemic immunohistochemistry (IHC) screening and additional fluorescence *in situ* hybridization (FISH) analysis on a tissue microarray (TMA) containing samples from 92 DLBCLs from patients with newly diagnosed or refractory or relapsed (r/r) DLBCL according to the ESMO Translational Research and Precision Medicine Working Group recommendations for the detection of NTRK fusions in daily practice and clinical research (13).

Materials and methods

Patients

In this prospective observational, single-center analysis, we studied 92 consecutive patients with DLBCL, aged 18 years or older, who were immunohistochemically screened for an NTRK fusion gene protein overexpression. Samples of all patients included in this analysis were previously diagnosed with DLBCL as part of the clinical routine at the Institute of Pathology of the University Medical Center Hamburg-Eppendorf between 2020 and 2022. Patients

with high-grade B-cell lymphoma with MYC and BCL2 and/or BCL6 rearrangements were not excluded from this study. DLBCL was defined according to the 2016 revision of the World Health Organization classification of lymphoid neoplasms criteria (23). If available, clinical data regarding patients' characteristics and DLBCL treatment were collected from the patient's electronic medical records (Figure 1). The Ann Arbor classification was used for disease staging assessment (24). The International Prognostic Index (IPI) was used to calculate prognostic risk scores (25).

The data cut-off was on December 21, 2022. The use of archived remnants of diagnostic tissues for manufacturing of tissue microarrays and their analysis for research purposes as well as patient data analysis has been approved by local laws (HmbKHG, §12) and by the local ethics committee (Ethics Commission Hamburg, WF-049/09). All work has been carried out in compliance with the Helsinki Declaration.

Tissue microarray (TMA)

The Institute of Pathology of the University Medical Center Hamburg-Eppendorf database includes 414 diagnoses of DLBCL for the years 2020 to 2022. Of these, 92 cases could be used to construct the TMA. The reasons for exclusion were mainly

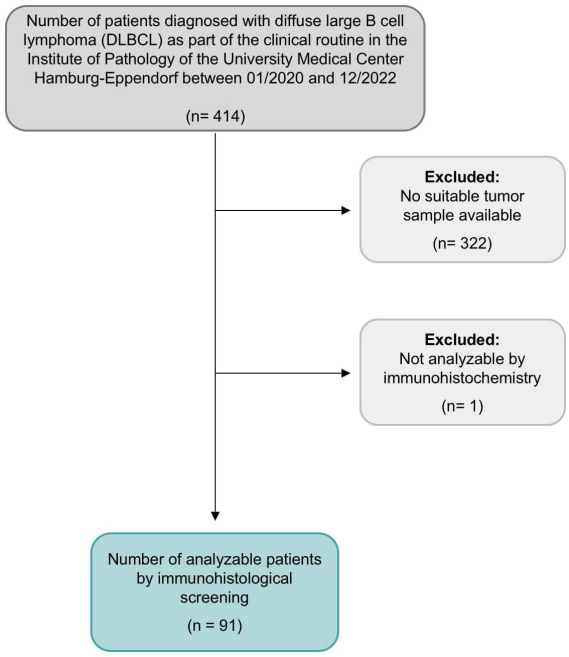

FIGURE 1
Flow chart of study design and population.

insufficient tissue quantities. Either because the tissue was already entirely or nearly completely utilized in the diagnostic workup or because it was a small needle biopsy containing too little material for tissue extraction for the TMA. Moreover, bone marrow biopsies are also generally unsuitable for TMAs. TMA construction was as previously described (26). In brief, tissue cylinders with a diameter of 0.6 mm each were taken from tumor-containing areas of selected "donor" tissue blocks and brought into empty recipient paraffin blocks. A large section of cerebral tissue was used as an on-slide positive control (27).

Immunohistochemistry (IHC)

Freshly prepared TMA sections were immunostained on one day in one experiment. Slides were deparaffinized and exposed to heat-induced antigen retrieval for 5 minutes in an autoclave at 121°C in pH 9 Dako Target Retrieval Solution buffer (Dako, Glostrup, Denmark). Primary Anti-Pan Trk antibody (rabbit monoclonal, EPR17341, Abcam, Cambridge, MA) was applied according to the manufacturer's instructions. The antibody reacts with a conserved proprietary peptide in the C-terminal part of TRK A, B and C. Bound antibody was then visualized using the EnVision Kit (Dako, Glostrup, Denmark) according to the manufacturer's instructions. The percentage of NTRK-positive tumor cells was estimated, and the staining intensity was semi-quantitatively recorded (0, 1+, 2+, 3+). For statistical analyses, the staining results were categorized into four groups: Negative: no staining at all, weak staining: staining intensity of 1+ in ≤ 70% or staining intensity of 2+ in ≤ 30% of tumor cells, moderate staining: staining intensity of 1+ in > 70%, staining intensity of 2+ in > 30% but in ≤ 70% or staining intensity of 3+ in ≤ 30% of tumor cells, strong staining: staining intensity of 2+ in > 70% or staining intensity of 3+ in > 30% of tumor cells.

Fluorescence *in situ* hybridization (FISH)

Freshly prepared TMA sections were pretreated (dewaxing, proteolysis) according to the instructions for use of the ZytoLight FISH-tissue Implementation Kit (Zyto Vision, Bremerhaven, Germany). 10 µl of SPEC NTRK1/NTRK2/NTRK3 Dual Color Break Apart Probe (Zyto Vision, Bremerhaven, Germany) was applied, posttreated and interpreted according to the manufactures manual. Hybridization quality was assessed semiquantitatively on a 1 - 3 scale (1=poor, 2=moderate, 3=good). Only results with quality 2 and 3 were evaluated.

Endpoints

The primary aim of this study was to evaluate the rate of immunohistochemical expression of NTRK fusion protein in tumor samples of patients with newly diagnosed or r/r DLBCL.

Statistical analysis

All statistical analyses were performed using Microsoft Excel for Mac, version 16.38 (Microsoft Cooperation, Redmon, Washington USA). Continuous values are presented as median. Nominal variables are expressed as numbers (%).

Results

Patients' characteristics

A total of 92 samples of 92 consecutive patients diagnosed with DLBCL were included in the analysis. The most frequent tissue samples originated from lymph nodes (38%), followed by the testis (9%). The remaining samples originated from other extranodal tissues, including the small intestine, colon, skin, spleen, liver, buccal mucosa, and nasal mucosa. Patients' demographics and baseline characteristics are presented in Table 1. The median age was 74 years (range 32-90), and the majority of patients were male (60%). In 41 (45%) patients, a germinal center B-cell-like cell of origin type was observed. Epstein-Barr-virus positivity was detectable in four patients (4%). Double hit expression was detectable in two patients (2%), whereas MYC-translocation was not assessed in 14 patients. IPI risk stratification showed high-risk DLBCL with IPI 4 or 5 in of 30 evaluable patients (17%, IPI was not assessable in 62 patients). In 13 patients, DLBCL transformed out of indolent lymphoma, including follicular lymphoma,

TABLE 1 Patients' characteristics.

Total number of analyzable patients, n	91
Age at DLBCL diagnosis, median (range)	74 (32-90)
Female sex, n (%)	37 (40)
Subtypes, n (%)	
Cell of origin type: Germinal enter B-cell-like	41 (45)
Epstein-Barr-virus positivity	4 (4)
Double hit	2 (2)
Triple hit	0
Ann Arbor stage, n (%)	
1A or 1B and 2A or 2B	18 (20)
3A or 3B	5 (5)
4A or 4B	14 (15)
Not evaluable	59 (65)
IPI, n (%)	
0-1	12 (13)
2-3	13 (14)
4-5	4 (4)
Not evaluable	62 (68)

lymphoplasmacytic lymphoma, chronic lymphatic lymphoma, and one case of angioimmunoblastic T-cell lymphoma.

Immunohistochemical findings

In the TMA, 91 out of 92 (99%) DLBCL were analyzable. The one non-informative case was excluded due to unequivocal tumor tissue on the slide. Positive staining was defined as any viable staining, whether nuclear, paranuclear, cytoplasmatic, or membranous. No positive case was detected with valid positive on slide control (Figures 2, 3).

Findings by FISH

For NTRK1, the hybridization quality was 2 and all spots were evaluable. For NTRK2 and NTRK3, the hybridization quality was 3 and 2, respectively, and all spots could be evaluated. All tests showed no break apart event (Figure 4).

Discussion

Up to now, the role of NTRK fusion genes and protein expression in lymphoma, particularly in DLBCL, has been scarcely investigated. For this reason, we aimed to investigate whether NTRK fusion proteins are expressed in samples of DLBCL patients. By conducting a systemic immunohistochemical screening for the expression of NTRK fusion proteins and an additional FISH analysis in a large cohort of 92 consecutive DLBCL samples, an NTRK fusion protein expression was undetectable in all analyzable samples. Our results are underlined by the few data sets provided by the National Cancer Institute Genomic Data Commons data portal in which NTRK3 receptor mutations (D98N) were detectable in only one of 28 (3.6%) provided cases of mature B-cell lymphoma, whereas mutations in NTRK1 and two were not detected at all (28). One of the few analyses describing the examination of NTRK fusions in B-cell lymphoma samples is a recently published study by Witte and colleagues. The authors reported two cases of NTRK3 mutations in a subset of patients with plasmablastic lymphoma using whole-exome and RNA-sequencing (22). Similar findings were reported by Li et al. who performed a whole-exome sequencing of matched tumor tissues and blood samples from 53 patients with primary gastrointestinal diffuse large B-cell lymphoma. NTRK2 and NTRK3 were detectable in two and one sample, respectively (29). To detect

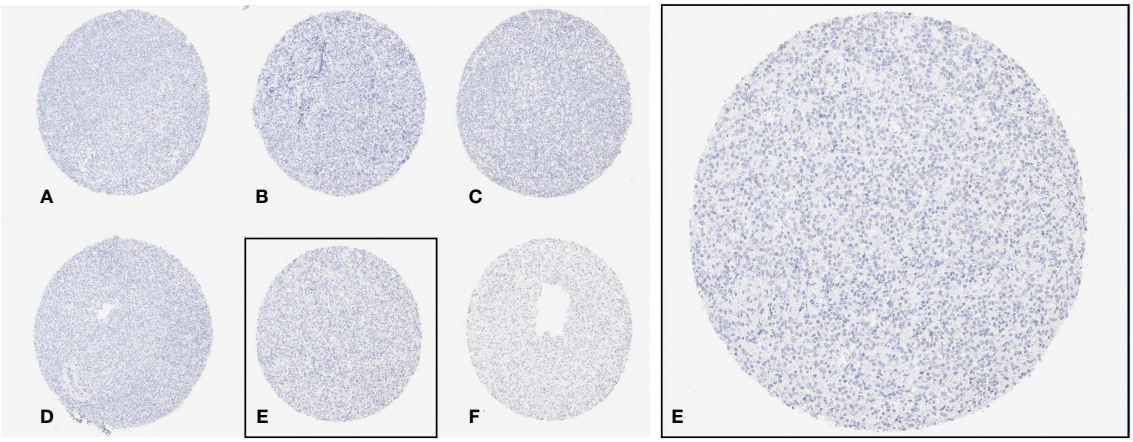

FIGURE 2
Left (40x): Overview of six spots from the TMA. Right (100x): Magnification of the spot e. **(A–F)** shows six exemplary TMA spots.

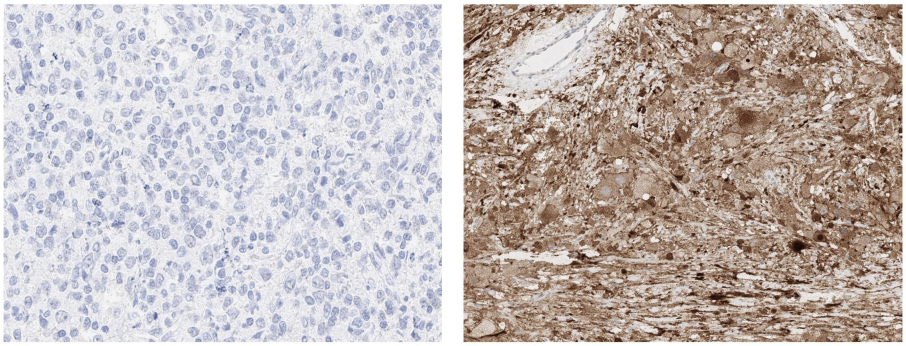

FIGURE 3
Left (400x): High magnification of spot e. No detectable positive signal. Right (100 x): Grey matter of the brain containing cell bodies with strong diffuse cytoplasmatic positivity. Of note are the negative vessels in the upper left corner.

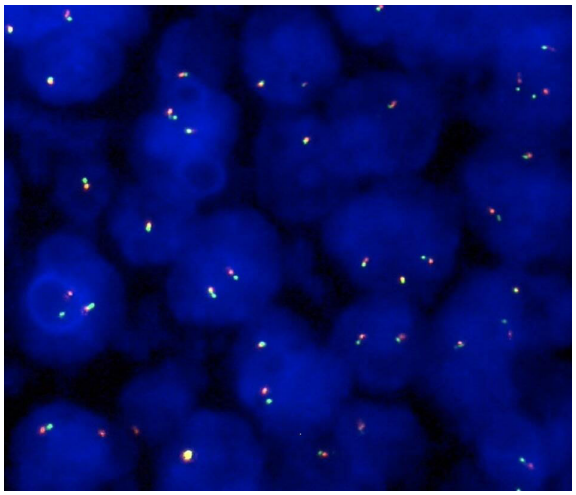

FIGURE 4
Representative example of interphase FISH finding using the NTRK2 probe (100x): Lymphoma cells lacking a translocation with two orange/green fusion signals.

NTRK fusions, several techniques are generally recommended by the ESMO Translational Research and Precision Medicine Working Group, including IHC, FISH, real-time polymerase-chain-reaction, and both RNA-based and DNA-based next-generation sequencing (13). Even though RNA-based sequencing is considered the gold standard for screening, it requires high-quality RNA for reliable sequencing and reducing the risk of false negative results (30). Moreover, next-generation sequencing remains an expansive technique that is not always widely available (13). However, IHC and FISH have been proven to have high sensitivity and specificity for detecting NTRK fusions or break aparts, respectively. False positive results are unlikely based on the limited expression of TRKA, TRKB, and TRKC in other tissues (13, 31–34). Both methods combine the advantages of rapidness, saving tumor material, and costs. Therefore a stepwise approach using IHC and/or FISH as a screening tool followed by RNA-based sequencing in cases of NTRK staining is recommended as one possible approach for the detection of NTRK fusions even in routine diagnostics (13). However, there remains a residual risk of false negative IHC results as recently described (35).

Even though no NTRK fusion protein expression and no NTRK break apart was detectable in our sample cohort, performing systemic screenings for NTRK fusions is necessary to further define the role of NTRK fusions not only in DLBCL but also in a multitude of lymphoma entities as long as the lack of reliable data exists. For this reason, additional analyses of NTRK fusions in cohorts of DLBCL by samples of similar size or larger and different detection technics are necessary to discuss our results.

Data availability statement

The raw data supporting the conclusions of this article will be made available by the authors, without undue reservation.

Author contributions

Conceptualization, SG, and SW. Methodology, SG, CB, and SW. Formal analysis, SG, and SW. Investigation, SG and SW. Resources, SW and CB. Data curation, SG and SW. Writing—original draft preparation, SG and SW. Writing—review and editing, JD, and CB. Visualization, SW. Supervision, JD and CB. Project administration, SG and SW. All authors contributed to the article and approved the submitted version.

Conflict of interest

The authors declare that the research was conducted in the absence of any commercial or financial relationships that could be construed as a potential conflict of interest.

Publisher's note

References

1. Morton LM, Wang SS, Devesa SS, Hartge P, Weisenburger DD, Linet MS. Lymphoma incidence patterns by WHO subtype in the united states, 1992-2001. *Blood* (2006) 107(1):265–76. doi: 10.1182/blood-2005-06-2508

2. van Leeuwen MT, Turner JJ, Joske DJ, Falster MO, Srasuebkul P, Meagher NS, et al. Lymphoid neoplasm incidence by WHO subtype in Australia 1982-2006. *Int J Cancer.* (2014) 135(9):2146–56. doi: 10.1002/ijc.28849

3. Smith A, Howell D, Patmore R, Jack A, Roman E. Incidence of haematological malignancy by sub-type: a report from the haematological malignancy research network. *Br J Cancer.* (2011) 105(11):1684–92. doi: 10.1038/bjc.2011.450

4. Hui D, Proctor B, Donaldson J, Shenkier T, Hoskins P, Klasa R, et al. Prognostic implications of extranodal involvement in patients with diffuse large b-cell lymphoma treated with rituximab and cyclophosphamide, doxorubicin, vincristine, and prednisone. *Leuk Lymphoma.* (2010) 51(9):1658–67. doi: 10.3109/10428194.2010.504872

5. Pavlovsky M, Cubero D, Agreda-Vasquez GP, Enrico A, Mela-Osorio MJ, San Sebastian JA, et al. Clinical outcomes of patients with b-cell non-Hodgkin lymphoma in real-world settings: Findings from the hemato-oncology Latin America observational registry study. *JCO Glob Oncol* (2022) 8:e2100265. doi: 10.1200/GO.21.00265

6. Bishop MR, Dickinson M, Purtill D, Barba P, Santoro A, Hamad N, et al. Second-line tisagenlecleucel or standard care in aggressive b-cell lymphoma. *N Engl J Med* (2022) 386(7):629–39. doi: 10.1056/NEJMoa2116596

7. Hutchings M, Mous R, Clausen MR, Johnson P, Linton KM, Chamuleau MED, et al. Dose escalation of subcutaneous epcoritamab in patients with relapsed or refractory b-cell non-Hodgkin lymphoma: an open-label, phase 1/2 study. *Lancet (London England).* (2021) 398(10306):1157–69. doi: 10.1016/S0140-6736(21)00889-8

8. Dickinson MJ, Carlo-Stella C, Morschhauser F, Bachy E, Corradini P, Iacoboni G, et al. Glofitamab for relapsed or refractory diffuse Large b-cell lymphoma. *N Engl J Med* (2022) 387(24):2220–31. doi: 10.1056/NEJMoa2206913

9. Hutchings M, Morschhauser F, Iacoboni G, Carlo-Stella C, Offner FC, Sureda A, et al. Glofitamab, a novel, bivalent CD20-targeting T-Cell-Engaging bispecific antibody, induces durable complete remissions in relapsed or refractory b-cell lymphoma: A phase I trial. *J Clin Oncol* (2021) 39(18):1959–70. doi: 10.1200/JCO.20.03175

10. Locke FL, Miklos DB, Jacobson CA, Perales MA, Kersten MJ, Oluwole OO, et al. Axicabtagene ciloleucel as second-line therapy for Large b-cell lymphoma. *N Engl J Med* (2022) 386(7):640–54. doi: 10.1056/NEJMoa2116133

11. Kamdar M, Solomon SR, Arnason J, Johnston PB, Glass B, Bachanova V, et al. Lisocabtagene maraleucel versus standard of care with salvage chemotherapy followed by autologous stem cell transplantation as second-line treatment in patients with relapsed or refractory large b-cell lymphoma (TRANSFORM): results from an interim analysis of an open-label, randomised, phase 3 trial. *Lancet (London England).* (2022) 399(10343):2294–308. doi: 10.1016/S0140-6736(22)00662-6

12. Locke FL, Hu Z-H, Siddiqi T, Jacobson CA, Nikiforow S, Ahmed S, et al. Real-world impact of time from leukapheresis to infusion (Vein-to-Vein time) in patients with relapsed or refractory (r/r) Large b-cell lymphoma (LBCL) treated with axicabtagene ciloleucel. *Blood* (2022) 140(Supplement 1):7512–5. doi: 10.1182/blood-2022-155603

13. Marchio C, Scaltriti M, Ladanyi M, Iafrate AJ, Bibeau F, Dietel M, et al. ESMO recommendations on the standard methods to detect NTRK fusions in daily practice and clinical research. *Ann Oncol* (2019) 30(9):1417–27. doi: 10.1093/annonc/mdz204

14. Skaper SD. The neurotrophin family of neurotrophic factors: an overview. *Methods Mol Biol* (2012) 846:1–12. doi: 10.1007/978-1-61779-536-7_1

15. Huang EJ, Reichardt LF. Neurotrophins: roles in neuronal development and function. *Annu Rev Neurosci* (2001) 24:677–736. doi: 10.1146/annurev.neuro.24.1.677

16. Amatu A, Sartore-Bianchi A, Siena S. NTRK gene fusions as novel targets of cancer therapy across multiple tumour types. *ESMO Open* (2016) 1(2):e000023. doi: 10.1136/esmoopen-2015-000023

17. Tacconelli A, Farina AR, Cappabianca L, Desantis G, Tessitore A, Vetuschi A, et al. TrkA alternative splicing: a regulated tumor-promoting switch in human neuroblastoma. *Cancer Cell* (2004) 6(4):347–60. doi: 10.1016/j.ccr.2004.09.011

18. Rubin JB, Segal RA. Growth, survival and migration: the trk to cancer. *Cancer Treat Res* (2003) 115:1–18. doi: 10.1007/0-306-48158-8_1

19. Cocco E, Scaltriti M, Drilon A. NTRK fusion-positive cancers and TRK inhibitor therapy. *Nat Rev Clin Oncol* (2018) 15(12):731–47. doi: 10.1038/s41571-018-0113-0

20. Administration USFaD. *FDA Approves larotrectinib for solid tumors with NTRK gene fusions 01.15. 2023* . Available at: https://www.fda.gov/drugs/fda-approves-larotrectinib-solid-tumors-ntrk-gene-fusions.

21. Joshi SK, Qian K, Bisson WH, Watanabe-Smith K, Huang A, Bottomly D, et al. Discovery and characterization of targetable NTRK point mutations in hematologic neoplasms. *Blood* (2020) 135(24):2159–70. doi: 10.1182/blood.2019003691

22. Witte HM, Kunstner A, Hertel N, Bernd HW, Bernard V, Stolting S, et al. Integrative genomic and transcriptomic analysis in plasmablastic lymphoma identifies disruption of key regulatory pathways. *Blood Adv* (2022) 6(2):637–51. doi: 10.1182/bloodadvances.2021005486

23. Swerdlow SH, Campo E, Pileri SA, Harris NL, Stein H, Siebert R, et al. The 2016 revision of the world health organization classification of lymphoid neoplasms. *Blood* (2016) 127(20):2375–90. doi: 10.1182/blood-2016-01-643569

24. Lister TA, Crowther D, Sutcliffe SB, Glatstein E, Canellos GP, Young RC, et al. Report of a committee convened to discuss the evaluation and staging of patients with hodgkin's disease: Cotswolds meeting. *J Clin Oncol* (1989) 7(11):1630–6. doi: 10.1200/JCO.1989.7.11.1630

25. International Non-Hodgkin's Lymphoma Prognostic Factors P. A predictive model for aggressive non-hodgkin's lymphoma. *N Engl J Med* (1993) 329(14):987–94. doi: 10.1056/NEJM199309303291402

26. Kononen J, Bubendorf L, Kallioniemi A, Barlund M, Schraml P, Leighton S, et al. Tissue microarrays for high-throughput molecular profiling of tumor specimens. *Nat Med* (1998) 4(7):844–7. doi: 10.1038/nm0798-844

27. Solomon JP, Linkov I, Rosado A, Mullaney K, Rosen EY, Frosina D, et al. NTRK fusion detection across multiple assays and 33,997 cases: diagnostic implications and pitfalls. *Mod Pathol* (2020) 33(1):38–46. doi: 10.1038/s41379-019-0324-7

28. Grossman RL, Heath AP, Ferretti V, Varmus HE, Lowy DR, Kibbe WA, et al. Toward a shared vision for cancer genomic data. *N Engl J Med* (2016) 375(12):1109–12. doi: 10.1056/NEJMp1607591

29. Li SS, Zhai XH, Liu HL, Liu TZ, Cao TY, Chen DM, et al. Whole-exome sequencing analysis identifies distinct mutational profile and novel prognostic biomarkers in primary gastrointestinal diffuse large b-cell lymphoma. *Exp Hematol Oncol* (2022) 11(1):71. doi: 10.1186/s40164-022-00325-7

30. Church AJ, Calicchio ML, Nardi V, Skalova A, Pinto A, Dillon DA, et al. Recurrent EML4-NTRK3 fusions in infantile fibrosarcoma and congenital mesoblastic nephroma suggest a revised testing strategy. *Mod Pathol* (2018) 31(3):463–73. doi: 10.1038/modpathol.2017.127

31. Chiang S, Cotzia P, Hyman DM, Drilon A, Tap WD, Zhang L, et al. NTRK fusions define a novel uterine sarcoma subtype with features of fibrosarcoma. *Am J Surg Pathol* (2018) 42(6):791–8. doi: 10.1097/PAS.0000000000001055

32. Hechtman JF, Benayed R, Hyman DM, Drilon A, Zehir A, Frosina D, et al. Pan-trk immunohistochemistry is an efficient and reliable screen for the detection of NTRK fusions. *Am J Surg Pathol* (2017) 41(11):1547–51. doi: 10.1097/PAS.0000000000000911

33. Negri T, Tamborini E, Dagrada GP, Greco A, Staurengo S, Guzzo M, et al. TRK-a, HER-2/neu, and KIT Expression/Activation profiles in salivary gland carcinoma. *Transl Oncol* (2008) 1(3):121–8. doi: 10.1593/tlo.08127

34. Yu X, Liu L, Cai B, He Y, Wan X. Suppression of anoikis by the neurotrophic receptor TrkB in human ovarian cancer. *Cancer Sci* (2008) 99(3):543–52. doi: 10.1111/j.1349-7006.2007.00722.x

35. Hondelink LM, Schrader AMR, Asri Aghmuni G, Solleveld-Westerink N, Cleton-Jansen AM, van Egmond D, et al. The sensitivity of pan-TRK immunohistochemistry in solid tumours: A meta-analysis. *Eur J Cancer.* (2022) 173:229–37. doi: 10.1016/j.ejca.2022.06.030

frontiers | Frontiers in Oncology

TYPE Systematic Review
PUBLISHED 30 March 2023
DOI 10.3389/fonc.2023.1169749

OPEN ACCESS

EDITED BY
Niklas Gebauer,
University Medical Center Schleswig-Holstein, Germany

REVIEWED BY
Hanno Maximilian Witte,
Bundeswehrkrankenhaus, Germany
Panpan Liu,
Sun Yat-sen University Cancer Center (SYSUCC), China

*CORRESPONDENCE
Zongxin Zhang
zhongxin1006@126.com

SPECIALTY SECTION
This article was submitted to Hematologic Malignancies, a section of the journal Frontiers in Oncology

RECEIVED 20 February 2023
ACCEPTED 20 March 2023
PUBLISHED 30 March 2023

CITATION
Cao D and Zhang Z (2023) Prognostic and clinicopathological role of geriatric nutritional risk index in patients with diffuse large B-cell lymphoma: A meta-analysis. *Front. Oncol.* 13:1169749. doi: 10.3389/fonc.2023.1169749

Prognostic and clinicopathological role of geriatric nutritional risk index in patients with diffuse large B-cell lymphoma: A meta-analysis

Dan Cao[1] and Zongxin Zhang[2]*

[1]Department of Hematology, Huzhou Central Hospital, Affiliated Central Hospital of Huzhou University, Huzhou, Zhejiang, China, [2]Clinical Laboratory, Huzhou Central Hospital, Affiliated Central Hospital of Huzhou University, Huzhou, Zhejiang, China

Background: Previous studies have explored the relationship between the geriatric nutritional risk index (GNRI) and survival outcomes of diffuse large B-cell lymphoma (DLBCL) cases, but the results were inconsistent. Consequently, the present meta-analysis was conducted to investigate how GNRI affects DLBCL and its function in terms of prognosis.

Methods: The Web of Science, PubMed, Embase, and Cochrane Library databases were thoroughly searched until January 18, 2023. We calculated combined hazard ratios (HRs) and 95% confidence intervals (CIs) to estimate the relationship between the GNRI and survival outcomes of patients with DLBCL.

Results: This meta-analysis included seven articles involving 2,353 cases. A lower level of GNRI predicted dismal overall survival (HR=1.40, 95% CI=1.25–1.56, p<0.001) and inferior progression-free survival (HR=1.46, 95% CI=1.19-1.80, p<0.001) of DLBCL patients. Moreover, a low GNRI was significantly related to Eastern Cooperative Oncology Group Performance Status ≥2 (odds ratio [OR] =4.55, 95% CI=2.75–7.54, p<0.001), Ann Arbor stage III–IV (OR=2.91, 95% CI=2.38–3.57, p<0.001), B symptoms (OR=3.51, 95% CI=2.34–5.29, p<0.001), and extranodal disease (OR=2.90, 95% CI=2.32–3.63, p<0.001).

Conclusion: A lower GNRI level predicted poorer short- and long-term prognosis in patients with DLBCL. A low GNRI was correlated with clinical factors of disease progression in DLBCL patients.

KEYWORDS

geriatric nutritional risk index, meta-analysis, diffuse large B-cell lymphoma, prognosis, clinical practice

Introduction

Among non-Hodgkin lymphoid (NHL) malignancies, diffuse large B-cell lymphoma (DLBCL) accounts for the highest proportion (30–40% of NHL cases) (1). Approximately 60% of the DLBCL cases can be treated using standard therapeutic regimens (such as rituximab, cyclophosphamide, doxorubicin, vincristine, and prednisone) (2). However, 45–50% of the cases relapse or become refractory after a complete response (3). The prognosis for patients experiencing relapse is poor because 80% of them ultimately die from DLBCL, even after treatment with subsequent regimens (4). The poor survival outcomes of DLBCL patients are partially due to the lack of effective prognostic markers. Therefore, identifying novel and readily available biomarkers is important for the prognosis of DLBCL.

Growing evidence has shown that nutritional status and immune responses play essential roles in tumor initiation, development, and metastasis (5, 6). Many parameters derived from laboratory examinations have drawn considerable attention because of their prognostic value. Recently, numerous studies reported the relationship between a series of serum-based parameters and the prognosis of DLBCL (7–10). These indexes include the lymphocyte-to-monocyte ratio (7), neutrophil-to-lymphocyte ratio (NLR) (8), C-reactive protein (9), and platelet-to-lymphocyte ratio (PLR) (10). The geriatric nutritional risk index (GNRI) is a nutritional marker that includes patient's body weight (BW), height, and serum albumin content. It is calculated by the formula: GNRI = 1.487 × serum albumin (g/L) + 41.7 × present/optimal BW (kg) (11). In clinical settings, the GNRI is used as a simple nutrition evaluation approach, and a low GNRI indicates poor nutritional status of patients (12, 13). In recent years, numerous studies have analyzed the role of GNRI in predicting the prognosis of DLBCL cases (14–20), but their findings remain controversial. For example, in some studies, low GNRI significantly predicted poor survival in DLBCL patients (14, 16, 19). However, other researchers have reported that the GNRI is not related to DLBCL survival (15). Previous studies that adopted different cut-off values of the GNRI could also contribute to the conflicting results. Therefore, we searched recent literatures and carried out a meta-analysis to identify whether the GNRI predicted DLBCL prognosis accurately.

Abbreviations: GNRI, geriatric nutritional risk index; DLBCL, diffuse large B-cell lymphoma; HR, hazard ratio; CI, confidence interval; OS, overall survival; PFS, progression-free survival; ECOG-PS, eastern cooperative oncology group performance status; NHL, non-Hodgkin lymphoid; R-CHOP, rituximab, cyclophosphamide, doxorubicin, vincristine and prednisone; LMR, lymphocyte-to-monocyte ratio; NLR, neutrophil-to-lymphocyte ratio; CRP, C-reactive protein; PLR, platelet-to-lymphocyte ratio; PRISMA, Preferred Reporting Items for Systematic Reviews and Meta-Analyses; NOS, Newcastle-Ottawa Scale; OR, odds ratio; ROC, receiver operating characteristic.

Materials and methods

Study guideline

This study was performed following the Preferred Reporting Items for Systematic Reviews and Meta-Analyses guidelines (21).

Literature search

Studies were identified in the Web of Science, PubMed, Embase, and Cochrane Library databases. The search strategies were as follows: (geriatric nutritional risk index or GNRI) and (diffuse large B-cell lymphoma or DLBCL or lymphoma). Detailed search strategies for each database are provided in Supplementary File 1. Retrieval timeline was from inception until January 18, 2023. Only publications published in the English language were considered. Relevant documents in references of the identified studies were also searched.

Eligibility criteria

Studies conforming to the following criteria were included (1): cases with a pathological diagnosis of DLBCL; (2) GNRI determined prior to anticancer therapy; (3) studies mentioning the function of GNRI in predicting prognosis, such as overall survival (OS), progression-free survival (PFS), recurrence-free survival (RFS), and cancer-specific survival (CSS); (4) studies with available hazard ratios (HRs) together with associated 95% confidence intervals (CIs) regarding patient outcomes; (5) studies with a threshold to classify high/low GNRI; and (6) articles written in the English language. Studies conforming to the following standards were excluded: (1) reviews, case reports, meeting abstracts, letters, and correspondences; (2) articles that included overlapping patients; and (3) animal studies.

Data collection and quality evaluation

Two independent reviewers (D.C. and Z.Z.) were responsible for data collection from qualified articles. Any disagreement between the reviewers was resolved through mutual negotiation until a consensus was reached. The following data were collected: name of first author, country, publication year, sample size, age, sex, study duration, follow-up, threshold GNRI, threshold measurement approach, study center, survival analysis, survival endpoints, treatment, and HRs with 95% CIs. The methodological quality of the eligible articles was evaluated using the Newcastle–Ottawa scale (NOS) (22). Articles with NOS scores of ≥6 were regarded as high-quality articles.

Statistical analysis

Combined HRs and 95% CIs were determined to estimate the relationship between the GNRI and survival outcomes in the

DLBCL cases. Heterogeneity among the enrolled articles was analyzed using I^2 statistics and the Cochran's Q test. An I^2 statistics of ≥50% and/or p<0.10 on the Cochran Q test indicated obvious heterogeneity, and the random-effects model was used; otherwise, the fixed-effects model was adopted. Diverse factor-stratified subgroup analyses were carried out to detect sources of heterogeneity. Correlations of GNRI with clinicopathological features in DLBCL were explored by combining odds ratios (ORs) and associated 95% CIs. The Begg's test was used for publication bias, while an asymmetry assessment was performed using a funnel plot. All statistical analyses were carried out using Stata software (version 12.0; Stata Corporation, College Station, TX, USA). Statistical significance was set at p<0.05 (two-sided), which represented statistical significance.

Ethnics statement

The need for ethical approval was waived from this work, and no informed consent was obtained because no patient information was involved.

Results

Study selection process

As shown in Figure 1, the original study selection detected 60 studies, and after removal of the duplicates, 32 records remained. Subsequently, titles and abstracts were scanned, and 21 articles were discarded because of their irrelevance. By reading the full texts of 11 articles, 4 articles were then eliminated due to no cut-off value of GNRI (n=3) and inclusion of overlapping patients (n=1). Finally, seven articles, involving 2,353 cases (14–20), were included in the present study (Figure 1; Table 1).

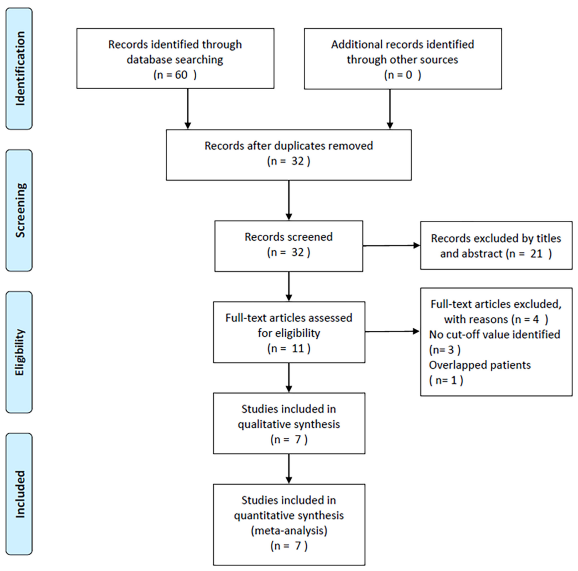

FIGURE 1
PRISMA flow diagram of the study selection process.

Qualified article characteristics

Table 1 shows the basic characteristics of the qualified articles. All the eligible articles were published between 2018–2022 (14–20). Three studies were conducted in Japan (14, 16, 18), two in China (15, 19), and one each in Taiwan (17) and Turkey (20). The sample size was 133–615 (median, 267). All the included studies had a retrospective design and enrolled DLBCL patients with Ann Arbor stage I–IV (14–20). The threshold GNRI was 92–106.26 (median, 96.8). Six studies analyzed thresholds with receiver operating characteristic (ROC) curves (14, 16–20), while one study selected cut-off values according to the literature (15). Five studies were carried out in a single center (14, 15, 17, 19, 20), and two were multicenter trials (16, 18). All seven articles mentioned the role of GNRI in predicting OS (14–20), and two studies reported an association between the GNRI and PFS (14, 17) in DLBCL. Six articles mentioned the HRs and 95% CIs through multivariate regression (14–18, 20), and one study adopted a univariate analysis (19). The NOS scores were 6–9 (median, 7), indicating high quality.

Prognostic value of GNRI for OS and PFS

Seven articles with 2,353 patients (14–20) reported GNRI values for predicting OS in DLBCL. No obvious heterogeneity (I^2 = 48.8%, p=0.069) was detected; therefore, we selected a fixed-effects model. According to Table 2 and Figure 2, the combined results were: HR=1.40, 95% CI=1.25–1.56, p<0.001, demonstrating that low GNRI was markedly associated with poor OS in DLBCL. Subgroup analysis by various factors was conducted (Table 2), which showed that the reduced GNRI significantly predicted poor OS, regardless of the study center, sample size, treatment, or survival analysis type. Furthermore, a lower GNRI markedly predicted poor OS when using a cut-off value of <98 when the patients' median age was ≥60 years, and cut-off values were determined using the ROC curve (Table 2). Two studies involving 681 patients reported an association between the GNRI and PFS in DLBCL (14, 17). Based on the combined data, a lower GNRI significantly predicted dismal PFS in DLBCL cases (HR=1.46, 95% CI=1.19–1.80, p<0.001; Figure 3 and Table 2).

Relationship of GNRI with clinicopathological factors

Five studies, involving 1,769 cases, mentioned the correlation between the GNRI and clinicopathological characteristics of DLBCL (14–17, 20). As shown in Table 3 and Figure 4, the combined results revealed a marked relation between the lower

TABLE 1 Baseline characteristics of included studies in this meta-analysis.

Study	Year	Country/ region	Sample size	Age (years) Median (range)	Gender (M/F)	Study period	Ann Arbor stage	Treatment	Follow-up (month) Median (range)	Cut-off value	Cut-off deter-mination	Study center	Survival endpoints	Survival analysis	NOS score
Kanemasa, Y.	2018	Japan	476	68(27-97)	266/210	2004-2017	I-IV	R-CHOP or R-CHP-COP	45	96.8	ROC curve	Single center	OS, PFS	Multivariate	8
Li, Z.	2018	China	267	59	156/111	2010-2016	I-IV	R-CHOP	1-72	98	Literature	Single center	OS	Multivariate	7
Matsukawa, T.	2020	Japan	615	69(20-97)	337/278	2008-2018	I-IV	R-CHOP	1-60	95.7	ROC curve	Multicenter	OS	Multivariate	7
Chuang, T. M.	2021	Taiwan	205	75(65-96)	107/98	2010-2019	I-IV	R-CHOP	1-140	92.5	ROC curve	Single center	OS, PFS	Multivariate	9
Lee, S.	2021	Japan	451	78(65-96)	223/228	2007-2017	I-IV	R-CHOP or R-CHP-COP	22.3(1-140.3)	92	ROC curve	Multicenter	OS	Multivariate	6
Yan, D.	2021	China	133	71(60-91)	67/66	2014-2018	I-IV	R-CHOP	35.2	106.26	ROC curve	Single center	OS	Univariate	7
Atas, U.	2022	Turkey	206	58.5	112/94	2008-2020	I-IV	R-CHOP	27.5(1-164)	104.24	ROC curve	Single center	OS	Multivariate	7

M, male; F, female; ROC, receiver operating characteristic; OS, overall survival; PFS, progression-free survival; NOS, Newcastle-Ottawa Scale; R-CHOP, rituximab with cyclophosphamide, doxorubicin, vincristine and prednisone; R-THP-COP, rituximab with cyclophosphamide, tetrahydropyranyl adriamycin, vincristine, prednisolone.

10.3389/fonc.2023.1169749

TABLE 2 Subgroup analysis of the prognostic value of GNRI for OS and PFS in patients with DLBCL.

Factors	No. of studies	No. of patients	Effects model	HR (95%CI)	p	Heterogeneity I^2(%) Ph	
OS							
Total	7	2,353	Fixed	1.40(1.25-1.56)	<0.001	48.8	0.069
Sample size							
<300	4	811	Fixed	1.44(1.11-1.86)	0.005	49.8	0.113
≥300	3	1,542	Random	1.60(1.17-2.19)	0.003	64.7	0.059
Cut-off value							
<98	4	1,747	Random	1.68(1.22-2.31)	0.001	60.3	0.056
≥98	3	606	Random	1.34(0.88-2.02)	0.171	51.8	0.126
Cut-off determination							
ROC curve	6	2,086	Fixed	1.43(1.27-1.60)	<0.001	40.6	0.134
Literature	1	267	–	0.81(0.44-1.48)	0.488	–	–
Study center							
Single center	5	1,287	Fixed	1.57(1.26-1.96)	<0.001	48.5	0.100
Multicenter	2	1,066	Random	1.46(1.06-2.01)	0.022	60.4	0.112
Survival analysis							
Univariate	1	133	–	1.48(1.06-2.07)	0.022	–	–
Multivariate	6	2,220	Random	1.55(1.18-2.04)	0.002	56.8	0.041
Median age (years)							
<60	2	473	Random	1.23(0.54-2.76)	0.623	73.0	0.054
≥60	5	1,880	Fixed	1.41(1.25-1.59)	<0.001	47.7	0.106
Treatment							
R-CHOP	5	1,426	Fixed	1.54(1.24-1.91)	<0.001	42.4	0.139
R-CHOP or R-CHP-COP	2	927	Random	1.55(1.00-2.40)	0.006	72.8	0.055
PFS							
Total	2	681	Fixed	1.46(1.19-1.80)	<0.001	44.0	0.181

ROC, receiver operating characteristic; OS, overall survival; PFS, progression-free survival; GNRI, geriatric nutritional risk index; DLBCL, diffuse large B-cell lymphoma; R-CHOP, rituximab with cyclophosphamide, doxorubicin, vincristine and prednisone; R-THP-COP, rituximab with cyclophosphamide, tetrahydropyranyl adriamycin, vincristine, prednisolone.

GNRI and Eastern Cooperative Oncology Group Performance Status (ECOG-PS) ≥2 (OR=4.55, 95% CI=2.75–7.54, p<0.001), Ann Arbor stage III–IV (OR=2.91, 95% CI=2.38–3.57, p<0.001), B symptoms (OR=3.51, 95% CI=2.34–5.29, p<0.001), and extranodal disease (OR=2.90, 95% CI=2.32–3.63, p<0.001). Nonetheless, the GNRI was not significantly related to sex in DLBCL (OR=0.93, 95% CI=0.77–1.12, p=0.436; Table 3; Figure 4).

Publication bias

We adopted the Begg's test and funnel plot to examine possible publication bias. As shown in Figure 5, symmetry was observed in the funnel plot, and the Begg's test (p=0.368 and 0.317 for OS and PFS, respectively) revealed no evidence of obvious publication bias.

Discussion

The role of GNRI in predicting prognosis in patients with DLBCL is controversial based on prior articles. We obtained data from seven articles, comprising 2,353 cases and showed that a lower GNRI markedly predicted worse OS and PFS in DLBCL patients. Based on subgroup analysis, the GNRI reliably predicted OS, especially when the cut-off value was <92. This meta-analysis also revealed that decreased GNRI was significantly associated with clinical factors representing aggressive biological behavior, i.e., ECOG-PS ≥2, Ann Arbor stage III–IV, B symptoms, and extranodal disorder. These factors are well known high-risk factors for disease progression and dismal outcomes in DLBCL cases. Taken together, low GNRI significantly predicted poor OS and PFS in DLBCL patients. To the best of our knowledge, this is the first meta-analysis to analyze the role of GNRI in predicting DLBCL prognosis.

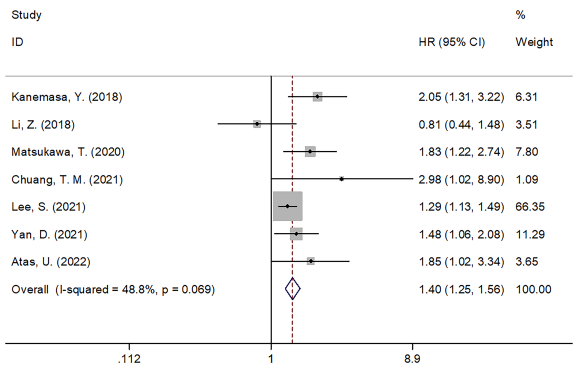

FIGURE 2
Forest plot of the association of GNRI with OS in patients with DLBCL.

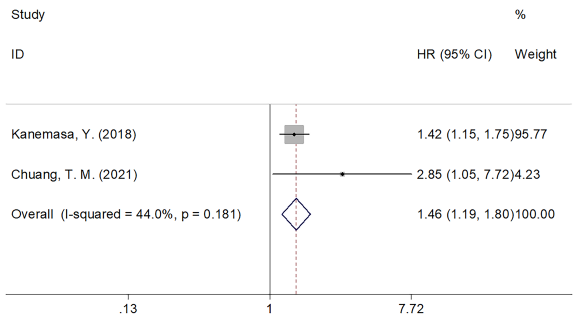

FIGURE 3
Forest plot of the association of GNRI with PFS in patients with DLBCL.

The GNRI is a beneficial tool for assessing nutritional status in clinical practice. There are several cancers for which the GNRI comprises serum albumin levels, BW, and height, which are identified as efficient prognostic factors (13, 23, 24). The correlation mechanism between the GNRI and DLBCL prognosis was interpreted based on components of the GNRI for cancer cases. Approximately 90% of the serum proteins are derived from albumin, which is produced by the liver. Albumin is essential to the human body (25). In addition to reflecting the nutritional status of the human body, serum albumin is a measure of inflammation (26). Albumin has a key effect in maintaining blood colloid osmotic pressure and delivering pharmaceuticals, hormones, cations, and fatty acids (27). Capillary permeability is increased by cancer-related inflammation, which allows serum albumin to escape into the interstitium. Second, >10% BW loss indicates protein-energy malnutrition (28). In comparison with normal-weight cases, underweight DLBCL cases have worse OS and PFS, according to a meta-analysis involving 8,753 participants (29). Patient outcomes have been shown to be significantly affected by weight, as a modifiable factor, and weight management should be aggressive during treatment (30). Finally, low GNRI, possibly caused by weight loss and decreased serum albumin content, is a reasonable and cost-effective prognostic marker for patients with DLBCL.

Notably, previous studies have also explored the prognostic value of several inflammatory parameters, such as the Glasgow prognostic score (GPS) (31), NLR (32), and PLR (33). These studies demonstrated that high GPS and elevated NLR and PLR remained effective prognostic indices for patients with DLBCL (31–33). The GNRI has several advantages and disadvantages compared with GPS, NLR, and PLR. The GNRI is a tool used for nutritional assessment. The nutritional status of patients could be directly reflected by the GNRI, but the GPS, NLR, and PLR have no such function. Second, the GNRI is a novel index that has drawn considerable attention in recent years. The clinical application of the GNRI is much more promising than that of the GPS, NLR, and PLR. However, disadvantages of the GNRI should also be acknowledged. Calculation of the GNRI is more complex than that of the GPS, NLR, and PLR.

We performed a subgroup analysis according to the median age and treatment regimens. As shown in Table 2, the results indicated that the GNRI remained a prognostic factor for OS in patients with a median age ≥60 years, and the prognostic role was not influenced by treatment strategies. Therefore, the GNRI could be a reliable prognostic indicator for DLBCL patients aged ≥60 years, whether they received the rituximab, cyclophosphamide, doxorubicin hydrochloride (hydroxydaunorubicin), vincristine sulfate (Oncovin), and prednisone (R-CHOP) or R-CHOP-like regimens. The association between the GNRI and clinicopathological factors was analyzed, and the results are shown in Figure 4 and Table 3. We do not think that these associations are causal because the sample size was relatively sufficient (five studies with 1,769 participants). Moreover, the p-value was <0.001 in these groups, indicating a positive relationship.

Recent meta-analyses have reported that the GNRI significantly predicts cancer prognosis (34–38). Zhang et al. conducted a meta-

TABLE 3 The association between GNRI and clinicopathological features in patients with DLBCL.

Variables	No. of studies	No. of patients	Effects model	OR (95%CI)	p	Heterogeneity I^2(%)	Ph
Gender (male vs female)	5	1,769	Fixed	0.93(0.77-1.12)	0.436	0	0.425
ECOG PS (≥2 vs <2)	5	1,769	Random	4.55(2.75-7.54)	<0.001	66.7	0.017
Ann Arbor stage (III-IV vs I-II)	5	1,769	Fixed	2.91(2.38-3.57)	<0.001	0	0.504
B symptom (present vs absent)	5	1,769	Random	3.51(2.34-5.29)	<0.001	56.3	0.058
Extranodal disease (yes vs no)	5	1,769	Fixed	2.90(2.32-3.63)	<0.001	40.2	0.153

GNRI, geriatric nutritional risk index; DLBCL, diffuse large B-cell lymphoma; ECOG PS, eastern cooperative oncology group performance status.

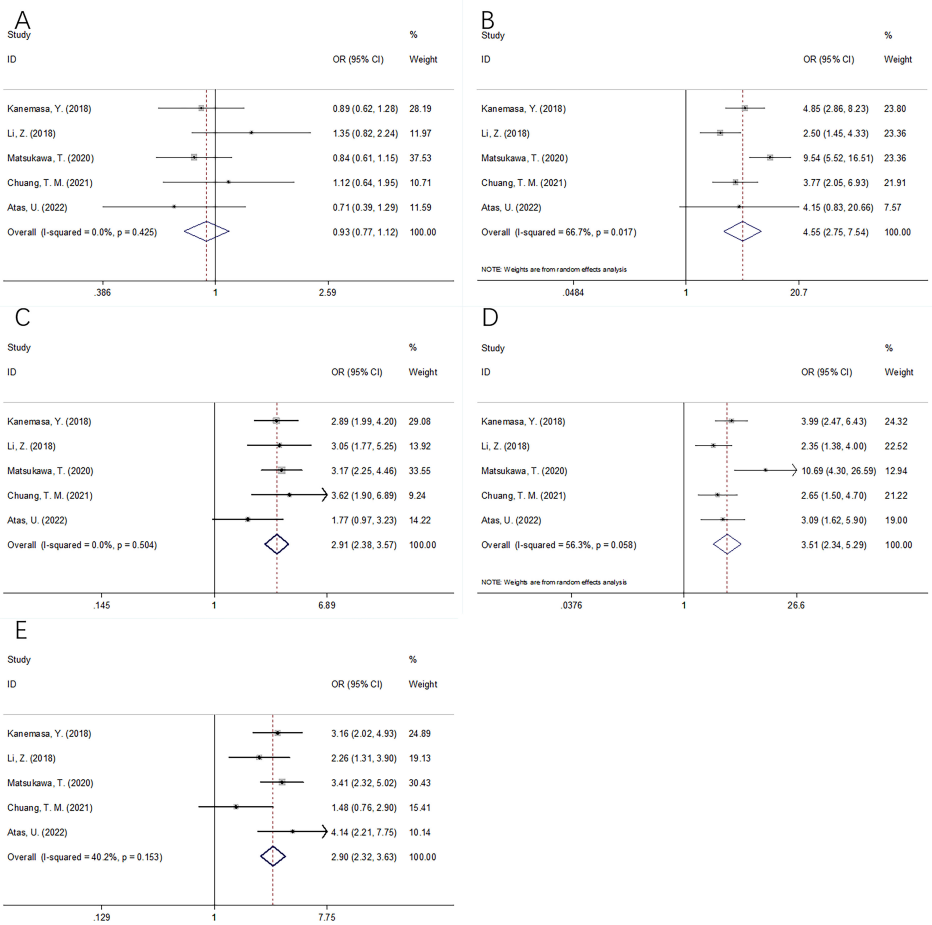

FIGURE 4
Forest plots of the correlation between GNRI and clinicopathological features in DLBCL patients. **(A)** Gender (male vs female); **(B)** ECOG PS (≥2 vs <2); **(C)** Ann Arbor stage (III-IV vs I-II); **(D)** B symptom (present vs absent); and **(E)** Extranodal disease (yes vs no).

analysis of 5,593 patients and showed that the GNRI performed well in predicting long-term survival, as well as complications among surgical gastric cancer cases (34). Zhou et al. reported that a low GNRI estimated dismal OS and CSS in esophageal cancer cases in a meta-analysis of 11 studies (39). A recent meta-analysis involving 3,440 participants showed that a lower GNRI before treatment predicted poorer OS and disease-free survival of colorectal cancer cases (40). Another meta-analysis enrolling 6,792 patients indicated that a lower GNRI strongly estimated dismal OS, RFS/PFS, and CSS in urological cancers (38). According to Wang et al., a low GNRI predicted dismal OS, RFS, and CSS in lung cancer cases (41).

Some limitations of the present study should be noted. First, the enrolled articles were retrospective studies, which are not as convincing as randomized controlled trials. Second, all the eligible studies were conducted in Asia. Therefore, the role of GNRI in predicting the prognosis of DLBCL in non-Asian populations

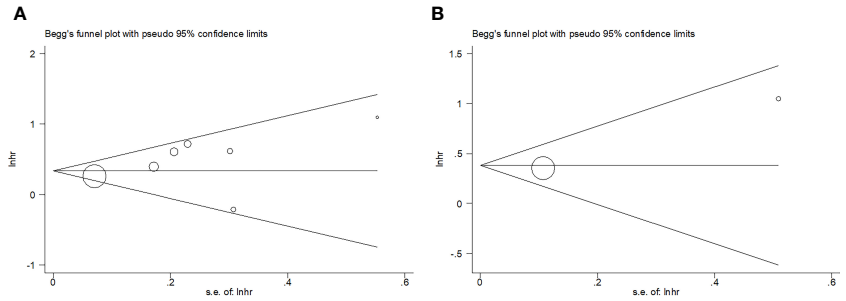

FIGURE 5
Publication bias. **(A)** OS, Begg's test, p=0.368; **(B)** PFS, Begg's test, p=0.317.

should be verified. Third, an optimum cut-off value of the GNRI was not determined in the included studies, which might have caused selection bias. Therefore, large-scale trials in multicenter regions should be conducted for further verification.

Conclusions

In summary, a low GNRI predicts poorer short- and long-term DLBCL prognosis. A low GNRI was correlated with clinical factors of disease progression in DLBCL.

Data availability statement

The original contributions presented in the study are included in the article/Supplementary Material. Further inquiries can be directed to the corresponding author.

Author contributions

DC and ZZ designed and conceived the study. DC and ZZ collected the data. DC analyze the data and performed the statistical analysis. ZZ gave the important guidance for statistical analysis and methodology. DC and ZZ provided critical intellectual contributions. DC drafted the manuscript. All authors contributed to the article and approved the submitted version.

Acknowledgments

We would like to thank Editage (www.editage.com) for English language editing.

Conflict of interest

The authors declare that the research was conducted in the absence of any commercial or financial relationships that could be construed as a potential conflict of interest.

Publisher's note

Supplementary material

The Supplementary Material for this article can be found online at: https://www.frontiersin.org/articles/10.3389/fonc.2023.1169749/full#supplementary-material

References

1. Susanibar-Adaniya S, Barta SK. 2021 Update on diffuse large b cell lymphoma: A review of current data and potential applications on risk stratification and management. *Am J Hematol* (2021) 96(5):617–29. doi: 10.1002/ajh.26151

2. Cheson BD, Nowakowski G, Salles G. Diffuse large b-cell lymphoma: New targets and novel therapies. *Blood Cancer J* (2021) 11(4):68. doi: 10.1038/s41408-021-00456-w

3. Crump M, Neelapu SS, Farooq U, Van Den Neste E, Kuruvilla J, Westin J, et al. Outcomes in refractory diffuse large b-cell lymphoma: Results from the international SCHOLAR-1 study. *Blood* (2017) 130(16):1800–8. doi: 10.1182/blood-2017-03-769620

4. He MY, Kridel R. Treatment resistance in diffuse large b-cell lymphoma. *Leukemia* (2021) 35(8):2151–65. doi: 10.1038/s41375-021-01285-3

5. Grivennikov SI, Greten FR, Karin M. Immunity, inflammation, and cancer. *Cell* (2010) 140(6):883–99. doi: 10.1016/j.cell.2010.01.025

6. Hanahan D, Weinberg RA. Hallmarks of cancer: The next generation. *Cell* (2011) 144(5):646–74. doi: 10.1016/j.cell.2011.02.013

7. Li YL, Pan YY, Jiao Y, Ning J, Fan YG, Zhai ZM. Peripheral blood lymphocyte/monocyte ratio predicts outcome for patients with diffuse large b cell lymphoma after standard first-line regimens. *Ann Hematol* (2014) 93(4):617–26. doi: 10.1007/s00277-013-1916-9

8. Wang J, Zhou M, Xu JY, Yang YG, Zhang QG, Zhou RF, et al. Prognostic role of pretreatment neutrophil-lymphocyte ratio in patients with diffuse large b-cell lymphoma treated with RCHOP. *Med (Baltimore)* (2016) 95(38):e4893. doi: 10.1097/md.0000000000004893

9. Hong JY, Ryu KJ, Lee JY, Park C, Ko YH, Kim WS, et al. Serum level of CXCL10 is associated with inflammatory prognostic biomarkers in patients with diffuse large b-cell lymphoma. *Hematological Oncol* (2017) 35(4):480–6. doi: 10.1002/hon.2374

10. Wang S, Ma Y, Sun L, Shi Y, Jiang S, Yu K, et al. Prognostic significance of pretreatment Neutrophil/Lymphocyte ratio and Platelet/Lymphocyte ratio in patients with diffuse Large b-cell lymphoma. *BioMed Res Int* (2018) 2018:9651254. doi: 10.1155/2018/9651254

11. Buzby GP, Knox LS, Crosby LO, Eisenberg JM, Haakenson CM, McNeal GE, et al. Study protocol: A randomized clinical trial of total parenteral nutrition in malnourished surgical patients. *Am J Clin Nutr* (1988) 47(2 Suppl):366–81. doi: 10.1093/ajcn/47.2.366

12. Ito Y, Abe A, Hayashi H, Momokita M, Furuta H. Prognostic impact of preoperative geriatric nutritional risk index in oral squamous cell carcinoma. *Oral Dis* (2022). doi: 10.1111/odi.14255

13. Pan Y, Zhong X, Liu J. The prognostic significance of geriatric nutritional risk index in elderly patients with bladder cancer after radical cystectomy. *Asian J Surg* (2022). doi: 10.1016/j.asjsur.2022.11.082

14. Kanemasa Y, Shimoyama T, Sasaki Y, Hishima T, Omuro Y. Geriatric nutritional risk index as a prognostic factor in patients with diffuse large b cell lymphoma. *Ann Hematol* (2018) 97(6):999–1007. doi: 10.1007/s00277-018-3273-1

15. Li Z, Guo Q, Wei J, Jin J, Wang J. Geriatric nutritional risk index is not an independent predictor in patients with diffuse large b-cell lymphoma. *Cancer Biomarkers* (2018) 21(4):813–20. doi: 10.3233/cbm-170754

16. Matsukawa T, Suto K, Kanaya M, Izumiyama K, Minauchi K, Yoshida S, et al. Validation and comparison of prognostic values of GNRI, PNI, and CONUT in newly diagnosed diffuse large b cell lymphoma. *Ann Hematol* (2020) 99(12):2859–68. doi: 10.1007/s00277-020-04262-5

17. Chuang TM, Liu YC, Hsiao HH, Wang HC, Du JS, Yeh TJ, et al. Low geriatric nutritional risk index is associated with poorer prognosis in elderly diffuse Large b-cell lymphoma patients unfit for intensive anthracycline-containing therapy: A real-world study. *Nutrients* (2021) 13(9):3243. doi: 10.3390/nu13093243

18. Lee S, Fujita K, Morishita T, Negoro E, Oiwa K, Tsukasaki H, et al. Prognostic utility of a geriatric nutritional risk index in combination with a comorbidity index in elderly patients with diffuse large b cell lymphoma. *Br J Haematol* (2021) 192(1):100–9. doi: 10.1111/bjh.16743

19. Yan D, Shen Z, Zhang S, Hu L, Sun Q, Xu K, et al. Prognostic values of geriatric nutritional risk index (GNRI) and prognostic nutritional index (PNI) in elderly patients with diffuse Large b-cell lymphoma. *J Cancer* (2021) 12(23):7010–7. doi: 10.7150/jca.62340

20. Atas U, Sozel H, Iltar U, Yucel OK, Salim O, Undar L. The prognostic impact of pretreatment geriatric nutritional risk index in patients with diffuse Large b-cell lymphoma. *Nutr Cancer* (2022) 75(2):591–8. doi: 10.1080/01635581.2022.2142248

21. Moher D, Liberati A, Tetzlaff J, Altman DG, Grp P. Preferred reporting items for systematic reviews and meta-analyses: The PRISMA statement. *PLoS Med* (2009) 6(7): e1000097. doi: 10.1371/journal.pmed.1000097

22. Stang A. Critical evaluation of the Newcastle-Ottawa scale for the assessment of the quality of nonrandomized studies in meta-analyses. *Eur J Epidemiol* (2010) 25 (9):603–5. doi: 10.1007/s10654-010-9491-z

23. Riveros C, Chalfant V, Bazargani S, Bandyk M, Balaji KC. The geriatric nutritional risk index predicts complications after nephrectomy for renal cancer. *Int Braz J urol* (2023) 49(1):97–109. doi: 10.1590/s1677-5538.Ibju.2022.0380

24. Grinstead C, George T, Han B, Yoon SL. Associations of overall survival with geriatric nutritional risk index in patients with advanced pancreatic cancer. *Nutrients* (2022) 14(18):3800. doi: 10.3390/nu14183800

25. Artigas A, Wernerman J, Arroyo V, Vincent JL, Levy M. Role of albumin in diseases associated with severe systemic inflammation: Pathophysiologic and clinical evidence in sepsis and in decompensated cirrhosis. *J Crit Care* (2016) 33:62–70. doi: 10.1016/j.jcrc.2015.12.019

26. Duran AO, Inanc M, Karaca H, Dogan I, Berk V, Bozkurt O, et al. Albumin-globulin ratio for prediction of long-term mortality in lung adenocarcinoma patients. *Asian Pacific J Cancer Prev* (2014) 15(15):6449–53. doi: 10.7314/apjcp.2014.15.15.6449

27. He J, Pan H, Liang W, Xiao D, Chen X, Guo M, et al. Prognostic effect of albumin-to-Globulin ratio in patients with solid tumors: A systematic review and meta-analysis. *J Cancer* (2017) 8(19):4002–10. doi: 10.7150/jca.21141

28. Collins N. Protein-energy malnutrition and involuntary weight loss: Nutritional and pharmacological strategies to enhance wound healing. *Expert Opin pharmacotherapy* (2003) 4(7):1121–40. doi: 10.1517/14656566.4.7.1121

29. Wang Z, Luo S, Zhao X. The prognostic impact of body mass index in patients with diffuse Large b-cell lymphoma: A meta-analysis. *Nutr Cancer* (2021) 73(11-12):2336–46. doi: 10.1080/01635581.2020.1823437

30. Duconseil P, Garnier J, Weets V, Ewald J, Marchese U, Gilabert M, et al. Effect of clinical status on survival in patients with borderline or locally advanced pancreatic adenocarcinoma. *World J Surg Oncol* (2019) 17(1):95. doi: 10.1186/s12957-019-1637-1

31. Hao X, Wei Y, Wei X, Zhou L, Wei Q, Zhang Y, et al. Glasgow Prognostic score is superior to other inflammation-based scores in predicting survival of diffuse large b-cell lymphoma. *Oncotarget* (2017) 8(44):76740–8. doi: 10.18632/oncotarget.20832

32. Mu S, Ai L, Fan F, Qin Y, Sun C, Hu Y. Prognostic role of neutrophil-to-lymphocyte ratio in diffuse large b cell lymphoma patients: an updated dose-response meta-analysis. *Cancer Cell Int* (2018) 18:119. doi: 10.1186/s12935-018-0609-9

33. Chen Y, Zhang Z, Fang Q, Jian H. Prognostic impact of platelet-to-lymphocyte ratio on diffuse large b-cell lymphoma: a meta-analysis. *Cancer Cell Int* (2019) 19:245. doi: 10.1186/s12935-019-0962-3

34. Zhang Q, Zhang L, Jin Q, He Y, Wu M, Peng H, et al. The prognostic value of the GNRI in patients with stomach cancer undergoing surgery. *J Pers Med* (2023) 13 (1):155. doi: 10.3390/jpm13010155

35. Xu J, Sun Y, Gong D, Fan Y. Predictive value of geriatric nutritional risk index in patients with colorectal cancer: A meta-analysis. *Nutr Cancer* (2023) 75(1):24–32. doi: 10.1080/01635581.2022.2115521

36. Yu J, Zhang W, Wang C, Hu Y. The prognostic value of pretreatment geriatric nutritional risk index in esophageal cancer: A meta-analysis. *Nutr Cancer* (2022) 74 (9):3202–10. doi: 10.1080/01635581.2022.2069273

37. Yang M, Liu Z, Li G, Li B, Li C, Xiao L, et al. Geriatric nutritional risk index as a prognostic factor of patients with non-small cell lung cancer: A meta-analysis. *Horm Metab Res* (2022) 54(9):604–12. doi: 10.1055/a-1903-1943

38. Wu Q, Ye F. Prognostic impact of geriatric nutritional risk index on patients with urological cancers: A meta-analysis. *Front Oncol* (2022) 12:1077792. doi: 10.3389/fonc.2022.1077792

39. Zhou J, Fang P, Li X, Luan S, Xiao X, Gu Y, et al. Prognostic value of geriatric nutritional risk index in esophageal carcinoma: A systematic review and meta-analysis. *Front Nutr* (2022) 9:831283. doi: 10.3389/fnut.2022.831283

40. Yuan F, Yuan Q, Hu J, An J. Prognostic role of pretreatment geriatric nutritional risk index in colorectal cancer patients: A meta-analysis. *Nutr Cancer* (2023) 75(1):276–85. doi: 10.1080/01635581.2022.2109692

41. Wang H, Li C, Yang R, Jin J, Liu D, Li W. Prognostic value of the geriatric nutritional risk index in non-small cell lung cancer patients: A systematic review and meta-analysis. *Front Oncol* (2021) 11:794862. doi: 10.3389/fonc.2021.794862

frontiers | Frontiers in Oncology

TYPE Brief Research Report
PUBLISHED 28 April 2023
DOI 10.3389/fonc.2023.1157646

OPEN ACCESS

EDITED BY
Francesco Piazza,
University of Padua, Italy

REVIEWED BY
Monica Balzarotti,
Humanitas Research Hospital, Italy
Liang Wang,
Capital Medical University, China

*CORRESPONDENCE
Adrián Mosquera Orgueira
adrian.mosquera.orgeira@sergas.es

RECEIVED 02 February 2023
ACCEPTED 17 April 2023
PUBLISHED 28 April 2023

CITATION
Mosquera Orgueira A, Díaz Arías JÁ, Serrano Martín R, Portela Piñeiro V, Cid López M, Peleteiro Raíndo A, Bao Pérez L, González Pérez MS, Pérez Encinas MM, Fraga Rodríguez MF, Vallejo Llamas JC and Bello López JL (2023) A prognostic model based on gene expression parameters predicts a better response to bortezomib-containing immunochemotherapy in diffuse large B-cell lymphoma. *Front. Oncol.* 13:1157646. doi: 10.3389/fonc.2023.1157646

A prognostic model based on gene expression parameters predicts a better response to bortezomib-containing immunochemotherapy in diffuse large B-cell lymphoma

Adrián Mosquera Orgueira[1,2]*, Jose Ángel Díaz Arías[1,2], Rocio Serrano Martín[1,2], Victor Portela Piñeiro[1,2], Miguel Cid López[1,2], Andrés Peleteiro Raíndo[1,2], Laura Bao Pérez[1,2], Marta Sonia González Pérez[1,2], Manuel Mateo Pérez Encinas[1,2], Máximo Francisco Fraga Rodríguez[1,2], Juan Carlos Vallejo Llamas[1,2] and José Luis Bello López[1,2]

[1]University Hospital of Santiago de Compostela, Servizo Galego de Saúde (SERGAS), Santiago de Compostela, Spain, [2]Health Research Institute of Santiago de Compostela, Santiago de Compostela, Spain

Diffuse Large B-cell Lymphoma (DLBCL) is the most common type of aggressive lymphoma. Approximately 60% of fit patients achieve curation with immunochemotherapy, but the remaining patients relapse or have refractory disease, which predicts a short survival. Traditionally, risk stratification in DLBCL has been based on scores that combine clinical variables. Other methodologies have been developed based on the identification of novel molecular features, such as mutational profiles and gene expression signatures. Recently, we developed the LymForest-25 profile, which provides a personalized survival risk prediction based on the integration of transcriptomic and clinical features using an artificial intelligence system. In the present report, we studied the relationship between the molecular variables included in LymForest-25 in the context of the data released by the REMoDL-B trial, which evaluated the addition of bortezomib to the standard treatment (R-CHOP) in the upfront setting of DLBCL. For this, we retrained the machine learning model of survival on the group of patients treated with R-CHOP (N=469) and then made survival predictions for those patients treated with bortezomib plus R-CHOP (N=459). According to these results, the RB-CHOP scheme achieved a 30% reduction in the risk of progression or death for the 50% of DLBCL patients at higher molecular risk (p-value 0.03), potentially expanding the effectiveness of this treatment to a wider patient population as compared with other previously defined risk groups.

KEYWORDS

machie learning, DLBCL - diffuse large B cell lymphoma, bortezomib, R-CHOP, lymphoma, genomics, gene expression

Introduction

Diffuse Large B-cell Lymphoma (DLBCL) is the most common type of aggressive lymphoma. Approximately 60% of patients achieve curation with the standard first line treatment, which is based on the combination of an anti-CD20 antibody (rituximab) with chemotherapy (cyclophosphamide, doxorubicin and vincristine) and prednisone (R-CHOP). The remaining patients have either refractory disease or relapse after achieving a remission, and this predicts an adverse prognosis (1). Traditionally, risk stratification has been based on scores that combine the value of different prognostic variables. Examples of these methods are the International Prognostic Index (IPI), the revised IPI (R-IPI), and the National Comprehensive Cancer Network IPI (NCCN-IPI) (2). Nevertheless, the accuracy of these scores is far from optimal, and other strategies are actively being explored based on novel molecular features. Earlier studies based on transcriptomic signatures revealed 3 prognostic groups based on their cell-of-origin (COO) status: activated B-cell–like (ABC), germinal-center B-cell–like (GCB) and unclassified (3). Furthermore, recent research reports proved that high risk lymphomas can also be identified as those which share a gene expression signature with either double & triple-hit DLBCLs or with Burkitt lymphomas (4). These lymphomas have been termed as molecular high-grade (MHG) by the academics (4). Finally, comprehensive classifications of DLBCL based on patterns of somatic mutations also exist, which are also associated with divergent clinical outcomes (5).

A few years ago, we presented a new prognostic tool in DLBCL based on a 102-gene expression profile (6). The data from this profile, when interpreted with machine learning tools, enabled the inference of personalized survival outcomes that were prognostically superior to those of the COO classification. Afterwards, we reproduced this profile in another cohort, and reduced the total number of genes in the signature to 19 variables which were prognostically independently of the IPI-related variables (7). The model was named LymForest-25. Finally, we validated the prognostic value of this signature in the UK population-based Haematological Malignancy Research Network database (8), confirming its superiority with respect to the COO and MHG classifications. Notably, the performance of the predictor continued to be high despite the exclusion of 2 genes which were not represented in the gene expression panel used in that study.

At the same time, a growing interest for improved treatments in DLBCL has emerged, and several trials have evaluated new upfront combinations during the last years. The ROBUST study was a randomized, phase III trial which explored the addition of lenalidomide to R-CHOP (R2-CHOP) vs standard R-CHOP, but failed to provide significant results (9). However, a tendency for an improved progression-free survival (PFS) with R2-CHOP was observed among patients with high risk disease (IPI ≥ 3). More recently, the POLARIX phase III trial evaluated a modified scheme of R-CHOP (pola-R-CHP), in which vincristine was replaced with polatuzumab vedotin, as compared with standard R-CHOP in patients with previously untreated intermediate-risk or high-risk DLBCL (10). A significant benefit in PFS was observed in the pola-R-CHP treatment branch, with a hazard ratio (HR) of 0.73. Notably, exploratory subgroup analysis evidenced that this benefit was more pronounced among patients with IPI ≥ 3 and in those with ABC phenotype. A different therapeutic strategy has been based on the incorporation of the proteasome inhibitor bortezomib into the R-CHOP scheme (RB-CHOP). Preclinical evidence indicated that bortezomib can exert antitumoral activity in B-cell lymphoma cell lines (11). This promoted clinical studies that ended up in the development of the REMoDL-B trial, a randomized phase III trial testing RB-CHOP vs R-CHOP in previously untreated DLBCL patients (12). The results of this trial indicated no evidence for a benefit of RB-CHOP over R-CHOP neither in PFS nor in overall survival (OS). However, exploratory *post-hoc* analysis evidenced a benefit for RB-CHOP in PFS in the MHG group, and a tendency towards a benefit in the ABC group (13).

Methods

In the present report, we aimed to reproduce the prognostic value of the LymForest gene expression profile in the publicly available data of the REMoDL-B trial (13), as well as to evaluate the possible predictive value of this signature. Briefly, normalized gene expression estimates were downloaded from the Gene Expression Omnibus (GEO), with ID GSE117556. This cohort contained data for 928 patients, out of which 469 were treated with R-CHOP and 459 were treated with RB-CHOP. Median follow-up was 29.37 months, and median overall survival was not reached. We created a random forest model of survival following previous specifications (7, 8), and this model was exclusively trained on the group of patients treated with R-CHOP. Out-of-bag metrics were derived for patients in this subgroup, and new predictions on patients treated with RB-CHOP were made based on the results of the training set. The values of the cumulative hazard function were used to calculate the c-indexes.

Results

Firstly, we decided to reproduce the machine learning predictions based on the expression of 17 out of 19 original genes. This was due to the fact that 2 genes (*FAM208B* and *TRAV6*) were not included in the Illumina HumanHT-12 WG-DASL V4.0 R2 expression beadchips. In the original UK population-based Haematological Malignancy Research Network database, the c-index of this signature was 0.612. In the case of the REMoDL-B trial cohort, the c-indexes were 0.619 and 0.640 for the R-CHOP and RB-CHOP treated patients, respectively. Then, we reasoned that the expression of one of the missing genes (the T-cell receptor alpha subunit variable region gene; *TRAV6*), could be substituted by the expression of the CD3 T-cell specific marker genes, namely *CD3D*, *CD3G* and *CD3E*. We observed that this strategy improved the c-index in the UK population-based Haematological Malignancy Research Network database (original c-index, 0.612; new c-index, 0.621). Hence, we performed the same

modification in the REMoDL-B trial cohort, obtaining a c-index of 0.668 in the group of patients treated with R-CHOP, and a small reduction of the c-index to 0.631 in those treated with RB-CHOP.

In a second approach, we evaluated the possible predictive value of this signature in the REMoDL-B trial. With this aim, we extracted the 2-year survival probabilities from the machine learning predictions. We chose this threshold because most of the relapses and lymphoma-related deaths are known to occur during this period of time (14). Initially, we explored the possible utility of the 17-gene model by splitting the patients into 2 halves and 3 tertiles of risk (Table 1). No statistically significant difference in PFS was observed between patients treated with RB-CHOP and R-CHOP in either the high or the low 50% risk groups. However, a significant advantage of RB-CHOP for those patients assigned to the higher 33% of risk was identified (p-value 0.03, HR 0.66). Then, we reproduced the same procedure with the model enriched in T-cell markers (Table 1). In this case, we observed a significantly higher PFS with RB-CHOP for the 50% of patients at higher risk (p-value 0.03, HR 0.70; Figure 1A), whereas no significant differences were observed for those patients assigned to the lower 50% of risk (Figure 1B). This effect appeared to be even more pronounced among patients in the higher 33% of risk (p-value 0.03, HR 0.66) (Figures 1C, D).

Discussion

Our data indicates a role for bortezomib-containing upfront treatments in patients with DLBCL who have high-risk molecular features. According to these results, the RB-CHOP scheme achieved a 30% reduction in the risk of progression or death for the 50% of DLBCL patients at higher molecular risk, potentially expanding the effectiveness of this treatment to a wider patient population as compared with other previously defined risk groups. Furthermore, we confirmed that the inclusion of T-cell markers in the gene expression signature enriches the prognostic performance of the signature in patients treated with R-CHOP, although their importance appears to diminish in patients treated with RB-CHOP. In conclusion, the standardization and implementation of machine learning-guided molecular risk scores based on transcriptomic features should be performed in the context of clinical trials evaluating novel upfront combinations in the upfront treatment of DLBCL. Additionally, the LymForest molecular profile improves previous transcriptomic signatures for both prognostication and drug-response prediction in patients with DLBCL requiring systemic immunochemotherapy. This strategy could also be explored to enrich the results of other trials aiming to improve R-CHOP as upfront treatment in DLBCL, such as those based on polatuzumab (pola-R-CHP) (10) and those aiming to incorporate immunotherapy (bispecific antibodies or CAR-T cells) (15, 16). This is relevant because most of the new drugs in the frontline setting face a substantial difficulty to improve R-CHOP due to its high effectivity in the global population, and therefore the development of biomarkers to guide their use is of the utmost interest.

Machine learning has the potential to play an important role in the *post hoc* analysis of clinical trials by enabling more comprehensive and accurate analysis of trial data. AI-based methods can process large amounts of data and identify patterns, relationships, and insights that may not be immediately apparent through traditional statistical methods. Additionally, AI techniques can help to identify potential safety concerns, optimize dosing regimens, and identify subgroups of patients who may benefit the most from a particular treatment. For example, machine learning algorithms can be used to identify the best predictive biomarkers or clusters of patients for a particular treatment, which can inform future trial design and clinical decision making. Several studies have demonstrated the potential of AI in the *post hoc* analysis of clinical trials. For instance, a recent study by *Yan et al. (2021)* used a machine learning algorithm to predict clinical outcomes in patients with colorectal cancer treated with immunotherapy, achieving better performance than traditional statistical methods (17). Recently, newer approaches in the prediction of response to targeted drugs and drug combinations from patients treated in routine clinical practice have been presented. For example, *Kong et al. (2022)* presented an approach to predict the response to immune check-point inhibitors based on the construction of a network of genes and proteins that are known to be involved in the immune response (18). Using machine learning algorithms, they identified patterns in the network that were associated with drug response, proving that their approach can accurately predict responses in several different types of cancer. In another approach, our group explored new methods to predict risk in multiple myeloma (MM) by the integration of clinical and biochemical data with gene expression profiling. By applying machine learning algorithms, we created a 50-variable model that can predict OS with high concordance (19). The model included patient age, ISS stage, serum B2-microglobulin, first-line treatment, and the expression of 46 genes as covariates. Importantly, we found that patients treated with the best-predicted drug combination were significantly less likely to die than patients treated with other schemes, particularly those treated with a triplet combination including bortezomib, an immunomodulatory drug and dexamethasone.

Validated and transparent machine learning algorithms are essential in medical applications because they can provide accurate and reliable predictions, which can aid clinicians in making optimal decisions (20). Despite this great potential, it is important to recognize their limitations and potential biases. It is crucial to fully understand the strengths and weaknesses of each algorithm and to ensure that they are appropriately validated and transparent. This requires ongoing research and collaboration between machine learning experts and clinicians (21). In the particular context of clinical trials, *post hoc* analysis can be used to analyze data from clinical trials and determine if a drug is effective and safe (22). Machine learning can be used to identify patterns and relationships that can later be used to develop new drugs or optimize existing ones. However, *post hoc* studies also have limitations, including the possibility of data overfitting and the inability to control for confounding variables due to their retrospective nature (23). In our particular case, we retrained a

TABLE 1 Results of the cox models testing for differential PFS outcomes of the different groups of patients analyzed in the text.

	17-gene model		CD3 genes + 17-gene model	
Groups	P-value	HR (95% CI)	P-value	HR (95% CI)
50% higher risk	0.29	0.84 (0.61-1.16)	2.94 x 10-2	0.70 (0.51-0.96)
50% lower risk	0.92	0.98 (0.67-1.43)	0.26	1.24 (0.85-1.82)
33% higher risk	3.5 x 10-2	0.66 (0.45-0.97)	2.88 x 10-2	0.66 (0.45-0.96)
34-65% risk	0.35	1.23 (0.79-1.92)	0.84	1.05 (0.67-1.65)
33% lower risk	0.97	0.99 (0.62-1.59)	0.36	1.25 (0.78-2.01)

P-values, hazard ratios (HR) and 95% confidence intervals of the HR are provided.

previously described prognostic model in the group of patients treated with R-CHOP, because this population was the target of our predictor (6–8). Afterwards, we used these predictions to risk stratify those patients treated with RB-CHOP and compare outcomes. However, though the use of an external cohort for training the predictor could be an option, this should have the same structure (e.g., inclusion and exclusion criteria, baseline characteristics…) as the original clinical trial data. This highlights the crucial importance of external validity in clinical trials, particularly for the construction of new machine learning predictors, and the need to discuss these issues with regulatory agencies for drug approval based on such types of evidence (24). Surely, a prospective validation of the findings on a new clinical trial or in a post-authorization real world cohort would provide more reliable information. Eventually, the growing application of machine learning in clinical trials will make these *post hoc* analysis more relevant, and regulators should pursue the development of good clinical practices to ensure a reliable and fair application (25, 26). This includes using appropriate statistical methods, validating the model on multiple datasets, and being transparent about its possible limitations. Another issue of relevance for the application of this technology relies on the need for genomic standardization, which should be pursued in order to lead to reliable results for patient care. Standardization of genomic

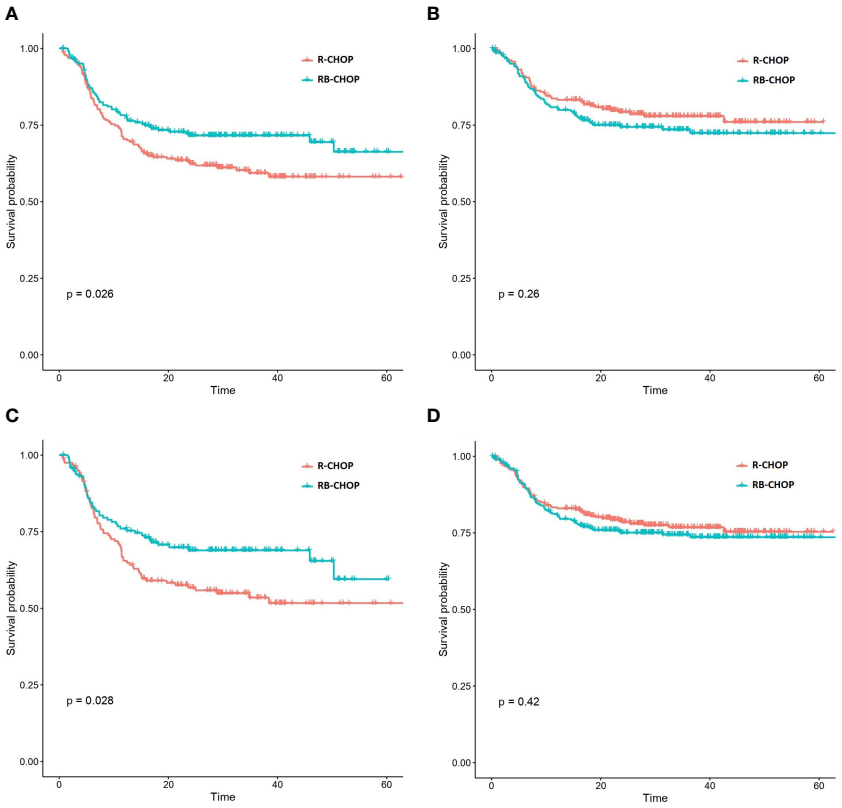

FIGURE 1
Kaplan-Meier curves representing the PFS of patients treated with RB-CHOP and R-CHOP according to their biological risk predicted by the CD3 markers & 17 gene expression signature. **(A, B)** Representation of RB-CHOP and R-CHOP curves for those patients in the higher 50% risk group **(A)** and in the lower 50%risk group **(B)**. **(C, D)** Representation of RB-CHOP and R-CHOP curves for those patients in the higher 33% risk group **(A)** and in the lower 67%risk group **(B)**.

tests involves ensuring that the tests are performed in a consistent and reliable manner across different laboratories, using well-defined protocols, standardized testing platforms and quality control measures (27). This will help to ensure that the results of the tests are accurate and can be compared across different settings and over time.

In conclusion, we present an evaluation of LymForest-25 machine-learning-based gene expression profile to risk stratify patients and predict treatment responses in patients with DLBCL within the REMoDL-B trial. The results suggest a role for bortezomib-containing upfront treatments in molecular high-risk patients. The standardization and implementation of machine learning-guided molecular risk scores based on transcriptomic features should be pursued in the context of clinical trials evaluating novel upfront combinations in the upfront treatment of DLBCL.

Data availability statement

The datasets presented in this study can be found in online repositories. The names of the repository/repositories and accession number(s) can be found in the article/supplementary material.

Funding

The authors declare that no support was provided in the forms of grants and/or equipment and grants for the development of this study.

Author contributions

AMO had the idea, designed the paper, analyzed the data and wrote the paper. JADA, MCL, APR, LBP, MSGP, MMPE, MFFR and JLBL reviewed the results, suggested modifications and approved the final publication. All authors contributed to the article and approved the submitted version.

Acknowledgments

The authors wish to thank the Supercomputing Center of Galicia (CESGA) for providing computational resources; and the REMoDL-B trial organizers for publicly sharing the clinical and gene expression data.

Conflict of interest

AMO reports honoraria for lectures and participation in advisory boards from Janssen, Takeda, Abbey, Amgen, Novartis, Gilead and AstraZeneca; research grants from Roche, Pfizer and Celgene-BMS and funds for conference organization from Jassen, Takeda, Abbey, Amgen, Novartis, Gilead, Roche, Bristol-Myers-Squibb, Glaxo-Smith-Klyne, Incyte and Pfizer.

The remaining authors declare that the research was conducted in the absence of any commercial or financial relationships that could be constructed as a potential conflict of interest.

Publisher's note

References

1. Feugier P, Van Hoof A, Sebban C, Solal-Celigny P, Bouabdallah R, Fermé C, et al. Long-term results of the r-CHOP study in the treatment of elderly patients with diffuse large b-cell lymphoma: a study by the groupe d'Etude des lymphomes de l'Adulte. *J Clin Oncol* (2005) 23(18):4117–26. doi: 10.1200/JCO.2005.09.131

2. Ruppert AS, Dixon JG, Salles G, Wall A, Cunningham D, Poeschel V, et al. International prognostic indices in diffuse large b-cell lymphoma: a comparison of IPI, r-IPI, and NCCN-IPI. *Blood* (2020) 135(23):2041–8. doi: 10.1182/blood.2019002729

3. Scott DW, Wright GW, Williams PM, Lih CJ, Walsh W, Jaffe ES, et al. Determining cell-of-origin subtypes of diffuse large b-cell lymphoma using gene expression in formalin-fixed paraffin-embedded tissue. *Blood* (2014) 123(8):1214–7. doi: 10.1182/blood-2013-11-536433

4. Sha C, Barrans S, Cucco F, Bentley MA, Care MA, Cummin T, et al. Molecular high-grade b-cell lymphoma: defining a poor-risk group that requires different approaches to therapy [published correction appears in J clin oncol. *2019 Apr 20;37 (12):1035]. J Clin Oncol* (2019) 37(3):202–12. doi: 10.1200/JCO.18.01314

5. Schmitz R, Wright GW, Huang DW, Johnson CA, Phelan JD, Wang JQ, et al. Genetics and pathogenesis of diffuse Large b-cell lymphoma. *N Engl J Med* (2018) 378 (15):1396–407. doi: 10.1056/NEJMoa1801445

6. Mosquera Orgueira A, Díaz Arias JÁ, Cid López M, Peleteiro Raíndo A, Antelo Rodríguez B, Aliste Santos C, et al. Improved personalized survival prediction of patients with diffuse large b-cell lymphoma using gene expression profiling. *BMC Cancer*. (2020) 20(1):1017. doi: 10.1186/s12885-020-07492-y

7. Mosquera-Orgueira A, Cid-Lopez M, Peleteiro-Raindo A, Díaz Arias JA, González Pérez MS, Antelo Rodríguez B, et al. LymForest-25: personally-tailored survival prediction of patients with diffuse large b-cell lymphoma using clinico-genomic prognostic models. *Supplement: 16th Int Conf Malignant Lymphoma Virtual Edition* (2021) 39(2):238. doi: 10.1002/hon.79_2880

8. Mosquera Orgueira A, Díaz Arías JÁ, Cid López M, Peleteiro Raíndo A, López García A, Abal García R, et al. Prognostic stratification of diffuse Large b-cell lymphoma using clinico-genomic models: validation and improvement of the LymForest-25 model. *Hemasphere* (2022) 6(4):e706. doi: 10.1097/HS9.0000000000000706

9. Nowakowski GS, Chiappella A, Gascoyne RD, Scott DW, Zhang Q, Jurczak W, et al. ROBUST: a phase III study of lenalidomide plus r-CHOP versus placebo plus r-CHOP in previously untreated patients with ABC-type diffuse Large b-cell lymphoma. *J Clin Oncol* (2021) 39(12):1317–28. doi: 10.1200/JCO.20.01366

10. Tilly H, Morschhauser F, Sehn LH, Friedberg JW, Trněný M, Sharman JP, et al. Polatuzumab vedotin in previously untreated diffuse Large b-cell lymphoma. *N Engl J Med* (2022) 386(4):351–63. doi: 10.1056/NEJMoa2115304

11. Strauss SJ, Higginbottom K, Jüliger S, Maharaj L, Allen P, Schenkein D, et al. The proteasome inhibitor bortezomib acts independently of p53 and induces cell death

via apoptosis and mitotic catastrophe in b-cell lymphoma cell lines. *Cancer Res* (2007) 67(6):2783–90. doi: 10.1158/0008-5472.CAN-06-3254

12. Davies A, Cummin TE, Barrans S, Maishman T, Mamot C, Novak U, et al. Gene-expression profiling of bortezomib added to standard chemoimmunotherapy for diffuse large b-cell lymphoma (REMoDL-b): an open-label, randomised, phase 3 trial. *Lancet Oncol* (2019) 20(5):649–62. doi: 10.1016/S1470-2045(18)30935-5

13. Davies AJ, Stanton L, Caddy J, Barrans S, Wilding S, Saunders GN, et al. Five-year survival results from the remodl-b trial (ISRCTN 51837425) show improved outcomes in diffuse Large b-cell lymphoma molecular subgroups from the addition of bortezomib to r-CHOP chemoimmunotherapy. *Blood* (2022) 140(Supplement 1):1770–2. doi: 10.1182/blood-2022-159976

14. Jakobsen LH, Bøgsted M, Brown PN, Arboe B, Jørgensen J, Larsen TS, et al. Minimal loss of lifetime for patients with diffuse Large b-cell lymphoma in remission and event free 24 months after treatment: a Danish population-based study. *J Clin Oncol* (2017) 35(7):778–84. doi: 10.1200/JCO.2016.70.0765

15. Dickinson MJ, Carlo-Stella C, Morschhauser F, Bachy E, Corradini P, Iacoboni G, et al. Glofitamab for relapsed or5 refractory diffuse Large b-cell lymphoma. *N Engl J Med* (2022) 387(24):2220–31. doi: 10.1056/NEJMoa2206913

16. Neelapu SS, Dickinson M, Munoz J, Ulrickson ML, Thieblemont C, Oluwole OO, et al. Axicabtagene ciloleucel as first-line6 therapy in high-risk large b-cell lymphoma: the phase 2 ZUMA-12 trial. *Nat Med* (2022) 28(4):735–42. doi: 10.1038/s41591-022-01731-4

17. Yan L, Wu Y, Wu Y, Zhang Q, Wang X. Prediction of clinical outcomes for immunotherapy of colorectal cancer using a machine learning algorithm. *Front Genet* (2021) 12:631321.

18. Kong J, Ha D, Lee J, Kim I, Park M, Im SH, et al. Network-based machine learning approach to predict immunotherapy response in cancer patients. *Nat Commun* (2022) 13(1):3703. doi: 10.1038/s41467-022-31535-6

19. Mosquera Orgueira A, González Pérez MS, Díaz Arias JÁ, Antelo Rodríguez B, Alonso Vence N, Bendaña López , et al. Survival prediction and treatment optimization of multiple myeloma patients using machine-learning models based on clinical and gene expression data. *Leukemia* (2021) 35(10):2924–35. doi: 10.1038/s41375-021-01286-2

20. Goldstein BA, Navar AM, Pencina MJ, Ioannidis JP. Opportunities and challenges in developing risk prediction models with electronic health records data: a systematic review. *J Am Med Inform Assoc* (2017) 24(1):198–208. doi: 10.1093/jamia/ocw042

21. Jha S, Topol EJ. Adapting to artificial intelligence: radiologists and pathologists as information specialists. *JAMA* (2016) 316(22):2353–4. doi: 10.1001/jama.2016.17438

22. Srinivas TR, Ho B, Kang J, Kaplan B. *Post hoc* Analyses: after the facts. *Transplantation* (2015) 99(1):17–20. doi: 10.1097/TP.0000000000000581

23. Curran-Everett D, Milgrom H. *Post-hoc* Data analysis: benefits and limitations. *Curr Opin Allergy Clin Immunol* (2013) 13(3):223–4. doi: 10.1097/ACI.0b013e3283609831

24. Futoma J, Simons M, Panch T, Doshi-Velez F, Celi LA. The myth of generalisability in clinical research and machine learning in health care. *Lancet Digit Health* (2020) 2(9):e489–92. doi: 10.1016/S2589-7500(20)30186-2

25. Hollis S, Fletcher C, Lynn F, Urban HJ, Branson J, Burger HU, et al. Best practice for analysis of shared clinical trial data. *BMC Med Res Methodol* (2016) 16 Suppl 1 (Suppl 1):76. doi: 10.1186/s12874-016-0170-y

26. Liu J, Chow SC. A proposal for *Post Hoc* subgroup analysis in support of regulatory submission. *Ther Innov Regul Sci* (2023) 57(2):196–208. doi: 10.1007/s43441-022-00459-0

27. Burke W, Ginsburg G, Terry S, Aronson N, Ashley EA, Billings PR, et al. *Roundtable on translating genomic-based research for health; board on health sciences policy; institute of medicine; center for medical technology policy. genome-based diagnostics: demonstrating clinical utility in oncology: workshop summary*. Washington (DC: National Academies Press (US (2013) 39(2):238.

frontiers | Frontiers in Medicine

TYPE Original Research
PUBLISHED 30 May 2023
DOI 10.3389/fmed.2023.1128295

OPEN ACCESS

EDITED BY
Hanno Maximilian Witte,
Bundeswehrkrankenhaus, Germany

REVIEWED BY
Niklas Gebauer,
University Medical Center Schleswig-Holstein, Germany
Conn Rother,
Federal Arms Hospital Ulm, Germany

*CORRESPONDENCE
Claudio Jommi
✉ claudio.jommi@uniupo.it

†These authors have contributed equally to this work

RECEIVED 20 December 2022
ACCEPTED 25 April 2023
PUBLISHED 30 May 2023

CITATION
Canales Albendea MÁ, Canonico PL, Cartron G, Deiters B, Jommi C, Marks R, Rioufol C, Sancho Cia JM, Santoro A and Wagner-Drouet EM (2023) Comparative analysis of CAR T-cell therapy access for DLBCL patients: associated challenges and solutions in the four largest EU countries. *Front. Med.* 10:1128295. doi: 10.3389/fmed.2023.1128295

Comparative analysis of CAR T-cell therapy access for DLBCL patients: associated challenges and solutions in the four largest EU countries

Miguel Á. Canales Albendea[1†], Pier Luigi Canonico[2†], Guillaume Cartron[3†], Barthold Deiters[4†], Claudio Jommi[2*†], Reinhard Marks[5†], Catherine Rioufol[6,7†], Juan M. Sancho Cia[8†], Armando Santoro[9,10†] and Eva M. Wagner-Drouet[11†]

[1]Department of Hematology, Clínica Universidad de Navarra, Pamplona, Spain, [2]Department of Pharmaceutical Sciences, Università del Piemonte Orientale, Novara, Italy, [3]Centre Hospitalier Universitaire de Montpellier, UMR-CNRS 5535, Montpellier, France, [4]GWQ ServicePlus AG, Düsseldorf, Germany, [5]Department of Medicine I, Medical Center, University of Freiburg, Freiburg, Germany, [6]Department of Pharmacy, Lyon Sud Hospital, Hospices Civils de Lyon, Lyon, France, [7]EA 3738 Center for Innovation in Cancerology of Lyon (CICLY)-Claude Bernard University Lyon I, Lyon, France, [8]ICO-IJC-Hospital Germans Trias i Pujol, Badalona, Spain, [9]Department of Biomedical Sciences, Humanitas University, Pieve Emanuele, Milan, Italy, [10]IRCCS Humanitas Research Hospital, Humanitas Cancer Center, Milan, Italy, [11]Department of Hematology and Oncology, University Medical Center, Mainz, Germany

Introduction: CAR T-cell therapy has emerged as a promising new immuno-oncology treatment that engages the patient's immune system to fight certain hematological malignancies, including diffuse large B-cell lymphoma (DLBCL). In the European Union (EU), CAR T-cell therapies have been approved for relapsed/refractory (R/R) DLBCL patients since 2018, but patient access is often still limited or delayed. This paper is aimed at discussing challenges to access and possible solutions in the largest four EU countries.

Methods: The analysis relied on literature review, market data collection, since homogeneous data coming from registries were not available, and discussion with experts coming from all four countries.

Results: We calculated that in 2020, between 58% and 83% of R/R DLBCL patients (EMA approved label population) or between 29% and 71% of the estimated medically eligible R/R DLBCL patients, were not treated with a licensed CAR T-cell therapy. Common challenges along the patient journey that may result in limited access or delays to CAR T-cell therapy were identified. These include timely identification and referral of eligible patients, pre-treatment funding approval by authorities and payers, and resource needs at CAR T-cell centers.

Discussion: These challenges, existing best practices and recommended focus areas for health systems are discussed here, with the aim to inform necessary actions for overcoming patient access challenges for current CAR T-cell therapies as well as for future cell and gene therapies.

KEYWORDS

CAR T-cell therapy, diffuse large B-cell lymphoma, patient access, health system, Germany, France, Italy, Spain

Highlights

- Despite approval of CAR T-cell therapies in EU-4 countries, their use in relapsed/refractory DLBCL patients remains limited, with between 29 and 71% of estimated eligible patients not receiving treatment in 2020.
- Systematic challenges along the patient journey can limit or delay CAR T-cell therapy access for eligible patients, including identification, referral, pre-treatment funding approval and center resource needs.
- Local best practices and actionable recommendations presented in this study can guide health system efforts to improve patient access for current and future cell and gene therapies.

1. Introduction

1.1. CAR T-cell cancer immunotherapy developments

CAR T-cell therapies are novel anti-cancer treatments that utilize the immune system, specifically immune T-lymphocytes, or T-cells, to fight tumor cells. Patient T-cells are genetically modified to express chimeric antigen receptors (CARs), which target specific cancer cell-associated surface proteins. When infused back into the patient's blood, CAR T-cells bind to cancer cells expressing these antigens and trigger a T-cell initiated cell destruction (1).

Six commercial CAR T-cell therapies have been approved by the U.S. Food and Drug Administration (FDA) and the European Medicines Agency (EMA) since 2017; four of them are designed to bind the B-lymphocyte antigen CD19 (Cluster of Differentiation 19) expressed on the cell surface of different types of lymphoma and leukemia, whereas the other two approved CAR T-cell therapies target the multiple myeloma-expressed B-cell maturation antigen BCMA (Supplementary Table 1). In 2020, EMA-approved CD19 CAR T-cell therapies covered the following indications: R/R diffuse large B-cell lymphoma (DLBCL) after at least two lines of therapy (2–4), with CAR T-cell therapy after only one line of chemoimmunotherapy approved by the EMA in October 2022 (5); R/R primary mediastinal large B-cell lymphoma after at least two lines of therapy (2, 4); R/R follicular lymphoma after at least two lines of therapy (2, 6); R/R mantle cell lymphoma after at least two lines of therapy including a Bruton's tyrosine kinase inhibitor (7); and R/R B-cell acute lymphoblastic leukemia in pediatric patients up to 25 years after at least two lines of therapy or after relapse post-transplant (2). Indications approved by EMA for BCMA CAR T-cell therapies include R/R multiple myeloma after at least three lines of systemic therapy, including an immunomodulatory agent, a proteasome inhibitor and an anti-CD38 antibody and with demonstrated disease progression on the last therapy line (8, 9).

The growing number of approved CAR T-cell therapies is fueled by a rapidly expanding pipeline with more than 500 "active" CAR T-cell trials listed by the beginning of 2022 ["active" status corresponding to CAR T-cell studies listed as "*recruiting*," "*enrolling by invitation*" or "*active, not recruiting*" on www.clinicaltrials.gov; (10)]. Ongoing research will likely increase the breadth of CAR immunotherapy applications and includes among others CAR T-cells targeting solid tumors, bispecific CAR T-cells targeting two different antigens, allogeneic "off-the-shelf" CAR T-cells and CAR NK (natural killer)-cells (1). Particularly for solid tumors, which constitute most of malignant neoplasms, CAR immunotherapy development may one day bring a much-needed novel treatment approach, akin to the successful application in different hematological cancers to date.

1.2. Access environment for DLBCL CAR T-cell therapies in EU-4 countries

In 2018/19, Germany, Italy and Spain granted reimbursement and commercial patient access for the CD19 CAR T-cell therapies *tisagenlecleucel* and *axicabtagene ciloleucel* in R/R DLBCL patients after at least two lines of therapy (11–15). France had already allowed patient access to *tisagenlecleucel* and *axicabtagene ciloleucel* before EMA market authorization, through its early access program (ATU), intended for therapies addressing a high unmet need without available alternatives [since 2021, the ATU/"*Temporary Authorization for Use*" program has been replaced by the APP/"*Early Access Authorization*" system (16)]. In 2019, both CAR T-cell therapies were approved by French authorities for statutory reimbursement listing and transitioned from the ATU program (17, 18). In the four European countries, integration of *tisagenlecleucel* and *axicabtagene ciloleucel* into care for R/R DLBCL patients was tightly controlled by the health authorities, including regulations for CAR T-cell center authorization, patient eligibility approval, data collection through registries and funding mechanisms (Table 1).

1.2.1. Center authorization and qualification

CAR T-cell therapies can be only provided by authorized CAR T-cell centers, that fulfil specific structural and organizational quality requirements defined by national authorities (13, 14, 19–21). In Spain, CAR T-cell centers were specifically designated by the Ministry of Health (22), and in Italy, due to the decentralized architecture of the health care system, by the respective regional authorities (13, 14), effectively authorizing only a sub-set of the centers that fulfill the quality criteria for active CAR T-cell therapy use. In France and Germany, centers fulfilling national criteria were authorized by regional health authorities or sick funds, respectively (20). In addition to authorization by authorities, pharmaceutical manufacturers have defined specific qualification procedures that centers need to complete before providing commercial CAR T-cell therapies.

1.2.2. Patient eligibility criteria

Beyond the EMA-approved R/R DLBCL indication for *tisagenlecleucel* and *axicabtagene ciloleucel*, patient eligibility criteria were further restricted at national level in Germany, Italy and Spain based on the selection criteria applied in the registrational trials (22–24, 26). In Germany, although not officially published, criteria for

TABLE 1 DLBCL CAR T-cell therapy implementation mechanisms across EU-4 countries – CAR T-cell center authorization, patient eligibility criteria, treatment approval processes, data collection and funding mechanisms in France, Germany, Italy, and Spain.

Country	France	Germany	Italy	Spain
CAR T-cell center authorization *(in addition to center qualification by manufacturer)*	CAR T-cell center criteria defined at national level (19). Center authorization by regional health authorities (19).	CAR T-cell center criteria defined at national level (20). Center authorization by sick funds (and their medical review boards) (20).	CAR T-cell center criteria defined at national level (13, 14). Center designation, authorization by regional health authorities (13, 14).	CAR-T center criteria, designation, and authorization at national level (21, 22).
Patient eligibility criteria	Patient eligibility criteria defined by CAR T-cell center.	Patient eligibility criteria defined by CAR T-cell center. Restrictions beyond EMA label may be applied by sick funds (and their medical review boards) for CAR-T cell product funding, that are based on clinical trial criteria and are evolving with new clinical evidence. The eligibility criteria applied by the sick funds' medical review boards can differ across German regions.	Patient eligibility criteria defined at national level. Restrictions beyond EMA label apply for CAR T-cell product funding, which are based on clinical trial criteria and additional 70 years age limit (increased to 75 years in May 2022 for *tisagenlecleucel*) (23–25).	Patient eligibility criteria defined at national level. Restrictions beyond EMA label apply for CAR T-cell product funding, which are based on clinical trial criteria (22).
Treatment approval	Center-level approval.	Pre-treatment approval by sick funds may be required/requested to minimize financial risks (26).	Center-level approval through completion of AIFA registry form with eligibility checklist (corresponding to an implicit authority approval) (23, 24). Additional pre-treatment approval may be required by the authorities of the region of patient origin.	Pre-treatment approval required by authorities of the region of patient origin and the national expert group (22, 27).
Registry for data collection *(in addition to EBMT registry requirement)*	National registry (DESCAR-T) (28). The registry is supporting yearly reassessment of approval based on real world effectiveness (17, 18, 29).	National registry (DRST) (26). In addition, data collection by sick funds is supporting outcome-based rebate agreements (29).	National AIFA registry (13, 14). The registry is supporting implementation of outcome-based staged payments (29).	National registry (VALTERMED) (27, 30). The registry is supporting implementation of outcome-based staged payments (29).
CAR T-cell product funding mechanisms	National funding for innovative, high-cost products through the "*Liste en Sus*" as well as the early access programs ATU/AAP (16, 29).	Sick fund-level funding, e.g., through application by the center for a NUB innovation funding (29).	National funding for innovative oncology products allocated to and managed by regional authorities ("*Fondo Farmaci Oncologici Innovativi*") (13, 14, 29).	Regional-level funding.

CAR T-cell therapy reimbursement have been developed by the sick funds' medical review boards under the guidance of the national Competence Center Oncology [KCO/"*Kompetenz-Centrum Onkologie*" (31)]. These patient eligibility criteria continue to evolve based on new clinical evidence, and their implementation by the sick funds' medical review boards differs across German regions. In Italy, in addition to the registrational trial criteria, a maximum patient age of 70 years was defined for CAR T-cell therapy by authorities (increased to 75 years in May 2022 for *tisagenlecleucel*) (23–25). In France, no eligibility criteria for DLBCL CAR T-cell therapies beyond EMA regulatory label were defined at the national level to our knowledge.

1.2.3. Pre-treatment approval

In France, patient eligibility for CAR T-cell therapy is assessed and confirmed at the discretion of the CAR T-cell center. In Germany, as long as no automatic funding process is implemented, sick funds supported by their medical review board decide on funding approval for each CAR T-cell therapy patient. Once automatic funding is established [via a NUB/"Neue Untersuchungs-und Behandlungsmethoden - New diagnostic and treatment method" funding for innovative medical procedures agreed at center level (29)], authorized centers can in theory provide CAR T-cell therapies within the label without pre-treatment approval by sick funds. However, due to the financial risks involved, centers may choose or be required by sick funds to collect this approval before use of the CAR T-cell therapy, despite existing NUB agreement (26). In Italy and Spain, authority approval is required for each patient before use of CAR T-cell therapy. In Italy, funding approval is sought by CAR T-cell centers through registration with the online AIFA registry platform (23, 24), but in addition, approval can also be required from the region of patient origin. In Spain, treatment approval must be given by the authorities of the region of patient origin as well as by a national expert group that confirms final eligibility for CAR T-cell therapy (27).

1.2.4. Registries

In France, Italy and Spain, CAR T-cell centers are required to collect patient outcome data in national CAR T-cell registries, which in France are also used to reassess CAR T-cell therapy approval based on demonstrated real-world effectiveness (17, 18, 28, 29), and in Italy and Spain, support outcome-based staged payments with pharmaceutical manufacturers (13–15, 29, 30). In Germany, CAR T-cell centers report data to the German Registry for Stem Cell Transplantation (DRST) (26). In addition, data collection for outcome-based rebate agreements with pharmaceutical manufacturers is managed by sick funds directly (29). In addition to national registries, European centers are requested to participate in data collection for the European Society for Blood and Marrow Transplantation (EBMT) CAR T-cell registry, also supporting post-authorization safety studies mandated by the EMA (32).

1.2.5. Funding mechanisms

Provided the above conditions are fulfilled, French and Italian authorized centers receive CAR T-cell product funding through a national financing mechanism for innovative, high-cost products ("*Liste en Sus*"/"*Supplementary List*" in France, "*Fondo Farmaci Oncologici Innovativi*"/"*Funds for Innovative Oncological Medicines*" in Italy) (13, 14, 29). Both in France and Italy, CAR T-cell product funding is conditioned by the centers providing information through the national registry to health authorities. In Italy, CAR-T cell product funding is allocated to the regions by the central government and managed by the regional authorities. In Spain, CAR T-cell product funding is managed at a regional level, and in Germany, CAR T-cell therapy funding *via* center-level NUB agreements is managed by the patient's sick fund individually (29).

1.3. DLBCL patients journey to CAR T-cell therapy

Before CAR T-cell therapy is indicated, DLBCL patients must undergo a multi-step diagnostic and therapeutic journey. After initial DLBCL diagnosis, patients start with a first line chemoimmunotherapy, generally using the combination regimen R-CHOP (33). Recently, the POLARIX trial has demonstrated significantly better PFS (Progression Free Survival) for the combination Polatuzumab vedotin + R-CHP compared with standard R-CHOP (34). However, it remains to be defined whether it will be considered as a new standard, bearing in mind the slight difference in PFS, no clear benefit in certain subgroups, and mainly, the lack of difference in OS (Overall Survival) (35). Otherwise, a consequence drawn from this first analysis is the reduction of patients receiving subsequent CAR T-cell therapy (34). Use of other R-CHOP-like regimens is generally not supported as first-line treatment due to lack of evidence for better outcomes and/or their higher toxicity vs. standard R-CHOP.

Up to 50% of DLBCL patients will be refractory to first line therapy or will experience relapse after initial response, thereby requiring second line therapy, which generally consists of salvage chemotherapy, followed by consolidation with autologous stem cell transplantation for those eligible (33). Around 80% of DLBCL patients undergoing second line therapy will be refractory or eventually relapse (33), becoming eligible for CAR T-cell therapy per the EMA regulatory label (2, 3). Based on our analysis, this corresponds to 14–21% of DLBCL patients in the EU-4 countries assessed (Supplementary Table 2). It must be noted that the above treatment pathway reflects patient reality in 2020, before EMA label for *axicabtagene ciloleucel* has been extended in October 2022 for use in DLBCL patient that relapses within 12 months from completion of, or is refractory to, first-line chemoimmunotherapy (3), which is likely to change the patient treatment pathway from second line on.

Once a patient is identified as a potential candidate for CAR T-cell therapy by their treating hematologist, support for confirmation of treatment choice and eligibility ideally is sought directly from a CAR T-cell center or from a specialized tumor board. Eligibility is confirmed through diagnostic tests according to local criteria, and the patient is subsequently referred to an authorized CAR T-cell center. As discussed previously, depending on the country, formal approval is required by payers and regional and/or national authorities before CAR T-cell therapy. For CAR T-cell production, the patient must undergo leukapheresis, usually at the authorized center, where T-cells are collected and shipped to a production facility of the pharmaceutical manufacturer. Before infusion of the CAR T-cells by the authorized center, patient will receive bridging therapy for disease control if required, and lymphodepleting conditioning chemotherapy to create an optimal environment for CAR T-cells expansion after infusion. After CAR T-cell infusion, guidelines recommend that the patient remains at the CAR T-cell center for 10 to 14 days, and in the vicinity of the center until day 28 post-infusion to ensure appropriate monitoring of adverse events. Usually, the patient is referred back to their referring physician for long-term follow-up and care (2, 3, 36).

Owing to the innovative nature and complexity of CAR T-cell therapy, implementation into routine care has proven challenging for health systems. This publication analyzes DLBCL patients' access to licensed CAR T-cell therapies in the four largest EU countries and discusses the main challenges for patient access and recommends solutions for overcoming these challenges for current and future CAR T-cell therapies.

2. DLBCL CAR T-cell therapy access situation in EU-4 countries in 2020: analysis of unpublished data

To assess the CAR T-cell therapy access situation for DLBCL patients across the EU-4 countries, we compared the EMA label population (R/R DLBCL patients after at least two therapy lines) as well as the estimated fraction that is considered medically eligible for CAR T-cell therapy, with the number of R/R DLBCL patients treated with licensed CAR T-cell therapies in the year 2020. To ensure comparability of the analysis across the EU-4 countries, a normalization by the respective population size was conducted (Supplementary Table 2). The size of the EMA DLBCL label population was derived or estimated based on publicly available data (Supplementary Table 2). The fraction of CAR T-cell therapy eligible patients was estimated based on the registrational trial information for *tisagenlecleucel* and *axicabtagene ciloleucel*, the same approach as used by HAS (French National Authority for Health) to estimate the number of potential CAR-T patients in France (using the average percentage of patients selected for CAR T-cell therapy that in the end received treatment; Supplementary Table 2). No publicly available data could be identified reporting the number of R/R DLBCL patients treated with licensed CAR T-cell therapies for the full year 2020

(January to December) in the EU-4 countries. Published registry data from France (DESCAR-T), Germany (DRST), Italy (AIFA) and Spain (VALTERMED) cover different timeframes, aggregating patients treated since registry opening, and may not be complete (26, 28, 37, 38). To overcome this limitation, our analysis used data and estimations for the total number of licensed CAR T-cell therapies (*tisagenlecleucel* and *axicabtagene ciloleucel*) for R/R DLBCL patients in France, Germany, and Italy in the year 2020, that were provided in personal communication by Kite Pharma Inc./ Gilead Sciences Inc. (39). For Spain, in response to a request for data disclosure, the Ministry of Health reported the number of R/R DLBCL patients for whom a licensed CAR T-cell therapy was requested in 2020, as well as the number of approved requests and the number of performed CAR T-cell therapies for these patients (40).

We analyzed patient access to CAR T-cell therapies across the 'EU-4' countries (France, Germany, Italy, and Spain), comparing the EMA DLBCL label population (R/R DLBCL patients after at least two lines of therapy) as well as the fraction estimated to be medically eligible with the number of R/R DLBCL patients effectively treated with a licensed CAR T-cell therapy in the year 2020 (Figure 1; Supplementary Table 2).

Based on public information and our calculations for the year 2020, the numbers of DLBCL patients relapsed/refractory after at least two therapy lines (corresponding to the EMA label population for DLBCL CAR T-cell therapies) were: 801 in France (12.3 per one million in habitants), 661 in Germany (7.9 per one million inhabitants), 638 in Italy (10.6 per one million in habitants), and 490 in Spain (10.5 per one million inhabitants) (Figure 1; Supplementary Table 2). However, not all R/R DLBCL patients with two or more lines of therapy are considered medically eligible for CAR T-cell therapy due to their general health and disease status. Based on the registrational trial information for *tisagenlecleucel* and *axicabtagene ciloleucel*, on average around 60% of selected patients had been treated in registrational trials. Therefore, we estimated that for the year 2020, 481 DLBCL patients in France would have been considered medically eligible to undergo licensed CAR T-cell therapy, 397 patients in Germany, 383 patients in Italy, and 294 patients in Spain [Figure 1; Supplementary Table 2; (17, 18)]. Based on information available for 2020, 340 DLBCL patients in France received a licensed CAR T-cell therapy [28 patients per month (39)], 250 DLBCL patients in Germany [21 patients per month (39)], 110 DLBCL patients in Italy [9 patients per month (39)], and 161 DLBCL patients in Spain [13 patients per month (40); Figure 1]. The above estimations for France and Italy are in range of DLBCL CAR T-cell therapy rates reported by the DESCAR-T registry (30 patients per month on average between December 2019 to January 2021) and the AIFA registry (8 patients per month on average between August 2019 and December 2020) (24, 28). For Germany, the DRST registry data from participating CAR T-cell centers suggests a lower monthly DLBCL CAR T-cell therapy rate than estimated by our analysis (15 patients per month on average between November 2018 and April 2021, after extrapolation to all 29 active centers in December 2020). This difference might be due to the published DRST registry data including a long time period (from November 2018) during which CAR T-cell therapy might have been used only by a few centers and clinical practice was slowly building up [Supplementary Table 2; (24, 26, 28, 39)].

This analysis indicates that in all four EU countries, less than 50% of DLBCL patients matching the EMA label indication received a CAR T-cell therapy in 2020 (Figure 1). Of the estimated CAR T-cell therapy eligible patients, approximately 7 in 10 DLBCL patients in France have been treated with a licensed CAR T-cell therapy in 2020 (71%; 42% of the EMA label population). In Germany and Spain, the CAR T-cell therapy rate was approximately 6 in 10 eligible DLBCL patients (63% and 55% respectively, 38% and 33% of the EMA label population), and in Italy, less than 3 in 10 eligible DLBCL patients received a CAR T-cell therapy in 2020 (29%, 17% of the EMA label population). It should be noted that despite a larger population size in Germany (83.8 million), the German Federal Joint Committee G-BA's

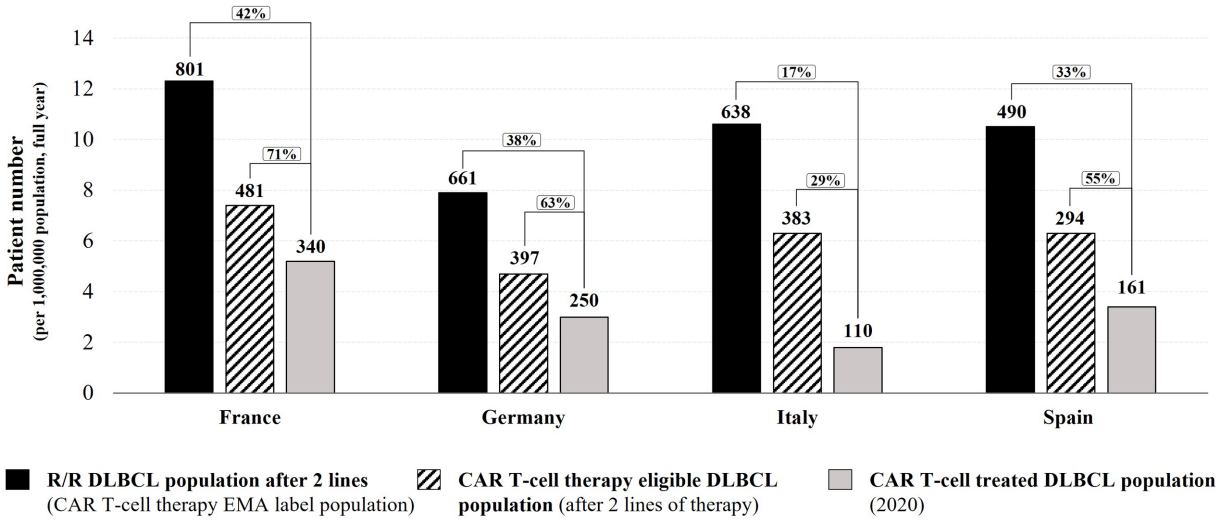

FIGURE 1
2020 DLBCL CAR T-cell therapy access analysis in Germany, France, Italy, and Spain. Numbers in graph indicate total patient numbers in the EU-4 countries. Bar graph height represents patient numbers normalized per 1 million inhabitants (relative to country population size in 2020). R/R – relapsed/refractory.

averaged estimations for the number of R/R DLBCL patients after at least two lines of therapy (661) is in range with estimations for Italy (638 patients in 60.5 million inhabitants) and is lower than estimations for France [801 patients in 65.3 million inhabitants; Figure 1; Supplementary Table 2; (12, 17, 18, 20, 41–44)]. As emphasized by the German HTA institute IQWiG in its assessment report, the estimation of R/R DLBCL patients after two lines of therapy in Germany might be underestimated due to data and methodical uncertainties (41); consequently, the rate of DLBCL CAR T-cell therapies in Germany in 2020 might be lower than reported in this analysis. In summary, between 29 and 71% of the estimated medically eligible patients did not receive a licensed CAR T-cell therapy in 2020, despite promising long-term efficacy and survival data (45–47). Reasons for this shortfall might include use of alternative therapies or clinical trial enrollment, restrictive funding criteria applied (e.g., CAR T-cell therapy not funded for DLBCL patients above a maximum age of 70 in Italy (increased to 75 years in May 2022) (23–25).

The number of authorized centers per population might also influence the overall CAR T-cell therapy rate. At the end of 2020, France, Germany, and Italy had a similar density of active DLBCL CAR T-cell centers (one center for two to three million inhabitants), whereas in Spain, center density was almost half of that (one center for five million inhabitants; Supplementary Figure 1; Supplementary Table 3). Of the EU-4 countries, Spain had the highest utilization of its DLBCL CAR T-cell centers as measured by the average number of DLBCL patients treated with licensed CAR T-cell therapies per center in 2020 (18 patients per center), followed by France (14 patients per center), Germany (9 patients per center) and Italy (6 patients per center; Supplementary Figure 1; Supplementary Table 3), indicating that Spain could partially compensate for its lower number of centers through a higher average treatment rate per center, although still not achieving overall CAR T-cell therapy rates at the level of France or Germany. Conversely, despite having a similar center density as France or Germany, average utilization of DLBCL CAR T-cell centers in Italy was the lowest, correlating with the lower rate of licensed CAR T-cell therapies overall. Unfortunately, no information on the theoretical CAR T-cell therapy capacity per center could be identified.

The following chapter will discuss challenges faced by DLBCL patients along their patient journey, which might contribute to the differences in CAR T-cell therapy rates observed among the EU-4 countries.

3. Challenges, best practices, and health system focus areas for DLBCL CAR T-cell therapy access in EU-4 countries: review of the literature and experts' opinion

To identify and discuss challenges, existing best practices, and potential health system recommendations for CAR T-cell therapy access in the EU-4 countries, the authors' professional experience, expertise and personal views were recorded through individual phone interviews (Supplementary Table 4 with interview questions). The authors have been selected based on their relevant expertise with CAR T-cell therapies in the four largest EU countries [convenience sample (48)] and the findings included in this chapter represent their personal viewpoints and experiences, substantiated by literature review.

To capture the challenges that might limit patient access to licensed CAR T-cell therapies and the differences seen across the EU-4 countries, we analyzed the key steps along the DLBCL patient journey, namely patient identification and referral (chapter "Patient identification and referral for CAR T-cell therapy"), patient approval before treatment (chapter "Patient approval before CAR T-cell therapy"), and CAR T-cell therapy delivery at authorized centers (chapter "CAR T-cell therapy delivery at authorized centers"). In addition to the identified challenges, we also discuss best practices and potential health system focus areas for improving patient access to CAR T-cell therapies.

3.1. Patient identification and referral for CAR T-cell therapy

3.1.1. Challenges for patient identification and referral

DLBCL is a fast-progressing disease, particularly in refractory patients, with a median overall survival of 6.3 months after start of second line therapy (33). Accurate and timely identification and referral of eligible R/R DLBCL patients for CAR T-cell therapy are therefore essential to ensure optimal outcomes and might represent a significant challenge for access to CAR T-cell therapies. Based on data available for Spain in 2020, for an estimated 294 medically eligible R/R DLBCL patients only 200 (68%) requests for licensed CAR T-cell therapy were submitted to the national expert group (40, 49), suggesting that up to one in three eligible patients were not identified or referred for CAR T-cell therapy.

Patient identification and selection for CAR T-cell therapy can be particularly challenging in small peripheral hospitals and clinics that treat many types of malignancies and may have only limited specific knowledge of the benefits and eligibility criteria of CAR T-cell therapies. Moreover, peripheral hospitals may not always be strongly connected with CAR T-cell centers or integrated with hemato-oncological care networks, where existing, which could support patient identification and referral for CAR T-cell therapies. The absence of clear and well-defined referral pathways for CAR T-cell therapies may also limit the likelihood and timeliness of referral of an eligible DLBCL patient to a CAR T-cell center. In addition, treating hematologists might be hesitant to refer eligible patients due to the perceived complexity and duration of the CAR T-cell therapy process, potentially prioritizing local treatment options, which further delay patient access to a CAR T-cell therapy. Despite being indicated after two lines of therapy, data from different European registries shows that many DLBCL patients treated or approved for treatment with CAR T-cell therapies had received three or more lines of prior therapies [71% of patients with at least three lines of therapy in the German DRST registry (26), 50% of patients in the French DESCAR-T registry (28), 42% of patients in the Italian AIFA registry (37), and 39% of patients in the UK national program (50)]. These findings suggest that referral of these patients potentially occurred too late and that timely identification and referral is a shared challenge across major European countries. Of note, it is likely that a number of patients included in these registries had already received several lines of therapy before CAR T-cell therapies became locally approved, and

therefore might have been overrepresented at the time of registry opening.

CAR T-cell center density per population (discussed above; Supplementary Figure 1; Supplementary Table 3) and moreover uneven geographical distribution of centers, may also have a role in creating referral delays or hesitancy, particularly if patients are required to travel over large distances to undergo CAR T-cell therapy. In Germany, personal experience from the authors suggests that travel distances of up to 2 hours to receive post-therapy follow-up or adverse event management create significant challenges, particularly for elderly patients. In Spain, where authorities designated nine CAR T-cell centers (and two "back-up" centers in case of capacity need), only six out of 17 regions had an active DLBCL CAR T-cell center by March 2021 (38). Out-of-region referral in Spain was reported to delay CAR T-cell therapy by 6 days compared to patients who have a CAR T-cell center in their region (67 days vs. 61 days median duration from treatment approval request to infusion, data from March 2019 – March 2021, including DLBCL and pediatric ALL CAR T-cell therapies) (22, 38). To ensure broader access to CAR T-cell therapy for lymphoma and leukemia patients across the country, the Spanish Ministry of Health (SNS) designated 15 new CAR T-cell centers in June 2022, including several in regions that did not have a CAR T center so far (51). In Italy, initial delays of center authorization and qualification by regional authorities and pharmaceutical manufacturers resulted in a geographically heterogeneous coverage of CAR T-cell centers. In December 2020, 70% of active CAR T-cell centers were concentrated in only four Italian regions (37). Regional inequities appear to have affected patient access in Italy. From August 2019–December 2020, DLBCL patients undergoing CAR T-cell therapies came from only 10 out of 20 regions (37).

3.1.2. Best practices and health system focus areas for patient identification and referral

Examples of successfully implemented best practices to address patient identification and referral challenges for CAR T-cell therapies are discussed in the following.

3.1.2.1. Educational activities

National and regional workshops and virtual roadshow events between CAR T-cell and referring centers provide an opportunity to discuss the CAR T-cell therapy process and patient eligibility criteria with referring physicians. Such meetings, as implemented by many European CAR T-cell centers, also support exchange of learnings and best practices for patient selection, such as for complex cases with specific comorbidities, reduced health status or age.

3.1.2.2. CAR T-cell therapy referral networks and quality criteria

To support early patient identification and timely referral, the hematology network around the Centre Hospitalier Universitaire de Montpellier has expanded its regional multi-disciplinary committee meeting to also include a CAR T-cell therapy dedicated segment. In the weekly virtual meeting, the committee reviews all presented DLBCL patients in the southern French region Occitania and advises referring physicians on CAR T-cell therapy eligibility and a course of treatment as soon as a patient fails first line therapy. The regional hematology network also defined clear pathways and quality criteria for the CAR T-cell therapy referral process (for instance final confirmation of patient eligibility must happen not more than 8 days after discussion in the regional committee, with clear responsibilities for diagnosis at both referring and CAR T-cell center). Similar network structures and regional dedicated multi-disciplinary meetings for CAR T-cell therapies exist also in other French regions (for instance implemented by the Hospices Civils de Lyon) and their development is supported by the French authorities through the National Cancer Plan (52). In the German region Rhineland-Palatinate, CAR T-cell centers and larger hospitals providing second-line therapy collaborate in a competence network for stem cell transplantation and cellular therapy, developing CAR T-cell therapy criteria and pathways, and organizing weekly virtual meetings to discuss individual patient cases. Outpatient hematology care providers are, at time of writing, not yet included in the network. In Spain, virtual weekly CAR T-cell committee meetings, now established in the Madrid region for example, also support referring centers with identification and referral of eligible patients. Beyond that, the Catalunya region has also established a well-defined hematology network with clear referral pathways that is also being used for CAR T-cell therapy patients. Small peripheral hospitals are strongly connected with larger hospitals, which in turn each have a designated reference CAR T-cell center where potential patients are referred to. The regional network also ensures continuous education of regional hospitals, ensuring that CAR T-cell therapy benefits, safety aspects and selection criteria are well known.

Based on the above discussed challenges and best practice examples, the authors suggest four key areas of focus for health systems to overcome challenges with patient identification and referral for CAR T-cell therapies (Table 2).

3.2. Patient approval before CAR T-cell therapy

3.2.1. Challenges

As discussed before, funding approval before CAR T-cell therapy is required in Spain (approval by the region of patient origin and by the national CAR T-cell therapy expert group). Depending on the center, pre-treatment funding approval may be required in Germany (approval by the patient's sick fund and medical review board), and in Italy (approval by the regional authorities). Without guarantee that the CAR T-cell product and procedure costs are funded, it is unlikely that authorized centers will initiate the treatment due to the high financial risks.

Collecting funding approval before CAR T-cell therapy can be a long and complex multi-step process adding administrative burden at the authorized centers and potentially resulting in delays in CAR T-cell

TABLE 2 Key health system focus areas for patient identification and referral challenges.

A. Focused referring center education on CAR T-cell therapy benefits/risks, patient selection and referral process, by CAR T-cell centers and hematology networks
B. Strengthened hematology networks, integrating referring centers through (virtual) tumor boards with a CAR T-dedicated segment and active communication among all network participants, including health authorities
C. Clear pathways, quality standards and responsibilities for patient referral for CAR T-cell therapy
D. Optimized geographical distribution of CAR T-cell centers to ensure equal access and minimal travel burden for patients

therapy access for patients. Registry data from patients treated in Germany and Spain report a median duration of 26 and 17 days respectively, from the moment of clinical decision for CAR T-cell therapy until leukapheresis, which besides other aspects also reflects the time required to receive external funding approval [Spanish data including DLBCL and also pediatric ALL patients; (26, 38)]. For patients whose health deteriorates during this wait time so much that they cannot undergo a CAR T-cell therapy in the end, such delays effectively restrict access to this therapy and its potential benefits. In Germany, personal experience from the authors indicates that it can take up to 4 weeks to receive funding approval by certain sick funds. These long timelines are in part also due to paper-based communication and the absence of an electronic information-sharing system. In addition, as no nationally harmonized criteria for CAR T-cell therapy eligibility are published and applied in Germany, decision making on patient eligibility can differ across sick funds, increasing financial and process uncertainties for CAR T-cell centers. In Spain, decisions for CAR T-cell therapy eligibility by the national expert group have occurred within 24 hours in 68% of "vital urgent cases" and within 72 hours in 79% of "non-vital urgent cases," however in a minority of cases the decisions took more time [data for March 2019 to March 2021 (38)]. Additional delays are thought to occur from the funding approval step with regional health authorities in Spain. For instance, based on author experience, decisions by authorities in the Catalunya region usually take around 2–3 days. Conversely, no additional delays are thought to occur in the Madrid region as the regional health authorities in Madrid only centralize and process requests for CAR T-cell therapy to the national expert group. In France and Italy, national financing mechanisms for innovative medicines are available for CAR T-cell therapies ["*Liste en Sus*" and "*Fondo Farmaci Oncologici Innovativi*" (29)] under the condition that information is provided through a national registry to authorities. This results in funding certainty for authorized centers and absence of a pre-treatment funding approval step in most cases. However, authorized private CAR T-cell centers in Italy cannot directly receive the national innovation funding, and instead require pre-treatment approval and CAR T-cell product purchase by the regional authorities or a public hospital in their place. In addition, for patients referred from other regions, to ensure that procedure costs are covered, authority approval from the region of patient origin may also be required in certain regions before initiation of therapy. This has resulted in delay in patient access to CAR T-cell therapies in Italy.

3.2.2. Best practices and health system focus areas

Examples of successfully implemented best practices to address patient approval challenges for CAR T-cell therapies are discussed in the following.

3.2.2.1. CAR T-cell therapy decision making by authorized centers

In France, authorized CAR T-cell centers decide on patient eligibility based on their medical assessment and in compliance with the licensed EMA label indication, but independent of an authority approval requirement. This approach has also allowed authorized centers to continuously refine patient selection based on their experiences and new evidence becoming available, effectively ensuring that all DLBCL patients that could benefit from CAR T-cell therapies have timely access to treatment. In Germany, most CAR T-cell centers have developed internal checklists over time based on their experience with the local sick fund process that allow them to anticipate specific requirements for eligibility decision making and to reduce the overall duration of pre-treatment funding approval.

3.2.2.2. National CAR T-cell therapy eligibility criteria and harmonized approval process

In Italy and Spain, the published and nationally harmonized DLBCL CAR T-cell therapy eligibility criteria, while restricting the eligible population beyond the EMA label, ensure transparency for patients and healthcare professionals and allow uniform decision-making on patient access to CAR T-cell therapies (23, 24, 38). In Germany, with the aim to work toward harmonization of patient eligibility criteria and decision-making, a monthly conference between the national Competence Center Oncology KCO, the sick fund's medical review boards and CAR T-cell centers, was initiated in 2021 (53). Centralized approval processes can also support ensuring equal access to CAR T-cell therapies for DLBCL patients. In the UK, a weekly National CAR T Clinical Panel (NCCP), composed of clinical experts, patient representatives and CAR T-cell center delegates decides on patient eligibility, prioritization, and referral to an appropriate center depending on available capacity and geographic vicinity (49, 54). A national CAR T-cell therapy board supporting efficient decision making on patient eligibility and referral was also established in the Netherlands by the hemato-oncology society HOVON (55). Similar to the centralized approval processes in the UK and the Netherlands, the Spanish national approval process aims to ensure equal patient access but is linked to prior regional authority approval, which may delay the process and potentially result in regionally heterogeneous decision-making. Of note, all described national approval processes may carry the risk of becoming bottlenecks to patient access in the future, when more patients in new indications are expected to become eligible for CAR T-cell therapy.

Based on the above discussed challenges and best practice examples the authors suggest three key areas of focus for health systems to overcome challenges with patient approval before CAR T-cell therapies (Table 3).

3.3. CAR T-cell therapy delivery at authorized centers

3.3.1. Challenges

CAR T-cell centers require specific capabilities, organization, and infrastructure to ensure optimal and timely delivery of CAR T-cell therapy to eligible patients. Specifically trained interdisciplinary teams are involved through various processes required for CAR T-cell therapy administration and patient management. Due to the

TABLE 3 Key health system focus areas for patient approval challenges.

A. Ensuring nationally harmonized and transparent CAR T-cell therapy eligibility criteria to support equal decision making and clarity on patient selection
B. Simplification of pre-treatment approval process through digitalization and reduction of number of process steps (e.g., single-step approval process, either at the regional or national level)
C. Decision making directly by authorized CAR T-cell centers without regional/national authority or payer pre-treatment approval requirement (for instance, with control through a registry documentation requirement)

complexity of CAR T-cell therapies, authorized centers may face challenges in providing CAR T-cell therapy capacity in a short time window to address the urgent medical need of R/R DLBCL patients, and in avoiding delays to other patient treatments that depend on similar center resources. With more patients expected to undergo CAR T-cell therapies in future indications, capacity challenges at authorized centers are likely to increase further.

Limited center resources for CAR T-cell therapy delivery may arise from lack of support from authorities to ensure financing for infrastructural and organizational investments required for CAR T-cell therapy. For instance, centers needed to invest in expanding their hematology wards and ICU beds, as CAR T-cell therapy patients were required to stay in the center for up to 3 weeks after infusions (2, 3, 26, 36, 38). Also, leukapheresis, cell therapy laboratory and pharmacy capacity needed to be increased, which proved to be difficult for certain CAR T-cell centers based on the authors' experience. Without financial support from authorities, such investments had to be covered by the centers independently, potentially resulting in delays with center authorization or limited overall CAR T-cell therapy capacity. In addition to challenges with infrastructural investments, the build-up of highly specialized teams, especially nurses, physicians, and pharmacists, requires significant training investment and may become increasingly difficult. CAR T-cell center quality criteria for instance, as introduced by the German Federal Joint Committee G-BA, include strict requirements on the professional qualifications of CAR T-cell therapy nurses (20), making it increasingly challenging to identify and recruit appropriately qualified nurses. Non-competitive compensation in public hospitals may increase staffing challenges further.

Moreover, beyond costs of the CAR T-cell product, centers must also cover costs of the procedure, including provision of specific care, monitoring, and hospital resources. Such costs might not be covered adequately through existing funding, resulting in additional financial challenges for authorized centers. In France for instance, a study reported that unlike CAR T-cell product costs, procedure costs were covered through a general, non-specific tariff resulting in an approximate €19,000 loss per DLBCL patient treated with CAR T-cell therapy (56). In Italy there are not CAR-T cell specific tariffs for the relevant inpatient service, which are classified according to the DRG (Diagnostic-Related-Groups) system. Currently, regions use different tariffs to cover CAR T-cell therapy procedures, for instance tariffs for allogeneic or autologous stem cell transplantation. There is no evidence whether these tariffs cover the relevant procedure costs (57). In Germany, hospitals may ask for funds for innovative and complex medicines/procedures through the NUB. Both CAR-T cell received a NUB 1 rank, which is granted to a medicine or procedure which is new, innovative, for a low number of patients and which requires higher resource (58). In Spain, the costs of the drug are covered by the patient's local hospital, whereas the cost of care and procedures are covered by the Autonomous Community where the treatment takes place, and subsequently refunded via the Health Cohesion Fund (30, 59, 60). In France, hospitals receive a flat supplement of 15,000 € per patient to cover the procedures associated with the CAR T treatment (61).

3.3.2. Best practices and health system focus areas

Examples of successfully implemented best practices to ensure adequate capabilities, organization, and infrastructure for CAR T-cell therapies are discussed in the following.

3.3.2.1. Constructive collaboration and support from health authorities

In France, CAR T-cell therapies were introduced in specialized centers with direct support from the regional health authorities, through collaborations that initiated already before EMA regulatory approval in the context of the ATU early access program (17, 18). Under the National Cancer Plan this collaboration between centers and authorities is expected to continue also for new CAR T-cell therapy indications and future capacity expansions required.

3.3.2.2. Optimizing CAR T-cell therapy capacity by utilizing network resources and reducing inpatient care

To optimize CAR T-cell therapy capacity and resource use, an approach taken by certain authorized centers is to delegate selected CAR T-cell therapy process steps within their network. In Spain, leukapheresis for CAR T-cell production is also provided at the level of certain specialized referring centers. Besides improving available capacity at the CAR T-cell center, this approach also reduces travel requirements for patients undergoing CAR T-cell therapy. Similarly, in France collaboration with the French Blood Collection Association EFS allowed to increase leukapheresis capacity outside of CAR T-cell centers. Furthermore, specialized rehabilitation centers for follow-up monitoring and accommodation after CAR T-cell infusion are being used to optimize bed capacity in CAR T-cell centers in Montpellier and Lyon. Moreover, reducing the requirement for inpatient procedures might also improve overall efficiency of resource usage. By conducting lymphodepletion in an outpatient setting, the Centre Hospitalier Universitaire de Montpellier was able to reduce hospitalization per patient by 3 days, effectively increasing their overall CAR T-cell therapy capacity. Other evidence suggests that in the future more procedures of CAR T-cell therapy may be provided in an outpatient setting (62).

Based on the above discussed challenges and best practice examples the authors suggest three key areas of focus for health systems to ensure adequate set-up of authorized centers for CAR T-cell therapies (Table 4).

4. Discussion

CAR T-cell therapies offer a promising new therapeutic approach to treating a number of severe cancers, including DLBCL where R/R patients previously had only very limited therapeutic options (33). Despite promising results of CAR T-cell therapies (45–47), our

TABLE 4 Key health system focus areas for ensuring adequate CAR T-cell center set-up.

A. Early and adequate authority support and coordinated capacity planning for CAR T-cell centers, also supporting professional training for specialized personnel
B. Leveraging network resources to optimize overall CAR T-cell therapy capacity (e.g., leukapheresis and post-infusion care performed in referring centers). Capacity optimization should also occur across networks, where patients are referred from one CAR T-cell center to another in case of limited treatment capacity
C. Sufficient CAR T-cell therapy procedure funding for authorized centers, ideally through a dedicated national tariff

analysis indicates that between 29% and 71% of the estimated eligible R/R DLBCL patients have not been treated with a licensed CAR T-cell therapy in 2020 in the EU-4 countries. While reasons for a low DLBCL CAR T-cell therapy rate can be diverse, including rapid disease progression and worsening of the patient's condition before treatment, use of alternative therapies or clinical trial enrollment, our analysis highlights a critical role for the health system in optimizing the patient's journey and access to CAR T-cell therapies. DLBCL CAR T-cell therapy rates were highest in France (71%). Reasons for this may include the early introduction of CAR T-cell therapy through the early access program ATU, allowing for early accumulation of expertise before EMA approval, the strongly embedded regional hematology networks supporting the CAR T-cell therapy patient journey, the national CAR T-cell therapy funding through the "*Liste en Sus*," as well as authority support driven by the National Cancer Plan (17, 18, 29, 52). Conversely in Italy, DLBCL CAR T-cell therapy rates were the lowest (29% of the estimated eligible patients) among the EU-4 countries in 2020 based on our analysis. Reasons for this may include the restrictive funding criteria for R/R DLBCL patients (including a maximum age for patient eligibility) and a lack of harmonized processes for managing CAR T-cell therapy pathways in a regionalized health care system, which could particularly result in challenges with timely patient identification and referral. The AIFA registry suggests that regional inequalities exist in patient access to CAR T-cell therapies, potentially also linked to a concentration of CAR T-cell centers in few Italian regions (37).

It must be noted that year 2020 has posed special challenges on the healthcare systems due to the COVID-19 pandemic, which affected all healthcare provisions, including specialized therapies like CAR T cell therapy. However, the authors are convinced that most of the barriers discussed in this manuscript are of systemic nature and not directly resulting from the pandemic situation, although they were likely further aggravated. Furthermore, the paper has carried out a cross-country comparison, and all analyzed countries have been affected by COVID-19 pandemic.

It should be noted that as we report data on the CAR T-cell therapy rate in 2020, the general patient access situation has likely evolved in the meantime, with additional expertise having been gained and additional CAR T-cell centers having been authorized. More research and systemic data collection will be needed to understand CAR T-cell therapy pathways and challenges along the patient journey in further detail. For instance, registries as implemented for CAR T-cell therapies in the EU-4 countries represent an important tool for tracking and improving health system performance for CAR T-cell therapy patients. However, these registries require further expansion (e.g., the inclusion of referral rates and timelines for CAR T-cell therapies) and need to provide a more systematic read out to support health system planners and decision-makers with the necessary information to focus improvement efforts.

5. Conclusion

Our analysis across the four largest health systems in the European Union has identified several challenges that can impact timely and equitable access to CAR T-cell therapy for eligible DLBCL patients. With additional CAR T-cell therapies for hematological cancers entering the market in the coming years (and potential future CAR T-cell treatments for solid tumors), we believe that it is crucial to ensure that health systems act on these challenges now and work to prepare a sustainable environment that will support patient access to future innovative therapies. The best practices and focus areas discussed in this article can serve as a blueprint to initiate improvements designed to fit within their national and local health system environments.

Data availability statement

The original contributions presented in the study are included in the article/Supplementary material, further inquiries can be directed to the corresponding author.

Author contributions

MÁCA, PLC, GC, JC, BD, CJ, RM, CR, AS, JMSC, and EMW-D contributed to the analysis of the CAR T-cell therapy access situation, barriers, and best practices, to the discussion of health system recommendations and to the writing of the manuscript. All authors contributed to the article and approved the submitted version.

Funding

Funding for journal publication fees and manuscript writing support by the agency Executive Insight was provided by Kite Pharma Inc./ Gilead Sciences Inc. Kite Pharma Inc./ Gilead Sciences Inc. contributed to the selection of authors but had no direct involvement in the preparation and development of the publication.

Conflict of interest

The authors declare that the research was conducted in the absence of any commercial or financial relationships that could be construed as a potential conflict of interest.

Publisher's note

Supplementary material

The Supplementary material for this article can be found online at: https://www.frontiersin.org/articles/10.3389/fmed.2023.1128295/full#supplementary-material

References

1. Larson RC, Maus MV. Recent advances and discoveries in the mechanisms and functions of CAR T cells. *Nat Rev Cancer*. (2021) 21:145–1. doi: 10.1038/s41568-020-00323-z

2. EMA (European medicines agency) [Internet] EPAR Kymriah. (2022a). Availanle at: https://www.ema.europa.eu/en/medicines/human/EPAR/kymriah [Accessed May 31, 2022].

3. EMA (European Medicines Agency) [Internet]. EPAR Yescarta. (2022b). Available at: https://www.ema.europa.eu/en/medicines/human/EPAR/yescarta [Accessed Apr 17, 2023].

4. EMA (European Medicines Agency) [Internet]. EPAR Breyanzi. (2022c). Available at: https://www.ema.europa.eu/en/medicines/human/EPAR/breyanzi [Accessed May 31, 2022].

5. Gilead [Internet]. Yescarta® CAR T-cell therapy quadruples median event-free survival duration over standard of care in second-line relapsed or refractory large B-Cell lymphoma. (2021). Available at: https://www.gilead.com/news-and-press/press-room/press-releases/2021/9/kite-submits-supplemental-biologics-license-application-to-us-food-and-drug-administration-for-earlier-use-of-yescarta-in-large-bcell-lymphomac [Accessed April 17, 2023].

6. EMA (European Medicines Agency) [Internet]. Opinion Yescarta (2022d). Available at: https://www.ema.europa.eu/en/documents/smop/chmp-post-authorisation-summary-opinion-yescarta-ii-42_en.pdf [Accessed May 31, 2022].

7. EMA (European Medicines Agency) [Internet]. EPAR Tecartus. (2022e) Avaialble at: https://www.ema.europa.eu/en/medicines/human/EPAR/tecartus [Accessed May 31, 2022].

8. EMA (European Medicines Agency) [Internet]. EPAR Abecma. (2022f). Available at: https://www.ema.europa.eu/en/medicines/human/EPAR/abecma [Accessed May 31, 2022].

9. EMA (European Medicines Agency) [Internet]. Opinion Carvykti (2022g). Available at: https://www.ema.europa.eu/en/medicines/human/summaries-opinion/carvykti [Accessed May 31, 2022].

10. Clinicaltrials.gov [Internet]. 544 studies found for: Recruiting, active, not recruiting, enrolling by invitation studies | cart. (2022). Avaialable at: https://clinicaltrials.gov/ct2/results?cond=&term=car+t&cntry=&state=&city=&dist= [Accessed May 31, 2022].

11. G-BA (Gemeinsamer Bundesausschuss) [Internet]. Axicabtagen Ciloleucel. (2019). Available at: https://www.g-ba.de/downloads/39-261-3771/2019-05-02_AM-RL-XII_Axicabtagen-Ciloleucel_D-406_D-416_BAnz.pdf [Accessed May 31, 2022].

12. G-BA (Gemeinsamer Bundesausschuss) [Internet]. Beschluss des Gemeinsamen Bundesausschussesüber eine Änderung der Arzneimittel Richelieu (AM-RL): Anlage XII – Nutzenbewertung von Arzneimitteln mit neuen Wirkstoffen nach § 35a SGB V Tisagenlecleucel (Neubewertung nach Fristablauf: Diffus großzelliges B-Zell-Lymphom). BAnz AT 28.10.2020 B4 (2020). Available at: https://www.g-ba.de/downloads/39-261-4456/2020-09-17_AM-RL-XII_Tisagenlecleucel_DLBCL_D-530_BAnz.pdf [Accessed May 31, 2022].

13. AIFA (Agenzia Italiana del Farmaco) [Internet]. Regime di rimborsabilita' e prezzo del medicinale per uso umano «Yescarta» (Determina n. DG/1643/2019). (2019a). Available at: https://www.aifa.gov.it/documents/20142/961234/Determina_DG-1643-2019_Yescarta.pdf/26464c52-5e7b-e97d-74d5-f66f69039fa0 [Accessed May 31, 2022].

14. AIFA (Agenzia Italiana del Farmaco) [Internet]. Regime di rimborsabilita' e prezzo del medicinale per uso umano «Kymriah» (2019b). Available at: https://www.aifa.gov.it/sites/default/files/Determina_50162_del_06.05.2019-KYMRIAH .pdf [Accessed May 31, 2022].

15. Ministerio de Sanidad [Internet]. Nota Informativa De La Reunión De La Comisión Interministerial De Precios De Los Medicamentos. (2019a). Available at: https://www.sanidad.gob.es/profesionales/farmacia/pdf/NOTA_INFORMATIVA_DE_LA_CIPM_185_web.pdf [Accessed May 31, 2022].

16. Legifrance [Internet]. Décret n° 2021–2869 du 30 juin 2021 relatif aux autorisations d'accès précoce et compassionnel de certains médicaments. (2021a). Available at: https://www.legifrance.gouv.fr/jorf/id/JORFTEXT000043728288 [Accessed May 31, 2022].

17. HAS (Haute Autorité de Santé) [Internet]. Kymriah (tisagenlecleucel). (2021a). Available at: https://www.has-sante.fr/jcms/c_2891692/fr/kymriah-tisagenlecleucel-car-t-anti-cd19-ldgcb [Accessed May 31, 2022].

18. HAS (Haute Autorité de Santé) [Internet]. Yescarta (axicabtagene ciloleucel). (2021b). Available at: https://www.has-sante.fr/jcms/p_3262244/en/yescarta-axicabtagene-ciloleucel [Accessed May 31, 2022].

19. Legifrance [Internet]. Arrêté du 19 mai 2021 limitant l'utilisation de médicaments de thérapie innovante à base de lymphocytes T génétiquement modifiés dits CAR-T Cells autologues à certains établissements de santé en application des dispositions de l'article L. 1151–1 du code de la santé publique. (2021b). Available at: https://www.legifrance.gouv.fr/jorf/id/JORFTEXT000043519089 [Accessed May 31, 2022].

20. G-BA (Gemeinsamer Bundesausschuss) [Internet]. Measures for quality assurance according to § 136a paragraph 5 SGB V: CAR T cells in B cell neoplasms. (2021). Available at: https://www.g-ba.de/beschluesse/4969/ [Accessed May 31, 2022].

21. Ministerio de Sanidad [Internet]. Criterios Y Estándares Para La Designación De Centros Para Utilizacion De Car-T En Linfoma Difuso De Células B Grandes Recidivante O Refractario, En Leucemia Linfoblástica Aguda De Células B Refractaria, Linfoma Recurrente O Refractario De Células De Manto Y Mieloma Múltiple En Recaida Y Refractario En El Sistema Nacional De Salud. (2021a). Available at: https://www.sanidad.gob.es/fr/profesionales/farmacia/pdf/20211202_Criterios_Estandares_Designacion_Centros_CART.PDF [Accessed May 31, 2022].

22. Ministerio de Sanidad [Internet]. Anexo 1. Solicitud De Valoración Por El Grupo De Expertos En La Utilización De Medicamentos Car A Nivel Sns. (2019b). Available at: https://www.sanidad.gob.es/profesionales/farmacia/pdf/20200206_Formulario_valoracion_grupo_expertos_CAR-T_tisagen_axicel.pdf [Accessed May 31, 2022].

23. AIFA (Agenzia Italiana del Farmaco) [Internet]. Scheda Yescarta DLBCL. (2019c). Available at: https://www.aifa.gov.it/documents/20142/936093/scheda_YESCARTA_DLBCL_12.11.2019.zip [Accessed May 31, 2022].

24. AIFA (Agenzia Italiana del Farmaco) [Internet]. Scheda Registro Kymriah DLBCL. (2021a). Available at: https://www.aifa.gov.it/documents/20142/1309641/Scheda_Registro_Kymriah_DLBCL_27.01.2021.zip [Accessed May 31, 2022].

25. AIFA (Agenzia Italiana del Farmaco) [Internet]. Modifica Registro KYMRIAH (DLCBL). (2022). Available at: https://www.aifa.gov.it/-/modifica-registro-kymriah-dlcbl- [Accessed May 31, 2022].

26. Bethge W, Martus P, Schmitt M, Holtick U, Subklewe M, Dreger P, et al. GLA/DRST real-world outcome analysis of CAR-T cell therapies for large B-cell lymphoma in Germany. *Blood*. (2022) 140:349–58. doi: 10.1182/blood.2021015209

27. Ministerio de Sanidad [Internet]. Procedimiento Para La Valoracion De Solicitudes Realizadas Por Los/Las Especialistas Del Sistema Nacional De Salud De Medicamentos Car-T Por El Grupo De Expertos En La Utilización De Medicamentos CAR. (2019c). Available at: https://www.sanidad.gob.es/fr/profesionales/farmacia/pdf/201906021_Procedimiento_Valoracion_Grupo_CAR_T.pdf [Accessed May 31, 2022].

28. Gouill S, Bachy E, Blasi R, Cartron G, Beauvais D, Bras F, et al. First results of DLBCL patients treated with CAR-T cells and enrolled in DESCAR-T registry, a French real-life database for CAR-T cells in hematologic malignancies. *Hematol Oncol*. (2021) 39. doi: 10.1002/hon.84_2879

29. Jørgensen J, Hanna E, Kefalas P. Outcomes-based reimbursement for gene therapies in practice: the experience of recently launched CAR-T cell therapies in major European countries. *J Mark Access Health Policy*. (2020) 8:1715536. doi: 10.1080/20016689.2020.1715536

30. Ministerio de Sanidad [Internet]. Plan De Abordaje De Las Terapias Avanzadas En El Sistema Nacional De Salud: Medicamentos Car. (2018). Available at: https://www.sanidad.gob.es/profesionales/farmacia/Terapias_Avanzadas.htm [Accessed May 31, 2022].

31. KCO (Kompetenz-Centrum Onkologie) [Internet]. (2022). Available at: https://www.kconkologie.de/ueber-uns/aufgaben-ziele/ [Accessed May 31, 2022].

32. EBMT (European Society for Blood and Marrow Transplantation) [Internet]. Data collection on CAR T-cells. (2022). Avaialble at: https://www.ebmt.org/registry/data-collection-car-t-cells [Accessed May 31, 2022].

33. Crump M, Neelapu SS, Farooq U, Neste EVD, Kuruvilla J, Westin J, et al. Outcomes in refractory diffuse large B-cell lymphoma: results from the international SCHOLAR-1 study. *Blood*. (2017) 130:1800–8. doi: 10.1182/blood-2017-03-769620

34. Tilly H, Morschhauser F, Sehn LH, Friedberg JW, Trněný M, Sharman JP, et al. Polatuzumab Vedotin in previously untreated diffuse large B-cell lymphoma. *N Engl J Med*. (2022) 386:351–3. doi: 10.1056/NEJMoa2115304

35. Major A, Cliff ERS, Ermann DA, Durani U, Russler-Germain DA. Frontline polatuzumab vedotin for diffuse large B-cell lymphoma: a survey of clinician impressions. *Ejhaem*. (2022) 3:930–5. doi: 10.1002/jha2.505

36. Yakoub-Agha I, Chabannon C, Bader P, Basak GW, Bonig H, Ciceri F, et al. Management of adults and children undergoing chimeric antigen receptor T-cell therapy: best practice recommendations of the European Society for Blood and Marrow Transplantation (EBMT) and the joint accreditation committee of ISCT and EBMT (JACIE). *Haematologica*. (2020) 105:297–6. doi: 10.3324/haematol.2019.229781

37. AIFA (Agenzia Italiana del Farmaco) [Internet] Osservatorio Nazionale sull'impiego dei Mediciniali. L'uso dei Farmaci in Italia. Rapporto Nazionale Anno 2020. Roma: Agenzia Italiana del Farmaco, (2021b). Available at: https://www.aifa.gov.it/-/rapporto-nazionale-osmed-2020-sull-uso-dei-farmaci-in-italia [Accessed May 31, 2022].

38. Ministerio de Sanidad [Internet]. *Informe De Seguimiento De La Dirección General De Cartera Común De Servicios Del Sistema Nacional De Salud (Sns) Y Farmacia Sobre El Plan Para El Abordaje De Las Terapias Avanzadas En El Sns*. (2022). Available at: https://www.sanidad.gob.es/profesionales/farmacia/pdf/20210718_Infor_MS_Seg_Plan_Terapias_Avanzadas_SNS.pdf [Accessed May 31, 2022].

39. Kite Pharma Inc./ Gilead Sciences S.r.l. Personal communication. (2021).

40. Ministerio De Sanidad. Solicitud de acceso a la información publica (Oct 2021) - personal communication from Spanish Ministry of Health on data query submitted. Solicitud de acceso a la información publica (Oct 2021) - personal communication from Spanish Ministry of Health on data query submitted (2021b).

41. IQWiG (Institut für Qualität und Wirtschaftlichkeit im Gesundheitswesen) [Internet]. Bewertung Tisagenlecleucel (diffuses grosszelliges B-Zell-Lymphom). Bericht Nr. 924 (09.06.2020). (2020). Available at: https://www.g-ba.de/downloads/92-975-3674/2020-03-15_

Bewertung-Therapiekosten-Patientenzahlen-IQWiG_Tisagenlecleucel_D-530.pdf [Accessed May 31, 2022].

42. AIRTUM Working Group; Busco S, Buzzoni C, Mallone S, Trama A, Castaing M, et al. Italian cancer figures--Report 2015: the burden of rare cancers in Italy. *Epidemiol Prev*. (2016) 40:1–120. doi: 10.19191/EP16.1S2.P001.035

43. Belleudi V, Trotta F, Fortinguerra F, Poggi FR, Olimpieri O, Santelli E, et al. Real world data to identify target population for new CAR-T therapies. *Pharmacoepidemiol Drug Saf*. (2021) 30:78–85. doi: 10.1002/pds.5165

44. Rocco AD, Cuneo A, Rocco AD, Merli F, Luca GD, Petrucci L, et al. Relapsed/refractory diffuse large B-cell lymphoma patients. A multicenter retrospective analysis of eligibility criteria for car-T cell therapy. *Leuk Lymphoma*. (2020) 62:1–11. doi: 10.1080/10428194.2020.1849676

45. Abramson JS, Palomba ML, Gordon LI, Lunning MA, Wang M, Arnason JE, et al. Two-year follow-up of transcend NHL 001, a multicenter phase 1 study of Lisocabtagene Maraleucel (liso-cel) in relapsed or refractory (R/R) large B-cell lymphomas (LBCL). *Blood*. (2021) 138:2840–0. doi: 10.1182/blood-2021-148948

46. Schuster SJ, Tam CS, Borchmann P, Worel N, McGuirk JP, Holte H, et al. Long-term clinical outcomes of tisagenlecleucel in patients with relapsed or refractory aggressive B-cell lymphomas (JULIET): a multicentre, open-label, single-arm, phase 2 study. *Lancet Oncol*. (2021) 22:1403–15. doi: 10.1016/S1470-2045(21)00375-2

47. Jacobson C, Locke FL, Ghobadi A, Miklos DB, Lekakis LJ, Oluwole OO, et al. Long-term (≥4 year and ≥5 year) overall survival (OS) by 12- and 24-month event-free survival (EFS): an updated analysis of ZUMA-1, the pivotal study of Axicabtagene Ciloleucel (Axi-Cel) in patients (pts) with refractory large B-cell lymphoma (LBCL). *Blood*. (2021) 138:1764. doi: 10.1182/blood-2021-148078

48. Lohr SL. *Sampling: design and analysis*. *2nd* ed. Boston: Brooks/Cole. (2010).

49. GENESIS-SEFH [Internet]. Axicabtagen ciloleucel en linfoma difuso de células B grandes refractario o en recaída (2019). Available at: http://gruposdetrabajo.sefh.es/genesis/genesis/Enlaces/InformesHosp_abc.htm [Accessed May 31, 2022].

50. Kuhnl A, Roddie C, Kirkwood AA, Tholouli E, Menne T, Patel A, et al. A national service for delivering CD19 CAR-Tin large B-cell lymphoma - The UK real-world experience. *Br J Haematol*. (2022) 198:492–502. doi: 10.1111/bjh.18209

51. Ministry of Health Ministry of Health doubles the network of CAR-T advanced therapy centers against serious diseases such as cancer [Internet] Available at: https://spaintoday.news/2022/06/10/the-ministry-of-health-doubles-the-network-of-car-t-advanced-therapy-centres-against-serious-diseases-such-as-cancer/ [Accessed October 3, 2022].

52. INCa (Institut national du cancer). *[Internet]. 2021–2030 France ten-year Cancer-control strategy Roadmap*. (2022) Available at: https://www.e-cancer.fr/Institut-national-du-cancer/Strategie-de-lutte-contre-les-cancers-en-France/La-strategie-decennale-de-lutte-contre-les-cancers-2021-2030 [Accessed May 31, 2022].

53. DAG-HSZT E. V. (Deutsche Arbeitsgemeinschaft Für Hämatopoetische Stammzelltransplantation Und Zelluläre Therapie EV) Falldiskussionen mit dem Kompetenz-Centrum Onkologie (KCO). CART-Indikationsdiskussionen mit dem KCO vom (2022). Available at: https://www.dag-kbt.de/Falldiskussionen.html [Accessed May 31, 2022].

54. NICE (National Institute for Health and Care Excellence) [Internet]. Cancer drugs fund – Data collection arrangement. Axicabtagene ciloleucel for treating diffuse large B-cell lymphoma and primary mediastinal B-cell lymphoma after 2 or more systemic therapies [ID1115]. (2018). Avaialble at: https://www.nice.org.uk/guidance/ta559/resources/managed-access-agreement-january-2019-pdf-6660053245 [Accessed May 31, 2022].

55. HOVON (Haemato Oncologie Stichting Volwassenen Nederland) [Internet]. Behandeladvies: lymfoom. (2022). Avaailable at: https://hovon.nl/nl/behandelrichtlijnen/lymfoom [Accessed May 31, 2022].

56. Jeanblanc G, Cartron G, N'Guessan K, Massetti M, Carette J. PCN167 estimation of the financial impact of chimeric antigen receptor (CAR) T-cell therapy for French hospitals. *Value Health*. (2020) 23:S452. doi: 10.1016/j.jval.2020.08.304

57. Jommi C, Bramanti S, Pani M, Ghirardini A, Santoro A. CAR T-cell therapies in Italy: patient access barriers and recommendations for health system solutions. *Front Pharmacol*. (2022) 13:915342. doi: 10.3389/fphar.2022.915342

58. Ronco V, Dilecce M, Lanati E, Canonico PL, Jommi C. Price and reimbursement of advanced therapeutic medicinal products in Europe: are assessment and appraisal diverging from expert recommendations? *J Pharm Policy Pract*. (2021) 14:30. doi: 10.1186/s40545-021-00311-0

59. Ministerio de Sanidad Real Decreto 1302/2006, de 10 de noviembre, por el que se establecen las bases del procedimiento para la designación y acreditación de los centros, servicios y unidades de referencia del Sistema Nacional de Salud. (2006). Available at: https://www.boe.es/buscar/doc.php?id=BOE-A-2006-19626#:~:text=A%2D2006%2D19626-,Real%20Decreto%201302%2F20062C20de%2010%20de20noviembre2C%20por,del%20Sistema%20Nacional%20de%20Salud [Accessed Apr 17, 2023].

60. Zozaya N, Villaseca J, Abdalla F, Calleja MA, Díez-Martín JL, Estévez J, et al. A strategic reflection for the management and implementation of CAR-T therapy in Spain: an expert consensus paper. *Clin Transl Oncol*. (2022) 24:968–0. doi: 10.1007/s12094-021-02757-9

61. ATIH Campagne tarifaire et budgétaire 2021. (2021). Available at: https://www.atih.sante.fr/sites/default/files/public/content/4004/notice_technique_complementaire_n_atih-234-7-2021_nouveautes_financement_2021-20210712.pdf [Accessed April 17, 2023].

62. Borogovac A, Keruakous A, Bycko M, Chakrabarty JH, Ibrahimi S, Khawandanah M, et al. Safety and feasibility of outpatient chimeric antigen receptor (CAR) T-cell therapy: experience from a tertiary care center. *Bone Marrow Transpl*. (2022) 138:4821–3. doi: 10.1182/blood-2021-153457

frontiers | Frontiers in Oncology

TYPE Original Research
PUBLISHED 09 June 2023
DOI 10.3389/fonc.2023.1172623

OPEN ACCESS

EDITED BY
Gaël Roué,
Josep Carreras Leukaemia Research Institute (IJC), Spain

REVIEWED BY
Jue Wang,
Huazhong University of Science and Technology, China
Joaquim Carreras,
Tokai University, Japan

*CORRESPONDENCE
Wanzhuo Xie
xiewanzhuo@zju.edu.cn

†These authors have contributed equally to this work and share first authorship

RECEIVED 23 February 2023
ACCEPTED 23 May 2023
PUBLISHED 09 June 2023

CITATION
Xu Y, Shen H, Shi Y, Zhao Y, Zhen X, Sun J, Li X, Zhou D, Yang C, Wang J, Huang X, Wei J, Huang J, Meng H, Yu W, Tong H, Jin J and Xie W (2023) Dyslipidemia in diffuse large B-cell lymphoma based on the genetic subtypes: a single-center study of 259 Chinese patients. *Front. Oncol.* 13:1172623. doi: 10.3389/fonc.2023.1172623

Dyslipidemia in diffuse large B-cell lymphoma based on the genetic subtypes: a single-center study of 259 Chinese patients

Yi Xu†, Huafei Shen†, Yuanfei Shi†, Yanchun Zhao, Xiaolong Zhen, Jianai Sun, Xueying Li, De Zhou, Chunmei Yang, Jinhan Wang, Xianbo Huang, Juying Wei, Jian Huang, Haitao Meng, Wenjuan Yu, Hongyan Tong, Jie Jin and Wanzhuo Xie*

Department of Hematology, The First Affiliated Hospital, College of Medicine, Zhejiang University, Hangzhou, Zhejiang, China

Background: Diffuse large B-cell lymphoma (DLBCL) is a kind of highly heterogeneous non-Hodgkin lymphoma, both in clinical and genetic terms. DLBCL is admittedly categorized into six subtypes by genetics, which contain MCD, BN2, EZB, N1, ST2, and A53. Dyslipidemia is relevant to a multitude of solid tumors and has recently been reported to be associated with hematologic malignancies. We aim to present a retrospective study investigating dyslipidemia in DLBCL based on the molecular subtypes.

Results: This study concluded that 259 patients with newly diagnosed DLBCL and their biopsy specimens were available for molecular typing. Results show that the incidence of dyslipidemia (87.0%, $p < 0.001$) is higher in the EZB subtype than in others, especially hypertriglyceridemia (78.3%, $p = 0.001$) in the EZB subtype. Based on the pathological gene-sequencing, patients with BCL2 gene fusion mutation are significantly correlative with hyperlipidemia (76.5%, $p = 0.006$) and hypertriglyceridemia (88.2%, $p = 0.002$). Nevertheless, the occurrence of dyslipidemia has no remarkable influence on prognosis.

Conclusion: In summary, dyslipidemia correlates with genetic heterogeneity in DLBCL without having a significant influence on survival. This research first connects lipids and genetic subtypes in DLBCL.

KEYWORDS

diffuse large B-cell lymphoma, molecular typing, dyslipidemia, hypertriglyceridemia, BN2 subtype, MCD subtype, EZB subtype, A53 subtype

Introduction

Diffuse large B-cell lymphoma (DLBCL) is characterized by aggressiveness and heterogeneity epigenetically and genetically. Besides, DLBCL accounts for approximately 35% of non-Hodgkin lymphoma (NHL) and is the most common lymphoma in adults (1). In 2018, the definition of molecular typing was initially propounded. Shipp et al. classified DLBCL into clusters 1–5 by genetic abnormality (2). Staudt et al. implemented molecular typing by analyzing genetic alterations and proposed four prominent subtypes: MCD (featured as the co-occurrence of *MYD88 L265p* and *CD79B* mutations), BN2 (featured as *BCL6* fusion mutations and *NOTCH2* mutations), EZB (featured as *EZH2* mutations and *BCL2* fusion mutations), and N1 (featured as *NOTCH1* mutations). Later, two other types were added, including ST2 (featured as *SGK1* and *TET2* mutations) and A53 (featured as *TP53* aneuploid mutations) (3, 4). Researchers had considered the influence of *MYC* mutations and therefore divided the EZB subtype into *MYC*-positive EZB isoforms and *MYC*-negative EZB isoforms (4). While the prior simple algorithm of six subtypes is more frequently being applied in clinical. Dyslipidemia has been considered correlative to multitudes of solid tumors, like breast cancer, prostate cancer, thyroid cancer, colorectal cancer, and lung cancer (5–9). Recently, researchers have found that a portion of hematologic malignancies is relative to the incidence of dyslipidemia, for instance, chronic leukemia and acute promyelocytic leukemia (10, 11). Ma et al. recently found that cholesterol biosynthesis relative axis may have an oncogenic activation in DLBCL with *BCL2-IGH* translocations (12). While the correlation between dyslipidemia and DLBCL has not been reported, especially on the genetic aspect. Therefore, we aim to investigate dyslipidemia in DLBCL in the context of molecular typing and explore the correlation between dyslipidemia and gene mutations.

In this retrospective study, we analyzed 259 DLBCL patients with gene sequencing to assess dyslipidemia in newly diagnosed DLBCL.

Methods

Patients and sample collection

A total of 259 newly diagnosed DLBCL patients were selected with indispensable pathological issues to analyze molecular typing. All patients were admitted to the clinic center affiliated with the First Affiliated Hospital of Zhejiang University School of Medicine from April 2014 to November 2022. A total of 121 genes covering exons, fusion-relevant introns and alternative splicing areas are analyzed. Six typing methods were applied in this study, which contain MCD, BN2, EZB, N1, ST2, and A53. In terms of dyslipidemia, we collected lipid indices, including triglycerides (TG), total cholesterol (TC), high-density lipoprotein cholesterol (HDL-C), and low-density lipoprotein cholesterol (LDL-C). Lipid profiles were stratified according to *The Guidelines on Prevention and Treatment of Blood Lipid Abnormality in Chinese Adults (Version 2016)* (13). Dyslipidemia is defined as a disease with an abnormality in lipids, usually with increased levels of TC and TG. Dyslipidemia is classified into different subtypes in clinical aspects, pathogenesis, and physical-chemistry aspects. According to the WHO criteria developed by Fredrickson, which discriminate by physical and chemical features. Dyslipidemia is categorized into six types (14). Due to the complexity of this classification, another standard is rather easier. Dyslipidemia is defined into four types: hypertriglyceridemia, hypercholesterolemia, hypoalbuminemia, and mixed hyperlipidemia (both hypertriglyceridemia and hypercholesterolemia). This method is now used more frequently in clinics, and in our study, this method was applied (15, 16).

All patients were initially treated with the first-line therapy recommended by the National Comprehensive Cancer Network (NCCN) (17). Patients with CD20 positivity were primely treated with rituximab in combination with cyclophosphamide, doxorubicin, vincristine, and prednisone (R-CHOP) or R-CHOP-like regimens. Older patients were medicated with a dose-decreased R-CHOP regimen. The R-DA-EPOCH regimen was administered to patients with poor left ventricular functions.

Diagnosis and prognosis indicators related to DLBCL were collected and concluded as follows: B symptoms, Ann Arbor stage, international prognosis index (IPI), Eastern Cooperative Oncology Group stage (ECOG stage), and results of immunohistochemistry (IHC). We also collected demographic and other clinical data from medical records that concluded: age, sex, height, weight, body mass index (BMI), white blood count (WBC), hemoglobin count, platelet counts, albumin, alanine transaminase (ALT), serum creatinine, lactate dehydrogenase (LDH), ferritin, C-reactive protein (CRP), β microglobulin (β-MG), fibrinogen, prothrombin time (PT), activated prothrombin time (APTT), thrombin time (TT), International normalized ratio (INR), D-dimer, and cytokines including interleukin-2 (IL-2), interleukin-4 (IL-4), interleukin-6 (IL-6), interleukin-10 (IL-10), interleukin-17α (IL-17α), tumor necrosis factor-α (TNF-α), and interferon-γ (IFN-γ). We collected a total of 22,375 samples.

The study was approved by the institutional Ethics Committee and conducted in accordance with the Declaration of Helsinki.

Classification of abnormality

According to the Guidelines on Prevention and Treatment of Blood Lipid Abnormality in Chinese Adults (Version 2016), we define dyslipidemia as hypertriglyceridemia, hypercholesterolemia, hypoalbuminemia, and mixed hyperlipidemia, which meets both hypertriglyceridemia and hypercholesterolemia.

The upper limits of normal TG, TC, and LDL were 1.70 mmol/L (150 mg/dl), 5.86 mmol/L (226.6 mg/dl), and 3.29 mmol/L (127.2 mg/dl), respectively. The lower limit of normal HDL was 0.78 mmol/L (30.2 mg/dl).

Definition of molecular subtypes

Biopsy samples and tissue sections from pathological entities, such as swollen lymph nodes and gastrointestinal tissues, were saved for analysis at the institute. The testing platform was the

Hiseq 4000 NGS platform (Illumina system), and the testing method was high-throughput sequencing, also called next-generation sequencing (NGS), contrary to the reference genome of GRCh37/hg19. This analysis covered 121 genes including exonic areas, intronic areas related to fusion mutations, and alternative splicing sites (3, 4). All these 121 genes are recorded in Figure 1 and Table S1. There were 2,876 cases of gene abnormalities occurring in 259 patients, including fusion mutations, copy number variation, gene amplification, missense variation, nonsense variation, frameshift insertion/deletion, and non-frameshift insertion/deletion. Besides, 2,790 protein-alternative mutations were found based on the analysis. The LymphGen algorithm was applied in the analysis for DLBCL subtype prediction with probability. The probability was analyzed in the Naïve Bayes algorithm [4]. All information was collected from the clinical center. All these gene abnormalities are listed in Table S2.

Statistical analysis

Data are presented as medians, absolute ranges, or frequencies. The Kruskal–Wallis H test was used to compare the distribution of numerical variables. The χ^2 test was used for qualitative variables. The relationships between clinical factors and dyslipidemia were assessed using univariable and multivariable logistic regression models. All multivariable analyses were adjusted for sex and age. The Kaplan–Meier method was used to estimate univariate survival curves, and the differences between curves were calculated via the log-rank test. Multivariable Cox proportional hazard regression models were used to assess the prognostic impact of hypertriglyceridemia with regard to overall survival (OS) and progress-free survival (PFS). Statistical analyses were performed using SPSS software (version 23.0) and GraphPad Prism (version 9.5). P-values below 0.05 were considered statistically significant.

A total of 121 genes being analyzed in DLBCL patients				
ALK	CDKN2B	GNA13	MYC	SGK1
AKT1	CDKN2C	HRAS	MYD88	SF3B1
AKT2	CD274	ID3	NF1	SOCS1
APC	CD70	IKZF1	NFKBIA	SPEN
ARID1A	CD79A	INPP5D	NFKB1	SMARCA4
ARID1B	CD79B	IRF4	NFKB2	STAT3
ARID2	CD83	JAK1	NFKBIE	STAT6
ATM	CD58	JAK2	NOTCH1	SYK
ATR	CIITA	JAK3	NOTCH2	TBL1XR1
B2M	CREBBP	KDM6A	NRAS	TCF3
BCL10	CTLA4	KDR	PAX5	TET2
BCL2	CTNNB1	KIT	PDCD1LG2	TNFAIP3
BCL6	CXCR4	KLHL6	PIK3R1	TNFRSF14
BCOR	CYLD	KMT2A	PIK3CA	TP53
BCORL1	DDX3X	KMT2C	PIK3CD	TP63
BIRC3	DNMT3A	KMT2D	PIM1	TP73
BTK	DTX1	KRAS	PLCG2	TRAF2
BRAF	EP300	LYN	POT1	TRAF3
CALR	ERBB4	MALT1	PRDM1	TRAF5
CARD11	EZH2	MAP2K1	PTEN	WHSC1
CCND1	FAS	MAP3K14	PTPN6	XPO1
CCND2	FAT1	MDM2	PTPRD	
CCND3	FBXO11	MED12	RB1	
CDKN1B	FBXW7	MEF2B	ROS1	
CDKN2A	FOXO1	MTOR	SETD2	

Prognosis-relevant gene
Diagnosis-relevant gene
Targeting medical gene
Both diagnosis-relavant and targeting medical gene
Both diagnosis and prognosis related gene

FIGURE 1
A total of 121 genes analyzed in DLBCL patients. Different colors represent different types, containing prognosis-relevant, diagnosis-relevant, and targeting medical-relevant genes.

Results

Patient characteristics

A total of 259 newly diagnosed DLBCL patients are categorized into six genetic subtypes, and the proportion of each type is 21.6% MCD subtype, 19.3% BN2 subtype, 8.9% EZB subtype, 3.5% N1 subtype, 4.2% ST2 subtype, and 12.4% A53 subtype, respectively (Figure 2). Besides, 30.1% of patients are unclassified, and this isoform is defined as a black control. To investigate the concrete genes influencing the lipids, we considered 60 familiar decisive molecular typing genes such as *BCL2*, *BCL6*, *TP53*, *MYD88*, *MYC*, *NOTCH2*, and *EZH2*. More details regarding genetic typing and gene translocation are shown in Figure 3.

We recorded and analyzed the initial concentration of lipids before DLBCL patients received any treatment. Results show that TG in the EZB subtype was higher than in the unclassified subtype (Kruskal–Wallis H test, p = 0.001). The median concentration of TG in these two groups is 2.01 mmol/L (range 1.76–2.48 mmol/L) and 1.16 mmol/L (range 0.84–1.58 mmol/L), respectively. More importantly, results show that in the EZB subtype, the incidence of hypertriglyceridemia is 78.3% compared with 19.2% in the unclassified subtype, 36.0% in the MCD subtype, and 18.2% in the ST2 subtype (chi-square test and Fisher's exact test, p <0.001, = 0.001, <0.001). In addition, dyslipidemia is discovered more commonly in the EZB subtype than in the unclassified subtype, with a significant statistical difference (87% vs 39.7%, p <0.001). The other three types of lipids (TC, HDL-C, and LDL-C), meanwhile, demonstrated no significant differences among the seven types.

According to the World Health Organization (WHO) classification of lymphoma, researchers put forward the concept of high-grade B-cell lymphoma based on three types of gene translocation: *BCL2*, *BCL6*, and *MYC*. Thus, we also analyzed the correlation between dyslipidemia and gene translocation. Based on pathological gene-sequencing, patients with *BCL2* gene fusion mutation are significantly more likely to have dyslipidemia (chi-square test, 76.5%, p = 0.006) and hypertriglyceridemia (chi-square test, 88.2%, p = 0.002) than patients without rearrangement of these three genes.

Other demography and clinical characteristics are demonstrated in Table 1.

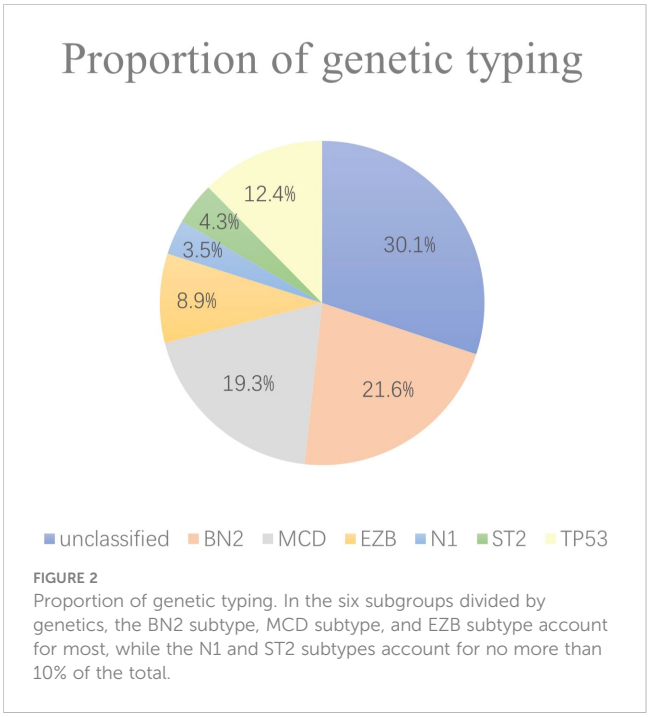

FIGURE 2
Proportion of genetic typing. In the six subgroups divided by genetics, the BN2 subtype, MCD subtype, and EZB subtype account for most, while the N1 and ST2 subtypes account for no more than 10% of the total.

Other clinical factors about dyslipidemia

Binary logistic regression is used to analyze other clinical elements related to hypertriglyceridemia and dyslipidemia. In univariable analysis, molecular typing, *BCL2* fusion translation, ferritin, and BMI were risk factors for hypertriglyceridemia (p <0.05). In terms of dyslipidemia, B symptoms, molecular typing, *BCL2* fusion translation, ferritin, CRP, and IL-6 have influenced dyslipidemia (p <0.05).

In multivariable analysis, results indicate that being one of the EZB subtypes (p = 0.002, OR 34.524, 95% CI 3.700–322.120) is correlative to hypertriglyceridemia. Besides, the level of BMI affects triglycerides (p = 0.002, OR 1.183, 95% CI 1.064–1.315). As for dyslipidemia, the EZB subtype is significantly associated with dyslipidemia (p = 0.020, OR 14.931, 95% CI 1.532–145.477). The influence of ferritin level is familiar (p = 0.026, OR 1.001, 95% CI 1.000–1.001). The detailed results of the logistic regression model are shown in Table 2.

Relation between dyslipidemia and survival

The median follow-up time is 12.3 months (range 1.1–105.0 months) among the 235 surviving patients. A total of 21 patients died, three of whom died of complications, and 18 patients died of disease progression. Significantly, only two patients died during induction treatment. Moreover, up to the cut-off time, disease progress occurred in 57 patients, and in 35 patients, disease progress occurred at the first assessment during therapy. Three patients were lost to follow-up. The 2-year OS and 2-year PFS rates were 81.7% and 61.3%, respectively. We interpret the influence of lipids on survival. Neither hypertriglyceridemia nor dyslipidemia significantly affected OS and PFS in DLBCL patients (hypertriglyceridemia: OS hazard ratio HR 0.855, 95% CI 0.353–2.075, p = 0.7336; PFS HR 0.824, 95% CI 0.482–1.407, p = 0.4730. dyslipidemia: OS hazard ratio HR 0.637, 95% CI 0.270–1.504, p = 0.3012; PFS HR 0.692, 95% CI 0.408-1.176, p = 0.1490, Figure 4). OS and PFS in different genetic subtypes showed no significant statistical divergence (Figure 5). Interestingly, OS in the A53 subgroup showed differences. The 32 patients who are defined as the A53 subgroup were divided into the HTG group and the non-HTG group by the level of triglycerides, and they also divided into the dyslipidemia group and the non-dyslipidemia group. Although the small number of samples precludes achieving a significant difference

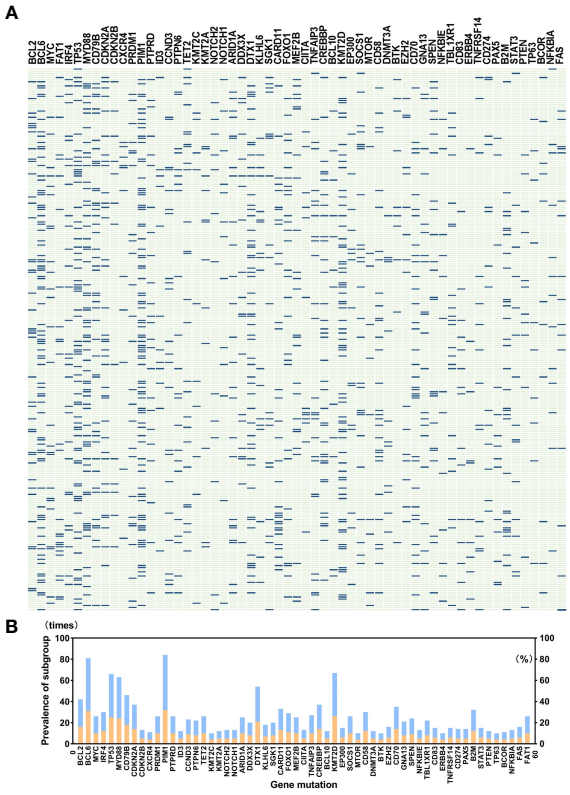

FIGURE 3
(A) shows gene mutations in detail in a total of 259 patients, and **(B)** indicates the prevalence of gene mutations. A total of 121 genes covering exon, fusion-relevant intron, and alternative splicing are analyzed, and we selected 60 types of gene mutations that occurred rather frequently or were molecular typing-related, like *BCL2*, *BCL6*, *MYC*, *MYD88*, *CD79B*, *PIM1*, *KMT2D*, *DTX1*, *TET2*, and *SGK1*. Panel **(B)** illustrates the prevalence of gene mutations; the blue band in the histogram represents mutation times, and the orange band shows percentage. Abnormalities of *BCL6*, *TP53*, *PIM1*, *MYD88*, and *KMT2D* occurred in more than 20% of patients, and *PIM1* mutations appeared most common.

in PFS, the OS showed significant results. The non-HTG group revealed better survival than the HTG group, while the non-dyslipidemia group showed worse survival than the dyslipidemia group (Figure 6). Relative parameters that significantly influenced survival were not discovered in either univariable or multivariable Cox regression models (Table S3).

Discussion

In our study, hypertriglyceridemia and dyslipidemia are associated with the molecular typing of DLBCL, and the most relevant is the EZB subtype. The other clinical factors also connect with dyslipidemia, including B symptoms, *BCL2* fusion translation, ferritin, and BMI. We demonstrated the correlation of dyslipidemia with the genetic type of DLBCL at the genetic level. While the incidence of hypertriglyceridemia and dyslipidemia has not influenced OS and PFS. Research shows that prostate cancer patients with high levels of triglycerides have a higher risk of relapse. But in some malignancies, dyslipidemia is not associated with a poor prognosis, such as gastric cancer and breast cancer (18–20). We conjectured that patients who have dyslipidemia were provided therapy to lower lipids, and dyslipidemia is not an independent prognosis factor. Besides, Schmitz et al. reported different OS in MCD, BN2, EZB, and N1 subtypes (3). In our study, OS and PFS did not show statistical differences. We inferred that it might be related to the small size of the patients and not enough follow-up time.

Dyslipidemia is characterized by abnormal serum triglycerides, cholesterol, low-density lipoprotein, and high-density lipoprotein. The Frederickson model was raised to systematically categorize dyslipidemia into five phenotypes. Type 2 is characterized by elevated levels of LDL, and the rest of the types are characterized by increased levels of various triglyceride-rich lipoprotein subfractions (16). A more practical model of dyslipidemia defines

TABLE 1 Characteristics of democracy and clinical factors in different types of DLBCL.

	Genetic typing							
	MCD n=50	BN2 n=56	EZB n=23	N1 n=9	ST2 n=11	A53 n=32	Unclassified n=78	P value
Age (years), range	66 (47-90)	62 (23-87)	60 (39-81)	70 (60-79)	69 (31-87)	64 (18-90)	58 (19-87)	0.001*[b]
Gender								0.747[a]
Male	30 (20.7)	29 (20.0)	15 (10.3)	5 (3.4)	8 (5.5)	18 (12.4)	40 (27.6)	
Female	20 (17.5)	27 (23.7)	8 (7.0)	4 (3.5)	3 (2.6)	14 (12.3)	38 (33.3)	
Height (cm), range	165 (149-180)	165 (147-184)	167 (151-182)	158 (145-170)	165.5 (156-177)	164.5 (155-180)	166 (150-186)	0.482[b]
Weight (Kg), range	60 (44-87)	61 (40-86)	65 (46-84)	55 (46-70)	58.75 (50-84)	61 (47-83)	61 (42-99)	0.530[b]
BMI (Kg/m^2), range	22.0 (17.0-22.4)	23.5 (14.7-29.4)	23.7 (16.5-29.0)	22.9 (17.1-25.1)	22.0 (18.7-26.8)	22.0 (18.4-29.3)	22.4 (16.2-33.9)	0.860[b]

(Continued)

TABLE 1 Continued

	Genetic typing							
	MCD n=50	BN2 n=56	EZB n=23	N1 n=9	ST2 n=11	A53 n=32	Unclassified n=78	P value
B symptoms, No. (%)	14 (20.0)	16 (22.9)	8 (11.4)	4 (5.7)	3 (4.3)	11 (15.7)	14 (20.0)	0.390[a]
Hans typing, No. (%)								0.001*[a]
Non-GCB	38 (22.2)	43 (25.1)	5 (2.9)	6 (3.5)	6 (3.5)	24 (14.0)	49 (28.7)	
GCB	11 (13.4)	12 (14.6)	18 (22.0)	2 (2.4)	5 (6.1)	1 (16.7)	2 (33.3)	
Unclassified	1 (16.7)	1 (16.7)	0 (0.0)	1 (16.7)	0 (0.0)	1 (16.7)	2 (33.3)	
BM involvement, No. (%)	14 (28.0)	9 (18.0)	3 (6.0)	3 (6.0)	5 (10.0)	5 (10.0)	11 (22.0)	0.119[a]
Ann Arbor stage, No. (%)								0.277[a]
I-II	10 (17.5)	14 (24.6)	4 (7.0)	0 (0.0)	0 (0.0)	9 (15.8)	20 (35.1)	
III-IV	40 (20.0)	41 (20.5)	18 (9.0)	9 (3.5)	11 (4.3)	32 (12.5)	58 (29.0)	
IPI score, No. (%)								0.175[a]
0-1	8 (14.5)	11 (20.0)	5 (9.1)	0 (0.0)	2 (3.6)	7 (12.7)	22 (40.0)	
2-3	18 (14.9)	30 (24.8)	11 (9.1)	3 (2.5)	6 (5.0)	16 (13.2)	37 (30.6)	
4-5	20 (27.4)	14 (19.2)	7 (9.6)	3 (2.5)	6 (8.2)	16 (13.2)	15 (20.5)	
WBC (10×10^9/L), range	5.2 (0.9-11.9)	6.7 (2.2-17.4)	7.0 (1.5-17.3)	3.7 (2.2-14.6)	7.1 (4.2-12.0)	6.6 (2.7-19.2)	5.6 (2.1-30.9)	0.093[b]
Hb (g/L), range	123.5 (46-160)	129 (69-162)	123 (93-174)	123 (57-148)	123 (51-153)	110 (57-156)	128 (54-166)	0.265[b]
PLT (10×10^9/L), range	171 (29-367)	202.5 (40-404)	229 (59-428)	155 (52-264)	218 (93-541)	227 (20-486)	225 (41-434)	0.163[b]
Ab (g/L), range	39.5 (23-51)	42.1 (24-50)	40.8 (32-48)	41.1 (30-47)	41.3 (29-47)	40.1 (27-53)	41.9 (23-52)	0.292[b]
ALT (U/L), range	17.5 (6-53)	17.5 (6-56)	12 (7-59)	23 (11-65)	15 (7-37)	17 (4-157)	17 (5-60)	0.616[b]
Scr (μmol/L), range	69 (34-168)	75 (32-152)	75 (49-285)	64 (36-133)	77 (55-110)	74 (37-266)	69 (42-193)	0.296[b]
LDH (IU/L), range	291 (94-2752)	329 (139-2259)	352 (131-772)	556 (215-1429)	248 (149-630)	280 (145-10540)	224 (118-2220)	0.034*[b]
Ferritin (ng/mL), range	462.6 (35-5102)	429.4 (24-40000)	355.8 (34-1224)	699.9 (80-12555)	333.9 (12-4533)	288.8 (5-3177)	182.6 (4-1616)	<0.001*[b]
CRP (mg/L), range	10.0 (0-167)	12.7 (0-160)	19.4 (0-120)	27.3 (2-167)	41.3 (2-230)	19.5 (1-118)	5.9 (0-80)	0.082[b]
β2-MG	2665 (0-7460)	2795 (1160-10980)	2470 (1150-16790)	4190 (1990-6500)	3550 (1450-12330)	2470 (1329-14400)	2070 (230-7700)	0.008*[b]
IL-6 (kU/L), range	14.1 (1.5-716.6)	9.0 (1.5-416.3)	10.5 (0.7-174.6)	10.3 (0.1-136.9)	26.4 (4.0-1436.1)	10.1 (2.9-378.6)	6.0 (0.4-424.3)	0.027*[b]
IL-10 (kU/L), range	10.0 (0.7-1046.7)	3.9 (0.7-2226.2)	4.6 (0.1-54.8)	39.9 (1.8-6007.0)	5.9(0.1-49.2)	4.6(0.1-512.6)	3.5 (0.1-475.9)	<0.001*[b]
TG (mmol/L), range	1.3 (0.6-6.2)	1.5 (0.5-3.7)	2.0 (0.5-5.3)	1.2 (0.5-2.6)	1.3 (0.7-2.7)	1.5 (0.6-22.0)	1.1 (0.4-5.4)	0.003*[b]
TC (mmol/L), range	3.6 (2.2-7.4)	4.1 (1.6-5.7)	4.3 (2.3-6.9)	4.9 (2.5-5.6)	4.2 (2.5-6.2)	4.1 (2.3-6.3)	4.1 (2.1-8.1)	0.177[b]

(Continued)

TABLE 1 Continued

	Genetic typing							
	MCD n=50	BN2 n=56	EZB n=23	N1 n=9	ST2 n=11	A53 n=32	Unclassified n=78	P value
HDL (mmol/L), range	0.9 (0.2-2.7)	1.1 (0.2-1.6)	0.9 (0.6-1.8)	1.1 (0.3-2.2)	0.9 (0.6-1.4)	0.9 (0.2-2.0)	1.0 (0.2-2.0)	0.092 [b]
LDL (mmol/L), range	2.1 (1.0-4.6)	2.2 (0.1-3.7)	2.3 (0.6-4.3)	2.7 (1.7-3.9)	2.2 (1.0-4.4)	2.3 (0.9-3.5)	2.4 (0.3-5.7)	0.285 [b]

BMI, Body Mass Index; Non-GCB, non-Germinal Center B-cell; GCB, Germinal Center B-cell; BM, bone marrow; IPI, International Prognostic Index; WBC, white blood cell; Hb, hemoglobin; PLT, platelet; Ab, albumin; ALT, alanine aminotransferase; Scr, serum creatinine; LDH, lactate dehydrogenase; CRP, C-reaction protein; β2-MG, β2-microglobulin; IL-6, Interleukin-6; IL-10, Interleukin-10; TG, triglyceride; TC, total cholesterol; HDL, high-density lipoprotein; LDL, low-density lipoprotein.
*Significantly different.
Continuous variables are presented as median with range and categorical variables are shown as frequency and percentage (No, %).
[a]Fisher's exact test. [b]Kruskal-Wallis test.

TABLE 2 Logistic regression models evaluating the associations between clinical variables and hypertriglyceridemia and dyslipidemia in DLBCL patients.

Dependent variable	Independent variable	Univariable analysis		Multivariable analysis	
		OR (95% CI)	P-value	OR (95% CI)	P-value
	Age	1.377 (0.816–2.321)	0.231	1.384 (0.715–2.677)	0.335
	Sex	0.989 (0.971–1.006)	0.199	0.879 (0.955–1.001)	0.062
	B symptoms	1.738 (0.989–3.053)	0.054	1.291 (0.627–2.661)	0.488
HTG	MCD subtype	3.150 (1.454–6.822)	0.004*	3.751 (0.721–19.507)	0.116
	BN2 subtype	2.362 (1.055–5.292)	0.037*	2.386 (0.907–6.272)	0.078
	EZB subtype	15.120 (4.387–47.260)	<0.001*	34.524 (3.700–322.120)	0.002*
	A53 subtype	2.520 (1.014–6.265)	0.047*	2.741 (0.977–7.692)	0.055
	BCL2 fusion mutation	4.104 (1.309-12.866)	0.015*	0.403 (0.034–4.814)	0.473
	ferritin	1.000 (1.000–1.001)	0.009*	1.000 (1.000–1.001)	0.167
	IL-10	1.001 (1.000–1.002)	0.096	1.001 (1.000–1.003)	0.135
	BMI	1.156 (1.058–1.265)	0.001*	1.183 (1.064–1.315)	0.002*
	Age	1.442 (0.877–2.371)	0.149	1.485 (0.805–2.739)	0.206
	Sex	0.990 (0.973–1.007)	0.238	0.976 (0.955–0.998)	0.035*
Dyslipidemia	B symptoms	2.178 (1.226–3.871)	0.008*	1.579 (0.764–3.264)	0.218
	MCD subtype	1.880 (0.938–3.768)	0.075	2.041 (0.405–10.287)	0.387
	BN2 subtype	1.642 (0.802–3.363)	0.175	1.261 (0.524–3.031)	0.605
	EZB subtype	10.108 (2.767–36.919)	<0.001*	14.931 (1.532–145.477)	0.020*
	A53 subtype	2.216 (0.958–5.126)	0.063	1.937 (0.732–5.123)	0.183
	BCL2 fusion mutation	7.232 (1.603–32.628)	0.010*	0.559 (0.041–7.714)	0.664
	ferritin	1.001 (1.000–1.002)	0.001*	1.001 (1.000–1.001)	0.026*
	IL-6	1.006 (1.000–1.009)	0.048*	1.002 (0.998–1.005)	0.306
	CRP	1.013 (1.011–1.019)	0.013*	1.000 (0.991–1.010)	0.979
	BMI	1.079 (0.992–1.172)	0.075	1.080 (0.975–1.195)	0.140

OR, odd ratio; CI, confidence interval; HTG, hypertriglyceridemia; IL-10, interleukin-10; BMI, Body Mass Index; IL-6, Interleukin-6; CRP, C-reactive protein.
*Significantly different.

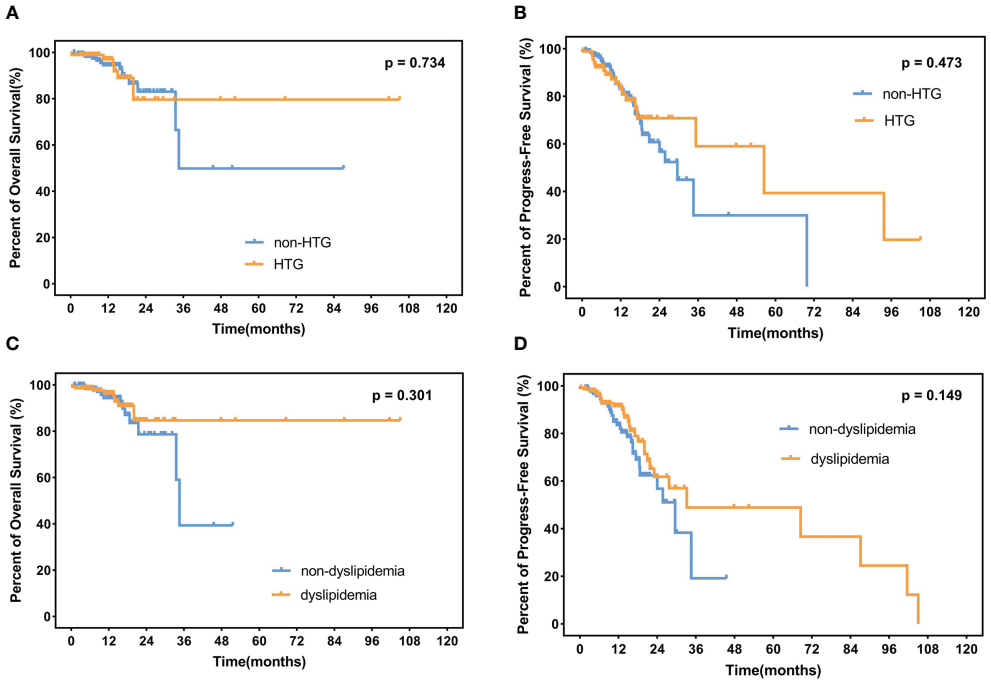

FIGURE 4
OS and PFS in patients. **(A)** Percent of OS and **(B)** progress-free survival in patients with or without HTG. **(C)** Percent of overall survival and **(D)** progress-free survival in dyslipidemia patients and non-dyslipidemia patients. OS, overall survival; PFS, progress-free survival; HTG, hypertriglyceridemia.

it as hypertriglyceridemia, hypercholesterolemia, hypo-HDL, and hyper-LDL. The recommended levels of TG, LDL, and HDL are 2–9.9 mmol/L, 3.4–4.9 mmol/L, and 0.7–0.9 mmol/L (15). Exorbitant levels of lipids express an increased risk of pancreatitis (21). In our retrospective study, two patients had high levels of triglycerides (28.02 and 22.00 mmol/L, respectively). While there were no episodes of acute pancreatitis. Elevated plasma LDL-cholesterol levels are the 8th leading risk factor for death in 2019 worldwide (22). A large study conducted in China indicated that the most common dyslipidemia subtypes are hypo-HDL (20.4%) and HTG (13.8%) (23). The mechanism related to primary dyslipidemia has not been proved definitively. According to genome-wide association studies (GWASes), *TMEM57*, *DOCK7*, *CELSR2*, *APOB*, *ABCG5*, *HMGCR*, *TRIB1*, *FADS2/S3*, *LDLR*, *NCAN*, and *TOMM40-APOE* appear to be related to increased TC levels. Similarly, *CELSR2-PSRC1-SORT1*, *PCSK9*, *NCAN-CILP2-PBX4*, *LDLR*, and *APOC1-APOE* are associated with variations in LDL levels (24). *D9N* and *N291S* variants have been associated with elevated TG, while the *S447X* variant appears to be related to depressed TG. Moreover, *APOA5*-related abnormalities appear to be potentially correlative to TG (25, 26). Besides, pre-B-cell leukemia transcription factor 4 (*PBX4/CILP2* locus) and B-cell CLL/lymphoma 3 genes are considered to be the association factors for dyslipidemia (27, 28). Secondary hyperlipidemia has been acknowledged as being

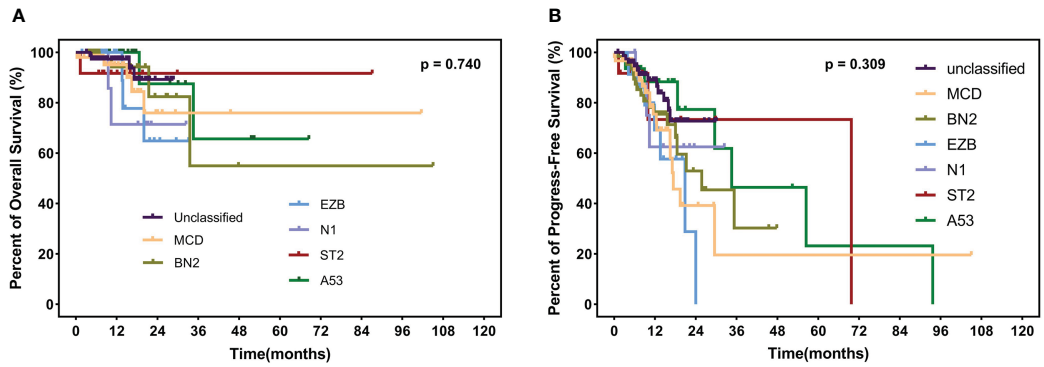

FIGURE 5
OS **(A)** and PFS **(B)** in different subtypes, including MCD, BN2, EZB, N1, ST2, A53, and unclassified subtypes. OS, overall survival; PFS, progress-free survival.

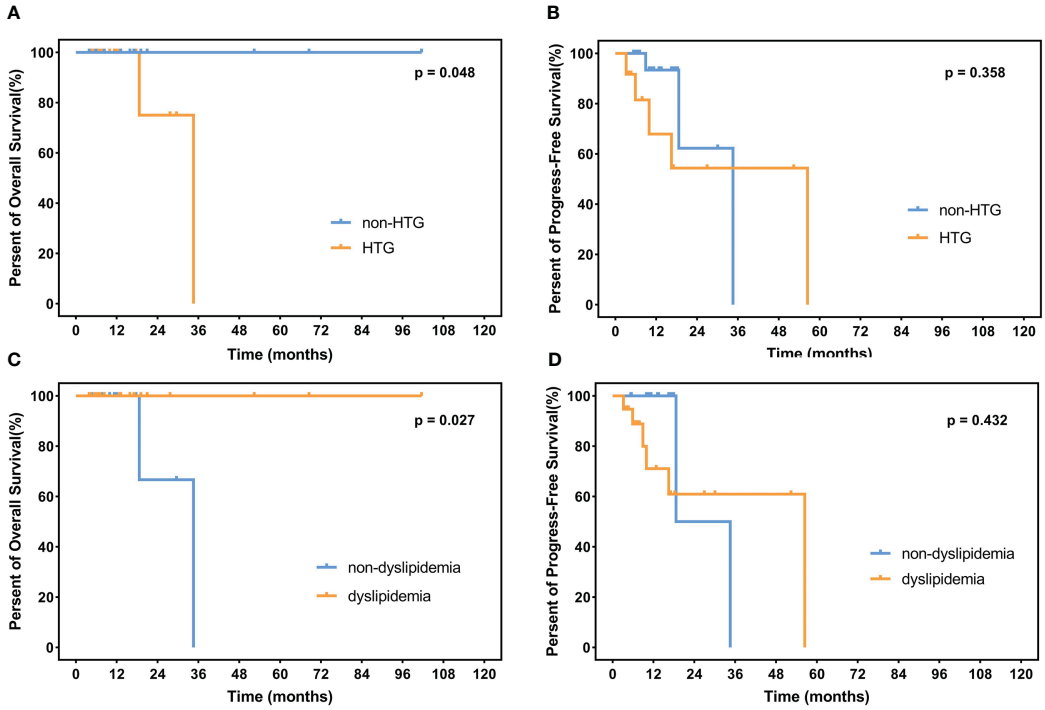

FIGURE 6
OS and PFS in the A53 subgroup. **(A)** illustrates OS in the HTG group and the non-HTG group with significant statistical differences. **(B)** shows PFS in these two groups without a significant statistical difference. **(C, D)** indicate OS and PFS in the dyslipidemia group and the non-dyslipidemia group, with a significant statistical difference only in OS. OS, overall survival; PFS, progress-free survival. HTG, hypertriglyceridemia.

associated with obesity, smoking, the metabolic syndrome, proinflammatory and prothrombotic biomarkers, and type 2 diabetes (29). Recently, the interaction between dyslipidemia-related genes and hematologic malignancy genes has been reported; for instance, the *PML/RARα* fusion protein and peroxisome proliferator-activated receptor-α have a synergistic effect on acute promyelocytic leukemia (30). Besides, the incidence of cardiovascular disease was higher in patients with DLBCL than in normal people (31).

Dyslipidemia has been reported to be associated with a multitude of solid tumors, such as breast cancer, prostate cancer, thyroid cancer, colorectal cancer, and lung cancer (5–9). In terms of hematologic malignancies, chronic lymphocyte leukemia and acute promyelocytic leukemia are reported to be associated with dyslipidemia and hypertriglyceridemia (11, 32). Whereas, the correlation between dyslipidemia and lymphoma or multiple myeloma has not been reported. More recently, studies aimed at lipids in DLBCL patients appeared to indicate a prognosis (33–35). Fundamental experiments investigated cholesterol and DLBCL. *SYK* inhibits cholesterol biosynthesis by modulating *PI3K/AKT*-dependent survival pathways (36). *SOX9–DHCR24*–cholesterol biosynthesis axis in *IGH-BCL2* fusion translation positive DLBCL plays an oncogenic role *via* upregulating cholesterol synthesis (12, 37). Based on molecular typing, the EZB subtype is characterized by *IGH-BCL2* fusion translation and the EZH2 mutation. Jiao et al. proposed the *SOX9–DHCR24*–cholesterol biosynthesis axis, which may interpret the association between the EZB subtype and dyslipidemia to some extent. *SOX9* was researched more frequently in other solid tumors like colon cancer, hepatocellular carcinoma, and breast cancer. *SOX9* plays an oncogenic role in GCB and *IGH-BCL2*-positive DLBCL. In other words, *SOX9*-positive DLBCLs are more likely to be categorized as EZB subtypes and are more likely to be associated with *NF-κB* signaling. SOX9 upregulates *DHCR24* expression, which is important in the cholesterol biosynthesis pathway (38–40). Other studies indicate that *BCL2* may influence lipid metabolism. Downregulation of *BCL2*-related transcription factors has been considered to affect carotid atherosclerosis and be associated with oxidized LDL trans-differentiation. Thus, we speculate that *BCL2* fusion influences lipid metabolism (41).

The concept of genetic typing was raised to provide potential nosology for precision medicine strategies in DLBCL. According to the research containing 574 DLBCL biopsy samples identified genes, the BN2 subtype is dominated by *NOTCH* pathway aberrations and the *NF-κB* pathway. Besides, the MCD subtype is characterized by *BCR* and *NF-κB* pathway aberrations. EZB subtype is enriched for *BCL2* translocation, *EZH2* mutation, and *REL* amplification, involving Janus-associated kinase–signal transducers and activators of transcription (*JAK-STAT*) signaling and the *PI3K* pathway. *BCR* has been shown to directly promote cholesterol biosynthesis through intermediate kinases downstream of *BCR* to maintain cell membrane integrity and *BCR* signaling (3, 42–46). Aimed at this, targeting cellular cholesterol provides new precise treatment strategies. Thaxton et al. investigated functional lipoprotein nanoparticles in DLBCL via targeting both cellular cholesterol uptake and *BCR*-associated

de novo cholesterol synthesis and achieved cellular cholesterol reduction and induced apoptosis in otherwise resistant ABC DLBCL cell lines (47).

We analyzed 259 DLBCL patients in the lipid aspect based on genetic typing and deduced the association between dyslipidemia and the EZB subtype without prognosis discrepancy. This study has some deficiencies. Firstly, it is a retrospective study with limitations in patient selection and analysis. Secondly, follow-up times are not long enough because there have been 121 types of gene sequencing analyses conducted in the clinical institution in recent years. Thirdly, the role of dynamic alterations in blood biomarkers during and after treatment was not taken into consideration during the analysis. Further prospective and multicenter research is needed to investigate dyslipidemia in DLBCL to instruct prognosis evaluation and treatment.

Conclusion

A total of 259 newly diagnosed DLBCL patients were categorized by genetic typing and analyzed for dyslipidemia. Significant differences were found in the EZB subtype; dyslipidemia and hypertriglyceridemia occurred in this isoform without influence on survival. In summary, the EZB subtype is exposed to higher risks of dyslipidemia and hypertriglyceridemia, which may guide clinical treatment strategies.

Data availability statement

The original contributions presented in the study are included in the article/Supplementary Material. Further inquiries can be directed to the corresponding author.

Ethics statement

The studies involving human participants were reviewed and approved by the Research Ethics Committee of the first affiliated Hospital, College of Medicine, Zhejiang University. Written informed consent was not required to participate in this study in accordance with the national legislation and the institutional requirements

Author contributions

WX contributed to the conception and design of the article. YX, HS, YS, and YZ wrote the manuscript. XZ, JS, XL, DZ, CY, JHW, XH, JYW, JH, HM, WY, HT, and JJ revised the manuscript. All authors contributed to the article and approved the submitted version.

Funding

This work was partially supported by grants from the National Program on Key Research Project of China (2022YFC2502700).

Acknowledgments

We thank all people involved in this study at nine medical centers.

Conflict of interest

The authors declare that the research was conducted in the absence of any commercial or financial relationships that could be construed as a potential conflict of interest.

Publisher's note

Supplementary material

The Supplementary Material for this article can be found online at: https://www.frontiersin.org/articles/10.3389/fonc.2023.1172623/full#supplementary-material

References

1. Rodriguez-Abreu D, Bordoni A, Zucca E. Epidemiology of hematological malignancies. *Ann Oncol* (2007) 18 Suppl 1:i3–8. doi: 10.1093/annonc/mdl443

2. Chapuy B, Stewart C, Dunford AJ, Kim J, Kamburov A, Redd RA, et al. Molecular subtypes of diffuse large b cell lymphoma are associated with distinct pathogenic mechanisms and outcomes. *Nat Med* (2018) 24(5):679–90. doi: 10.1038/s41591-018-0016-8

3. Schmitz R, Wright GW, Huang DW, Johnson CA, Phelan JD, Wang JQ, et al. Genetics and pathogenesis of diffuse Large b-cell lymphoma. *N Engl J Med* (2018) 378 (15):1396–407. doi: 10.1056/NEJMoa1801445

4. Wright GW, Huang DW, Phelan JD, Coulibaly ZA, Roulland S, Young RM, et al. A probabilistic classification tool for genetic subtypes of diffuse Large b cell lymphoma with therapeutic implications. *Cancer Cell* (2020) 37(4):551–68.e14. doi: 10.1016/j.ccell.2020.03.015

5. Yao X, Tian Z. Dyslipidemia and colorectal cancer risk: a meta-analysis of prospective studies. *Cancer Causes Control* (2015) 26(2):257–68. doi: 10.1007/s10552-014-0507-y

6. Hao B, Yu M, Sang C, Bi B, Chen J. Dyslipidemia and non-small cell lung cancer risk in Chinese population: a case-control study. *Lipids Health Dis* (2018) 17(1):278. doi: 10.1186/s12944-018-0925-z

7. Song Y, Lee HS, Park G, Kang SW, Lee JW. Dyslipidemia risk in thyroid cancer patients: a nationwide population-based cohort study. *Front Endocrinol (Lausanne)* (2022) 13:893461. doi: 10.3389/fendo.2022.893461

8. Rice KR, Koch MO, Cheng L, Masterson TA. Dyslipidemia, statins and prostate cancer. *Expert Rev Anticancer Ther* (2012) 12(7):981–90. doi: 10.1586/era.12.75

9. Schairer C, Freedman DM, Gadalla SM, Pfeiffer RM. Lipid-lowering drugs, dyslipidemia, and breast cancer risk in a Medicare population. *Breast Cancer Res Treat* (2018) 169(3):607–14. doi: 10.1007/s10549-018-4680-7

10. Li K, Wang F, Yang ZN, Cui B, Li PP, Li ZY, et al. PML-RARalpha interaction with TRIB3 impedes PPARgamma/RXR function and triggers dyslipidemia in acute promyelocytic leukemia. *Theranostics* (2020) 10(22):10326–40. doi: 10.7150/thno.45924

11. Mozessohn L, Earle C, Spaner D, Cheng SY, Kumar M, Buckstein R. The association of dyslipidemia with chronic lymphocytic leukemia: a population-based study. *J Natl Cancer Inst* (2017) 109(3). doi: 10.1093/jnci/djw226

12. Shen Y, Zhou J, Nie K, Cheng S, Chen Z, Wang W, et al. Oncogenic role of the SOX9-DHCR24-cholesterol biosynthesis axis in IGH-BCL2+ diffuse large b-cell lymphomas. *Blood* (2022) 139(1):73–86. doi: 10.1182/blood.2021012327

13. Zhu JR, Gao RL, Zhao SP, Lu GP, Zhao D, Li JJ. Chinese guidelines for the management of dyslipidemia in adults. *J Geriatr Cardiol* (2018) 15(1):1–29. doi: 10.11909/j.issn.1671-5411.2018.01.011

14. Fredrickson DS, Levy RI, Lees RS. Fat transport in lipoproteins–an integrated approach to mechanisms and disorders. *N Engl J Med* (1967) 276(4):215–25. doi: 10.1056/NEJM196701262760406

15. Garg A, Garg V, Hegele RA, Lewis GF. Practical definitions of severe versus familial hypercholesterolaemia and hypertriglyceridaemia for adult clinical practice. *Lancet Diabetes Endocrinol* (2019) 7(11):880–6. doi: 10.1016/S2213-8587(19)30156-1

16. Berberich AJ, Hegele RA. A modern approach to dyslipidemia. *Endocr Rev* (2022) 43(4):611–53. doi: 10.1210/endrev/bnab037

17. Zelenetz AD, Gordon LI, Chang JE, Christian B, Abramson JS, Advani RH, et al. NCCN Guidelines(R) insights: b-cell lymphomas, version 5.2021. *J Natl Compr Canc Netw* (2021) 19(11):1218–30. doi: 10.6004/jnccn.2021.0054

18. Allott EH, Howard LE, Cooperberg MR, Kane CJ, Aronson WJ, Terris MK, et al. Serum lipid profile and risk of prostate cancer recurrence: results from the SEARCH database. *Cancer Epidemiol Biomarkers Prev* (2014) 23(11):2349–56. doi: 10.1158/1055-9965.EPI-14-0458

19. Pih GY, Gong EJ, Choi JY, Kim MJ, Ahn JY, Choe J, et al. Associations of serum lipid level with gastric cancer risk, pathology, and prognosis. *Cancer Res Treat* (2021) 53(2):445–56. doi: 10.4143/crt.2020.599

20. Goto W, Kashiwagi S, Kamei Y, Watanabe C, Aomatsu N, Ikeda K, et al. Relationship between serum lipid levels and the immune microenvironment in breast cancer patients: a retrospective study. *BMC Cancer* (2022) 22(1):167. doi: 10.1186/s12885-022-09234-8

21. Berglund L, Brunzell JD, Goldberg AC, Goldberg IJ, Sacks F, Murad MH, et al. Evaluation and treatment of hypertriglyceridemia: an endocrine society clinical practice guideline. *J Clin Endocrinol Metab* (2012) 97(9):2969–89. doi: 10.1210/jc.2011-3213

22. Pirillo A, Casula M, Olmastroni E, Norata GD, Catapano AL. Global epidemiology of dyslipidaemias. *Nat Rev Cardiol* (2021) 18(10):689–700. doi: 10.1038/s41569-021-00541-4

23. Zhang M, Deng Q, Wang L, Huang Z, Zhou M, Li Y, et al. Prevalence of dyslipidemia and achievement of low-density lipoprotein cholesterol targets in Chinese adults: a nationally representative survey of 163,641 adults. *Int J Cardiol* (2018) 260:196–203. doi: 10.1016/j.ijcard.2017.12.069

24. Jeemon P, Pettigrew K, Sainsbury C, Prabhakaran D, Padmanabhan S. Implications of discoveries from genome-wide association studies in current cardiovascular practice. *World J Cardiol* (2011) 3(7):230–47. doi: 10.4330/wjc.v3.i7.230

25. Hegele RA, Pollex RL. Hypertriglyceridemia: phenomics and genomics. *Mol Cell Biochem* (2009) 326(1-2):35–43. doi: 10.1007/s11010-008-0005-1

26. Khalil YA, Rabès JP, Boileau C, Varret M. APOE gene variants in primary dyslipidemia. *Atherosclerosis* (2021) 328:11–22. doi: 10.1016/j.atherosclerosis.2021.05.007

27. Vrablik M, Hubacek JA, Dlouha D, Lanska V, Rynekrova J, Zlatohlavek L, et al. Impact of variants within seven candidate genes on statin treatment efficacy. *Physiol Res* (2012) 61(6):609–17. doi: 10.33549/physiolres.932341

28. Miao L, Yin RX, Pan SL, Yang S, Yang DZ, Lin WX. BCL3-PVRL2-TOMM40 SNPs, gene-gene and gene-environment interactions on dyslipidemia. *Sci Rep* (2018) 8(1):6189. doi: 10.1038/s41598-018-24432-w

29. Yuan G, Al-Shali KZ, Hegele RA. Hypertriglyceridemia: its etiology, effects and treatment. *CMAJ* (2007) 176(8):1113–20. doi: 10.1503/cmaj.060963

30. Wu S, Li S, Jin P, Zhang Y, Chen L, Jin W, et al. Interplay between hypertriglyceridemia and acute promyelocytic leukemia mediated by the cooperation of peroxisome proliferator-activated receptor-alpha with the PML/RAR alpha fusion protein on super-enhancers. *Haematologica* (2022) 107(11):2589–600. doi: 10.3324/haematol.2021.280147

31. Ekberg S, Harrysson S, Jernberg T, Szummer K, Andersson PO, Jerkeman M, et al. Myocardial infarction in diffuse large b-cell lymphoma patients - a population-based matched cohort study. *J Intern Med* (2021) 290(5):1048–60. doi: 10.1111/joim.13303

32. Sun J, Lou Y, Zhu J, Shen H, Zhou D, Zhu L, et al. Hypertriglyceridemia in newly diagnosed acute promyelocytic leukemia. *Front Oncol* (2020) 10:577796. doi: 10.3389/fonc.2020.577796

33. Xu J, Wei Z, Zhang Y, Chen C, Li J, Liu P. A novel scoring system based on the level of HDL-c for predicting the prognosis of t-DLBCL patients: a single retrospective study. *BioMed Res Int* (2018) 2018:2891093. doi: 10.1155/2018/2891093

34. Gao R, Liang JH, Wang L, Zhu HY, Wu W, Cao L, et al. Low serum cholesterol levels predict inferior prognosis and improve NCCN-IPI scoring in diffuse large b cell lymphoma. *Int J Cancer* (2018) 143(8):1884–95. doi: 10.1002/ijc.31590

35. Zhang Y, Chen Q, Lu C, Yu L. Prognostic role of controlling nutritional status score in hematological malignancies. *Hematology* (2022) 27(1):653–8. doi: 10.1080/16078454.2022.2078040

36. Chen L, Monti S, Juszczynski P, Ouyang J, Chapuy B, Neuberg D, et al. SYK inhibition modulates distinct PI3K/AKT- dependent survival pathways and cholesterol biosynthesis in diffuse large b cell lymphomas. *Cancer Cell* (2013) 23(6):826–38. doi: 10.1016/j.ccr.2013.05.002

37. Russo V. Cholesterol: a putative oncogenic driver for DLBCL. *Blood* (2022) 139(1):5–6. doi: 10.1182/blood.2021014300

38. Xia P, Chen J, Liu Y, Cui X, Wang C, Zong S, et al. MicroRNA-22-3p ameliorates alzheimer's disease by targeting SOX9 through the NF-kappaB signaling pathway in the hippocampus. *J Neuroinflamm* (2022) 19(1):180. doi: 10.1186/s12974-022-02548-1

39. Heckman CA, Mehew JW, Boxer LM. NF-kappaB activates bcl-2 expression in t (14;18) lymphoma cells. *Oncogene* (2002) 21(24):3898–908. doi: 10.1038/sj.onc.1205483

40. Buhrmann C, Brockmueller A, Mueller AL, Shayan P, Shakibaei M. Curcumin attenuates environment-derived osteoarthritis by Sox9/NF-kB signaling axis. *Int J Mol Sci* (2021) 22(14):7645. doi: 10.3390/ijms22147645

41. Rykaczewska U, Zhao Q, Saliba-Gustafsson P, Lengquist M, Kronqvist M, Bergman O, et al. Plaque evaluation by ultrasound and transcriptomics reveals BCLAF1 as a regulator of smooth muscle cell lipid transdifferentiation in atherosclerosis. *Arterioscler Thromb Vasc Biol* (2022) 42(5):659–76. doi: 10.1161/ATVBAHA.121.317018

42. Kuliszkiewicz-Janus M, Malecki R, Mohamed AS. Lipid changes occuring in the course of hematological cancers. *Cell Mol Biol Lett* (2008) 13(3):465–74. doi: 10.2478/s11658-008-0014-9

43. Lionakis MS, Dunleavy K, Roschewski M, Widemann BC, Butman JA, Schmitz R, et al. Inhibition of b cell receptor signaling by ibrutinib in primary CNS lymphoma. *Cancer Cell* (2017) 31(6):833–43.e5. doi: 10.1016/j.ccell.2017.04.012

44. Phelan JD, Young RM, Webster DE, Roulland S, Wright GW, Kasbekar M, et al. A multiprotein supercomplex controlling oncogenic signalling in lymphoma. *Nature* (2018) 560(7718):387–91. doi: 10.1038/s41586-018-0290-0

45. Davis RE, Ngo VN, Lenz G, Tolar P, Young RM, Romesser PB, et al. Chronic active b-cell-receptor signalling in diffuse large b-cell lymphoma. *Nature* (2010) 463(7277):88–92. doi: 10.1038/nature08638

46. Wilson WH, Wright GW, Huang DW, Hodkinson B, Balasubramanian S, Fan Y, et al. Effect of ibrutinib with r-CHOP chemotherapy in genetic subtypes of DLBCL. *Cancer Cell* (2021) 39(12):1643–53.e3. doi: 10.1016/j.ccell.2021.10.006

47. Rink JS, Yang S, Cen O, Taxter T, McMahon KM, Misener S, et al. Rational targeting of cellular cholesterol in diffuse Large b-cell lymphoma (DLBCL) enabled by functional lipoprotein nanoparticles: a therapeutic strategy dependent on cell of origin. *Mol Pharm* (2017) 14(11):4042–51. doi: 10.1021/acs.molpharmaceut.7b00710

frontiers | Frontiers in Oncology

TYPE Systematic Review
PUBLISHED 20 July 2023
DOI 10.3389/fonc.2023.1188478

OPEN ACCESS

EDITED BY
Onder Alpdogan,
Thomas Jefferson University, United States

REVIEWED BY
Luis Colomo,
Hospital del Mar, Parc de Salut Mar, Spain
Panagiotis Tsirigotis,
National and Kapodistrian University of Athens, Greece

*CORRESPONDENCE
Vanja Zeremski
vanja.zeremski@med.ovgu.de

RECEIVED 17 March 2023
ACCEPTED 05 July 2023
PUBLISHED 20 July 2023

CITATION
Zeremski V, Kropf S, Koehler M, Gebauer N, McPhail ED, Habermann T, Schieppati F and Mougiakakos D (2023) Induction treatment in high-grade B-cell lymphoma with a concurrent *MYC* and *BCL2* and/or *BCL6* rearrangement: a systematic review and meta-analysis.
Front. Oncol. 13:1188478.
doi: 10.3389/fonc.2023.1188478

Induction treatment in high-grade B-cell lymphoma with a concurrent *MYC* and *BCL2* and/or *BCL6* rearrangement: a systematic review and meta-analysis

Vanja Zeremski[1]*, Siegfried Kropf[2], Michael Koehler[1,3], Niklas Gebauer[4], Ellen D. McPhail[5], Thomas Habermann[6], Francesca Schieppati[7] and Dimitrios Mougiakakos[1]

[1]Department of Hematology and Oncology, Medical Center, Otto-von-Guericke University Magdeburg, Magdeburg, Germany, [2]Department for Biometry and Medical Informatics, Otto-von-Guericke University Magdeburg, Magdeburg, Germany, [3]Specialty Practice for Psycho-Oncology, Magdeburg, Germany, [4]Department of Hematology and Oncology, University Hospital of Schleswig-Holstein, Luebeck, Germany, [5]Department of Laboratory Medicine and Pathology, Mayo Clinic, Rochester, MN, United States, [6]Division of Hematology, Mayo Clinic, Rochester, MN, United States, [7]Hematology, ASST Spedali Civili di Brescia, Lombardy, Italy

Background and aim: High-grade B cell lymphomas with concomitant *MYC* and *BCL2* and/or *BCL6* rearrangements (HGBCL-DH/TH) have a poor prognosis when treated with the standard R-CHOP-like chemoimmunotherapy protocol. Whether this can be improved using intensified regimens is still under debate. However, due to the rarity of HGBCL-DH/TH there are no prospective, randomized controlled trials (RCT) available. Thus, with this systematic review and meta-analysis we attempted to compare survival in HGBCL-DH/TH patients receiving intensified vs. R-CHOP(-like) regimens.

Methods: The PubMed and Web of Science databases were searched for original studies reporting on first-line treatment in HGBCL-DH/TH patients from 08/2014 until 04/2022. Studies with only localized stage disease, ≤10 patients, single-arm, non-full peer-reviewed publications, and preclinical studies were excluded. The quality of literature and the risk of bias was assessed using the Methodological Index for Non-Randomized Studies (MINORS) and National Heart, Lung, and Blood Institute (NHLBI) Quality Assessment Tool for Observational Cohort and Cross-Sectional Studies. Random-effect models were used to compare R-CHOP-(like) and intensified regimens regarding 2-year overall survival (2y-OS) and 2-year progression-free survival (2y-PFS).

Results: Altogether, 11 retrospective studies, but no RCT, with 891 patients were included. Only four studies were of good quality based on aforementioned criteria. Intensified treatment could improve 2y-OS (hazard ratio [HR]=0.78 [95% confidence interval [CI] 0.63-0.96]; p=0.02) as well as 2y-PFS (HR=0.66 [95% CI 0.44-0.99]; p=0.045).

Conclusions: This meta-analysis indicates that intensified regimens could possibly improve 2y-OS and 2y-PFS in HGBCL-DH/TH patients. However, the significance of these results is mainly limited by data quality, data robustness, and its retrospective nature. There is still a need for innovative controlled clinical trials in this difficult to treat patient population.

Systematic review registration: https://www.crd.york.ac.uk/prospero, identifier CRD42022313234.

KEYWORDS

high-grade B cell lymphoma, double-hit lymphoma (DHL), triple-hit lymphoma (THL), induction treatment, meta-analysis

Introduction

Large B cell lymphomas (LBCLs) represent a rather heterogeneous group of B cell-derived entities (1). The underlying genetic, morphologic, and clinical features of LBCLs can vary substantially translating into different outcomes. More than 20 years ago it was suggested that LBCLs harboring *MYC*, *BCL2*, and/or *BCL6* translocation (double-hit [DH] or triple-hit [TH] lymphoma) fare poorly under standard-intensity chemotherapeutic regimen (2). It was however not until 2017 that this subgroup was introduced as a separate entity and defined as "high-grade B-cell lymphoma with *MYC* and *BCL2* and/or *BCL6* rearrangements" (HGBCL-DH/TH) in the WHO classification (3). Most recently, cases with *MYC*/*BCL6* rearrangement were separated from this group due to the divergent mechanisms of pathogenesis (1).

HGBCL-DH/TH patients frequently present with high-risk features including advanced stage, a high International Prognostic Index (IPI) score, and ≥1 extranodal localization. Furthermore, central nervous system involvement is common (4–8). Earlier works have repeatedly confirmed that HGBCL-DH/TH patients have inferior outcome following standard DLBCL treatment (i.e., R-CHOP), especially in advanced stage (9–12). Consequently, intensified regimens (i.e., DA-EPOCH-R, R-CODOX-M/IVAC, R-hyperCVAD, and GMALL protocol) have been introduced and are currently widely used in first-line setting (13–16). In fact, even adoptive CAR T cells therapy is currently being evaluated as a frontline approach in this highly vulnerable patient population (17). However, data addressing the significance of an intensified first-line therapy have been scarce and rather disputable. Several studies implied that intensified regimens could improve progression-free survival (PFS) (7, 18); yet benefit in terms of overall survival (OS) was rarely reported. Recently, we retrospectively analyzed a large, multi-center HGBCL-DH/TH cohort of 259 patients and could not identify a significant advantage of employing intensified regimens over R-CHOP(-like) regimens (neither for PFS nor for OS) (19).

Thus, we decided to re-evaluate this issue and to possibly gain additional insights that would help guide the treatment of this difficult-to-treat population. With this aim, we performed a meta-analysis of recently published studies and compared survival outcome of intensified regimens to R-CHOP(-like) strategies in newly diagnosed HGBCL-DH/TH patients.

Methods

This systematic review and meta-analysis was preformed following the Preferred Reporting Items for Systematic Reviews and Meta-Analyses (PRISMA) guidelines (20). The protocol was registered at PROSPERO International Prospective Register of Systematic Reviews (CRD 42022313234).

Selection criteria and search strategy

The Population, Intervention, Control, Outcome, Study (PICOS) approach was used to define the inclusion criteria (Table 1) (21). Eligible studies were included in the analysis if treatment related outcomes were reported. The primary endpoint in our study was 2-year OS (2y-OS) of patient groups receiving different induction regimens (intensified regimen vs. R-CHOP[-like]). Furthermore, we compared 2-year PFS (2y-PFS) between these 2 groups. In case of eligible studies not reporting on treatment related outcome, the authors were contacted in order to obtain missing data necessary for analysis. The exclusion criteria were also reported in Table 1. Literature search for studies published from 08/2014 until 04/2022 was carried out using the PubMed and Web of Science databases. The following keywords were used, with the use of wildcard characters to account for variations in spelling and plurals: "*MYC/BCL2*" OR "*MYC/BCL6*" AND "lymphoma", "double-hit" OR "triple-hit" AND "lymphoma". Two of the authors independently performed the screening and identified studies, data selection, and data extraction. Disagreements were resolved by a consensus-based discussion. For studies with multiple publications or overlapping patient cohorts, the most complete dataset amongst all available publications was used.

TABLE 1 Inclusion and exclusion criteria for selection of the articles.

PICOS inclusion criteria	
Population	Newly diagnosed HGBCL patients with concurrent *MYC* and *BCL2* and/or *BCL6* rearrangement (according to WHO 2017) aged ≥18 years
Intervention	Intensified front-line treatment (i.e. DA-EPOCH-R, R-CHOEP, R-Hyper-CVAD, R-CODOX-M/IVAC, B-ALL protocol, R-CHOP with upfront autologous SCT)
Control	Standard front-line treatment (R-CHOP[-like]: R-CHOP and its modified versions [i.e. R-miniCHOP, R-CHOP with lenalidomide or ibrutinib])
Outcome	2-years overall survival and/or progression-free survival
Study design	Randomized clinical trials, retrospective trials and case series written in English language and published between August 2014 and April 2022 (including e-publications available ahead of print)
Exclusion criteria	
	Studies ≤10 patients, single-arm studies, reviews, preclinical trials, case reports, abstracts, posters

PICOS, Population, Intervention, Control, Outcome, Study; HGBCL, high-grade B-cell lymphoma; SCT, Stem cell transplantation.

Study quality assessment

Methodological Index for Non-Randomized Studies (MINORS) was used to assess the quality of included observational studies (22). The MINORS consists of 12 indexes: 1) a clearly stated aim; 2) inclusion of consecutive patients; 3) prospective collection of data; 4) endpoints appropriate to the aim of the study; 5) unbiased assessment of the study endpoint(s); 6) a follow-up period appropriate to the aim of the study; 7) loss to follow-up less than 5%; 8) prospective calculation of the study size; 9) an adequate control group; 10) contemporary groups (control and studied group should be managed during the same time period, no historical comparison); 11) baseline equivalence of groups and 12) an adequate statistical analysis. The items were scored 0 if not reported; 1 when reported but inadequate; and 2 when reported and adequate. Studies were considered as high quality if the total score was ≥17, medium quality if the total score was 9-16, and low quality if the total score was <9 (22). In addition, the NHLBI Quality Assessment Tool for Observational Cohort and Cross-Sectional Studies (NHLBI, National Heart, Lung, and Blood Institute) was used (23). NHLBI developed a set of tailored quality assessment tools to assist reviewers in focusing on concepts that are key to a study's internal validity. We used the study rating tool on the range of items included in each tool to judge each study to be of "good," "fair," or "poor" quality. In general terms, a "good" study has the least risk of bias, and results are considered to be valid. A "fair" study is susceptible to some bias deemed not sufficient to invalidate its results. The fair quality category is likely to be broad, so studies with this rating will vary in their strengths and weaknesses. A "poor" rating indicates significant risk of bias (23). The study quality was assessed by two authors.

Data analysis

All statistical analyses were performed using SPSS software, version 28 (IBM Statistics, Armonk, NY, USA). Heterogeneity between studies was assessed using I^2 statistics, with I^2 above 50% being considered as an indicator for distinct heterogeneity. As large heterogeneity among the studies was observed particularly for PFS, the random-effects model has been applied consistently for all analyses. The hazard ratio (HR) with a corresponding 95% confidence interval (95% CI) for OS and PFS was utilized to compare the prognostic survival. HR and 95% CI were directly extracted from the Cox proportional hazards models used for the univariate analyses of the original studies. When it was not possible to obtain these values from the original studies, we estimated them from survival curves (where possible) using the methods described by Parmar et al. (24) or we derived them from the reported estimates and CIs for 2yOS or 2yPFS in the two treatment arms via normal approximation. HR less than 1.0 indicated an advantage for intensified treatment as compared to standard treatment in terms of improving 2y-OS and 2y-PFS. p values ≤0.05 were considered statistically significant. Potential publication bias was examined using funnel plot and Eggers' test. Robustness of results was assessed by iterative omission of single studies from the analysis (so-called leave-one-out analysis).

Results

Study selection and description of studies

Altogether 2411 records were identified through database searches. After initial screening, 108 full-text articles were further selected for eligibility. The flowchart of the reviews shows the detailed process of selection (Figure 1). Finally, 11 relevant studies, comprising a total of 891 HGBCL-DH/TH patients, were included (6, 7, 18, 25–32). We identified no prospective, randomized controlled trials (RCT); all studies included in the meta-analysis were of retrospective design. Three authors provided additional individual patient data on request (26, 27, 29). Characteristics of included studies are outlined in Table 2. *MYC* translocation partner was rarely stated, therefore we did not report on this data. Studies conducted exclusively on HGBCL-DH/TH patients with localized stage (n=3) were excluded, in order to avoid selection bias. Eight out of 11 eligible studies were published from 2019 onwards (6, 18, 26–29, 31, 32). Only four studies were primarily designed to compare induction treatment in HGBCL-DH/TH patients (6, 7, 18, 31).

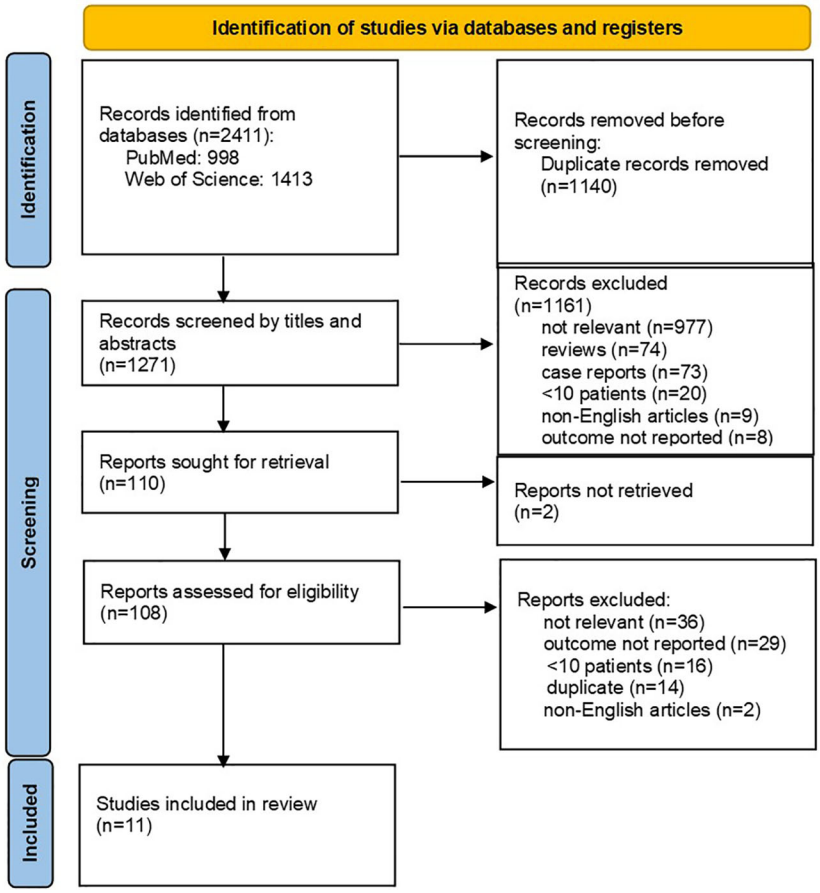

FIGURE 1
PRISMA flow diagram.

Quality assessment

No standardized assessment tools exist for observational studies. We used the MINORS scale to assess study quality (Supplementary Table S1). The final scores for each study ranged from 13 to 19. Overall, the studies included in the meta-analysis were of intermediate reliability. Four studies were considered to be high-quality studies (6, 26, 27, 31). We additionally assessed studies for bias based on the 14 criteria in the NHLBI tool for quality assessment (NHLBI). About a half (54.5%) of the studies were of good quality and showed low risk of bias. All studies lacked the following features: blinded study, exposure reassessment over time, provided sample size justification, power description or variance/effect estimates. Key methodological strengths in the included studies were rare.

Outcome

All studies were analyzed regarding 2y-OS and included 464 patients that received an intensified treatment and 412 with standard R-CHOP-like protocol. The study by Tisi et al., compared R-CHOP to two different treatment groups: i.e., DA-EPOCH-R and "intensive regimens" (R-CODOX-M/IVAC, R-Hyper-CVAD/R-MA, GMALL protocol) (18). Only patients treated within the "intensive regimens" cohort were included in our analysis (as this cohort included more patients than the DA-EPOCH-R group). Intensified treatment resulted in improved 2y-OS in all patients (intensified treatment *vs.* standard treatment: HR=0.78 [95% CI 0.63-0.96]; p=0.02; Figure 2). There was no heterogeneity among studies (I^2 = 0%; p=0.43). A sensitivity analysis was performed using the so-called leave-one-out approach in order to evaluate the robustness of the results. The statistically significant combined effect size for the impact of intensified treatment on 2y-OS was found to be lost when omitting one of the following studies: Laude et al., Petrich et al. and Zhang et al. (Supplementary Table S2) (6, 7, 31). No publication bias with regard to 2y-OS was evident (p=0.11 in Egger's test; funnel plots are presented in Supplementary Figure S1).

Seven studies with available data for 2y-PFS were included in the meta-analysis; altogether, 358 patients treated with intensified and 325 patients treated with standard treatment. Intensified treatment was shown to result in prolonged 2y-PFS as compared to standard treatment (HR=0.66 [95% CI 0.44-0.99]; p=0.045, Figure 3). A significant heterogeneity between the results of the individual studies (I^2 = 66.7%; p=0.02) was noticed. The study by Kuenstner et al. was shown to be the key contributor to this between-study heterogeneity after performing the so-called leave-

TABLE 2 Characteristics of included studies.

Study	Country	Sample size (*N*)	Participant group (*n*)	Treatment arm, n (%)	age, median (range)	*BCL2* +/- *BCL6* translocation, n (%)	advanced stage	high IPI, n (%)	FU months, median (range)	2y-PFS, %	2y-OS, %
de Jonge et al., 2016[§#]	Netherland	26	17	R-CHOP, 10 (58.8) intensified[1], 7 (41.2)	64.5 (41–80)	8 (80.0) 7 (100)	9 (90.0) 7 (100.0)	na	40.5 (5.6-75.4)	na	36.0 53.6
Kuenster et al., 2021[§#]	Germany	47	34	R-CHOP-like[2], 21 (61.8) intensified[2], 13 (38.2)	73 (45-82) 60 (35-77)	11 (52.4) 10 (76.9)	10 (47.6) 12 (92.3)	13 (61.9) 9 (69.2)	92 (70.3-113.7)	42.9 23.1	61.9 46.2
Laude et al., 2021[#]	France	156	156	R-CHOP-like[3], 99 (63.5) intensified[3], 57 (36.5)	66 58	76 (76.8) 46 (80.7)	85 (85.9) 55 (98.2)	69 (75.0) 39 (72.0)	32 (28-39)	40.0 50.7	na
McPhail et al., 2019[§#]	USA	100	70	R-CHOP, 32 (45.7) intensified[4], 38 (54.3)	66 (44-79) 59 (29-83)	25 (83.3) ns, 2 28 (82.4) ns, 4	na	na	28.9 (14.3-43.5)	29.8 53.9	41.5 57.5
Miyaoka et al., 2022[§]	Japan	50	21	R-CHOP-like[5], 15 (71.4) intensified[5], 6 (28.6)	67 (49-79) 57.5 (39-73)	13 (86.6) 4 (66.7)	10 (66.7) 4 (66.7)	10 (66.7) 1 (16.7)	78 (0-179.3)	na	41.5 57.5
Petrich et al., 2014[#]	USA	311	311	R-CHOP, 100 (32.0) intensified[6], 211 (57.9)	60 (19-87)*	295 (95.0)*	255 (81.0) *	na	23 (1-126)**	na	na
Schieppati et al., 2020[§#]	Italy	95	24	R-CHOP, 7 (29.2) intensified[7], 17 (70.8)	68 (59-88) 62 (27-76)	5 (71.5) 14 (82.3)	6 (85.7) 16 (94.1)	4 (57.1) 11 (64.7)	45 (28.6-58.1)	42.9 73.1	42.9 58.8
Tisi et al., 2019	Italy	100	76	R-CHOP[8], 27 (33.3) intensified[8] 34 (42.0) DA-EPOCH-R, 15 (19.0)	61 (21-85)*	57 (70.4)*	70 (86.0)*	56 (69.0) *	33**	40 50 64	34 64 66
Yoshida et al., 2015[§]	Japan	22	12	R-CHOP, 7 (58.3) intensified, 5[9] (41.6)	66 (54-88) 58 (46-64)	7 (100.0) 5 (100.0)	6 (75.9) 5 (71.4)	4 (57.1) 4 (80.0)	14 (5.6-22.4)	na	51.4 40.0
Zhang F. et al, 2019	China	139	139	R-CHOP, 76 (54.7) intensified, 63[10] (45.3)	57 (18-81)*	*BCL2*, 109 (78.4)*	54 (71.1) 36 (57.1)	34 (44.8) 42 (66.7)	18 (4-39)	45.4 63.6	47.8 67.4
Zhang J. et al. 2020[§#]	China	51	31	R-CHOP-like[11], 18 (58.1) intensified, 13[11] (41.9)	56.5 (26-72) 42 (19-68)	ns	13 (72.2) 9 (61.5)	na	16 (10.4-21.5)	na	87.7 58.6

Sample size (N) refers to the total number of patients in each study, whereas the participant group (n) refers to the number of HGBCL-DH/TH patients included in this meta-analysis (i.e. HGBCL-DH/TH patients who received [curative] induction treatment and had reported treatment outcome).

[§]available individual patient data, [#]including HGBCL-DH/TH arising from low-grade lymphomas, * data for all patients; **follow-up for all living patients.

ns, not specified; na, not applicable.

[1] intensified regimens: DA-EPOCH-R (dose-adjusted, rituximab, etoposide, prednisone, vincristine, cyclophosphamide and doxorubicin) 71.4%, R-CHOP+up-front autologous stem cell transplantation (SCT) 28.6%; R-DHAP (rituximab, dexamethasone, cisplatin, high-dose cytarabine) 14.2%.

[2] R-CHOP-like: R-CHOP(rituximab, cyclophosphamide, doxorubicin, vincristine, prednisone), R-miniCHOP.

intensified regimens: GMALL (German multicenter acute lymphoblastic leukemia) protocol 61.5%, R-CHOEP (rituximab, cyclophosphamide, doxorubicin, vincristine, etoposide, prednisone) 23.1%, DA-EPOCH-R 7.7%, other 7.7%.

[3] R-CHOP-like not further specified.

intensified regimens: DA-EPCOH-R 24.6%, R-ACVBP (rituximab, doxorubicin, cyclophosphamide, vindesine, bleomycin and prednisone) 28.1%, R-COPADEM (rituximab, cyclophosphamide, vincristine, prednisone, doxorubicin and methotrexate) 47.3%.

[4] intensified regimens: R-CHOEP 44.7%, R-CODOX-M/IVAC 39.5%, R-hyperCVAD (rituximab, cyclophosphamide, vincristine, doxorubicin and dexamethasone) 15.8%.

[5] R-CHOP-like: R-CHOP, R-COP (rituximab, cyclocphosphamid, vincristine, prednisone).

intensified regimens: DA-EPOCH-R 66.7%, R-hyper-CVAD 33.3%, R-CODOX-M 16.7%.

[6]intensified regimens: R-Hyper-CVAD n=65, DA-EPOCH-R n=64, R-CODOX-M/IVAC n=42, R-ICE n=9, other n=10; up-front autologous SCT n=39, up-front allogeneic SCT n=14.

[7]intensified regimens: DA-EPOCH-R (+/- up-front autologous stem cell transplantation) 58.9%, GMALL 35.3%, R-CHOP+up-front autologous SCT 5.9%.

[8]R-CHOP-like: R-CHOP, R-COMP (R-CHOP with liposomal anthracycline), R-miniCHOP, R-megaCHOP, R-M/VACOP-B (rituximab, methotrexate, etoposide, doxorubicin, cyclophosphamide, vincristine, prednisone and bleomycin).

intensified regimens: R-CODOX-M/IVAC, GMALL, R-Hyper-CVAD/R-MA (rituximab, cyclophosphamide, vincristine, doxorubicin and dexamethasone/ rituximab,high-dose methotrexate and cytarabine), upfront autologous SCT (accurate treatment distribution not known).

[9]intensified regimens: R-CODOX-M/IVAC (rituximab, cyclophosphamide, doxorubicin, vincristine, methotrexate/ifosfamide, etoposide, high-dose cytarabine) 60.0%, R-hyper-CVAD 20.0%, R-ESHAP (rituximab, etoposide, methylprednisolone, high-dose cytarabine and cisplatin) 20.0%.

[10]intensified regimens: DA-EPOCH-R (100 %).

[11]R-CHOP-like: R-CHOP, R-CHOP + lenalidomide, R-CHOP + HD-MTX.

intensified regimens: DA-EPOCH-R +/- HD-MTX or +/- i.th. MTX (76.9%); R-CODOX-M/IVAC (15.4%), other (7.6%).

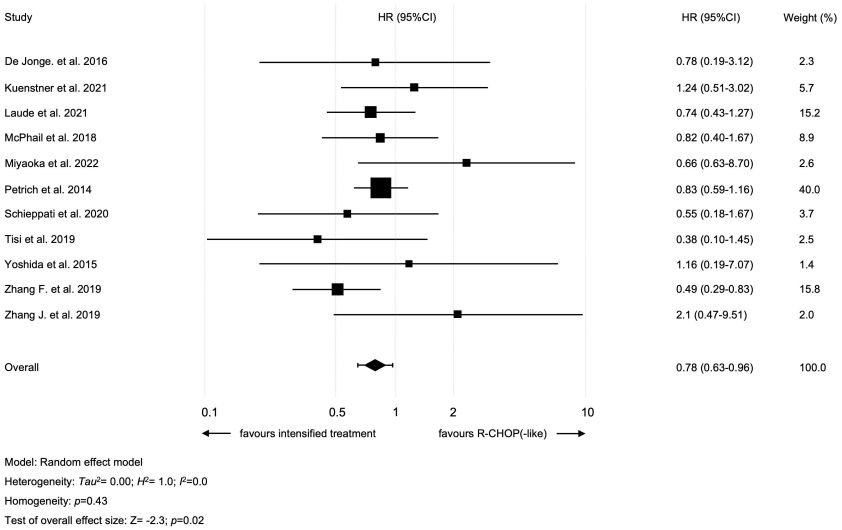

FIGURE 2
Forest plot of 2-year overall survival.

one-out sensitivity analysis (26). Following exclusion of this study, the combined effect size for the impact of intensified treatment on 2y-PFS was found to be stronger (HR=0.57 [95% CI 0.45-0.7]; p<0.01) and there was no longer heterogeneity among studies (I^2 = 0%; p=0.60) (Supplementary Table S3). There were no hints on publication bias regarding 2y-PFS (p=0.41 in the Egger's test; funnel plots are presented in Supplementary Figure S2).

Toxicity

Treatment toxicity was only questioned within two studies (6, 31). As expected, Laude et al. observed significantly higher rates of grade 3/4 hematological toxicities and mucositis in the intensified arm (neutropenia, thrombocytopenia, anemia, and mucositis; all p=0.01). Surprisingly, Zhang et al. reported no difference between these standard versus intensified approaches. Also, neutropenia rates were unexpectedly low in patients treated with intensified regimens (20.6%). Due to the small sample size we refrained from further statistical analyses.

Discussion

This systematic review of published studies from 2014 to 2022, which compared survival rates according to induction treatment in newly diagnosed HGBCL-DH/TH patients, yielded 11 retrospective studies. Only four of them were primarily designed to compare outcome between intensified treatment and R-CHOP(-like) standard protocols.

Regarding OS, previous data has been rather controversial. A few single-arm, prospective studies reported impressive survival

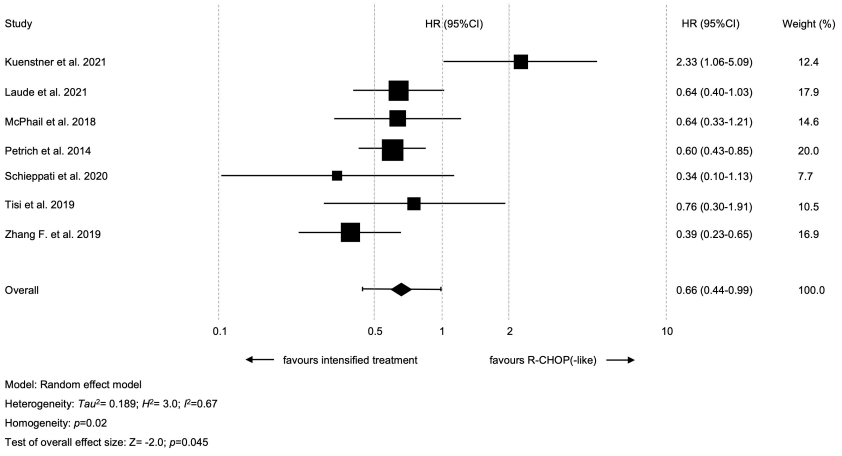

FIGURE 3
Forest plot of 2-year progression-free survival.

rates using various intensified regimens, as follows: 4-year OS of 82% with DA-EPOCH-R, 2y-OS of 76% with R-CODOX-M/R-IVAC and 5-year OS of 83% with Nordic Lymphoma Group protocol (R-CHOP/R-CHOEP combined with high-dose methotrexate and intrathecal liposomal cytarabine) (33–35). Given the rarity of HGBCL-DH/TH, these studies included only a small number of HGBCL-DH/TH patients (n=24 and n<10 patients, respectively). Conversely, retrospective studies reported comparably low survival rates when applying these (or similar) intensified regimens, with only a few of them reporting a 2y-OS of >60% (18, 31), indicating a potential selection bias toward enrollment of healthier patients in prospective studies.

R-CHOP in combination with lenalidomide was prospectively investigated in 82 LBCL patients with *MYC* translocation (also including 24% patients with *MYC* single-hit translocation) within the HOVON-2 trial (36). This resulted in 2y-OS of 73% and 2-year event-free survival (2y-EFS) of 63%. The REMoDL trial, that compared R-CHOP plus bortezomib *vs*. R-CHOP, included 35 HGBCL-DH/TH patients (37). Median OS at 30 months was 58.5% and 38.9%, respectively.

According to this systematic review, and to the best of our knowledge, no prospective trials have directly compared the efficacy of intensified treatment and R-CHOP(-like) so far. A previously published meta-analysis (7), including 11 retrospective trials (published between 2009 and 2014) with altogether 394 patients, did not find any difference in OS between the two approaches (R-CHOP *vs.* R-EPOCH: HR=0.77 [95% CI 0.51-1.13]; p=0.19; R-CHOP *vs.* other intensified regimens [R-Hyper-CVAD, R-CODOX-M/IVAC, R-ICE, and other]: HR 0.89 [95%CI 0.62-1.13]; p=0.53). Of note, 5 of the included studies have only reported preliminary results in abstract format and not the final study data. Howlett et al. also included double-expressors (DEL) as well as LBCLs with amplifications and/or extra copies of *MYC*, *BCL2* and *BCL6* in their analysis (38). These, however, have to be distinguished from HGBCL-DH/TH as their prognosis does not seem to differ significantly from DLBCL (NOS) (11, 29, 39, 40). Furthermore, DEL and HGBCL-DH/TH are considered to have different underlying biology. DEL arise from "activated" B-cells in contrast to HGBCL-DH/TH with germinal B-center origin (10, 41).

Our current meta-analysis suggests that 2y-OS can be improved using intensified regimes (HR=0.78; p=0.02). Still, this needs to be interpreted with caution, as the analysis was found to be insufficiently robust. So-called leave-one-out analysis with any of the three largest trials (Laude et al. n=156, Petrich et al. n=311, Zhang F. et al. n=139) was associated with loss of statistical significance (6, 7, 31).

Regarding PFS, previously published data are also rather contradictory. The earlier mentioned meta-analysis by Howlett et al. demonstrated prolonged PFS when using R-EPOCH (HR=0.66 [95% CI 0.44-0.96]; p=0.03). The use of other intensified regimens, however, did not lead to statistically significant improvement of PFS (HR=0.74 [95% CI 0.51-1.05]; p=0.09) (38). In our recently published multi-center analysis on HGBCL-DH/TH patients (also including 7 trials with 209 patients from this meta-analysis) neither 2y-OS nor 2y-PFS was shown to be improved with regimens other than R-CHOP(-like) (R-CHOP [-like] *vs.* intensified treatment rates for 2y-OS were 54.2% *vs.* 55.2% [p=0.87] and 2yPFS 44.4% *vs.* 48.4% [p=0.63], respectively) (19). A subgroup analysis of different intensified regimens (i.e., R-EPOCH *vs.* other treatments) was not carried out. These results were in line with recently published data on 154 HGBCL-DH/TH patients (42). Magnusson et al. reported 4-year OS rates of 54.5% and 49.6% in patients treated with R-CHOP and R-EPOCH, respectively. However, the present meta-analysis did demonstrate an improved 2y-PFS using intensified regimens over R-CHOP (-like) (HR=0.66; p=0.045). Interestingly, one study included in this meta-analysis showed improved 2y-PFS with R-CHOP(-like) protocols (26). This is possibly explained by selection bias as these patients were older (median age 73 *vs*. 60 years), had less frequently advanced stage disease (47.6% *vs*. 92.3%), and less often concomitant *BCL2* translocation (52.4% *vs.* 76.9%), signifying an enrichment in the pathogenetically and clinically divergent MYC/*BCL6* rearranged subgroup. In fact, excluding this study from the meta-analysis, enhanced the cumulative effect (HR=0.56; p<0.01).

When comparing induction regimens in HGBCL-DH/TH patients, it needs to be mentioned that there is a relevant heterogeneity among this group. Namely, localized stage HGBCL-DH/TH result in high 2y-OS >80% using R-CHOP (with/without consolidative radiation) (43, 44), which is comparable to outcome in DLBCL patients (45). Thus, intensified treatment does not seem to be required in these patients. On the other hand, transformed HGBCL-DH/TH (with a prior history of low grade lymphoma) seem to perform poorly comparing to *de novo* HGBCL-DH/TH.

McPhail et al. reported a median OS of 10.8 months and 22 months in patients with transformed and *de novo* HGBCL-DH/TH, respectively (27). Conversely, Li et al. failed to reproduce these results (46). It is to be mentioned that a number studies do not evaluate/report whether prior low-grade lymphoma was present or not, leaving this issue still unresolved.

HGBCL-DH/TH also encompasses both large cell and high grade morphology, and in some studies high grade morphology shows an association with poorer outcome (27). In addition, the prognostic role of *BCL6* rearrangement is not clear. There are data that suggest that patients with concomitant *MYC*/*BCL6* rearrangement (in the absence of a *BCL2* rearrangement) have a better survival as compared to patients harboring a *MYC/BCL2* rearrangement (47). In fact, gene expression profile and mutational spectra in *MYC*/*BCL6* were shown to differ noticeably from *MYC*/*BCL2* lymphomas (26, 48). Consequently, *MYC/BCL6* LBCLs are now excluded from the HGBCL-DH entity, according to the recently revised 2022 WHO classification (1). Depending on the morphological features they are classified as DLBCLs NOS or HGBLs NOS. The recently updated International Consensus Classification also redefined the term of HGBCL-DH. It now comprises two groups: HGBCL with *MYC/BCL2* rearrangements (with or without *BCL6* rearrangement) and a new provisional entity, HBGBL with *MYC/BCL6* rearrangements (49). Finally, the prognostic significance of the *MYC* translocation partner (immunoglobulin [Ig] *vs*. non-Ig) is not clarified yet. Two large trials (Lunenburg Lymphoma Biomarker Consortium and GELY/LYSA trial) showed that adverse prognosis of *MYC* rearrangement is confined solely to *MYC*/Ig translocation (50, 51). However,

several studies failed to show a difference in outcome between *MYC*/Ig and *MYC*/non-Ig rearranged cases (27, 46, 52). The heterogeneity among HGBCL-DH/TH patients possibly explains discordant outcomes in previously published studies.

Another important issue that needs to be considered, is the high heterogeneity among "intensified regimens". This term includes basically all regimens beyond R-CHOP(-like) (Table 2). Some of the previously published studies suggest that treatment outcome can significantly vary among intensified regimens (5, 29). In fact, "more intensified regimens" (i.e. GMALL protocol, R-CODOX-M/IVAC) yield poorer survival rates comparing to DA-EPOCH-R, possibly due to increased toxicity. Further treatment escalation, in terms of consolidative autologous stem cell transplantation, also failed to improve survival rates, especially after intensified induction (53, 54).

The results of our meta-analysis suggest that intensified induction improves 2y-PFS and possibly 2y-OS. One could however argue, whether a superior 2y-PFS suffices to justify the use of an intensified induction. In LBCLs, 2-years 2y-EFS was shown to be a robust parameter for long-term survival (55). Whether this also applies to HGBCL-DH/TH remains to be elucidated. In order to significantly improve OS, new consolidation strategies may be a reasonable approach. Actually, first results of upfront use of CAR T cells in high-risk DLBCL, including 16 HGBCL patients, showed promising results (estimated 12 months OS was 91%) (17). Another phase II study explored blinatumomab consolidation after R-CHOP treatment in high-risk DLBCL (12 HGBCL-DH/TH patients). A notable proportion of patients (i.e., 7/8) with persistent disease after induction (either partial remission or stable disease) did achieve a complete remission after treatment with blinatumomab (56).

However, there are some limitations of this meta-analysis and the applicability of its conclusions. Firstly, the data presented here are derived from retrospective studies and subject to potential sources of bias inherent to this methodology, including missing data, and a non-uniform follow-up. In part, the small size of included studies (<50 patients in six studies) with wide 95% CIs of the estimated HRs in some of them may influenced the reliability of the results. Then, the issue of treatment-related toxicity could not be addressed here, given the scarcity of reported data. Furthermore, most of the studies had a more exploratory design. Evaluating whether there was adequate statistical analysis or an adequate control group was therefore challenging in terms of bias assessment.

In summary, this meta-analysis represents a comprehensive review of the treatment of HGBCL-DH/TH patients. Given the rarity of this entity there is obviously a lack of large high-quality studies. In the absence of a more robust data set, this meta-analysis provides the rationale for using intensified induction protocols for appropriately selected advances stage patients or to preferentially treat them within clinical trials. Moreover, each patient should be counseled on the risks and benefits of such treatment intensification including the limitation of the available data. However, to definitely clarify the question of the optimal induction in HGBCL-DH/TH patients, prospective, randomized trials are promptly needed.

Data availability statement

The original contributions presented in the study are included in the article/Supplementary Material. Further inquiries can be directed to the corresponding author.

Author contributions

VZ designed and performed the research, interpreted data and wrote the manuscript. SK analyzed and interpreted data. MK performed the research, interpreted data and reviewed the manuscript. NG, EM and TH reviewed the manuscript. DM interpreted data and wrote the manuscript. All authors contributed to the article and approved the submitted version.

Funding

TH reported funding by MER P50 CA97274.

Conflict of interest

Author TH reported following disclosures institutional fees: Data Monitoring Committee: Seagen, Tess Therapeutics, Eli Lilly & Co., Scientific Advisory Board: Eli Lilly & Co., Morphosys, Incyte, Biegene, Loxo Oncology, Research Support: Genentech, Sorrento. Author NG reported the following disclosures: Scientific Advisory Board: Roche, Takeda, Astra Zeneca. Travel Support: Beigene, Janssen, Roche.

The remaining authors declare that the research was conducted in the absence of any commercial or financial relationships that could be construed as a potential conflict of interest.

Publisher's note

Supplementary material

The Supplementary Material for this article can be found online at: https://www.frontiersin.org/articles/10.3389/fonc.2023.1188478/full#supplementary-material

References

1. Alaggio R, Amador C, Anagnostopoulos I, Attygalle AD, Araujo IB, Berti E, et al. The 5th edition of the world health organization classification of haematolymphoid tumours: lymphoid neoplasms. *Leukemia* (2022) 36:1720–48. doi: 10.1038/s41375-022-01620-2

2. Kramer MH, Hermans J, Wijburg E, Philippo K, Geelen E, van Krieken JH, et al. Clinical relevance of BCL2, BCL6, and MYC rearrangements in diffuse large b-cell lymphoma. *Blood* (1998) 92:3152–62. doi: 10.1182/blood.V92.9.3152

3. Swerdlow SH ed. *WHO classification of tumours of haematopoietic and lymphoid tissues*. Lyon: International Agency for Research on Cancer (2017). p. 585.

4. Pedersen MØ, Gang AO, Poulsen TS, Knudsen H, Lauritzen AF, Nielsen SL, et al. Double-hit BCL2/MYC translocations in a consecutive cohort of patients with large b-cell lymphoma - a single centre's experience. *Eur J Haematol* (2012) 89:63–71. doi: 10.1111/j.1600-0609.2012.01787.x

5. Oki Y, Noorani M, Lin P, Davis RE, Neelapu SS, Ma L, et al. Double hit lymphoma: the MD Anderson cancer center clinical experience. *Br J Haematol* (2014) 166:891–901. doi: 10.1111/bjh.12982

6. Laude M-C, Lebras L, Sesques P, Ghesquieres H, Favre S, Bouabdallah K, et al. First-line treatment of double-hit and triple-hit lymphomas: survival and tolerance data from a retrospective multicenter French study. *Am J Hematol* (2021) 96:302–11. doi: 10.1002/ajh.26068

7. Petrich AM, Gandhi M, Jovanovic B, Castillo JJ, Rajguru S, Yang DT, et al. Impact of induction regimen and stem cell transplantation on outcomes in double-hit lymphoma: a multicenter retrospective analysis. *Blood* (2014) 124:2354–61. doi: 10.1182/blood-2014-05-578963

8. Tomita N, Tokunaka M, Nakamura N, Takeuchi K, Koike J, Motomura S, et al. Clinicopathological features of lymphoma/leukemia patients carrying both BCL2 and MYC translocations. *Haematologica* (2009) 94:935–43. doi: 10.3324/haematol.2008.005355

9. Barrans S, Crouch S, Smith A, Turner K, Owen R, Patmore R, et al. Rearrangement of MYC is associated with poor prognosis in patients with diffuse large b-cell lymphoma treated in the era of rituximab. *J Clin Oncol* (2010) 28:3360–5. doi: 10.1200/JCO.2009.26.3947

10. Green TM, Young KH, Visco C, Xu-Monette ZY, Orazi A, Go RS, et al. Immunohistochemical double-hit score is a strong predictor of outcome in patients with diffuse large b-cell lymphoma treated with rituximab plus cyclophosphamide, doxorubicin, vincristine, and prednisone. *J Clin Oncol* (2012) 30:3460–7. doi: 10.1200/JCO.2011.41.4342

11. Landsburg DJ, Falkiewicz MK, Petrich AM, Chu BA, Behdad A, Li S, et al. Sole rearrangement but not amplification of MYC is associated with a poor prognosis in patients with diffuse large b cell lymphoma and b cell lymphoma unclassifiable. *Br J Haematol* (2016) 175:631–40. doi: 10.1111/bjh.14282

12. Landsburg DJ, Nasta SD, Svoboda J, Morrissette JJ, Schuster SJ. 'Double-hit' cytogenetic status may not be predicted by baseline clinicopathological characteristics and is highly associated with overall survival in b cell lymphoma patients. *Br J Haematol* (2014) 166:369–74. doi: 10.1111/bjh.12901

13. Aurer I, Dreyling M, Federico M, Tilly H, Linton K, Kimby E, et al. Double hit lymphoma diagnosis and treatment in Europe-a cross-sectional survey of clinical practice by the EHA lymphoma working party (EHA LyG). *Hemasphere* (2020) 4:e481. doi: 10.1097/HS9.0000000000000481

14. Dunleavy K. Double-hit lymphoma: optimizing therapy. *Hematol Am Soc Hematol Educ Program* (2021) 2021:157–63. doi: 10.1182/hematology.2021000247

15. Li L-R, Wang L, He Y-Z, Young KH. Current perspectives on the treatment of double hit lymphoma. *Expert Rev Hematol* (2019) 12:507–14. doi: 10.1080/17474086.2019.1623020

16. National Comprehensive Cancer Network. *B cell lymphoma*. Available at: https://www.nccn.org/professionals/physician_gls/pdf/b-cell.pdf.

17. Neelapu SS, Dickinson M, Munoz J, Ulrickson ML, Thieblemont C, Oluwole OO, et al. Axicabtagene ciloleucel as first-line therapy in high-risk large b-cell lymphoma: the phase 2 ZUMA-12 trial. *Nat Med* (2022) 28:735–42. doi: 10.1038/s41591-022-01731-4

18. Tisi MC, Ferrero S, Dogliotti I, Tecchio C, Carli G, Novo M, et al. MYC rearranged aggressive b-cell lymphomas: a report on 100 patients of the fondazione italiana linfomi (FIL). *Hemasphere* (2019) 3:e305. doi: 10.1097/HS9.0000000000000305

19. Zeremski V, McPhail ED, Habermann TM, Schieppati F, Gebauer N, Vassilakopoulos T, et al. Treatment intensification might not improve survival in high-grade b-cell lymphoma with a concurrent MYC and BCL2 and/or BCL6 rearrangement: a retrospective, multicenter, pooled analysis. *Hematol Oncol* (2023) 1–5. doi: 10.1002/hon.3130

20. Page MJ, McKenzie JE, Bossuyt PM, Boutron I, Hoffmann TC, Mulrow CD, et al. The PRISMA 2020 statement: an updated guideline for reporting systematic reviews. *BMJ* (2021) 372:n71. doi: 10.1136/bmj.n71

21. Richardson WS, Wilson MC, Nishikawa J, Hayward RS. The well-built clinical question: a key to evidence-based decisions. *ACP J Club* (1995) 123:A12–3. doi: 10.7326/ACPJC-1995-123-3-A12

22. Slim K, Nini E, Forestier D, Kwiatkowski F, Panis Y, Chipponi J. Methodological index for non-randomized studies (minors): development and validation of a new instrument. *ANZ J Surg* (2003) 73:712–6. doi: 10.1046/j.1445-2197.2003.02748.x

23. National Heart, Blood and Lung Institute. Available at: https://www.nhlbi.nih.gov/health-topics/study-quality-assessment-tools.

24. Parmar MK, Torri V, Stewart L. Extracting summary statistics to perform meta-analyses of the published literature for survival endpoints. *Stat Med* (1998) 17:2815–34. doi: 10.1002/(SICI)1097-0258(19981230)17:24<2815::AID-SIM110>3.0.CO;2-8

25. de Jonge AV, Roosma TJ, Houtenbos I, Vasmel WL, van de Hem K, de Boer JP, et al. Diffuse large b-cell lymphoma with MYC gene rearrangements: current perspective on treatment of diffuse large b-cell lymphoma with MYC gene rearrangements; case series and review of the literature. *Eur J Cancer* (2016) 55:140–6. doi: 10.1016/j.ejca.2015.12.001

26. Künstner A, Witte HM, Riedl J, Bernard V, Stölting S, Merz H, et al. Mutational landscape of high-grade b-cell lymphoma with MYC-, BCL2 and/or BCL6 rearrangements characterized by whole-exome sequencing. *Haematologica* (2022) 107:1850–63. doi: 10.3324/haematol.2021.279631

27. McPhail ED, Maurer MJ, Macon WR, Feldman AL, Kurtin PJ, Ketterling RP, et al. Inferior survival in high-grade b-cell lymphoma with MYC and BCL2 and/or BCL6 rearrangements is not associated with MYC/IG gene rearrangements. *Haematologica* (2018) 103:1899–907. doi: 10.3324/haematol.2018.190157

28. Miyaoka M, Kikuti YY, Carreras J, Itou A, Ikoma H, Tomita S, et al. AID is a poor prognostic marker of high-grade b-cell lymphoma with MYC and BCL2 and/or BCL6 rearrangements. *Pathol Int* (2022) 72:35–42. doi: 10.1111/pin.13182

29. Schieppati F, Balzarini P, Fisogni S, Re A, Pagani C, Bianchetti N, et al. An increase in MYC copy number has a progressive negative prognostic impact in patients with diffuse large b-cell and high-grade lymphoma, who may benefit from intensified treatment regimens. *Haematologica* (2020) 105:1369–78. doi: 10.3324/haematol.2019.223891

30. Yoshida M, Ichikawa A, Miyoshi H, Kiyasu J, Kimura Y, Arakawa F, et al. Clinicopathological features of double-hit b-cell lymphomas with MYC and BCL2, BCL6 or CCND1 rearrangements. *Pathol Int* (2015) 65:519–27. doi: 10.1111/pin.12335

31. Zhang F, Li L, Zhang L, Li X, Fu X, Wang X, et al. Prognostic analysis of CD5 expression in double-hit diffuse large b-cell lymphoma and effectiveness comparison in patients treated with dose-adjusted EPOCH plus rituximab/R-CHOP regimens. *Blood Lymphat Cancer* (2019) 9:33–43. doi: 10.2147/BLCTT.S216292

32. Zhang J, Weng Z, Huang Y, Li M, Wang F, Wang Y, et al. High-grade b-cell lymphoma with MYC, BCL2, and/or BCL6 Translocations/Rearrangements: clinicopathologic features of 51 cases in a single institution of south China. *Am J Surg Pathol* (2020) 44:1602–11. doi: 10.1097/PAS.0000000000001577

33. Dunleavy K, Fanale MA, Abramson JS, Noy A, Caimi PF, Pittaluga S, et al. Dose-adjusted EPOCH-r (etoposide, prednisone, vincristine, cyclophosphamide, doxorubicin, and rituximab) in untreated aggressive diffuse large b-cell lymphoma with MYC rearrangement: a prospective, multicentre, single-arm phase 2 study. *Lancet Haematol* (2018) 5:e609–17. doi: 10.1016/S2352-3026(18)30177-7

34. McMillan AK, Phillips EH, Kirkwood AA, Barrans S, Burton C, Rule S, et al. Favourable outcomes for high-risk diffuse large b-cell lymphoma (IPI 3-5) treated with front-line r-CODOX-M/R-IVAC chemotherapy: results of a phase 2 UK NCRI trial. *Ann Oncol* (2020) 31:1251–9. doi: 10.1016/j.annonc.2020.05.016

35. Leppä S, Jørgensen J, Tierens A, Meriranta L, Østlie I, de Nully Brown P, et al. Patients with high-risk DLBCL benefit from dose-dense immunochemotherapy combined with early systemic CNS prophylaxis. *Blood Adv* (2020) 4:1906–15. doi: 10.1182/bloodadvances.2020001518

36. Chamuleau ME, Burggraaff CN, Nijland M, Bakunina K, Mous R, Lugtenburg PJ, et al. Treatment of patients with MYC rearrangement positive large b-cell lymphoma with r-CHOP plus lenalidomide: results of a multicenter HOVON phase II trial. *Haematologica* (2020) 105:2805–12. doi: 10.3324/haematol.2019.238162

37. Davies A, Cummin TE, Barrans S, Maishman T, Mamot C, Novak U, et al. Gene-expression profiling of bortezomib added to standard chemoimmunotherapy for diffuse large b-cell lymphoma (REMoDL-b): an open-label, randomised, phase 3 trial. *Lancet Oncol* (2019) 20:649–62. doi: 10.1016/S1470-2045(18)30935-5

38. Howlett C, Snedecor SJ, Landsburg DJ, Svoboda J, Chong EA, Schuster SJ, et al. Front-line, dose-escalated immunochemotherapy is associated with a significant progression-free survival advantage in patients with double-hit lymphomas: a systematic review and meta-analysis. *Br J Haematol* (2015) 170:504–14. doi: 10.1111/bjh.13463

39. Huang S, Nong L, Wang W, Liang L, Zheng Y, Liu J, et al. Prognostic impact of diffuse large b-cell lymphoma with extra copies of MYC, BCL2 and/or BCL6: comparison with double/triple hit lymphoma and double expressor lymphoma. *Diagn Pathol* (2019) 14:81. doi: 10.1186/s13000-019-0856-7

40. Sermer D, Bobillo S, Dogan A, Zhang Y, Seshan V, Lavery JA, et al. Extra copies of MYC, BCL2, and BCL6 and outcome in patients with diffuse large b-cell lymphoma. *Blood Adv* (2020) 4:3382–90. doi: 10.1182/bloodadvances.2020001551

41. Lenz G, Wright G, Dave SS, Xiao W, Powell J, Zhao H, et al. Stromal gene signatures in large-b-cell lymphomas. *N Engl J Med* (2008) 359:2313–23. doi: 10.1056/NEJMoa0802885

42. Magnusson T, Narkhede M, Mehta A, Goyal G. No difference in overall survival between r-CHOP and r-EPOCH among patients with advanced stage MYC-rearranged, double hit, or triple hit diffuse large b-cell lymphoma. In: *EHA 2021 virtual congress* (2021).

43. Barraclough A, Alzahrani M, Ettrup MS, Bishton M, van Vliet C, Farinha P, et al. COO and MYC/BCL2 status do not predict outcome among patients with stage I/II DLBCL: a retrospective multicenter study. *Blood Adv* (2019) 3:2013–21. doi: 10.1182/bloodadvances.2019000251

44. Torka P, Kothari SK, Sundaram S, Li S, Medeiros LJ, Ayers EC, et al. Outcomes of patients with limited-stage aggressive large b-cell lymphoma with high-risk cytogenetics. *Blood Adv* (2020) 4:253–62. doi: 10.1182/bloodadvances.2019000875

45. Kumar A, Lunning MA, Zhang Z, Migliacci JC, Moskowitz CH, Zelenetz AD. Excellent outcomes and lack of prognostic impact of cell of origin for localized diffuse large b-cell lymphoma in the rituximab era. *Br J Haematol* (2015) 171:776–83. doi: 10.1111/bjh.13766

46. Li S, Saksena A, Desai P, Xu J, Zuo Z, Lin P, et al. Prognostic impact of history of follicular lymphoma, induction regimen and stem cell transplant in patients with MYC/BCL2 double hit lymphoma. *Oncotarget* (2016) 7:38122–32. doi: 10.18632/oncotarget.9473

47. Ye Q, Xu-Monette ZY, Tzankov A, Deng L, Wang X, Manyam GC, et al. Prognostic impact of concurrent MYC and BCL6 rearrangements and expression in *de novo* diffuse large b-cell lymphoma. *Oncotarget* (2016) 7:2401–16. doi: 10.18632/oncotarget.6262

48. Cucco F, Barrans S, Sha C, Clipson A, Crouch S, Dobson R, et al. Distinct genetic changes reveal evolutionary history and heterogeneous molecular grade of DLBCL with MYC/BCL2 double-hit. *Leukemia* (2020) 34:1329–41. doi: 10.1038/s41375-019-0691-6

49. Campo E, Jaffe ES, Cook JR, Quintanilla-Martinez L, Swerdlow SH, Anderson KC, et al. The international consensus classification of mature lymphoid neoplasms: a report from the clinical advisory committee. *Blood* (2022) 140:1229–53. doi: 10.1182/blood.2022015851

50. Rosenwald A, Bens S, Advani R, Barrans S, Copie-Bergman C, Elsensohn M-H, et al. Prognostic significance of MYC rearrangement and translocation partner in diffuse Large b-cell lymphoma: a study by the lunenburg lymphoma biomarker consortium. *J Clin Oncol* (2019) 37:3359–68. doi: 10.1200/JCO.19.00743

51. Copie-Bergman C, Cuillière-Dartigues P, Baia M, Briere J, Delarue R, Canioni D, et al. MYC-IG rearrangements are negative predictors of survival in DLBCL patients treated with immunochemotherapy: a GELA/LYSA study. *Blood* (2015) 126:2466–74. doi: 10.1182/blood-2015-05-647602

52. Aukema SM, Kreuz M, Kohler CW, Rosolowski M, Hasenclever D, Hummel M, et al. Biological characterization of adult MYC-translocation-positive mature b-cell lymphomas other than molecular burkitt lymphoma. *Haematologica* (2014) 99:726–35. doi: 10.3324/haematol.2013.091827

53. Chen AI, Leonard JT, Okada CY, Gay ND, Chansky K, Fan G, et al. Outcomes of DA-EPOCH-R induction plus autologous transplant consolidation for double hit lymphoma. *Leuk Lymphoma* (2018) 59:1884–9. doi: 10.1080/10428194.2017.1406085

54. Landsburg DJ, Falkiewicz MK, Maly J, Blum KA, Howlett C, Feldman T, et al. Outcomes of patients with double-hit lymphoma who achieve first complete remission. *J Clin Oncol* (2017) 35:2260–7. doi: 10.1200/JCO.2017.72.2157

55. Maurer MJ, Habermann TM, Shi Q, Schmitz N, Cunningham D, Pfreundschuh M, et al. Progression-free survival at 24 months (PFS24) and subsequent outcome for patients with diffuse large b-cell lymphoma (DLBCL) enrolled on randomized clinical trials. *Ann Oncol* (2018) 29:1822–7. doi: 10.1093/annonc/mdy203

56. Katz DA, Morris JD, Chu MP, David KA, Thieblemont C, Morley NJ, et al. Open-label, phase 2 study of blinatumomab after frontline r-chemotherapy in adults with newly diagnosed, high-risk DLBCL. *Leuk Lymphoma* (2022) 63:2063–73. doi: 10.1080/10428194.2022.2064981

frontiers | Frontiers in Oncology

TYPE Original Research
PUBLISHED 03 August 2023
DOI 10.3389/fonc.2023.1159484

OPEN ACCESS

EDITED BY
Gaël Roué,
Josep Carreras Leukaemia Research Institute (IJC), Spain

REVIEWED BY
Malgorzata Bobrowicz,
Medical University of Warsaw, Poland
David Chiron,
INSERM U1232 Centre de Recherche en Cancérologie et Immunologie Nantes Angers (CRCINA), France

*CORRESPONDENCE
Brian Lee
brian.lee1@northwestern.edu

†Deceased

RECEIVED 06 February 2023
ACCEPTED 04 July 2023
PUBLISHED 03 August 2023

CITATION
Lee B, Pierpont T, August A and Richards K (2023) Monoclonal antibodies binding to different epitopes of CD20 differentially sensitize DLBCL to different classes of chemotherapy. *Front. Oncol.* 13:1159484. doi: 10.3389/fonc.2023.1159484

Monoclonal antibodies binding to different epitopes of CD20 differentially sensitize DLBCL to different classes of chemotherapy

Brian Lee[1]*, Tim Pierpont[2], Avery August[2] and Kristy Richards[3†]

[1]Department of Biochemistry and Molecular Genetics, Northwestern University Feinberg School of Medicine, Chicago, IL, United States, [2]Department of Microbiology and Immunology, College of Veterinary Medicine, Cornell University, Ithaca, NY, United States, [3]Department of Biomedical Sciences, College of Veterinary Medicine, Cornell University, Ithaca, NY, United States

Introduction: Rituximab (R), an anti-CD20 monoclonal antibody (mAb) and the world's first approved antibody for oncology patients, was combined with the CHOP chemotherapy regimen and markedly improved the prognosis of all B- cell–derived lymphomas, the most common hematological malignancy worldwide. However, there is a 35% disease recurrence with no advancement in the first-line treatment since R was combined with the archetypal CHOP chemotherapy regimen nearly 30 years ago. There is evidence that R synergizes with chemotherapy, but the pharmacological interactions between R and CHOP or between newer anti-CD20 mAbs and CHOP remain largely unexplored.

Methods: We used *in vitro* models to score pharmacological interactions between R and CHOP across various lymphoma cell lines. We compared these pharmacological interactions to ofatumumab, a second-generation anti-CD20 mAb, and CHOP. Lastly, we used RNA-sequencing to characterize the transcriptional profiles induced by these two antibodies and potential molecular pathways that mediate their different effects.

Results: We discovered vast heterogeneity in the pharmacological interactions between R and CHOP in a way not predicted by the current clinical classification. We then discovered that R and ofatumumab differentially synergize with the cytotoxic and cytostatic capabilities of CHOP in separate distinct subsets of B-cell lymphoma cell lines, thereby expanding favorable immunochemotherapy interactions across a greater range of cell lines beyond those induced by R-CHOP. Lastly, we discovered these two mAbs differentially modulate genes enriched in the JNK and p38 MAPK family, which regulates apoptosis and proliferation.

Discussion: Our findings were completely unexpected because these mAbs were long considered to be biological and clinical equivalents but, in practice, may perform better than the other in a patient-specific manner. This finding may have immediate clinical significance because both immunochemotherapy combinations

are already FDA-approved with no difference in toxicity across phase I, II, and III clinical trials. Therefore, this finding could inform a new precision medicine strategy to provide additional therapeutic benefit to patients with B-cell lymphoma using immunochemotherapy combinations that already meet the clinical standard of care.

KEYWORDS

rituximab, ofatumumab, chemotherapy, R-CHOP, B-cell lymphoma, DLBCL

Introduction

Non-Hodgkin's lymphoma is the most common hematological malignancy worldwide, encompassing a heterogenous group of disorders that rank fifth highest in cancer mortality and seventh in cancer incidence (1). Rituximab (R) is the first monoclonal antibody (mAb) used in oncology treatment, and its addition to the CHOP [cyclophosphamide (C); doxorubicin (H), a topoisomerase II inhibitor; vincristine (O), an anti-microtubule drug; and prednisone (P), a glucocorticoid steroid] combination chemotherapy regimen doubled the average cure rates from approximately 30% to 60% of patients with non-Hodgkin's B-cell lymphoma without increasing toxicity (2–6). R was subsequently combined with other chemotherapy regimens across all lymphoma subtypes, and these new immunochemotherapy combinations improved the prognosis of all B-cell–derived lymphoproliferative diseases (7–12). However, at least eight clinical trials utilizing either more intensive chemotherapy, small-molecule inhibitors, or newer mAbs have all generally failed to improve upon the R-CHOP regimen success (13–21). These combinations had either worse or similar clinical outcomes or higher toxic fatality rates. Therefore, despite over 20 years since R-CHOP was introduced, clinical protocol for the first-line treatment of diffuse large B-cell lymphoma (DLBCL) has remained virtually unchanged. R is an anti-CD20 antibody whose binding induces cell death through four different mechanisms: 1) direct signaling induced cell death, 2) complement-dependent cytotoxicity (CDC), 3) antibody-dependent cell-mediated cytotoxicity (ADCC), and 4) antibody-dependent phagocytosis (ADP) (22). Newer anti-CD20s, ofatumumab (OF) and obinutuzumab, which preferentially activate CDC and ADCC, respectively, were combined with conventional chemotherapy but did not improve prognosis in patients with DLBCL in their respective 2017 and 2019 phase III clinical trials compared with R-CHOP (18–21).

There is evidence that mAbs such as R sensitizes or confers resistance in B-cell cancers to chemotherapeutics through modulation of anti-apoptotic factors (23–25). Strategies that downregulate these anti-apoptotic factors may have a high therapeutic potential because this approach has already been applied to other cancers, leading to FDA-approved drugs such as venetoclax to treat leukemia (26). However, interactions between R and CHOP or between newer anti-CD20s and CHOP have not been studied, despite the potential that differential interactions could lead to better or worse outcomes depending on the mAb choice for specific patients. Furthermore, the direct mechanisms of cell death induced by anti-CD20s are poorly understood (22). Therefore, understanding how R and other anti-CD20 mAbs interact with CHOP can advise new therapeutic strategies and even help elucidate anti-CD20's direct biological effects.

Here, we scored and characterized the pharmacological interactions between R and the individual components of CHOP. We then compared these interactions to those between OF and CHOP to identify any potential differential immunochemotherapy interactions. Last, we compared the transcriptional profiles of R and OF binding to mechanistically understand their differences.

Materials and methods

Cell lines and cell culture

Activated B-cell (ABC) subtypes (HBL1, U2932, SUDHL2, and TMD8) and germinal center B-cell (GCB) subtypes (SUDHL4, HT, LY18, and WSL-DLCL2) were maintained in Roswell Park Memorial Institute (RPMI) 1640 with 2 mM L-glutamine (Gibco), supplemented with 10% Fetal bovine serum (FBS) heat-inactivated (HI) at 56°C for 30 min (Gibco), penicillin (100 µg/mL) and streptomycin (100 µg/mL) (Gibco), and 1 mM N-2-hydroxyethylpiperazine-N-2-ethane sulfonic acid (HEPES) (Gibco). Cells were incubated at 37°C with 5% CO_2 and maintained in a log growth phase. Cell viability and growth phase were measured using trypan blue exclusion assay, and cells were only used in a log growth phase with viability greater than 90% for all cell lines.

Reagents

R (Rituxan™, Genentech, Inc.) and OF (Arzerra™, GlaxoSmithKline, Inc.) were obtained through the North Carolina Cancer Hospital pharmacy. Cyclophosphamide was replaced with its active metabolite 4-hydroperoxycyclophosphamide (Toronto Research Chemicals), which was dissolved in Dimethyl sulfoxide

(DMSO) purged with nitrogen gas to make a stock concentration of 20 mM and sealed in vials with nitrogen gas at −80°C. Doxorubicin and vincristine (Selleckchem) were dissolved in Phosphate buffered saline (PBS) to make a stock concentration of 20 mM and were stored at −80°C. Prednisone was replaced with a more soluble biological and clinical analog, dexamethasone (Selleckchem), which was dissolved in PBS to make a stock concentration of 20 mM and stored at −80°C. We made this substitution because prednisone is metabolically converted to the more biologically active form prednisolone, in which the 11-C ketone is reduced to a more soluble 11-C hydroxyl, and dexamethasone has this more soluble substituent conferring its similar properties to prednisone in treating hematological malignancies (27). Pooled AB human serum (HS) was obtained from Sigma-Aldrich.

Dose–response curves and analysis of pharmacological interactions

Survival dose–response curves for each of the CHOP drugs, with or without R, were generated to characterize the pharmacological interactions between R and CHOP. Cells were resuspended in fresh media the day before and seeded at 1.0×10^5 cells/mL in 96-well flat bottom plates and treated for 48 h with varying concentrations of chemotherapeutic, with or without R (at 20 μg/mL) in triplicate. This concentration of R was used because pharmacokinetic studies have shown that R serum levels were, on average, 20.3 μg/mL 3 months after their infusion (28). Viability was measured using a CellTiter-Blue reduction assay by adding 10% CellTiter-Blue at 45.5 h after treatment and taking fluorescence readings at 540 nm/620 nm on a microplate reader (BioTek Synergy 2) at 46 and 48 h after treatment. Baseline fluorescent values at 46 h were subtracted from 48-h values to measure change in reduction potentials. By means of reduction potential, dose–response curves were made for each of the CHOP drugs with and without R (20 μg/mL) for two ABC subtypes (U2932 and HT) and two GCB subtypes (HBL1 and SUDHL4).

The chemotherapeutic-only dose–response curve was standardized to a medium-only control, and the R + chemo dose–response curve was standardized to an R-treated control by dividing fluorescent output of these two treatment groups by their respective controls. A 15% DMSO all-kill control was subtracted from both the numerator and denominator. Therefore, the viability was calculated by the following equations:

$$Viability\ \ (/control) = \frac{\Delta Fluorescence_{chemo} - \Delta Fluorescence_{DMSO}}{\Delta Fluorescence_{media} - \Delta Fluorescence_{DMSO}}$$

$$Viability\ \ (/control) = \frac{\Delta Fluorescence_{R+chemo} - \Delta Fluorescence_{DMSO}}{\Delta Fluorescence_{R} - \Delta Fluorescence_{DMSO}}$$

To design a dose–response curve with least squares fit, we transformed the drug concentrations to logarithmic scale and standardize viability to run between 0% and 100%. We then used the following equation to generate a sigmoidal regression fit into our dose–response data, where Hill slope coefficient is determined on the basis of the data

$$Viability = \frac{100}{1 + 10^{\log(IC50 - [drug] \times Hill\ \ Slope)}}$$

To assess the magnitude and statistical significance of these pharmacological interactions, we interpolated Half-maximal inhibitory concentration (IC_{50}) values based on our nonlinear regression equation and their associated p-value using extra-sum-of-squares F-test. Last, we use the combination index analysis based on the Loewe additivity criteria and the response additivity analysis to score the pharmacological interactions as synergistic or antagonistic.

Growth inhibition and cell death analysis

Trypan blue exclusion assay was used to characterize the pharmacological interactions observed in the experiments above. Cells were treated as described above and mixed with an equal volume of 0.4% trypan blue dye solution, and viability was determined by light microscopy. Percent dead was calculated as proportion of dead cells over total cells, whereas growth inhibition was calculated as total cells, both dead and alive, over total cells in medium-only conditions. The results were representative of three independent experiments.

Complement-dependent cytotoxicity

CDC assays were performed using pooled human AB serum (Krackler Scientific) and R (20 μg/mL). Cell lines were incubated with varying proportions of HI FBS and HS totaling 10% net serum that induced approximately 50% cell death (10% HS and no HI FBS for HBL1 and HT, 5% HS and 5% HI FBS for U2932, and 2% HS and 8% HI FBS for SUDHL4). As a control, cells were incubated in HI HS (HI; 56°C for 30 min) and HI FBS in analogous concentrations. HI FBS was used to recapitulate growth conditions as similarly as possible to those used to generate dose–response curves and pharmacological analysis in Figure 1. To investigate the pharmacological interactions between CDC and chemotherapeutic, dose–response curves were created by treating cells with chemo as described above with or without CDC (HS + R + chemo and HS + chemo). As a control comparison, cells were also treated with HI + R + chemo and HI + chemo. Viability was measured using CellTiter-Blue as described above, and the pharmacological interactions were scored as described above on the basis of the relative curve shifts.

Focused comparison between R + chemo and OF + chemo

Abbreviated experiments comparing differential interactions between R + chemo and OF + chemo were performed by treating all eight cell lines with physiologically relevant concentrations of C (<27 μM), H (<1.1 μM), O (9.3×10^{-2} μM), and P (3.1×10^3 μM) based on the C_{max} of pharmacokinetic studies for each drug (29–32), with or without R or OF (10 μg/mL). Cell lines were treated for 48 h, and viability was measured using CellTiter-Blue as described earlier.

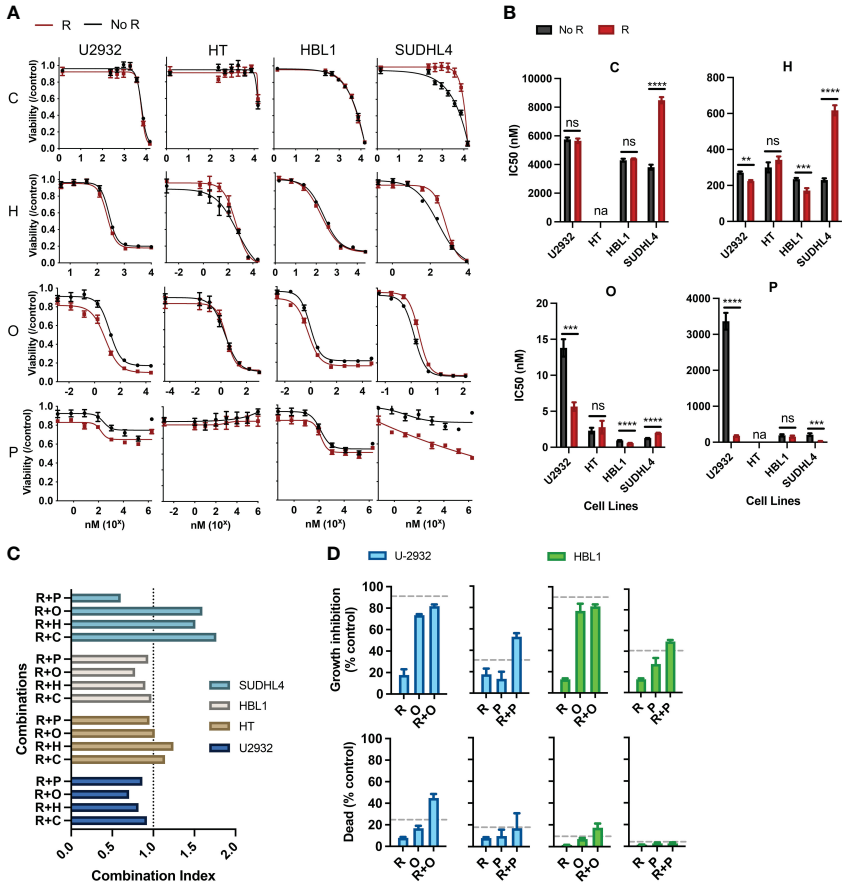

FIGURE 1
Rituximab directly synergizes and antagonizes the cytotoxic and cytostatic potential of chemotherapy. **(A)** Two ABC subtypes (HBL1 and SUDHL4) and two GCB subtypes (U2932 and HT) were treated with one of the CHOP drugs (0–15 μM C, 0–50 μM H, 0–0.125 μM O, and 0–1.8 × 10^3 μM P) with or without R (20 μg/mL) for 48 h, and viability was measured using cell titer reduction assay. C_{max} for each drug are C (<27 μM), H (<1.1 μM), O (9.3 × 10^2 μM), and P (3.1 × 10^3 μM). No R (black curve) was standardized to a media control, whereas R (red curve) was standardized to R-treated group. This figure is representative of at least five experiments performed in triplicates. **(B)** IC_{50} of chemo and R + chemo combinations were also compared. *p < 0.05; **p < 0.01; ***p < 0.001; ****p < 0.0001. ns, not significant; na indicates that IC_{50} was unavailable due to dose–response curves not following sigmoidal relationship necessary for its calculation. **(C)** Combination index of each R + chemo combinations was scored. **(D)** HBL1 and U2932 cells were treated as indicated and trypan blue exclusion assay used to determine the percent of dead cells and percentage growth inhibition relative to a medium-only control. The dashed lines represent the expected additive effect of the sum of the individual drugs. This figure is representative of at least three experiments performed in triplicates.

RNA extraction and gene expression analysis

TMD8 and U2932 cells were split and cultured separately for a week to create two biological replicates per cell line. These replicates were then treated with R, OF, or human Immunoglobulin G1 (IgG1) isotype (SouthernBiotech) control for 4 h, followed by collection of RNA for sequencing. RNA from 8.0 × 10^7 TMD8 and U2932 cells was extracted using the standard TRIzol protocol. Agarose gel (1%) was used to validate intact RNA by identifying the 28S and 18S ribosomal RNA bands. The library preparation, sequencing, and initial quality check were performed by the Cornell TREx sequencing facility (https://rnaseqcore.vet.cornell.edu/index.html). Specifically, fastq files are first processed with trim-galore to remove low quality bases and adapter sequences. Trimmed reads are then aligned to a human reference genome from Ensembl using STAR. Last, raw counts generated by STAR for annotated genes were analyzed with DESeq2.

Reverse transcription/quantitative PCR

RNA was extracted using TRIzol reagent (Invitrogen) or an RNAeasy kit (Invitrogen), and Complementary DNA (cDNA) was generated using a You Prime First-beads kit (GE Healthcare). Quantitative PCR was then performed using a 7500 Fast Real-Time PCR instrument (Applied Biosystems). Data were analyzed using the comparative threshold cycle $2^{-\Delta\Delta CT}$ method, and the values were expressed as fold change compared to respective cell lines treated with IgG-isotype antibody. Primer sequences for eight randomly selected genes are provided in Table 1.

TABLE 1 Validation of RNA sequencing (RNA-seq) using quantitative reverse transcription (qRT)-PCR.

Gene	Name	Primers	
ATP2A3	ATPase sarcoplasmic/endoplasmic reticulum Ca^{2+} transporting 3	Forward	5′-GCTCCAGATATCTCTGCCTGTC-3′
BCL2A1	BCL2-related protein A1	Forward	5′-TATGCTGGTAGAGTCAGTGGC-3′
		Reverse	5′-TATGCTGGTAGAGTCAGTGGC-3′
CDKN2C	Cyclin-dependent kinase inhibitor 2C	Forward	5′ATTTGGAAGGACTGCGCTGC-3′
		Reverse	5′-GCAGTCTCCTGGCAATCTCG-3′
DUSP5	Dual-specificity phosphatase A5	Forward	5′-CTGCAGCTCCTGTGGGAC-3′
		Reverse	5′-CACTGCCGAGGTAGAGGAAG-3′
RPSKA5	Ribosomal protein S6 kinase A5	Forward	5′-GGAGAGATTGTGCTTGCCCT-3′
		Reverse	5′-TCTGTCAGCACCACATGGC-3′
KCNMB4	Potassium calcium-activated channel subfamily M regulatory beta subunit 4	Forward	5′-GGTTCCCAGCCATTTACTTGC-3′
		Reverse	5′-CATGAGTGCGATGCAGAAGC-3′
NDFIP	Thioredoxin-interacting protein	Forward	5′-GGCAGCTGCTCATAGAACAAG-3′
		Reverse	5′-AAGGAATGTCGGGTTGATGC-3′
NLRC3	NLR family card protein containing 3	Forward	5′-TCGAGGCCCGGGAGAAC-3′
		Reverse	5′-GCGCCTTGGTGTCTTCATTTG-3′

Pathway enrichment and visual analysis of differentially expressed genes

Kyoto Encyclopedia of Genes and Genomes (KEGG; www.genome.jp/kegg/pathway.html) pathway analysis was conducted to identify the most significant enriched pathways. Differentially expressed genes were mapped onto biologically relevant pathways using their manually annotated pathway database.

Statistical analysis

All values are presented as mean ± standard deviation of the mean (SD) of data from experiments performed at least in triplicate. For comparisons between two groups, unpaired Student's t-test was used. P-values for IC_{50}'s were calculated using extra-sum-of-squares F-test. For multiple comparisons, one-way ANOVA was used with Bonferroni correction to adjust p-values based on the number of comparisons performed.

Results

Rituximab directly potentiates or antagonizes the cytotoxic and cytostatic potential of chemotherapy

R has been shown to affect chemotherapeutic responses separately from its immune effector functions (CDC, ADCC, and ADP), but such interactions within the R-CHOP regimen remain largely unexplored. Therefore, we scored the pharmacological interactions between R and the individual constituents of CHOP using CellTiter-Blue reduction assays, which measure the cumulative metabolic potential of living cells after treatment. We considered drug interactions in terms of potentiation and antagonism based on the criteria set by Gessner (33). Namely, we defined potentiation as a non-killing response that enhances killing by another drug and antagonism as a non-active response that reduces killing by another drug. We assigned R as the non-killing drug because previous studies, and our findings, show that R alone induces limited direct killing in most DLBCL cell lines, and this criterion was used to study the effects of R with other chemotherapy drugs (22, 34, 35).

Pharmacodynamic interactions between R and C, H, O, or P were first assessed in two ABC-subtype (U2932 and HT) and two GCB-subtype (HBL1 and SUDHL4) DLBCL. A viability dose–response curve was created with chemotherapy treatment along a concentration range spanning the entire drug effect. Another viability dose–response curve was created across the same concentration range with the addition of R (20 μg/mL). Cells were incubated for 48 h, and cell viability was measured using luminescent reduction assay (CellTiter-Blue). Chemo viability was normalized to untreated viability, whereas R + chemo viability was normalized to R-treated. This strategy removed any killing directly induced by R, thereby allowing for a direct comparison of the chemo-only and R + chemo dose–response curves for pharmacological interactions. Therefore, if the viability curve of R + chemo shifted to the right relative to chemo-only, then viability was higher with the addition of R to chemotherapy, indicating antagonism. If the two curves overlap, then there is no indication of interaction. Last, if the R + chemo viability curve shifted to the left relative to chemo-only, then viability is reduced with the addition of R, indicating a potentiation.

All chemotherapy drugs, with the exception of P, induced a significant loss of viability, with P having more modest effects (Figure 1A). Although P is cytotoxic to DLBCL in the first-line clinical care, the observed limited cytotoxicity in cell culture is consistent with other reported *in vitro* studies, likely reflecting selection for prednisone resistance through the establishment of cell lines from post-treatment patients (36). R potentiated O and P in HBL1 and U2932 but did not interact with chemotherapy in HT. R antagonized C, H, and O in SUDHL4 and potentiated P in SUDHL4 (Figure 1A). Therefore, R + chemo interactions were highly heterogenous, with different cell lines having differential responses to the same drugs, but not in a way predicted by the classical clinical classifications, namely, ABC and GCB subtypes. This heterogeneity in pharmacological interactions, ranging from antagonism to potentiation, was unexpected because R has been characterized as a general potentiator of chemotherapy in the field (22, 34, 35, 37). This heterogeneity in drug response illustrates the wide biological heterogeneity of DLBCL and possibly contributes to the variability in patient response to R-CHOP (38). To further quantify the magnitude and statistical significance of these pharmacological interactions, we compared the IC_{50}'s of C, H, or O, with or without R (Figure 1B). In addition, to assess R + chemo interactions as synergistic or antagonistic, we use combination index analysis based on the Loewe additivity criteria (Figure 1C). Similar to our previous finding, R synergizes and antagonizes with chemotherapy in an ABC- and GCB-independent manner.

Our initial approach so far measured cell viability using CellTiter-Blue assay, which measures the cumulative metabolic reduction of living cells after treatment. Although this assay measures the total metabolism, and therefore viability, of the remaining cell population, it cannot differentiate potentiation and antagonism in terms of the cytotoxic or cytostatic effects. Therefore, we used a trypan blue exclusion assay, able to distinguish cell death from cell growth inhibition, to further characterize observed the pharmacological interactions in terms of the cytotoxic and cytostatic effects (34). We specifically examined interactions between R + O and R + P in HBL1 and U2932 cell lines because these combinations and their respective cell lines showed potentiation. R + O led to additive and greater than additive killing in HBL1 and U2932, respectively (Figure 1D). R + P induced greater than additive growth inhibition in both cell lines. Therefore, R can synergistically augment the cytotoxic and cytostatic potential of chemotherapy.

R also induces cell killing through other immune effector functions, and interactions between these immune mechanisms and chemotherapy remain unexplored in the R-CHOP regimen. Therefore, we investigated the interactions between R induced CDC and chemotherapy. Although we observed that R can kill DLBCL via CDC when HS was present versus when HI HS was present, we observed that CDC does not synergize with nor antagonize chemotherapy (Supplementary Figure 1).

Rituximab and ofatumumab differentially potentiate chemotherapy in DLBCL

There are no studies on the pharmacological interactions between newer anti-CD20 antibodies and CHOP. We therefore compared the pharmacological interactions between R + chemo and OF+ chemo to potentially identify any differences in immunochemotherapy interactions, which may elucidate molecular pathways that drive these immunochemotherapy interactions. R binds to the large loop on the extracellular domain of CD20, whereas OF binds an area distinct from the area bound by

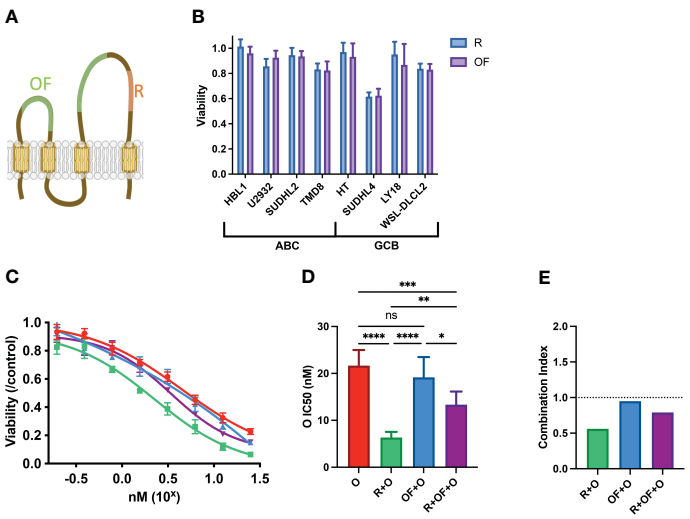

FIGURE 2
Rituximab and ofatumumab induce similar levels of direct killing but differentially synergize with chemotherapy. **(A)** Depiction of R and OF epitopes on CD20. **(B)** Direct killing induced by R and OF across eight cell lines. **(C)** Dose–response curve of O, R + O, OF + O, and R + OF + O. **(D)** IC_{50} of the effect of O, R + O, OF + O, and R + OF + O on U2932 cells. *p < 0.05; **p < 0.01; ***p < 0.001; ****p < 0.0001. ns, not significant. **(E)** Combination index of respective anti-CD20 + chemo combinations. This figure is representative of at least three experiments performed in triplicates.

R, a region encompassing the small and large loop (Figure 2A). However, they both exhibit similar levels of direct killing and performed similarly in clinical trials (18–21). We determined their similarities *in vitro* via measurement of their direct killing on four ABC-subtype DLBCLs (HBL1, U2932, SUDHL2, andTMD8) and four GCB-subtype DLBCLs (HT, SUDHL4, LY18, and WSL-DLBCL2) and found that that they were comparable in their ability to reduce viability (Figure 2B). Although anti-CD20s usually induce limited direct killing, we note that R induces a significant viability reduction in SUDHL4.

Although R and OF seemed to induce similar direct effects, we compared their pharmacological interactions with chemotherapy. Because we previously observed that R potentiated chemotherapy in U2932, we treated U2932 with different doses of O alone, in combination with R and in combination with OF (Figure 2C). Unexpectedly, despite R and OF inducing similar levels of direct killing, they differentially potentiated killing by O. R potentiated O to a greater extent than OF. We also combined R + OF + O to determine whether R and OF together potentiate chemotherapy in an additive or synergistic manner (Figure 2C). We find that these two antibodies sensitized U2932 to chemotherapy intermediate between R + O and R + OF. These findings that R potentiated O in U2932, OF potentiated O to a more limited extent, and combining the two anti-CD20s with O led to an intermediate effect may suggest that R and OF interfere with one another for their respective CD20 epitope and that simply giving them both together would not compensate for any differential interactions with CHOP. This interference could possibly be due to the relatively small size of CD20, causing R and OF to sterically interfere with one another for their respective epitopes (39). To quantify the magnitude and the statistical significance of these differences, we compared the IC_{50}'s of these of these immunochemotherapy

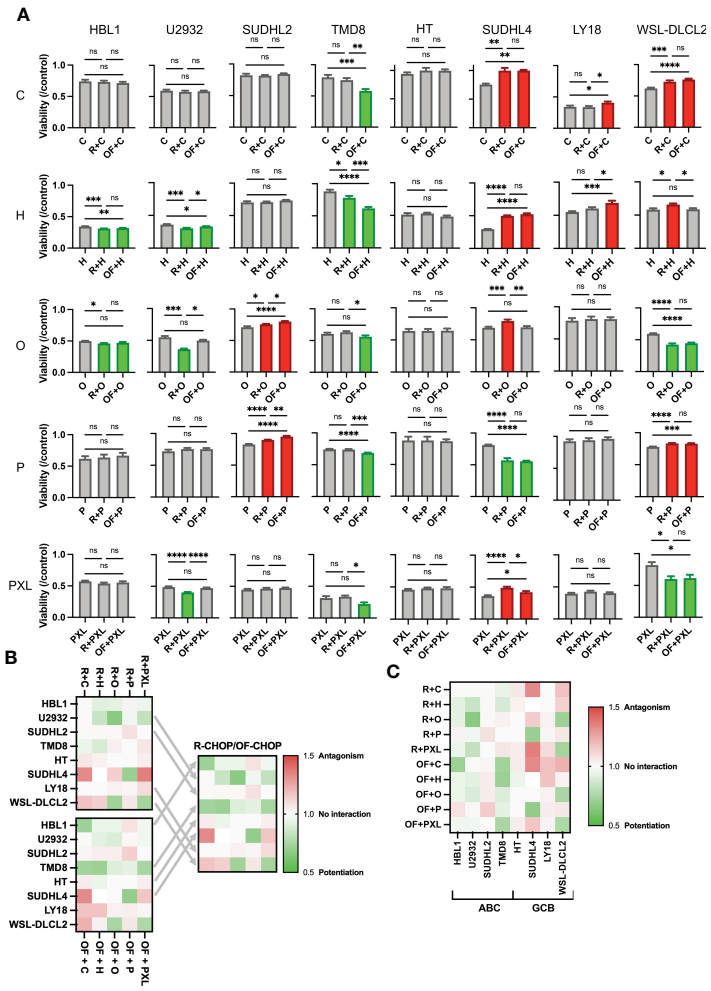

FIGURE 3
Rituximab and ofatumumab differentially synergize with chemotherapy, thereby expanding favorable immunochemotherapy interactions across a greater range of cell lines versus R-CHOP alone. **(A)** Comparison of the effect of R + CHOP versus OF + CHOP interactions across eight cell lines. For a given graph, the left bar represents viability of chemo-only, the middle bar represents R + chemo, and the right bar represents OF + chemo. Paclitaxel (PXL) was also tested. Green indicates potentiation, red indicates antagonism, and gray indicates no interaction. One-way ANOVA was used with p-value adjusted using Bonferroni corrections for multiple comparisons. *p < 0.05; **p < 0.01; ***p < 0.001; ****p < 0.0001. ns, not significant. This figure is representative of at least three experiments. **(B)** Heat map displaying combination indexes using R-CHOP only, OF-CHOP only, and cell line-tailored use of anti-CD20s with CHOP. **(C)** Heat map globally displaying combination indexes using either of the two mAbs with CHOP.

interactions (Figure 2D). In addition, we use combination index analysis based on the Loewe additivity criteria and observe that R synergizes with chemotherapy, whereas OF does not (Figure 2E).

To determine whether this difference in pharmacological interaction was occurring in a U2932 cell–specific manner, all other seven cell lines mentioned previously were treated using a single physiologically relevant dose of one of the CHOP drugs independently or in combination with R or OF. Physiological concentrations were based on the C_{max} of each drug based on pharmacokinetic studies C (<27 μM), H (<1.1 μM), O (9.3×10^{-2} μM), and P (3.1×10^{3} μM) (29–32). R + Paclitaxel (PXL) was also examined as previous published studies demonstrated that R + PXL synergistically induces apoptosis (40). R + chemo and OF + chemo were compared to a chemo-only treatment group to score pharmacological interactions. R + chemo and OF + chemo were then compared to each other to score differential interactions between the two anti-CD20 mAbs. Although we found that R and OF induced comparable levels of direct killing, they unexpectedly potentiated chemotherapy differentially in six of eight cell lines (Figure 3A). R exhibited more favorable interactions with chemotherapy in U2932 (ABC), SUDHL2 (ABC), and LY18 (GCB), whereas OF exhibited more favorable chemotherapy interactions in TMD8 (ABC), SUDHL4 (GCB), and WSL-DLCL2 (GCB). Using the preferred anti-CD20 antibody along with chemotherapy reduced or eliminated antagonism and enhanced or induced potentiation with at least one of the CHOP drugs and all four in some cases. Therefore, tailored use of these anti-CD20 mAbs to each cell line expanded therapeutically favorable immunochemotherapy interactions across a greater range of cell lines than using R-CHOP or OF-CHOP alone. The expansion of synergy through cell line–specific use of these anti-CD20s with chemotherapy is illustrated through a heat map of the combination index of all pharmacological interactions (Figure 3B). Tailored use of these antibodies leads to expansion of synergy (green) and reduction in antagonism (red).

Last, a heat map of all pharmacological interactions using combination index analysis displays these interactions globally (Figure 3C). From this perspective, we observe that anti-CD20s preferentially synergize chemotherapy in the ABC subtype and antagonize chemotherapy in the GCB subtype.

Comparison of gene expression profiles induced by rituximab and ofatumumab

Our finding that R and OF differentially synergize with CHOP in a cell line–specific manner suggests that additional biomarkers that predict the differential response are needed before any trials can be considered. To this end, we investigated the transcriptional profiles of R and OF to determine whether changes could help elucidate the mechanisms behind these pharmacological differences. We analyzed the transcriptomes of cell lines that showed favorable interactions using either R + chemo or OF + chemo. Because U2932 exhibited favorable interactions using R + chemo combinations and TMD8 showed favorable interactions using OF + chemo interactions, we analyzed the gene expression profiles induced by R and OF for these two cell lines. Four hours was chosen as the incubation time because it was the earliest time point at which differential pharmacological interactions were detected, thereby allowing us to identify the earliest transcriptional profiles that drive pharmacological differences (data not shown). To validate our RNA sequencing data, we measured the gene expression levels of eight randomly selected genes using qRT–PCR and compared them to those found using RNA sequencing (Supplementary Figure 2).

Fifty of the most variably expressed genes were hierarchically clustered on a heat map to visualize the global differences between cell lines treated with IgG isotype, R, or OF (Figure 4A). The heat maps show distinct gene expression profiles between cells treated with IgG isotype and anti-CD20 antibody but far smaller differences in gene expression profiles between cells treated with either R or OF.

Next, Venn diagrams of gene expression profiles were generated to quantify the number of upregulated and downregulated genes induced by R and OF (Figures 4B, C). In U2932, although both mAbs caused substantial changes compared to the isotype control, R and OF induced remarkably similar gene expression profiles compared to each other. R upregulated 723 genes and downregulated 530 genes, and OF upregulated 737 genes and downregulated 608 genes. There was only one differentially expressed gene between R and OF at a false discovery rate (FDR) of 0.3. For TMD8, R and OF induced substantial transcriptional changes compared to the isotype control and had more different gene expression profiles compared to each other. R upregulated 697 genes and downregulated 649 genes, and OF upregulated 692 genes and downregulated 539 genes. R preferentially upregulated 3 genes versus OF, whereas OF preferentially upregulated 19 genes versus R at an FDR = 0.10, a threshold used in previous cancer drug studies (41–46).

We then used volcano plots to show the top 10 most significant differentially expressed genes induced by R and OF (Figure 4D). In U2932, R preferentially downregulated Deltex E3 Ubiquitin Ligase 2 (DTX2) compared to OF. In TMD8, OF preferentially upregulated genes associated with apoptosis and chemosensitization (Synaptojanin 2 (SYNJ2), Cathepsin D (CTSD), TNF alpha induced protein 8 like 1 (TNFAIP8L1), and Chromosome 8 Open Reading Frame 82 (C8orf82)) and growth inhibition (transforming growth factor-beta 1 (TGFB1), Interleukin 4-induced gene-1 (IL4I1), and Kruppel-like transcription factor 2 (KLF2)) in DLBCLs compared to R. In summary, our data suggests that there is strong concordance in the gene expression profiles induced by R and OF, with subtle transcriptional differences between R and OF.

We next wanted to understand whether the directionality of these transcriptional differences between R and OF in TMD8 was cell line specific. We measured the fold changes of the 22 differentially expressed genes induced by R and OF in both TMD8 and U2932. In both cell lines, R preferentially downregulated these genes (Figure 5A), whereas OF preferentially upregulated these genes (Figure 5B). Interestingly, the directionality of these differences was conserved in 21 of the 22 genes across both cell lines (Figure 5C). Therefore, we conclude that these transcriptional differences between R and OF are conserved across cell lines.

Next, we proceeded to identify any biological pathways enriched within genes differentially expressed by R and OF. The

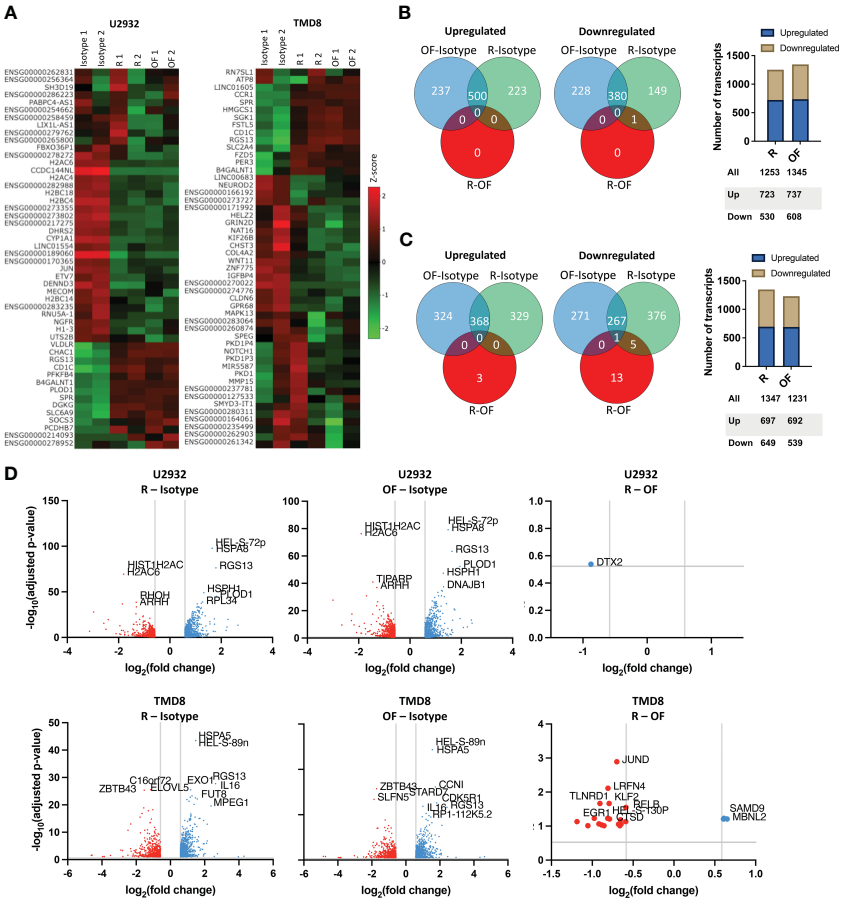

FIGURE 4
Rituximab and ofatumumab activate similar transcriptional profiles but differentially modulate a small subset of genes. **(A)** Heat map of the 50 most variable genes expressed by U2932 and TMD8 treated with R, OF, or IgG isotype control (20 μg/mL) for 4 hours. Venn diagrams and distribution of upregulated and downregulated genes in U2932 **(B)** and TMD8 **(C)**. **(D)** Volcano plots of differentially expressed genes between R and isotype, OF and isotype, and R and OF in U2932 and TMD8. The top 10 most significant differentially expressed genes were labeled in all graphs.

KEGG is an integrated database resource consisting of curated databases manually mapped into molecular networks to biologically interpret sequencing data. We performed gene enrichment analysis using this database to identify enriched molecular pathways. Because of the remarkably similar gene expression changes induced by R and OF in U2932, we were unable to perform gene enrichment analysis for U2932. However, we found enrichment of nine pathways in TMD8 (Figure 5D). Among these pathways, the Mitogen-activated protein kinase (MAPK) pathway is the most significantly enriched and the most biologically relevant pathway, with previous studies showing that this pathway is modulated by R in sensitizing B-cell lymphomas to chemotherapy (47, 48). Therefore, our gene enrichment analysis suggests that R and OF may exert distinct effects through differential regulation of the MAPK signaling pathway.

Because the MAPK pathway comprises many families that modulate a broad spectrum of physiological processes, ranging from cell survival to apoptosis, it is important to identify which families of the MAPK pathway may be differentially modulated by R and OF (49). Therefore, using the KEGG database, we mapped differentially expressed genes with other known molecularly interacting genes to identify the most biologically relevant MAPK family (Figure 5E). Among the differentially modulated MAPK families, we find the c-Jun N-terminal kinases (JNK) and p38 MAPK pathway most biologically relevant to our findings for two reasons. First, we see that chemotherapy also upregulates this pathway. Second, previous studies have shown that upregulation of this pathway sensitizes DLBCLs to chemotherapy, such as vindesine and cyclophosphamide (50, 51). Therefore, these results may suggest that OF potentiates the cytotoxic and cytostatic potential of chemotherapy through complementary upregulation of the JNK and p38 MAPK signaling pathway, leading to enhanced downstream apoptosis and inhibition of proliferation.

Discussion

Our work revealed vast heterogeneity in the pharmacological interactions within the R-CHOP regimen, illustrating the wide genetic and phenotypic heterogeneity expected of DLBCL. This finding may explain why some patients are cured by R-CHOP, whereas other patients relapse. We then demonstrated, for the first

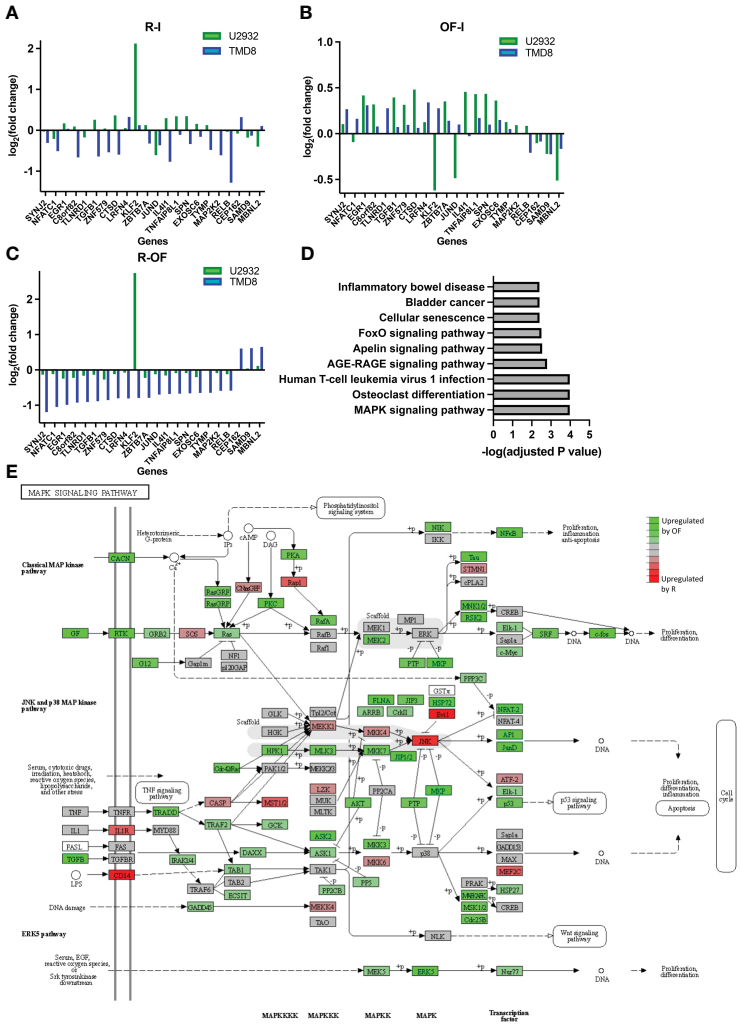

FIGURE 5
Ofatumumab differentially upregulates genes enriched in the JNK and p38 MAPK pathway over rituximab. **(A)** Fold changes of the significant differentially expressed genes modulated by R. **(B)** Fold changes of the significant differentially expressed genes modulated by OF. **(C)** Difference in fold changes of significant differentially expressed genes between the two anti-CD20s. **(D)** Gene enrichment analysis using the KEGG database. **(E)** These differences in TMD8 were mapped with related genes using the KEGG database to identify which specific family of the MAPK signaling pathway was most biologically relevant and, therefore, most likely involved in differential pharmacological interactions. Green represents genes that were preferentially upregulated by OF over R, whereas red represents genes preferentially upregulated by R over OF.

time, that two FDA-approved anti-CD20s can differentially potentiate CHOP in a cell line–specific manner. The observed difference between R and OF was unexpected because they have similar direct killing capacities *in vitro* and were comparable in their clinical efficacy in phase III clinical trials (18–21). For this reason, these findings reveal novel mechanisms of different anti-CD20 mAbs independent of their ability to modulate immune function. Although we observe that R and OF preferentially synergize with chemotherapy in a cell line–specific manner, we also observe that these anti-CD20s generally synergize with chemotherapy more in ABC DLBCLs and antagonize chemotherapy more in GCB DLBCLs. This paradoxical role of these anti-CD20s could possibly be explained by the fact that R is known to simultaneously activate pro-survival pathway Akt, which drives lymphomagenesis in GCB, and to downregulate pro-survival pathway NF-kB, which drives lymphomagenesis in ABC but not in GCB (52–54).

Our initial findings of the pharmacological interactions between R and CHOP validated previous studies that showed that R potentiates some chemotherapies (35). R potentiated cytotoxic chemotherapy drugs such as O and cytostatic properties of glucocorticoids such as P. However, our findings also demonstrated that R can antagonize chemotherapy in some cell lines, as we observed in SUDHL2 and SUDHL4. This finding is unexpected because R has been characterized as a general chemotherapy potentiator in the field. It is possible that this interaction could advise the use R and chemotherapy concurrently, pre-administration, or post-administration of chemotherapy to avoid an unfavorable immunochemotherapy interaction, which is a recognized important question in the field (55). Last, we characterized interactions between CDC and chemotherapy in R-CHOP, which remained largely unexplored (34).

We also compared the transcriptional profiles of DLBCLs bound by R and OF to uncover potential mechanisms for these

pharmacological differences. We found that, compared to R, OF preferentially upregulates genes enriched in the p38 MAPK pathway, leading to downstream apoptosis and growth inhibition. This transcriptional difference could mechanistically explain how R and OF differentially potentiate chemotherapy for two reasons. First, on the basis of KEGG analysis, chemotherapy upregulates this same pathway, and, therefore, potentiated killing and growth inhibition may occur through functional complementation. In addition, a previous study found that an organic molecule activating p38 MAPK synergized with vinblastine and cyclophosphamide to kill DLBCLs (50). Interestingly, previous studies show that R sensitizes B-cell lymphomas to chemotherapy through inhibition, rather than upregulation of p38 MAPK, suggesting that R and OF may sensitize DLBCLs to chemotherapy through opposite modulation of p38 MAPK (24, 47).

R and OF were presumed to have similar direct signaling activities, based on previous studies and our findings (39). However, our results from *in vitro* experiments found that these two mAbs that bind to different epitopes on CD20 can initiate different downstream mechanisms that potentiate different classes of chemotherapy. A previous report showed that R and a non-clinical anti-CD20 mAb induced different transcriptional profiles (56). Therefore, it is conceivable that targeting other CD20 epitopes could elicit different pathways and activate favorable immunochemotherapy interactions across a broader range of DLBCLs. These findings may advise a new design strategy for new anti-CD20s that focus on targeting different epitopes of CD20 to expand favorable immunochemotherapy interactions across a greater range of DLBCLs. This strategy is particularly clinically relevant since the expiration of the R patent in 2016, because there has been a breakthrough in other anti-CD20 biologics such as ocrelizumab, ublituximab, and obinutuzumab, which are already approved for use in patients. Given the usage of anti-CD20s in nearly all B-cell pathologies, the findings of this paper may also have potential therapeutic value in a broad range of B-cell–related diseases including multiple sclerosis, chronic lymphocytic leukemia, rheumatoid arthritis, Burkitt leukemia, and others.

Further studies will be needed to address limitations of our findings and test their potential implications. In this study, we scored the pharmacological interactions between R and chemotherapy and between CDC and chemotherapy. However, R is cytotoxic to DLBCL by ADCC and ACP, and we cannot exclude that these mechanisms could also interact with chemotherapy. Indeed, there has been a study showing that dexamethasone enhances R-mediated ADCC through increased phosphatidylserine exposure on DLBCLs (34). Therefore, studying the pharmacological interactions between cellular-mediated effects and chemotherapy could elucidate additional immunochemotherapy interactions specific to the *in vivo* setting.

Our transcriptome analysis reveals a mechanistically plausible finding explaining the pharmacological differences between R and OF, validated by correlating gene fold expression using qRT-PCR (Supplementary Figure 1). However, DLBCL is characterized by a notable degree of biological heterogeneity, and our analysis is limited to a few select cell lines. Therefore, we present our transcriptional analysis as hypothesis-generating, rather than conclusive across all DLBCLs. Furthermore, the direct effects of anti-CD20 are known to activate direct signaling and transcriptional pathways, necessitating further investigation through a multi-omics approach (57). Ultimately, whole-exome, transcriptomic, and phosphoproteomic analysis would provide additional mechanistic insight into these findings and elucidate potential baseline biomarkers predicting favorable outcomes using either R or OF.

Data availability statement

The datasets presented in this study can be found in online repositories. The names of the repository/repositories and accession number(s) can be found below: GEO, accession number GSE228687.

Author contributions

BL: conceptualization, method design, data analysis, experimentation, validation, writing, and funding acquisition. TP: conceptualization, method design, data analysis, experimentation, validation, writing, and funding acquisition. AA: conceptualization, method design, data analysis, writing, funding acquisition, methodology, project administration, resources, and supervision. KR: conceptualization, method design, data analysis, writing, funding acquisition, methodology, project administration, resources, and supervision. All authors contributed to the article and approved the submitted version.

Funding

This work was supported, in part, by grants from the Dextra Undergraduate Research Endowment, Cornell Agriculture and Life Sciences Endowment, Paul Schreuers Memorial Endowment, Goldberg Foundation, National Institutes of Health (5R01 CA185372 to KR, TP, and BL and T32GM008152-35 to BL), and National Institute of Allergy and Infectious Diseases (AI29422, AI120701, and AI138570 to AA and TP).

Acknowledgments

We would like to thank Veronika Kottisch and Stephanie Rosenbloom for preparation of 4-hydroperoxycyclophosphamide. We would also like to thank Yimon Aye and Ari Melnick for helpful discussions. We thank Suzin Webb for providing managerial support through the entirety of this project.

Conflict of interest

The authors declare that the research was conducted in the absence of any commercial or financial relationships that could be construed as a potential conflict of interest.

Publisher's note

All claims expressed in this article are solely those of the authors and do not necessarily represent those of their affiliated organizations, or those of the publisher, the editors and the reviewers. Any product that may be evaluated in this article, or claim that may be made by its manufacturer, is not guaranteed or endorsed by the publisher.

Supplementary material

The Supplementary Material for this article can be found online at: https://www.frontiersin.org/articles/10.3389/fonc.2023.1159484/full#supplementary-material

References

1. García Zueco JC, Delgado P. Epidemiology of non-Hodgkin's lymphomas. *Sangre (Barc)* (1994) 39:267–75. doi: 10.3390/medsci9010005

2. Coiffier B, Sarkozy C. Diffuse large B-cell lymphoma: R-CHOP failure—what to do? *Hematol: Am Soc Hematol Educ Program* (2016) 2016:366. doi: 10.1182/asheducation-2016.1.366

3. Coiffier B, Lepage E, Briere J, Herbrecht R, Tilly H, Bouabdallah R, et al. CHOP chemotherapy plus rituximab compared with CHOP alone in elderly patients with diffuse large-B-cell lymphoma. *N Engl J Med* (2002) 346:235–42. doi: 10.1056/NEJMoa011795

4. Pfreundschuh M, Kuhnt E, Trümper L, Osterborg A, Trneny M, Shepherd L, et al. CHOP-like chemotherapy with or without rituximab in young patients with good-prognosis diffuse large-B-cell lymphoma: 6-year results of an open-label randomised study of the MabThera International Trial (MInT) Group. *Lancet Oncol* (2011) 12:1013–22. doi: 10.1016/S1470-2045(11)70235-2

5. Habermann TM, Weller EA, Morrison VA, Gascoyne RD, Cassileth PA, Cohn JB, et al. Rituximab-CHOP versus CHOP alone or with maintenance rituximab in older patients with diffuse large B-cell lymphoma. *J Clin Oncol* (2006) 24:3121–7. doi: 10.1200/JCO.2005.05.1003

6. Lenz G, Dreyling M, Hoster E, Wörmann B, Dührsen U, Metzner B, et al. Immunochemotherapy with rituximab and cyclophosphamide, doxorubicin, vincristine, and prednisone significantly improves response and time to treatment failure, but not long-term outcome in patients with previously untreated mantle cell lymphoma: results of a prospective randomized trial of the German Low Grade Lymphoma Study Group (GLSG). *J Clin Oncol* (2005) 23:1984–92. doi: 10.1200/JCO.2005.08.133

7. Nencioni A, Cea M, Moran E, Carbone F, Augusti V, Patrone F, et al. Monoclonal antibodies for non-hodgkin's lymphoma: State of the art and perspectives. *Clin Dev Immunol* (2010) 2010. doi: 10.1155/2010/428253

8. Marcus R, Imrie K, Solal-Celigny P, Catalano JV, Dmoszynska A, Raposo JC, et al. Phase III study of R-CVP compared with cyclophosphamide, vincristine, and prednisone alone in patients with previously untreated advanced follicular lymphoma. *J Clin Oncol* (2008) 26:4579–86. doi: 10.1200/JCO.2007.13.5376

9. Van Oers MHJ, Klasa R, Marcus RE, Wolf M, Kimby E, Gascoyne RD, et al. Rituximab maintenance improves clinical outcome of relapsed/resistant follicular non-Hodgkin lymphoma in patients both with and without rituximab during induction: results of a prospective randomized phase 3 intergroup trial. *Blood* (2006) 108:3295–3301. doi: 10.1182/blood-2006-05-021113

10. Forstpointner R, Dreyling M, Repp R, Hermann S, Hänel A, Metzner B, et al. The addition of rituximab to a combination of fludarabine, cyclophosphamide, mitoxantrone (FCM) significantly increases the response rate and prolongs survival as compared with FCM alone in patients with relapsed and refractory follicular and mantle cell lymphomas: Results of a prospective randomized study of the German Low-Grade Lymphoma Study Group. *Blood* (2004) 104:3064–71. doi: 10.1182/blood-2004-04-1323

11. Herold M, Scholz CW, Rothmann F, Hirt C, Lakner V, Naumann R, et al. Long-term follow-up of rituximab plus first-line mitoxantrone, chlorambucil, prednisolone and interferon-alpha as maintenance therapy in follicular lymphoma. *J Cancer Res Clin Oncol* (2015) 141:1689–95. doi: 10.1007/s00432-015-1963-9

12. Adams CM, Clark-Garvey S, Porcu P, Eischen CM. Targeting the bcl-2 family in B cell lymphoma. *Front Oncol* (2019) 1:636. doi: 10.3389/fonc.2018.00636

13. Landsburg DJ, Falkiewicz MK, Maly J, Blum KA, Howlett C, Feldman T, et al. Outcomes of patients with double-hit lymphoma who achieve first complete remission. *J Clin Oncol* (2017) 35:2260–7. doi: 10.1200/JCO.2017.72.2157

14. Younes A, Sehn LH, Johnson P, Zinzani PL, Hong X, Zhu J, et al. Randomized phase III trial of ibrutinib and rituximab plus cyclophosphamide, doxorubicin, vincristine, and prednisone in non–germinal center B-cell diffuse large B-cell lymphoma. *J Clin Oncol* (2019) 37:1285–95. doi: 10.1200/JCO.18.02403

15. Castellino A, Chiappella A, LaPlant BR, Pederson LD, Gaidano G, Macon WR, et al. Lenalidomide plus R-CHOP21 in newly diagnosed diffuse large B-cell lymphoma (DLBCL): long-term follow-up results from a combined analysis from two phase 2 trials. *Blood Cancer J* (2018) 8. doi: 10.1038/s41408-018-0145-9

16. Wilson WH, Dunleavy K, Pittaluga S, Hegde U, Grant N, Steinberg SM, et al. Phase II study of dose-adjusted EPOCH and rituximab in untreated diffuse large B-cell lymphoma with analysis of germinal center and post-germinal center biomarkers. *J Clin Oncol* (2008) 26:2717–24. doi: 10.1200/JCO.2007.13.1391

17. Dayanand K. A phase I/II trial of vorinostat (SAHA) in combination with rituximab-CHOP in patients with newly diagnosed advanced stage diffuse large B-cell lymphoma (DLBCL): SWOG S0806. *Physiol Behav* (2018) 176:139–48. doi: 10.1002/ajh.25010

18. van Imhoff GW, McMillan A, Matasar MJ, Radford J, Ardeshna KM, Kuliczkowski K, et al. Ofatumumab versus rituximab salvage chemoimmunotherapy in relapsed or refractory diffuse large B-cell lymphoma: the ORCHARRD study. *J Clin Oncol* (2017) 35:544–51. doi: 10.1200/JCO.2016.69.0198

19. Peyrade F, Bologna S, Delwail V, Emile JF, Pascal L, Fermé C, et al. Combination of ofatumumab and reduced-dose CHOP for diffuse large B-cell lymphomas in patients aged 80 years or older: an open-label, multicentre, single-arm, phase 2 trial from the LYSA group. *Lancet Haematol* (2017) 4:e46–55. doi: 10.1016/S2352-3026(16)30171-5

20. Czuczman MS, Hess G, Gadeberg OV, Pedersen LM, Goldstein N, Gupta I, et al. Chemoimmunotherapy with ofatumumab in combination with CHOP in previously untreated follicular lymphoma. *Br J Haematol* (2012) 157:438–45. doi: 10.1111/j.1365-2141.2012.09086.x

21. Vitolo U, Trněný M, Belada D, Burke JM, Carella AM, Chua N, et al. Obinutuzumab or rituximab plus cyclophosphamide, doxorubicin, vincristine, and prednisone in previously untreated diffuse large B-cell lymphoma. *J Clin Oncol* (2017) 35:3529–37. doi: 10.1200/JCO.2017.73.3402

22. Pierpont T, Limper C, Richards KL. Past, present, and future of rituximab-the world's first oncology monoclonal antibody therapy. *Front Oncol* (2018) 8. doi: 10.3389/fonc.2018.00163

23. Demidem A, Lam T, Alas S, Hariharan K, Hanna N, Bonavida B, et al. Chimeric anti-CD20 (IDEC-C2B8) monoclonal antibody sensitizes a B cell lymphoma cell line to cell killing by cytotoxic drugs. *Cancer Biother Radiopharm* (2009) 12:177–86. doi: 10.1089/cbr.1997.12.177

24. Alas S, Emmanouilides C, Bonavida B. Inhibition of interleukin 10 by rituximab results in down-regulation of bcl-2 and sensitization of B-cell non-hodgkin's lymphoma to apoptosis 1. *Clin Cancer Res* (2001) 7:709–723. doi: 10.1038/sj.onc.1207336

25. Olejniczak SH, Hernandez-Ilizaliturri FJ, Clements JL, Czuczman MS. Acquired resistance to rituximab is associated with chemotherapy resistance resulting from decreased bax and bak expression. *Clin Cancer Res* (2008) 14:1550–60. doi: 10.1158/1078-0432.CCR-07-1255

26. *Venclyxto*. European Medicines Agency, European Union. (2016). Available at: https://www.ema.europa.eu/en/medicines/human/EPAR/venclyxto.

27. Labar B, Suciu S, Willemze R, Muus P, Marie J-P, Fillet G, et al. Dexamethasone compared to prednisolone for adults with acute lymphoblastic leukemia or lymphoblastic lymphoma: final results of the ALL-4 randomized, phase III trial of the EORTC Leukemia Group. *Haematologica* (2010) 95:1489. doi: 10.3324/haematol.2009.018580

28. NL B, Grillo-López AJ, White CA, Bence-Bruckler I, Maloney D, Czuczman M, et al. Association of serum Rituximab (IDEC-C2B8) concentration and anti-tumor response in the treatment of recurrent low-grade or follicular non-Hodgkin's lymphoma. *Ann Oncol* (1998) 9:995–1001. doi: 10.1023/A:1008416911099

29. Joy MS, La M, Wang J, Bridges AS, Hu Y, Hogan SL, et al. Cyclophosphamide and 4-hydroxycyclophosphamide pharmacokinetics in patients with glomerulonephritis secondary to lupus and small vessel vasculitis. *Br J Clin Pharmacol* (2012) 74:445–455. doi: 10.1111/j.1365-2125.2012.04223.x

30. Barpe DR, Rosa DD, Froehlich PE. Pharmacokinetic evaluation of doxorubicin plasma levels in normal and overweight patients with breast cancer and simulation of dose adjustment by different indexes of body mass. *Eur J Pharm Sci* (2010) 41:458–63. doi: 10.1016/j.ejps.2010.07.015

31. Yang F, Jiang M, Lu M, Hu P, Wang H, Jiang J, et al. Pharmacokinetic behavior of vincristine and safety following intravenous administration of vincristine sulfate liposome injection in chinese patients with malignant lymphoma. *Front Pharmacol* (2018) 9. doi: 10.3389/fphar.2018.00991

32. Sagcal-Gironella ACP, Sherwin CMT, Tirona RG, Rieder MJ, Brunner HI, Vinks AA, et al. Pharmacokinetics of prednisolone at steady state in young patients with systemic lupus erythematosus on prednisone therapy: an open-label, single-dose study. *Clin Ther* (2011) 33:1524–36. doi: 10.1016/j.clinthera.2011.09.015

33. Gessner PK. A straightforward method for the study of drug interactions: an isobolographic analysis primer. *J Am Coll Toxicol* (1988) 7:987–1012. doi: 10.3109/10915818809014529

34. Rose AL, Smith BE, Maloney DG. Glucocorticoids and rituximab *in vitro*: synergistic direct antiproliferative and apoptotic effects. *Blood* (2002) 100:1765–73. doi: 10.1182/blood.V100.5.1765.h81702001765_1765_1773

35. Jazirehi A, Bonavida B. Cellular and molecular signal transduction pathways modulated by rituximab (rituxan, anti-CD20mAb) in non-Hodgkin's lymphoma: implications in chemosensitization and therapeutic intervention. *Oncogene* (2007) 26:6184–93. doi: 10.1038/sj.onc.1208349

36. Knutson SK, Warholic NM, Johnston LD, Klaus CR, Wigle TJ, Iwanowicz D, et al. Synergistic anti-tumor activity of EZH2 inhibitors and glucocorticoid receptor agonists in models of germinal center non-hodgkin lymphomas. *PloS One* (2014) 9. doi: 10.1371/journal.pone.0111840

37. Jazirehi AR, Huerta-Yepez S, Cheng G, Bonavida B. Rituximab (Chimeric anti-CD20 monoclonal antibody) inhibits the constitutive nuclear factor-KB signaling pathway in non-hodgkin's lymphoma B-cell lines: role in sensitization to chemotherapeutic drug-induced apoptosis. *Cancer Res* (2005) 65:264–276. doi: 10.1158/0008-5472.264.65.1

38. Sangaletti S, Iannelli F, Zanardi F, Cancila V, Portararo P, Botti L, et al. Intra-tumour heterogeneity of diffuse large B-cell lymphoma involves the induction of diversified stroma-tumour interfaces. *EBioMedicine* (2020) 61:103055. doi: 10.1016/j.ebiom.2020.103055

39. Klein C, Lammens A, Schäfer W, Georges G, Schwaiger M, Mössner E, et al. Epitope interactions of monoclonal antibodies targeting CD20 and their relationship to functional properties. *MAbs* (2013) 5:22–33. doi: 10.4161/mabs.22771

40. Mukhtar E, Adhami VM, Mukhtar H. Targeting microtubules by natural agents for cancer therapy. *Mol Cancer Ther* (2014) 13:275–84. doi: 10.1158/1535-7163.MCT-13-0791

41. Schlager S, Salomon C, Olt S, Albrecht C, Ebert A, Bergner O, et al. Inducible knock-out of BCL6 in lymphoma cells results in tumor stasis. *Oncotarget* (2020) 11:875–90. doi: 10.18632/oncotarget.27506

42. Diaferia GR, Balestrieri C, Prosperini E, Nicoli P, Spaggiari P, Zerbi A, et al. Dissection of transcriptional and cis -regulatory control of differentiation in human pancreatic cancer. *EMBO J* (2016) 35:595–617. doi: 10.15252/embj.201592404

43. Docking TR, Parker JDK, Jädersten M, Duns G, Chang L, Jiang J, et al. A clinical transcriptome approach to patient stratification and therapy selection in acute myeloid leukemia. *Nat Commun* (2021) 12:1–15. doi: 10.1038/s41467-021-22625-y

44. Hernández-Verdin I, Kirasic E, Wienand K, Mokhtari K, Eimer S, Loiseau H, et al. Molecular and clinical diversity in primary central nervous system lymphoma. *Ann Oncol* (2022) 15:186–199. doi: 10.1016/j.annonc.2022.11.002

45. Wu H, Wang C, Wu Z. Gene expression PROPER: comprehensive power evaluation for differential expression using RNA-seq. *Bioinformatics* (2015) 31:233–41. doi: 10.1093/bioinformatics/btu640

46. Locatelli SL, Consonni FM, Careddu G, Serio S, Viswanadha S, Vakkalanka SKVS, et al. RNA sequencing reveals mechanisms underlying modulation of hodgkin lymphoma cells and tumor microenvironment by the PI3K δ/γ Inhibitor, RP6530. *Blood* (2017) 130. doi: 10.1182/blood.V130.Suppl_1.2476.2476

47. Vega MI, Huerta-Yepaz S, Garban H, Jazirehi A, Emmanouilides C, Bonavida B, et al. Rituximab inhibits p38 MAPK activity in 2F7 B NHL and decreases IL-10 transcription: Pivotal role of p38 MAPK in drug resistance. *Oncogene* (2004) 23:3530–40. doi: 10.1038/sj.onc.1207336

48. Pedersen IM, Buhl AM, Klausen P, Geisler CH, Jurlander J. The chimeric anti-CD20 antibody rituximab induces apoptosis in B-cell chronic lymphocytic leukemia cells through a p38 mitogen activated protein-kinase-dependent mechanism. *Blood* (2002) 99:1314–9. doi: 10.1182/blood.V99.4.1314

49. Cargnello M, Roux PP. Activation and function of the MAPKs and their substrates, the MAPK-activated protein kinases. *Microbiol AND Mol Biol Rev* (2011) 75:50–83. doi: 10.1128/MMBR.00031-10

50. Yu X, Wang X, Wang X, Zhou Y, Li Y, Wang A, et al. TEOA inhibits proliferation and induces DNA damage of diffuse large B-cell lymphoma cells through activation of the ROS-dependent p38 MAPK signaling pathway. *Front Pharmacol* (2020) 11:1392. doi: 10.3389/fphar.2020.554736

51. Liao Y, Hung M-C. Regulation of the activity of p38 mitogen-activated protein kinase by Akt in cancer and adenoviral protein E1A-mediated sensitization to apoptosis. *Mol Cell Biol* (2003) 23:6836–48. doi: 10.1128/MCB.23.19.6836-6848.2003

52. Edelmann J, Dokal AD, Vilventhraraja E, Holzmann K, Britton D, Klymenko T, et al. Rituximab and obinutuzumab differentially hijack the B cell receptor and NOTCH1 signaling pathways. *iScience* (2021) 24:102089. doi: 10.1016/j.isci.2021.102089

53. Davis RE, Brown KD, Siebenlist U, Staudt LM. Constitutive nuclear factor B activity is required for survival of activated B cell-like diffuse large B cell lymphoma cells. *J Exp Med* • (2001) 194:1861–74. doi: 10.1084/jem.194.12.1861

54. Compagno M, Lim WK, Grunn A, Nandula SV, Brahmachary M, Shen Q, et al. Mutations of multiple genes cause deregulation of NF-kB in diffuse large B-cell lymphoma. *Nature* (2009) 459:717–21. doi: 10.1038/nature07968

55. Pavanello F, Zucca E, Ghielmini M. Rituximab: 13 open questions after 20 years of clinical use. *Cancer Treat Rev* (2017) 53:38–46. doi: 10.1016/j.ctrv.2016.11.015

56. Franke A, Niederfellner GJ, Klein C, Burtscher H. Antibodies against CD20 or B-cell receptor induce similar transcription patterns in human lymphoma cell lines. *PloS One* (2011) 6:e16596. doi: 10.1371/journal.pone.0016596

57. Czuczman MS, Olejniczak S, Gowda A, Kotowski A, Binder A, Kaur H, et al. Acquirement of rituximab resistance in lymphoma cell lines is associated with both global CD20 gene and protein down-regulation regulated at the pretranscriptional and posttranscriptional levels. *Clin Cancer Res* (2008) 14:1561–70. doi: 10.1158/1078-0432.CCR-07-1254

frontiers | Frontiers in Oncology

TYPE Original Research
PUBLISHED 28 August 2023
DOI 10.3389/fonc.2023.1089187

OPEN ACCESS

EDITED BY
Gaël Roué,
Josep Carreras Leukaemia Research Institute (IJC), Spain

REVIEWED BY
Zhiwu Jiang,
Chinese Academy of Sciences (CAS), China
Conn Rother,
Federal Arms Hospital Ulm, Germany
Joaquim Carreras,
Tokai University, Japan

*CORRESPONDENCE
Xiaoxi Li
lixiaoxi@ujs.edu.cn
Hui Qian
lstmmmlst@163.com

†These authors have contributed equally to this work and share first authorship

RECEIVED 04 November 2022
ACCEPTED 18 July 2023
PUBLISHED 28 August 2023

CITATION
Li X, Deng M, Zhang C, Luo L and Qian H (2023) Establishment of a primary renal lymphoma model and its clinical relevance. *Front. Oncol.* 13:1089187. doi: 10.3389/fonc.2023.1089187

Establishment of a primary renal lymphoma model and its clinical relevance

Xiaoxi Li*†, Minyao Deng†, Chenxiao Zhang, Lingli Luo and Hui Qian*

Department of Laboratory Medicine, School of Medicine, Jiangsu University, Zhenjiang, Jiangsu, China

Extranodal dissemination is an important feature of aggressive B-cell lymphoma. Owing to the lack of available animal models, the study on extranodal dissemination of lymphoma is greatly limited. Here, we identified a novel cell line, named MA-K, which originated from the Eμ-Myc;Cdkn2a$^{-/-}$ cell line, named MA-LN in this study. Compared to MA-LN, MA-K tended to disseminate in the kidney rather than the lymph nodes in the lymphoma transplantation model, resembling human primary renal lymphoma. The transcriptome analysis revealed that MA-K had undergone transcriptional evolution during the culture. The specialized transcriptional pattern analysis we proposed in this study identified that the FOXO1-BTG1-MYD88 pattern was formed in MA-K. Further analysis found that the translation pathway was the most enriched pathway in specially expressed genes (SEGs) in MA-K. Among the SEGs, three upregulated genes, RPLP2, RPS16, and MRPS16, and five downregulated genes, SSPN, CD52, ANKRD37, CCDC82, and VPREB3, in MA-K were identified as promising biomarkers to predict the clinical outcomes of human DLBCL. Moreover, the joint expression of the five-gene signature could effectively predict clinical outcomes of human DLBCL in three groups. These findings suggested that the MA-K cell line had strong clinical relevance with human aggressive B-cell lymphoma. Moreover, the MA-K primary renal lymphoma model, as a novel syngenetic mouse model, will be greatly useful for both basic research on lymphoma dissemination and preclinical efficacy evaluation of chemotherapy and immunotherapy.

KEYWORDS

primary renal lymphoma, extranodal lymphoma, extranodal dissemination, MA-K, MCD subtype, LymphGen, aggressive B-cell lymphoma, translation pathway

Introduction

B-cell lymphoma is a B-lymphoid hyperplasia disease with high heterogeneity. While most lymphomas primarily present in lymph nodes, extranodal dissemination of lymphoma is a common clinical feature observed in most subtypes of Non-Hodgkin's B-cell lymphoma (B-NHL), including diffused large B-cell lymphoma (DLBCL, NOS) (1, 2), Burkitt's lymphoma (BL) (3, 4), and high-grade B-cell lymphoma (HGBL) (5, 6). The disseminated organs include the central nervous system (CNS) (7), skin (8), and uterus (9). Primary renal lymphoma (PRL) is a rare malignant lymphoma and most of the PRL cases are DLBCL (10). Patients with extranodal lymphoma, such as CNS lymphoma, often have poor clinical outcome. Classification of DLBCL based on transcriptional profile (11) and genetic variation (2) links the extranodal lymphoma to the activated B-cell-like (ABC) subtype and the MCD (including $MYD88^{L265P}$ and CD79B mutations) subtype. However, because of the lack of available animal models, the genetic and non-genetic factors of extranodal lymphoma are still unclear.

The Eμ-Myc transgenic mouse is a well-established spontaneous B-cell lymphoma mouse model (12) resembling the translocation of oncogenic Myc to the enhancer of immunoglobulin heavy (IgH) μ gene in human BL. Unlike human BL and DLBCL that originated from the mature B stage, the later stage of B-cell differentiation, Eμ-Myc lymphoma mainly originates from the pro-B and pre-B stage. Hence, Eμ-Myc transgenic mouse is not an ideal model to resemble the aggressive phenotype of human B-cell lymphoma, such as extranodal dissemination. In the combined Eμ-Myc transgenic mouse and genetically engineered modified mouse (GEMM) models, the knockout of tumor suppressor genes (TSGs), such as p53 and Arf (13, 14), could significantly accelerate lymphomagenesis and shorten survival time. Transcriptome analysis on a large cohort of Eμ-Myc transgenic mice (15) revealed that the onset of Eμ-Myc lymphoma dramatically varied and BL-like and DLBCL-like transcriptional characteristics were identified in early-onset and late-onset lymphoma, respectively. In addition, genomic analysis (16) identified that disruptive mutations in Bcor contributed to spontaneously lymphomagenesis of Eμ-Myc transgenic mouse. Given that lymph node is still the major disseminated site in most Eμ-Myc-based mouse models, understanding the mechanism of extranodal dissemination is still difficult and challenging.

Because of ease of establishing a syngeneic lymphoma transplantation model, a type of the GEM-derived allograft (GDA) model (17), the Eμ-Myc;$Cdkn2a^{-/-}$ cell line, which usually gives rise to lymphoma in lymph nodes, is widely used for *in vivo* efficacy evaluation (18, 19). In this study, we reported a Eμ-Myc;$Cdkn2a^{-/-}$ derived cell line that could give rise to extranodal lymphoma, specifically to kidney, in a GDA model. To distinguish it from the parental Eμ-Myc;$Cdkn2a^{-/-}$ cell line, we named the kidney-disseminated cell line as the MA-K cell line, in which the M referred to Myc and the A referred to Arf. Because of the strong clinical relevance of extranodal dissemination and aggressive B-cell lymphoma, we further analyzed the transcriptome profile of MA-K and explored prognostic biomarkers of human DLBCL inspired by the transcriptome of MA-K. Translation pathway was the most enriched pathway in SEGs in MA-K. Eight SEGs in MA-K, RPLP2, RPS16, MRPS16, SSPN, CD52, VPREB3, CCDC82, and ANKRD37, were identified as promising prognostic biomarkers of human DLBCL. Together, we report that a novel MA-K cell line with renal tropism in the GDA model has strong clinical relevance with aggressive DLBCL. The MA-K GDA model will be applied to explore the genetic and non-genetic mechanism of PRL, as well as to evaluate the preclinical efficacy of chemotherapy and immunotherapy.

Materials and methods

Cell lines

The *Eμ-Myc;*$Cdkn2a^{-/-}$ cell line, also named MA-LN in this study, was a kind gift from Prof. Michael Hemann at MIT in 2011 and preserved in the laboratory of Prof. Hai Jiang at CEMCS, CAS. The MA-K cell line was established from the *Eμ-Myc;*$Cdkn2a^{-/-}$ cell line in our laboratory. The *Eμ-Myc;*$Cdkn2a^{-/-}$ cell line and the MA-K cell line were cultured in 45% DMEM, 45% IMDM, and 10% fetal bovine serum (Biosera, FB-1058), supplemented with 100 U/ml penicillin and streptomycin, and 25 μM β-mercaptoethanol.

Lymphoma transplantation model

All mice were housed in a specific pathogen-free environment at the Laboratory Animal Research Center in Jiangsu University and treated in strict accordance with protocols, which were approved by the Animal Care and Use Committee of Laboratory Animal Research Center, Jiangsu University.

Six-week C57BL/6JGpt female mice were purchased from the GemPharmatech (Nanjing, CN). A total of 10^6 MA-LN cells or MA-K cells in 200 μl of DPBS were injected into C57BL/6 female recipient mice *via the* tail vein. Recipient mice transplanted with the MA-LN cell line usually grew a palpable mass at axillary lymph nodes at the 4th week post-transplantation. Instead, typical symptoms, including hunch back, dull hair, movement retardation, and abdominal bulge, were usually observed in MA-K recipient mice at the 4th week post-transplantation. Recipient mice transplanted with MA-LN or MA-K were monitored until any one of the above-mentioned symptoms arose and were sacrificed for evaluating lymphoma dissemination.

H&E staining and imaging

For histological H&E staining, lymphomas were fixed in 10% formalin overnight and subsequently transferred into 70% ethanol, embedded in paraffin according to standard protocols. Sections (8 μm) were stained with H&E and images from the whole slide were acquired by Pannoramic MIDI (3DHISTECH) and analyzed by CaseViewer software (3DHISTECH).

RNA extraction and RNA sequencing

Two replicates of MA-LN and MA-K, collected at different times, were applied to RNA sequencing. Total RNA was extracted using the Trizol reagent kit (15596018, Invitrogen) according to the manufacturer's protocol. RNA library construction and sequencing were performed by Gene Denovo Biotechnology Co. (Guangzhou, China). The enriched mRNA by Oligo(dT) beads was fragmented into short fragments using fragmentation buffer and reversely transcribed into cDNA by using NEBNext Ultra RNA Library Prep Kit for Illumina (#7530, New England Biolabs). The purified double-stranded cDNA fragments were end repaired, A base added, and ligated to Illumina sequencing adapters. The ligation reaction was purified with the AMPure XP Beads (1.0×). Ligated fragments were subjected to size selection by agarose gel electrophoresis and polymerase chain reaction (PCR) amplified. The resulting cDNA library was sequenced using Illumina Novaseq6000.

Specially expressed genes analysis

For each transcription region, an FPKM (fragment per kilobase of transcript per million mapped reads) value was calculated to quantify its expression abundance and variations, using RSEM software.

To filter SEGs with biological significance, we divided the gene expression level into three levels as FPKM ≥ 10, FPKM ≥ 1, and FPKM < 1. Inactive genes or basal expressed genes were defined as FPKM < 1. Active genes were defined as FPKM ≥ 1. SEGs were filtered as follows. Inactive genes (FPKM < 1) in both groups were directly excluded for SEGs analysis. For active genes (FPKM ≥ 1) in both groups, genes with $Log_2(FC) \leq -2$ and $Log_2(FC) \geq 2$ were filtered as SEGs. In the case of inactive genes (FPKM < 1) in one of the groups, active genes (FPKM ≥ 10) in another group were directly listed into SEGs. All SEGs were listed in Data Sheet 1.

Pathway enrichment analysis and protein–protein interaction (PPI) enrichment of SEGs were performed with Metascape (https://metascape.org). PPI enrichment analysis had been carried out with the following databases: STRING and BioGrid. Only physical interactions in STRING (physical score > 0.132) and BioGrid were used.

Survival analysis

Survival analysis was performed with the online tool SurvExpress (20). A human DLBCL dataset [Lenz Staudt Lymphoma GSE10846 (21), n = 420] was chosen for survival analysis. The prognostic index (PI) was calculated by the expression value and the Cox model to generate the risk groups. The optimization algorithm was applied in risk grouping. The SurvExpress program was performed according to the tutorial.

Statistical analysis

Depending on the type of experiment, log-rank test or f-test was used as indicated in figure legends. p-values <0.05 were considered significant (* < 0.05, ** < 0.01, *** < 0.001).

Results

Establishment of primary renal lymphoma model

The Eμ-Myc;Cdkn2a$^{-/-}$ cell line, also called MA-LN in this study, is a cell line widely used to establish the lymphoma transplantation model, a type of GDA model. M refers to Myc gene and A refers to Arf gene. MA-LN lymphoma typically presented in lymph nodes (LNs) in recipient mice (Figure 1A), and the progression of lymphoma could be well monitored by touching the palpable mass arising in the axillary lymph nodes.

The MA-LN cell line was first introduced to establish the MA-LN GDA model in 2011. In 2021, we began to notice some obvious symptoms that we had never seen before, including hunch back, dull hair, movement retardation, and abdominal bulge, instead of palpable mass at LNs. Anatomical results showed that lymphoma was mainly disseminated at the kidney and LNs and spleens were no longer involved (Figure 1B), which was highly similar to human PRL. Despite the differences of disseminated sites, there was no difference in survival time of MA-LN and MA-K recipient mice (Figure 1C).

Considering that we had changed the source of recipient mice, we suspected that the source difference of recipient mice probably contributed to kidney dissemination of lymphoma. Hence, we successively replaced recipient mice from three different sources. The results showed that lymphoma was still disseminated at the kidney.

A study (22) had proven that cancer cell lines could evolve in culture, forming genetic and transcriptional heterogeneity and different drug responses. Therefore, we proposed that the Eμ-Myc;Cdkn2a$^{-/-}$ cell line had evolved into a novel and stable cell line, renamed as MA-K, indicating the tendency of MA-K to kidney dissemination in the GDA model.

The histological analysis of MA-LN lymphoma showed that the lymphoma mass was mainly composed of lymphoma cells (Figure 1D). For MA-K lymphoma, we analyze several affected kidneys and typical H&E staining sections were presented (Figure 1E; Supplementary Image 1). According to HE staining images, we found that MA-K lymphoma can infiltrate kidneys from both renal glomerulus (#1) and renal capsule (#2 and #3). Because of the lack of *in vivo* tracing analysis of pathological progression, we cannot describe the detailed process of kidney dissemination. We speculated that MA-K lymphoma first infiltrated from glomerulus, and then the oversized lymphoma on the outer surface of the kidney could invade the kidney from the renal capsule.

MA-K had specialized transcriptional patterns and abnormal expression of LymphGen

To identify the molecular characteristics of MA-K cells, we performed RNA-Seq analysis and 12,809 genes were initially detected in MA-LN and MA-K. To obtain differentially expressed genes (DEGs) with biological significance, we removed genes with

10.3389/fonc.2023.1089187

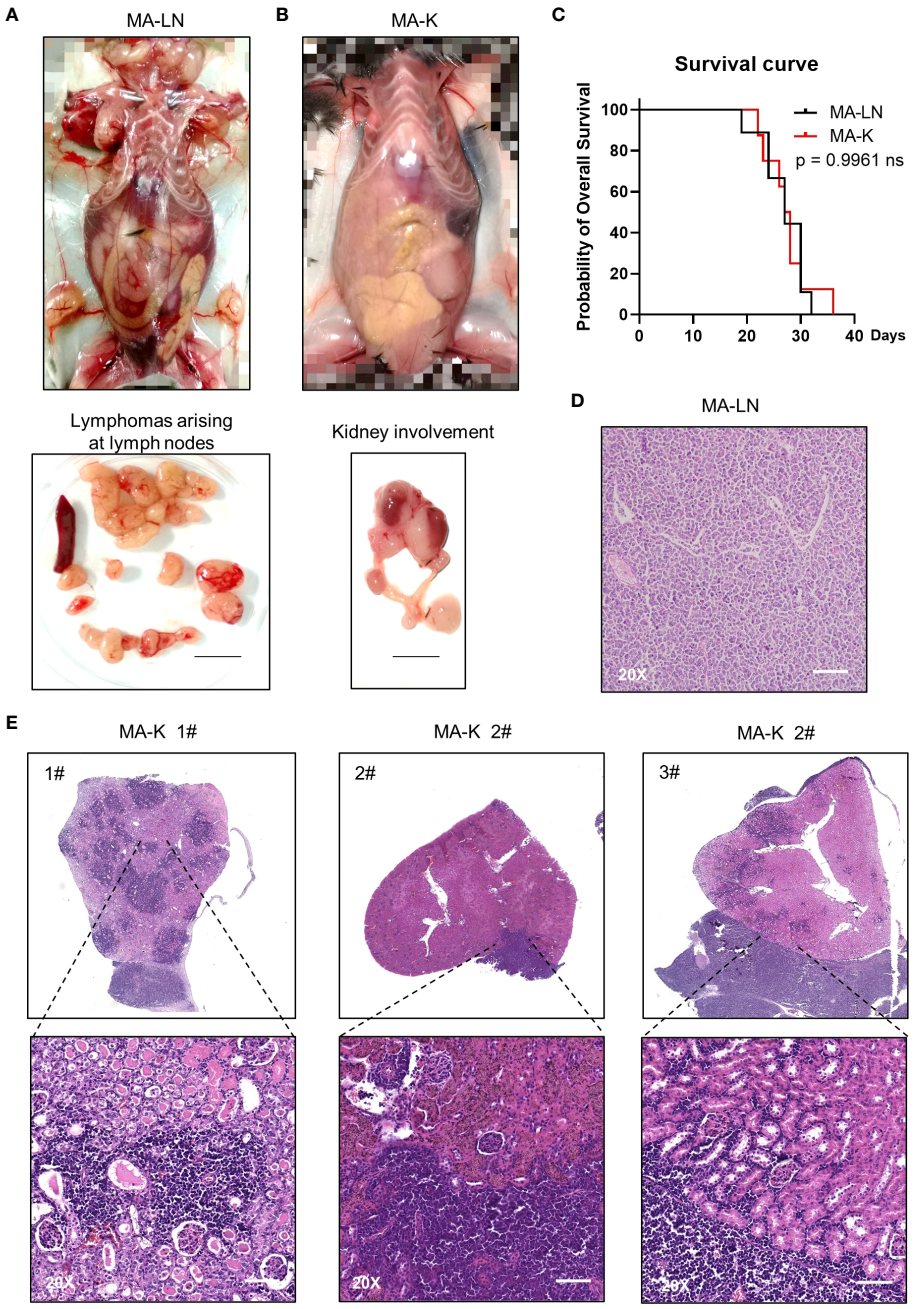

FIGURE 1
MA-K tends to disseminate in the kidney of recipient mice in the lymphoma transplantation model. **(A)** A representative picture showing the disseminated sites of MA-LN lymphoma in recipient mouse. The lymphomas were dissociated from mandibular lymph nodes, axillary lymph nodes, and inguinal lymph nodes of the recipient mice. Spleen was not enlarged. Bar, 1 cm. **(B)** A representative picture showing the unaffected lymph nodes and affected kidney and ureter in MA-K recipient mice. Bar, 1 cm. **(C)** Kaplan–Meier plots of MA-LN and MA-K recipient mice. MA-LN, $n = 9$; MA-K, $n = 8$. The equality of survival curves was tested using a log-rank test. **(D)** A representative H&E staining section of MA-LN lymphoma. Bar in 20× image, 200 μm. **(E)**. Representative H&E staining sections of primary renal lymphoma arising in MA-K recipient mice. Bar in 20× image, 200 μm.

FPKM < 1 and 8,547 genes were left. Surprisingly, approximately 20% of genes (1,905 of 8,547) had differentially expressed more than twice, indicating that MA-K was completely different from MA-N at the transcriptional level. Given that cancer cell lines could transcriptionally evolve in culture (22), we attributed the huge transcriptional difference to transcriptional selection and adaptation during the culture.

To identify the molecular patterns of MA-LN and MA-K, we proposed the specialized transcriptional pattern (STP) and specially expressed genes (SEGs), instead of routinely DEGs, to describe the molecular pattern of the individual sample. Four reference genes, Gapdh, Actb, Hsp90ab1, and Myc, were used as the reference gene panel to determine the quality and comparability of FPKM data. A total of 44 LymphGen genes were selected to perform STP analysis.

Owing to basic expression level (FPKM < 1), Bcl2, Bcl6, Bcl10, and other LymphGen genes were not included in the panel of 44 LymphGen genes. Compared to MA-LN, 14 downregulated SEGs and 3 upregulated SEGs [$\log_2$(FC) ≤ 1 and $\log_2$(FC) ≥ 1] in MA-K were identified in 44 LymphGen genes (Figure 2A). The observation indicated that gene inactivation by transcriptional inhibition was happening during the evolution of MA-K, which is consistent with high-frequency inactivation mutations in human B-NHL.

To test whether the gene expression level of SEGs in MA-K could predict clinical outcome, we performed survival analysis using a human DLBCL dataset (Lenz Staudt Lymphoma GSE10846, n = 420). We assumed that the STP of MA-K was associated with poor prognosis. The SurvExpress program was used to validate if the gene expression status could predict prognosis, in which the expression data of a single gene or multiple genes was calculated to the risk score, also called the prognostic index (PI) (20). The human DLBLC dataset (Lenz Staudt Lymphoma GSE10846, n = 420) was chosen, which contained detailed clinical information and had been adopted by many studies.

The results showed that most genes were associated with clinical relevance, while most of the gene expression level in risk groups was contrary to expectations (Figure 2B). Only FOXO1, BTG1, and MYD88 were in line with expectations (Figure 2C), indicating that the abnormal transcriptional pattern for specialized lymphoma was very complicated due to the heterogeneity of lymphoma. Although the significance of transcriptional evolution of MA-K was not fully understood, most LymphGen genes were indeed significantly altered at the transcriptional level.

Translation pathway is altered in MA-K with clinical relevance

To filter SEGs with biological significance, we analyzed the expression data as follows (Figure 3A). Inactive genes or basic expressed genes (defined as FPKM < 1) in both MA-LN and MA-K had been excluded in the 8,547 genes. For active genes (FPKM ≥ 1) in both, genes with $\log_2$(FC) ≤ 2 and $\log_2$(FC) ≥ 2 were filtered as SEGs. In the case of inactive genes in one, active genes (FPKM ≥ 10) in another were filtered as SEGs. All SEGs are listed in Data Sheet 1. A total of 360 SEGs were identified, specifically 100 upregulated SEGs and 260 downregulated SEGs in MA-K.

The pathway enrichment analysis revealed that translation pathway was the most affected pathway in SEGs (Figure 3B). In addition, the PPI network analysis discovered two core PPI networks in SEGs (Figure 3C). A core PPI network involved proteins in the translation machine, including the mitochondrial translation machine (Figure 3D). Another core PPI network involved proteins in Focal adhesion-MAPK, Unidentified, and Leukocyte Differentiation (Figure 3E). Together, the results suggested that the alteration of translation pathway and others presented the molecular features of MA-K cells.

Considering that many ribosomal proteins were abnormally regulated in tumors, we further analyzed the clinical relevance of the expression level of ribosomal proteins in human DLBCL. Survival analysis revealed that the high expression level of RPLP2, RPS16, and MRPS16, upregulated in MA-K, was significantly correlated with the poor prognosis of human DLBCL (Figure 3F).

Together, the transcriptional profiles discovered that translation pathway and others were largely altered in MA-K.

Identification of the five-gene signature to predict prognosis of human DLBCL

Next, we investigated the clinical relevance of MA-K by evaluating the ability of SEGs in MA-K to predict prognosis of human DLBCL. Owing to too many SEGs in MA-K, we only chose 50 SEGs filtered with Log_2(FC) < −3 or Log_2(FC) > 3 for survival analysis (Figure 4A). Finally, five genes, downregulated in MA-K to MA-L, SSPN, CD52, VPREB3, CCDC82, and ANKRD37, were significantly correlated with poor prognosis of human DLBCL (Figure 4B).

To investigate whether the five genes had a synergistic effect on the predicted clinical outcome, we compared the hazard ratio (HR) and p-value of three-gene and four-gene combinations in two risk groups. Notably, the five-gene signature showed improved prognostic prediction (HR = 2.39, 95% confidence interval: 3.37 to 4.76, p = 4.621e-12) and a four-gene signature that removed ANKRD37 was similar to the five-gene signature, even better on HR. The results indicated that SSPN, CD52, VPREB3, and CCDC82 were independent prognostic biomarkers, and the four-gene or five-gene signature could be developed as a promising prognostic biomarker panel for human DLBCL (Figure 4C).

To further evaluate the usefulness of the five-gene signature, we tested its performance in three risk groups. The survival curves of high-, medium-, and low-risk groups were well stratified by the five-gene signature (log-rank equal curves p = 8.46e-14) and the individual genes were also significantly differential expressed in each risk group (Figure 4D). The p-value of the four-gene signature was a little worse than the five-gene signature (log-rank equal curves p = 1.465e-13).

We also noticed that the expression level of SSPN was the most different in three risk groups (p = 2.43e-61). Given that SSPN is a membrane protein, it suggests that SSPN, detectable by immune-based assay, is a promising prognostic biomarker for human DLBCL. These results not only identified the five-gene signature as a potential prognostic biomarker of human DLBCL, but also highlighted the clinical relevance between the MA-K cell model and human aggressive DLBCL.

Discussion

This study reports a novel murine cell line, named MA-K. Compared to the parental Eμ-Myc;Cdkn2a$^{-/-}$ cell line, called MA-LN in this study, MA-K cells tend to invade the kidney in a lymphoma transplantation model, resembling human PRL. Kidney involvement is a type of extranodal lymphoma and is associated with poor prognosis in human aggressive B-cell lymphoma. Although lymphoma arising in the kidney is rare (10), the remarkable behavior of MA-K model, in which lymphoma did not start

10.3389/fonc.2023.1089187

A LymphGen transcriptional pattern in MA-LN and ML-K

Categories	Symbol	MA-LN-R1	MA-LN-R2	MA-K-R1	MA-K-R2	Log2FC
Reference genes	Gapdh	2503.73	3048.98	2110	2375.41	-0.31
	Actb	893.21	852.08	655.25	549.2	-0.54
	Hsp90ab1	1684.08	1861.82	2493.44	2065.07	0.36
	Myc	781.54	690.77	891.83	876.55	0.26
Lymphoma related genes	Cd19	337.44	298.47	164.06	154.76	-1.00
	Cd274	2.31	1.01	1.63	2.61	0.35
	Trp53	131.93	131.4	89.88	74.27	-0.68
	Ddx3x	191.97	228.2	383.78	332	0.77
	Foxo1	13.93	12.32	3.74	4.18	-1.73
MCD genes	Pim1	20.59	15.55	3.51	4.75	-2.13
	Btg1	44.2	37.18	8.74	12.75	-1.92
	Tbl1xr1	12.14	12.87	23.2	20.86	0.82
	Btg2	82.8	73.36	9.06	16.66	-2.60
	Setd1b	23.65	20.42	6.57	7.1	-1.69
	Klhl14	3.3	2.01	2.96	1.89	-0.13
	Grhpr	31.86	37.56	28.04	36.62	-0.10
	Irf4	59.32	62.99	51.11	48.46	-0.30
BN2 genes	Notch2	33.7	26.94	17.59	18.51	-0.75
	Bcl10	13.45	13.51	17.89	17.3	0.38
	Spen	20.51	20.1	13.08	11.71	-0.71
	Klf2	54.68	53.37	6.99	7.55	-2.89
EZB genes	Tnfrsf14	6.92	8.7	2.96	2.12	-1.62
	Kmt2d	54.06	45.11	18.92	21.35	-1.30
	Crebbp	18.42	17.37	9.54	9.57	-0.91
	Ezh2	50.48	58.84	59.55	63.28	0.17
	Ep300	45.45	42.65	27.09	28.21	-0.67
	Gna13	30.18	31.52	30.83	32.85	0.05
	Stat6	39.8	37.8	18.9	22.43	-0.91
ST2 genes	Dusp2	37.12	29	11.85	21.45	-0.99
	Sgk1	7.69	6.04	14.57	19.76	1.32
	Junb	73.49	49.82	13.92	17.56	-1.97
BCR subunits	Cd79a	677.06	500.12	163.27	164.65	-1.84
	Cd79b	472.77	389.85	125.69	127.68	-1.77
BCR-dependent NF-κB pathway	Syk	100.65	96.66	49.18	46.71	-1.04
	Btk	92.94	90.34	80.75	94.68	-0.06
	Plcg2	90.05	72.65	70.47	61.11	-0.31
	Card11	27.63	21.94	15.74	15.38	-0.67
	Bcl10	13.45	13.51	17.89	17.3	0.38
	Malt1	18.75	16.54	11.93	12.43	-0.53
	Traf6	21	22.62	24.51	22.74	0.12
	Map3k7	17.47	17.28	32.27	27.86	0.79
IκB kinase	Ikbkb	32.08	31.44	25.47	25.3	-0.32
	Chuk	19.86	23.92	48.4	52.84	1.21
	Ikbkg	7.48	7.78	10.23	11.19	0.49
MYD88 pathway	Tlr9	12.96	9.33	2.8	4.19	-1.67
	Myd88	16.24	15.77	34.35	29.68	1.00
	Irak1	58.48	54.26	35.29	33.53	-0.71
	Irak4	8.44	7.01	3.83	4.46	-0.90

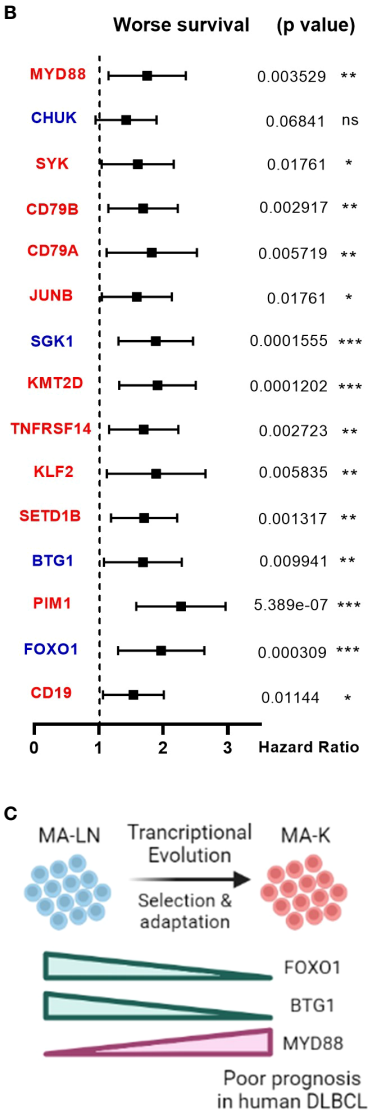

FIGURE 2
LymphGen signature in specialized transcriptional pattern of MA-K and clinical relevance. **(A)** Expression level of LymphGen genes in MA-LN and MA-K. FPKM were used to evaluate the gene expression abundance in MA-LN and MA-K. The reference gene panel including Gapdh, Actb, Hsp90ab1, and Myc was presented to the quality and comparability of FPKM data. Log_2(FC) was calculated by the average FPKM. FC, fold change. **(B)** Forest plot of indicated genes in two risk groups. *p*-values of the log-rank test were shown. The hazard ratio (HR), confidence interval, and *p*-value in forest plot were obtained from the SurvExpress program. **(C)** Diagram for the formation of FOXO1-BTG1-MYD88 pattern during the evolution of MA-K. Created with BioRender.com. A p-value< 0.05 was regarded as statistically significance. (* < 0.05, ** < 0.01, *** < 0.001). ns, no significance.

primarily in lymph nodes in recipient mice, is a notable feature for most kinds of human primary extranodal lymphoma.

Dissemination into extranodal sites and primary extranodal localization are indeed biologically and clinically distinct scenarios. If lymphoma first presents in lymph nodes and then disseminates to extranodal tissues/organs with progression, it is not primary extranodal lymphoma, but secondary extranodal lymphoma. If lymphoma first appears in extranodal tissues/organs, this situation is considered as primary extranodal lymphoma. MA-LN cells mainly home to lymph nodes and form nodal lymphoma, while MA-K cells do not home to peripheral lymphatic organs such as lymph nodes and spleens. Therefore, we define the MA-K lymphoma model as a PRL model.

In addition, we notice that there is no difference in survival time between MA-K and MA-LN recipient mice. We assume that the survival time is determined by multiple factors, including the disease progression and therapeutic response. In this study, although there was no significant difference in survival time between MA-LN and MA-K recipient mice, the criteria for their experimental end points were largely different. The end point of MA-LN is obvious and palpable mass at lymph nodes. In this situation, the MA-LN recipient mice are in good condition. If the swollen lymph nodes are removed surgically or treated with drugs, the survival time of recipient mice should be significantly prolonged. The end point of MA-K is moribund status; at this point, the kidney damage is already very severe. In this case, it will

10.3389/fonc.2023.1089187

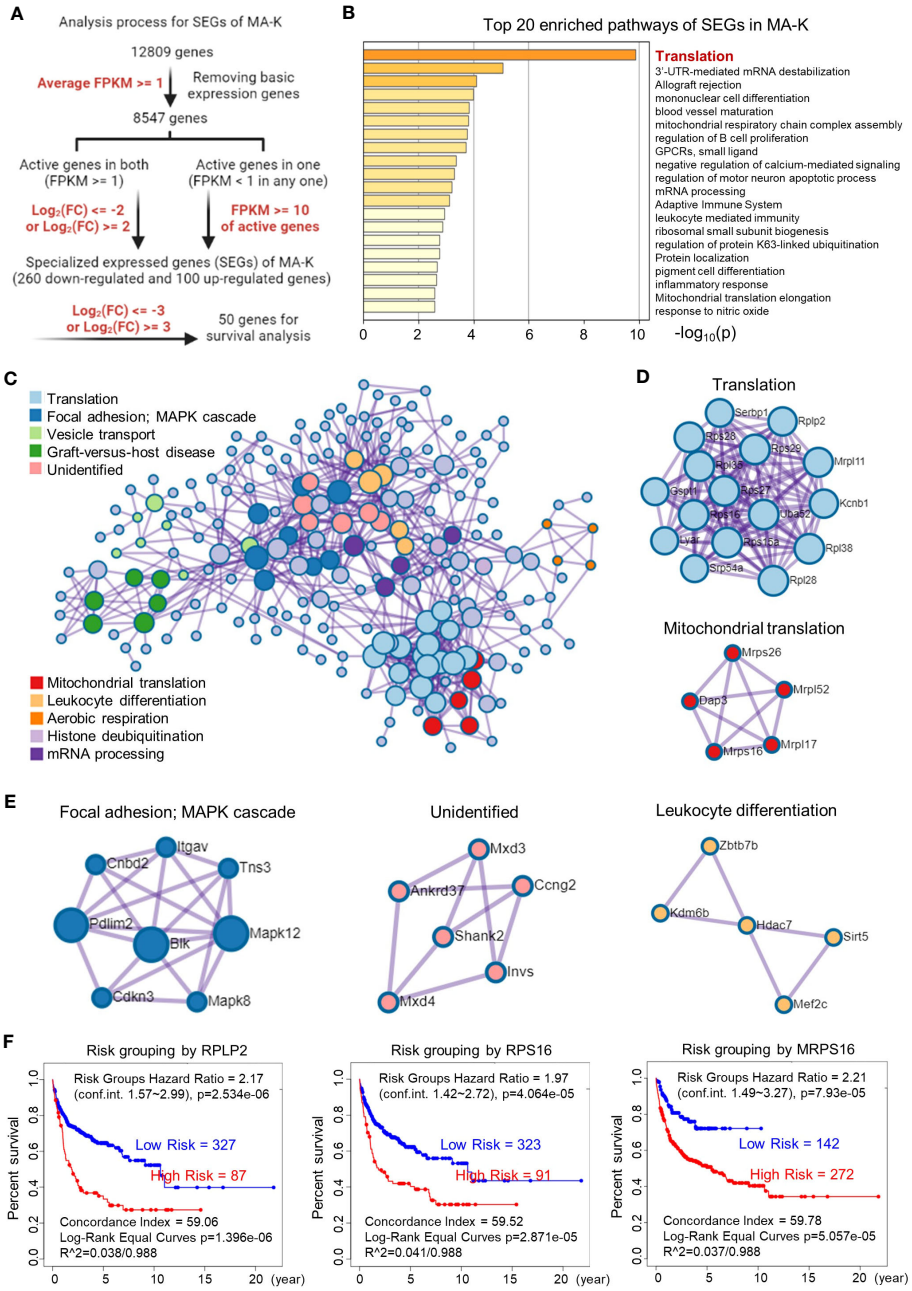

FIGURE 3
Translation-related proteins, altered in MA-K, are associated with prognosis of human DLBCL. **(A)** The analysis process of SEGs in MA-K. Filter parameters were highlighted in red. Inactive genes or basic expressed genes were defined as FPKM < 1 and excluded in SEGs analysis. Active genes were defined as FPKM ≥ 1. Created with BioRender.com. **(B)** The top 20 enriched pathways of SEGs in MA-K. In total, 360 SEGs were selected as described in Materials and methods and applied to pathway enrichment analysis. *p*-values are calculated based on the cumulative hypergeometric distribution. **(C)** The protein–protein interaction (PPI) networks of SEGs. **(D)** Genes in the PPI network including translation and mitochondrial translation. **(E)** Genes in the PPI network including Focal adhesion-MAPK, Unidentified, and Leukocyte differentiation. **(F)**. Kaplan–Meier plots of RPLP2, RPS16, and MRPS16 in human DLBCL. Red, high-risk group. Blue, low-risk group. Risk groups were generated based on the prognostic index (PI) for each gene and the optimization algorithm was applied in risk grouping. The number of each risk group was indicated in the plots. The equality of survival curves was tested using a log-rank test. A human DLBCL dataset (Lenz Staudt Lymphoma GSE10846, *n* = 420) was chosen for survival analysis.

be difficult for existing treatment interventions to extend the survival time of MA-K recipient mice.

Extranodal dissemination is also one of the key indicators for international prognostic index (IPI) in human lymphoma, indicating that extranodal dissemination indeed is associated with poor outcome in DLBCL patients. Although we currently do not know which genes/molecules are key biomarkers of extranodal lymphoma, similar to EMT markers in solid tumors, based on the features of extranodal dissemination and malignant progression we observed in MA-K model, we propose that

10.3389/fonc.2023.1089187

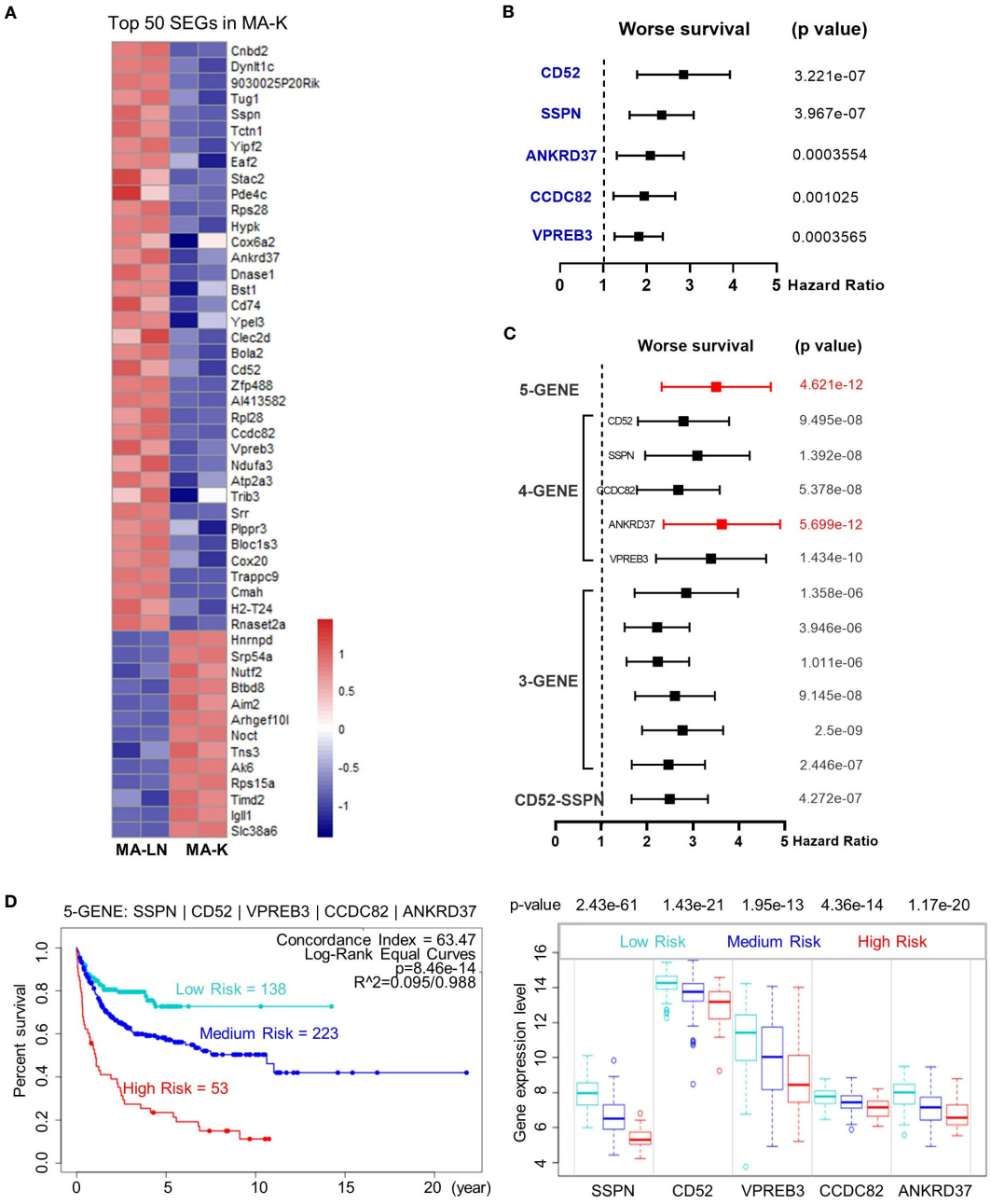

FIGURE 4
The five-gene signature, altered in MA-K, predicts the prognosis of human DLBCL. **(A)** Heatmap of SEGs in MA-K. Fifty SEGs in MA-K [$\log_2$(FC) ≤ 3 and $\log_2$(FC) ≥ 3] were analyzed. FPKM of selected SEGs were used to generate the heatmap in R studio. **(B)** Forest plot of SSPN, CD52, VPREB3, CCDC82, and ANKRD37 in two risk groups. *p*-values of the log-rank test were shown. The hazard ratio (HR), confidence interval, and *p*-value in forest plot were obtained from the SurvExpress program. **(C)** Forest plot of different combinations of SSPN, CD52, VPREB3, CCDC82, and ANKRD37 in two risk groups. *p*-values of the log-rank test were shown. The hazard ratio (HR), confidence interval, and *p*-value in forest plot were obtained from the SurvExpress program. **(D)** Kaplan–Meier plots of the five-gene signature and box plot of gene expression by three risk groups. Red, high-risk group. Cyan, medium-risk group. Blue, low-risk group. Risk groups were generated based on the prognostic index (PI) for each gene set and the optimization algorithm was applied in risk grouping. The number of each risk group was indicated in the plots. The *p*-value of gene expression by three risk groups in box plot was obtained from an *f*-test. A human DLBCL dataset (Lenz Staudt Lymphoma GSE10846, *n* = 420) was chosen for survival analysis.

compared to MA-LN, the MA-K cell line and PRL model are more aggressive.

The MA-K cell line originates from the MA-LN cell line and is identified as its kidney dissemination in recipient mice. Although we do not know how the MA-K cell line was formed, we can confirm that MA-K is largely different from the parent MA-LN at the transcriptional level. Given that cancer cell lines could undergo the genetic and non-genetic evolution in culture (22, 23), we attribute the formation of MA-K to transcriptional selection and adaptation (TSA). We propose that both the genetic mechanism,

such as abnormal B-cell differentiation, and the non-genetic mechanism, such as cell plasticity at transcriptional selection and adaptation, are involved in the evolution of MA-K. Enlarged spleen is a common feature in Eμ-Myc and its derived lymphoma mouse models, but no enlarged spleens were observed in the MA-K recipient mice. Given that spleen and lymph nodes are both peripheral lymphoid organs, we speculate that the MA-K cell line had lost key genes that guide the homing ability of lymphoma cells to the peripheral lymphoid organs, ultimately leading to extranodal presentation.

To establish the relevance of MA-K and human aggressive B-cell lymphoma, we analyzed STP in MA-K by 44 LymphGen genes. FOXO1 is frequently mutated in the EZB-MYC+ subtype (2). BTG1 is frequently mutated in the MCD subtype. Oncogenically active mutations in MYD88 are observed in many extranodal lymphoma of DLBCL (9, 24–28) and classified into the MCD subtype (2). FOXO1, BTG1, and MYD88 are in line with expectations, indicating that MA-K shares the molecular pattern of MCD and EZB-MYC+ subtypes.

To confirm the clinical relevance of MA-K, we re-examined the SEGs in MA-K from two perspectives. In terms of signal pathway enrichment, we found that translation-related ribosomal proteins were enriched in MA-K, and the high expression of these genes was also correlated with the poor prognosis of human DLBCL. Emerging evidence suggested that dysregulation of onco-ribosomes could facilitate the oncogenic translation program and increase the risk of developing malignancy, including tumor behavior, therapeutic response, and clinical outcome (29–31). RPLP2, RPS16, and MRPS16, discovered in this study, had been reported to play oncogenic roles in various tumors (32–34). Hence, the gain of onco-ribosomes in MA-K suggests that pharmaceutical inhibition of translation may be a potential therapeutic vulnerability of aggressive B-cell lymphoma, and this strategy should be evaluated in the MA-K GDA model and clinical trials. Whether abnormal activation of ribosomal proteins contributes to extranodal dissemination of lymphoma and other aggressive phenotypes should be further explored. In terms of top SEGs, we chose the top 50 SEGs for evaluation of prognostic biomarkers. The five genes, downregulated in MA-K, were correlated with poor prognosis of human DLBCL, suggesting that these genes played negative regulation in aggressive progression of human DLBCL. Owing to the limitation of gene expression datasets with clinical information, we only evaluated the clinical relevance between MA-K and human DLBCL.

Meanwhile, CD52 and SSPN, as membrane proteins, probably directly participate in the interaction between lymphoma cells and tumor microenvironment and finally determine lymphoma dissemination. In terms of molecular classification and molecular diagnosis, we propose that CD52 and SSPN are ideal prognostic biomarkers to predict the clinical outcomes. As a specific antigen in all blast cells, CD52 had been developed as a promising therapeutic target by mono-antibody (Alemtuzumab) in many clinical trials (35–38). However, CD52 was downregulated in MA-K and the low expression of CD52 was correlated with the poor prognosis of human DLBCL, suggesting that patients could not benefit from anti-CD52 immunotherapy and even worse. If CD52 is a negative regulator for aggressive B-cell lymphoma, targeting CD52 will directly accelerate malignant transformation of lymphoma, such as extranodal dissemination. Hence, the adoption of anti-CD52 immunotherapy in clinical trials needs to be carefully reassessed.

In conclusion, the MA-K GDA model is a syngeneic lymphoma transplantation model in which lymphoma arising in recipient mice usually disseminated at the kidney, highly resembling human PRL. SEGs in MA-K reveal that MA-K has strong clinical relevance with human aggressive DLBCL and onco-ribosomes, and others, such as CD52 and SSPN, are identified as promising prognostic biomarkers in human DLBCL. Further studies on the MA-K cell line will provide more meaningful insights into the genetic and non-genetic mechanism of extranodal lymphoma. Moreover, the MA-K GDA model could be developed as a novel preclinical model of aggressive B-cell lymphoma and widely used for efficacy evaluation of chemotherapy and immunotherapy.

Data availability statement

The datasets presented in this study can be found in online repositories. The names of the repository/repositories and accession number(s) can be found in the article/Supplementary Material.

Ethics statement

The animal study was reviewed and approved by the Animal Care and Use Committee of Laboratory Animal Research Center, Jiangsu University.

Author contributions

XL conceptualized and designed the experiments, and wrote the manuscript. HQ helped with designing the experiments and reviewing the manuscript. MD and CZ performed the mouse experiments. XL analyzed the transcriptome data. LL performed the prognostic analysis. All authors discussed the results and commented on the manuscript. XL and HQ jointly supervised the study. All authors contributed to the article and approved the submitted version.

Funding

This work was supported by the National Natural Science Foundation of China (Grant Number 81900200), the Natural Science Foundation of Jiangsu Province (Grant Number BK20190840), and the Foundation of State Key Laboratory of Cell Biology (Grant Number SKLCB2018KF008).

Conflict of interest

The authors declare that the research was conducted in the absence of any commercial or financial relationships that could be construed as a potential conflict of interest.

Publisher's note

All claims expressed in this article are solely those of the authors and do not necessarily represent those of their affiliated organizations, or those of the publisher, the editors and the reviewers. Any product that may be evaluated in this article, or claim that may be made by its manufacturer, is not guaranteed or endorsed by the publisher.

Supplementary material

The Supplementary Material for this article can be found online at: https://www.frontiersin.org/articles/10.3389/fonc.2023.1089187/full#supplementary-material

References

1. Sehn LH, Salles G. Diffuse large B-cell lymphoma. *N Engl J Med* (2021) 384:842–58. doi: 10.1056/NEJMra2027612

2. Wright GW, Huang DW, Phelan JD, Coulibaly ZA, Roulland S, Young RM, et al. A probabilistic classification tool for genetic subtypes of diffuse large B cell lymphoma with therapeutic implications. *Cancer Cell* (2020) 37:551–568.e14. doi: 10.1016/j.ccell.2020.03.015

3. Bociek RG. Adult burkitt's lymphoma. *Clin Lymphoma* (2005) 6:11–20. doi: 10.3816/clm.2005.n.021

4. Blum KA, Lozanski G, Byrd JC. Adult Burkitt leukemia and lymphoma. *Blood* (2004) 104:3009–20. doi: 10.1182/blood-2004-02-0405

5. Olszewski AJ, Kurt H, Evens AM. Defining and treating high-grade B-cell lymphoma, NOS. *Blood* (2022) 140:943–54. doi: 10.1182/blood.2020008374

6. Ok CY, Medeiros LJ. High-grade B-cell lymphoma: a term re-purposed in the revised WHO classification. *Pathology* (2020) 52:68–77. doi: 10.1016/j.pathol.2019.09.008

7. Schaff LR, Grommes C. Primary central nervous system lymphoma. *Blood* (2022) 140:971–9. doi: 10.1182/blood.2020008377

8. Willemze R, Jaffe ES, Burg G, Cerroni L, Berti E, Swerdlow SH, et al. WHO-EORTC classification for cutaneous lymphomas. *Blood* (2005) 105:3768–85. doi: 10.1182/blood-2004-09-3502

9. Cao X-X, Li J, Cai H, Zhang W, Duan M-H, Zhou D-B. Patients with primary breast and primary female genital tract diffuse large B cell lymphoma have a high frequency of MYD88 and CD79B mutations. *Ann Hematol* (2017) 96:1867–71. doi: 10.1007/s00277-017-3094-7

10. Cheng X, Huang Z, Li D, Wang Y. Enormous primary renal diffuse large B-cell lymphoma: A case report and literature review. *J Int Med Res* (2019) 47:2728–39. doi: 10.1177/0300060519842049

11. Alizadeh AA, Eisen MB, Davis RE, Ma C, Lossos IS, Rosenwald A, et al. Distinct types of diffuse large B-cell lymphoma identified by gene expression profiling. *Nature* (2000) 403:503–11. doi: 10.1038/35000501

12. Adams JM, Harris AW, Pinkert CA, Corcoran LM, Alexander WS, Cory S, et al. The c-myc oncogene driven by immunoglobulin enhancers induces lymphoid Malignancy in transgenic mice. *Nature* (1985) 318:533–8. doi: 10.1038/318533a0

13. Schmitt CA, McCurrach ME, de StanChina E, Wallace-Brodeur RR, Lowe SW. INK4a/ARF mutations accelerate lymphomagenesis and promote chemoresistance by disabling p53. *Genes Dev* (1999) 13:2670–7. doi: 10.1101/gad.13.20.2670

14. Eischen CM, Weber JD, Roussel MF, Sherr CJ, Cleveland JL. Disruption of the ARF–Mdm2–p53 tumor suppressor pathway in Myc-induced lymphomagenesis. *Genes Dev* (1999) 13:2658–69. doi: 10.1101/gad.13.20.2658

15. Mori S, Rempel RE, Chang JT, Yao G, Lagoo AS, Potti A, et al. Utilization of pathway signatures to reveal distinct types of B lymphoma in the Eμ-myc model and human diffuse large B-cell lymphoma. *Cancer Res* (2008) 68:8525–34. doi: 10.1158/0008-5472.CAN-08-1329

16. Lefebure M, Tothill RW, Kruse E, Hawkins ED, Shortt J, Matthews GM, et al. Genomic characterisation of Eμ-Myc mouse lymphomas identifies Bcor as a Myc co-operative tumour-suppressor gene. *Nat Commun* (2017) 8:14581. doi: 10.1038/ncomms14581

17. Day C-P, Merlino G, Van Dyke T. Preclinical mouse cancer models: A maze of opportunities and challenges. *Cell* (2015) 163:39–53. doi: 10.1016/j.cell.2015.08.068

18. Zhao B, Pritchard JR, Lauffenburger DA, Hemann MT. Addressing genetic tumor heterogeneity through computationally predictive combination therapy. *Cancer Discovery* (2014) 4:166–74. doi: 10.1158/2159-8290.CD-13-0465

19. Ferrao PT, Bukczynska EP, Johnstone RW, McArthur GA. Efficacy of CHK inhibitors as single agents in MYC-driven lymphoma cells. *Oncogene* (2012) 31:1661–72. doi: 10.1038/onc.2011.358

20. Aguirre-Gamboa R, Gomez-Rueda H, Martínez-Ledesma E, Martínez-Torteya A, Chacolla-Huaringa R, Rodriguez-Barrientos A, et al. SurvExpress: an online biomarker validation tool and database for cancer gene expression data using survival analysis. *PloS One* (2013) 8:e74250. doi: 10.1371/journal.pone.0074250

21. Lenz G, Wright G, Dave SS, Xiao W, Powell J, Zhao H, et al. Stromal gene signatures in large-B-cell lymphomas. *N Engl J Med* (2008) 359:2313–23. doi: 10.1056/NEJMoa0802885

22. Ben-David U, SIranosian B, Ha G, Tang H, Oren Y, Hinohara K, et al. Genetic and transcriptional evolution alters cancer cell line drug response. *Nature* (2018) 560:325–30. doi: 10.1038/s41586-018-0409-3

23. Marine J-C, Dawson S-J, Dawson MA. Non-genetic mechanisms of therapeutic resistance in cancer. *Nat Rev Cancer* (2020) 20:743–56. doi: 10.1038/s41568-020-00302-4

24. Ngo VN, Young RM, Schmitz R, Jhavar S, Xiao W, Lim K-H, et al. Oncogenically active MYD88 mutations in human lymphoma. *Nature* (2011) 470:115–9. doi: 10.1038/nature09671

25. Kraan W, van Keimpema M, Horlings HM, Schilder-Tol EJM, Oud MECM, Noorduyn LA, et al. High prevalence of oncogenic MYD88 and CD79B mutations in primary testicular diffuse large B-cell lymphoma. *Leukemia* (2014) 28:719–20. doi: 10.1038/leu.2013.348

26. Nakamura T, Tateishi K, Niwa T, Matsushita Y, Tamura K, Kinoshita M, et al. Recurrent mutations of CD79B and MYD88 are the hallmark of primary central nervous system lymphomas. *Neuropathol Appl Neurobiol* (2016) 42:279–90. doi: 10.1111/nan.12259

27. Hattori K, Sakata-Yanagimoto M, Okoshi Y, Goshima Y, Yanagimoto S, Nakamoto-Matsubara R, et al. MYD88 (L265P) mutation is associated with an unfavourable outcome of primary central nervous system lymphoma. *Br J Haematol* (2017) 177:492–4. doi: 10.1111/bjh.14080

28. Schrader AMR, Jansen PM, Willemze R, Vermeer MH, Cleton-Jansen A-M, Somers SF, et al. High prevalence of MYD88 and CD79B mutations in intravascular large B-cell lymphoma. *Blood* (2018) 131:2086–9. doi: 10.1182/blood-2017-12-822817

29. Elhamamsy AR, Metge BJ, Alsheikh HA, Shevde LA, Samant RS. Ribosome biogenesis: A central player in cancer metastasis and therapeutic resistance. *Cancer Res* (2022) 82:2344–53. doi: 10.1158/0008-5472.CAN-21-4087

30. Pelletier J, Thomas G, Volarević S. Ribosome biogenesis in cancer: new players and therapeutic avenues. *Nat Rev Cancer* (2018) 18:51–63. doi: 10.1038/nrc.2017.104

31. Bursać S, Prodan Y, Pullen N, Bartek J, Volarević S. Dysregulated ribosome biogenesis reveals therapeutic liabilities in cancer. *Trends Cancer* (2021) 7:57–76. doi: 10.1016/j.trecan.2020.08.003

32. Liao Y, Shao Z, Liu Y, Xia X, Deng Y, Yu C, et al. USP1-dependent RPS16 protein stability drives growth and metastasis of human hepatocellular carcinoma cells. *J Exp Clin Cancer Res* (2021) 40:201. doi: 10.1186/s13046-021-02008-3

33. Wang Z, Li J, Long X, Jiao L, Zhou M, Wu K. MRPS16 facilitates tumor progression *via the* PI3K/AKT/Snail signaling axis. *J Cancer* (2020) 11:2032–43. doi: 10.7150/jca.39671

34. Artero-Castro A, Castellvi J, García A, Hernández J, Ramón y Cajal S, Lleonart ME. Expression of the ribosomal proteins Rplp0, Rplp1, and Rplp2 in gynecologic tumors. *Hum Pathol* (2011) 42:194–203. doi: 10.1016/j.humpath.2010.04.020

35. Geisler CH, van T' Veer MB, Jurlander J, Walewski J, Tjønnfjord G, Itälä Remes M, et al. Frontline low-dose alemtuzumab with fludarabine and cyclophosphamide prolongs progression-free survival in high-risk CLL. *Blood* (2014) 123:3255–62. doi: 10.1182/blood-2014-01-547737

36. Faderl S, Thomas DA, O'Brien S, Garcia-Manero G, Kantarjian HM, Giles FJ, et al. Experience with alemtuzumab plus rituximab in patients with relapsed and

refractory lymphoid Malignancies. *Blood* (2003) 101:3413–5. doi: 10.1182/blood-2002-07-1952

37. Uppenkamp M, Engert A, Diehl V, Bunjes D, Huhn D, Brittinger G. Monoclonal antibody therapy with CAMPATH-1H in patients with relapsed high- and low-grade non-Hodgkin's lymphomas: a multicenter phase I/II study. *Ann Hematol* (2002) 81:26–32. doi: 10.1007/s00277-001-0394-7

38. Lundin J, Osterborg A, Brittinger G, Crowther D, Dombret H, Engert A, et al. CAMPATH-1H monoclonal antibody in therapy for previously treated low-grade non-Hodgkin's lymphomas: a phase II multicenter study. European Study Group of CAMPATH-1H Treatment in Low-Grade Non-Hodgkin's Lymphoma. *J Clin Oncol* (1998) 16:3257–63. doi: 10.1200/JCO.1998.16.10.3257

Frontiers in Oncology

Advances knowledge of carcinogenesis and tumor progression for better treatment and management

The third most-cited oncology journal, which highlights research in carcinogenesis and tumor progression, bridging the gap between basic research and applications to imrpove diagnosis, therapeutics and management strategies.

Discover the latest Research Topics

See more →

Frontiers

Avenue du Tribunal-Fédéral 34
1005 Lausanne, Switzerland
frontiersin.org

Contact us

+41 (0)21 510 17 00
frontiersin.org/about/contact